



FACULTY OF SCIENCE AND TECHNOLOGY

MASTER'S THESIS

Study program/ Specialization: Masters Degree in Mechanical and Structural Engineering – Civil Engineering	Spring semester, 2012 Open
Writer: Jan Tveiten	 (Writer's signature)
Faculty supervisor: Jasna Bogunovic Jakobsen External supervisor(s):	
Title of thesis: Dynamic analysis of a suspension bridge.	
Credits (ECTS): 30	
Key words: Suspension bridge Steel bridge Eigen value analysis Dynamic analysis	Pages: 90 + enclosure: 80 Stavanger, 11/6-2012

PREFACE

This master thesis is the final part of my Master degree in structural and material science at the University of Stavanger. The thesis consists of collecting and studying data for the Lysefjord Bridge in light of the deterioration of the main cables and to carry out some static and dynamic analysis of the bridge to see if any load case could indicate reasons for the wire breakage. Data is given from the Norwegian Public Roads Administration (Statens Vegvesen)

The existing finite element model of the bridge is modeled in ABAQUS. The model is analyzed with emphasis on the dynamic aspects of the bridge. Studies of the eigenfrequencies and eigenmodes have been done, both from the finite element model results and by simpler theoretical calculations. Wind loading and vortex induced vibrations of the bridge girder has been looked into. Cables forces from the loads have been checked.

The wire fractures observed in the main cables have been summarized and analyzed with respect to weather conditions in the area. Data on the weather in the area has been provided by the Lysefjord Weather Station, downloaded through www.wunderground.com.

The thesis consists of;

- A presentation of the static and dynamic characteristics of a suspension bridge
- A summary of the wire fractures in the main cables on Lysefjord Bridge
- A weather analysis at the time of the wire fractures
- Verification of the existing finite element model in ABAQUS
- An eigenvalue, wind, temperature and traffic analysis of the bridge model
- A verification of the finite element model results by theoretical calculations

Contents

Faculty of Science and Technology	i
Preface	i
Table of Figures	ii
Table of Tables	iv
Acknowledgments	v
1 Introduction	1
2 Suspension bridges	3
2.1. Stiffening girder	4
2.2. Support of stiffening girder	5
2.3. Main Cables	6
2.4. Hanger cables	7
2.5. Towers	7
2.6. Anchor piers	9
3 Fracturing of main cables	10
3.1. The main cables	10
3.2. Possible causes for wire fractures	11
3.3. SoundPrint® acoustic monitoring system	12
3.4. Weather around Lysefjord Bridge	15
4 Finite element model	22
4.1. ABAQUS software	22
4.2. ABAQUS model	23
4.3. Basic model loads	33
5 Results of ABAQUS analysis	42
5.1. Deformed model	42
5.2. Temperature loads	43
5.3. Traffic load model	44
5.4. Motion induced wind loads	44
5.5. Eigenfrequencies and eigenmodes	46
5.6. Vortex Induced Vibrations	59
6 Validation of eigenfrequencies and eigenmodes	72
6.1. Basic definitions	72
6.2. Basic assumptions	73
6.3. Vertical asymmetric modes	73
6.4. Vertical symmetric modes	74
6.5. Torsional eigenfrequencies and modes	76
7 Conclusion	79
8 Future recommendations	81
Bibliography	82
APPENDIX A: Drawings	84
APPENDIX B: Girder cross section calculations	93
APPENDIX C: Calculation of shear center	95
APPENDIX D: Calculation of Steinman eigen modes	98
APPENDIX E: ABAQUS files	100
APPENDIX F: FORTRAN files	158

TABLE OF FIGURES

Figure 1-1: Plan and section of Lysefjord Bridge[1].....	1
Figure 2-1: Bakke bridge.....	3
Figure 2-2: Main components of a suspension bridge [30].....	4
Figure 2-3: Cross section of bridge girder at Lysefjord Bridge [7]	5
Figure 2-4: Pendulum support north side [30]	5
Figure 2-5: Fixed support north side [30]	6
Figure 2-6: Pendulum support south side [30]	6
Figure 2-7: Detail of hanger attachment to main cables Lysefjord Bridge [30]	7
Figure 2-8: North tower Lysefjord Bridge [30]	8
Figure 3-1: Main cable cross section Lysefjord Bridge [7]	10
Figure 3-2: Cumulative wire breaks since bridge opening	11
Figure 3-3: Surface defects on examined z wire from Lysefjord Bridge[27]	12
Figure 3-4: Acoustic sensor on main span	13
Figure 3-5: Acoustic sensor on backstay cable.....	13
Figure 3-6: Wire breaks east cable [3]	14
Figure 3-7: Wire breaks west cable [3]	14
Figure 3-8: Wire breaks by month [3]	15
Figure 3-9: Wind velocity distribution at Forsand weather station from January 1 st 2009 to December 31 st 2011	16
Figure 3-10: Temperature distribution at the Forsand weather station from January 1 st 2009 to December 31 st 2011	16
Figure 3-11: Cable breaks as function of temperature.....	17
Figure 3-12: Cable breaks as function of wind velocity.....	18
Figure 3-13: Wire breaks as function of day	18
Figure 3-14: Wire breaks as function of temperature east/west side.....	19
Figure 3-15: Wire breaks as function of wind east/west side.....	19
Figure 3-16: Wire breaks as function of weekday east/west side	20
Figure 3-17: Time between wire fractures.....	20
Figure 4-1: Element model of Lysefjord Bridge	23
Figure 4-2: Element and node numbering scheme man span.....	24
Figure 4-3: Cross section of bridge girder with cable, hanger, dummy elements and mass node points	25
Figure 4-4: Vertical bridge geometry.....	27
Figure 4-5: Vertical cable geometry.....	28
Figure 4-6: Vertical distance between cable and girder	28
Figure 4-7: Girder cross section with initial shear stress distribution	30
Figure 4-8: Mass positions in cross section.....	32
Figure 4-9 : Rotation of girder cross section	36
Figure 4-10: Wind force diagram for bridge cross section.....	39
Figure 4-11: Traffic load position along bridge.....	41
Figure 4-12: Traffic load placement on east side of bridge.....	41
Figure 5-1: Cable force increase due to temperature	43
Figure 5-2: Angle dependent lift force.....	45
Figure 5-3: Angle dependent moment.....	45
Figure 5-4: Horizontal symmetric modes.....	49

Figure 5-5: Horizontal asymmetric modes.....	49
Figure 5-6: Vertical symmetric modes	50
Figure 5-7: Vertical asymmetric modes	50
Figure 5-8:Torsional symmetric modes.....	51
Figure 5-9: Torsional asymmetric modes	51
Figure 5-10: Horizontal coupled modes.....	52
Figure 5-11: First three coupled horizontal/torsion modes	54
Figure 5-12: Coupled horizontal and torsional modes	54
Figure 5-13: Symmetric torsional modes without cable mass in mass moment.....	56
Figure 5-14: Asymmetric torsional modes without cable mass in mass moment	57
Figure 5-15: First three horizontal main cable modes with high energy and different shape	58
Figure 5-16: First three vertical main cable modes with high energy and different shape.....	59
Figure 5-17: Vortexes around bridge girder.....	60
Figure 5-18: Map of Lysefjord bridge and surrounding terrain.	62
Figure 5-19: Vertical displacement in girder quarter points due to harmonic vortex shedding lift force on half the bridge.....	63
Figure 5-20: Asymmetric wind velocity and force on bridge	64
Figure 5-21: Vertical displacement [m] in girder quarter points on tapered harmonic wind lift load	64
Figure 5-22: Vertical displacement [m] in girder quarter points on tapered harmonic wind lift load with varying vortex shedding frequency	65
Figure 5-23: Vertical displacement [m] in center point bridge first harmonic symmetric wind lift load.	66
Figure 5-24: Vertical displacement [m] of quarter points on bridge VIV second symmetric lift load.	67
Figure 5-25: Percent increase of cable force at max oscillation due to VIV second symmetric wind lift load.....	67
Figure 5-26: Symbol explanation [22]	69
Figure 5-27: First symmetric vertical mode shape.....	69

TABLE OF TABLES

Table 3-1: Statistics for wind and temperature graphs	17
Table 3-2: Statistical values for cable break data.....	17
Table 4-1: Shear calculation constants.....	30
Table 4-2: Masses in cross section.....	32
Table 4-3: Weight of structure.....	34
Table 4-4: Wind coefficients.....	36
Table 4-5: Rotation independent wind forces	39
Table 4-6: Cable loads from lorry on crossbeam between hangers	41
Table 5-1: Alvsat and ABAQUS values for eigenfrequencies	48
Table 5-2: Frequencies and periods of horizontal coupled modes	52
Table 5-3: Modes above energy threshold	52
Table 5-4: Mode intersection set at threshold level.....	53
Table 5-5: Frequencies without cable mass in mass moment	55
Table 5-6: Number of modes with energy above threshold.....	57
Table 5-7: Critical wind velocities for vortex induced vibrations	61
Table 5-8: Length coefficients.....	69
Table 6-1: Bridge constants.....	73
Table 6-2: Bleich and ABAQUS vertical symmetric frequency table	76
Table 6-3: Torsional symmetric frequencies.....	78

ACKNOWLEDGMENTS

I wish to thank my thesis supervisor Professor Jasna Bogunovic Jakobsen for her help and guidance throughout this work. In addition, special thanks to Ove Mikkelsen for help in questions regarding ABAQUS. Thanks to Roger Gulsvik Ebeltoft and Per Slyngstad from The Norwegian Public Roads Administration for providing information about the bridge. Thanks to Erik Tveiten and Johan Tesdal for help in validating results when needed. Thanks to Birgitte Gran for comments and suggestions along the road.

And finally, thanks to my wife for supporting me through this study.

1 Introduction

Lysefjord Bridge is a suspension bridge with a total length of 637 m. The bridge consists of 3 spans, the main span is 446 m and the side spans are 34.5 m and 156.5 m. The bridge was opened on December 18th 1997. Since the opening, a number of fractures in the wires of the main cables have occurred, and the fracture rate is has not flattened out. A number of analyses have been carried out on the bridge since then, and surveillance equipment have been mounted to monitor the wire fractures in the cables. There is also a plan to monitor the wind velocity and the bridge girder response, as a collaboration project between the University of Stavanger and the Norwegian Public Roads Administration.

Aims of this thesis is to become familiar with the load carrying characteristics of a suspension bridge, in particular the non-linear and dynamic aspects of the structure. Vortex induced vibrations from wind loads will be studied, so will the eigenfrequencies and eigenmodes of the system. Steigen [1] has made an element model of the bridge in ABAQUS where the finite element analysis will be run. Also theoretical calculations will be done to verify the results.

In 2009 an acoustic monitoring system was mounted on the bridge. The system monitors the main and the backstay cables for fractures, and the company running the equipment issues reports on a quarterly basis reporting findings. These reports have data on the time and position of the fracture event.

There is also a local weather station at the mouth of Lysefjord at Forsand. Data will be taken from here and matched to the fracture records to see if correlations can be identified. Simple graphs and tables will be used to look for correlations.

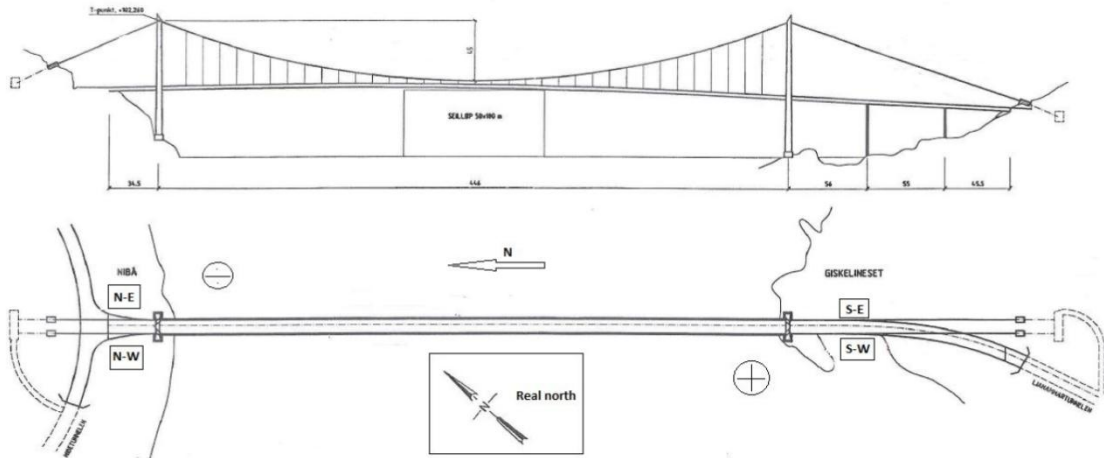


Figure 1-1: Plan and section of Lysefjord Bridge[1]

The thesis starts out by presenting the various structural elements of a suspension bridge in chapter 2. Some of the details from Lysefjord Bridge are presented to provide the basis for the element model.

Chapter 3 describes the wire fractures in the main cables of Lysefjord Bridge. The main cable system is described, together with previous analysis work of the fractures. The cable monitoring system is mentioned, together with registered findings by the monitoring system. Figures showing the fracture positions are also presented.

Chapter 4 discusses the finite element model in ABAQUS. Some parts will be detailed, like finding the shear center and mass moment of inertia of the bridge girder. Other parts will just be used as modeled in Steigen [1]. The loads on the model will be discussed, and in particular some detail about the way the FORTRAN subroutines are chosen to be run when needed.

Chapter 5 discusses the results of the analysis, and uses results to run additional analysis of the bridge. Accurate wind loads on the bridge girder is found by adjusting wind forces according to the rotation of the girder. Eigenfrequency analysis has been done on the three first symmetric and asymmetric eigenmodes for the horizontal, vertical and torsional directions. Vortex induced vibrations will be studied using simple sinusoidal load variation along the time axis.

Chapter 6 performs a theoretical validation of the eigenfrequencies and eigenmodes found in chapter 5. The theory for the validation have some assumptions that are slightly different from the ABAQUS model. These will be described. The eigenfrequencies found will be compared to both the Alvsat and ABAQUS values.

The software tools used in this thesis will be ABAQUS [14] for finite element analysis, Maple [15] and OpenAxiom [16] for symbolic math work, Matlab [17] and Octave [18] for general numerical analysis and FORTRAN and Python [19] for programming tasks.

2 Suspension bridges

The principle of carrying load by suspending a rope, chain or cable across an obstacle has been known since ancient times. The suspension bridge is one type of cable supported bridges. Suspension bridges are lighter per unit length than any other type of bridge form. Thus they dominate the genre of long span bridges in the world. The first known suspension bridge built in Norway was the Bakke Bridge in Vest Agder, see Figure 2-1. It was built in 1842, and it is still in operation today. Bakke Bridge is part of a spectacular piece of old road in Vest Agder/Rogaland called Tronåsen. This drive can be recommended.

There are a number of suspension bridges in Norway, about 200 at date. The longest suspension bridge in Norway will be the Hardanger Bridge, under construction at the time of writing. The main span will be 1310m with a total length of 1380 m.



Figure 2-1: Bakke bridge

The structural system of a cable supported bridge consists of [6]

- Towers supporting the cable system and transforming the loads to the foundation.
- Main cables supporting the stiffening girder
- Anchor bolts providing hold down support for horizontal and vertical forces
- Hanger cables connecting the stiffening girder to the main cable
- Stiffening girder with bridge deck

For descriptions of a wide array of suspension bridges, see [6].

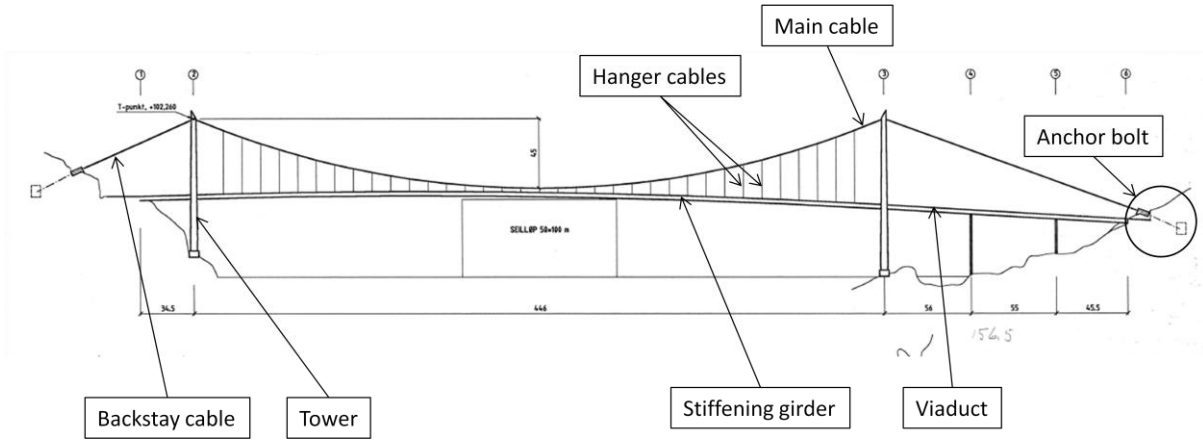


Figure 2-2: Main components of a suspension bridge [30]

2.1. Stiffening girder

The main function of the stiffening girder is to stiffen the bridge structure and to distribute the loads acting on the bridge. It distributes concentrated load on to the bridge deck, and nowadays has a significant contribution to the torsional stiffness of the system. This was not the case when the cross sections consisted of vertical and possibly horizontal trusses to carry vertical and horizontal loads in earlier days.

The most famous suspension bridge collapse is the Tacoma Narrows Bridge in Washington in the 1940's. A number of unfortunate factors contributed to the collapse, but the bridge slenderness, the aerodynamic shape of the girder cross section and the lack of torsion stiffness contributed to the collapse. No dynamic analysis of the bridge was carried out, only a static analysis. The bridge was built for a static wind force of 160 km/h, but collapsed at a much lower wind speed.

The bridge girder widely used today in Norway is quite narrow, similar to the one used at Tacoma Narrows. Other countries with larger traffic may have wider bridge girders. The aerodynamic shape has changed to avoid vortex induced vibration. And since the cross section is closed, the torsion stiffness is dramatically improved.

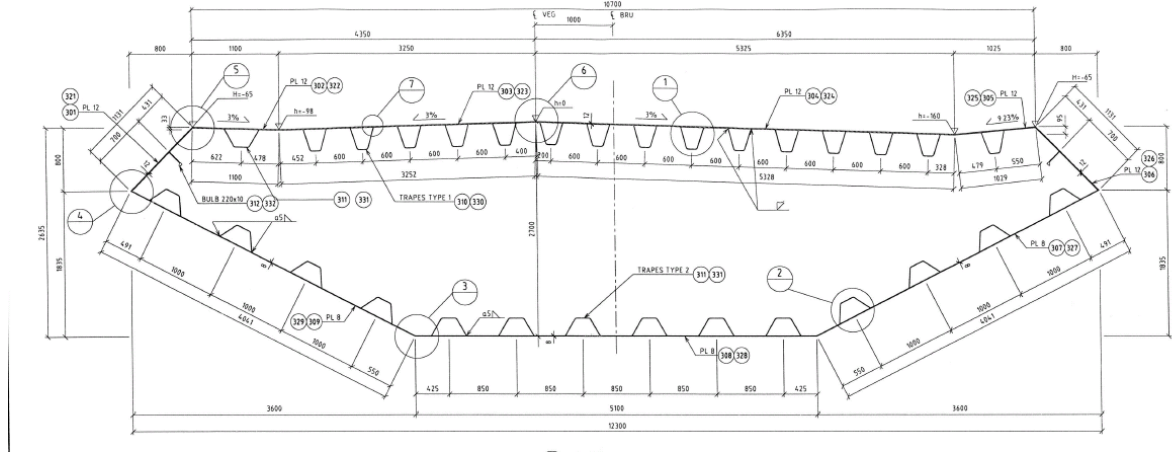


Figure 2-3: Cross section of bridge girder at Lysefjord Bridge [7]

2.2. Support of stiffening girder

The support of the stiffening girder holds the bridge fixed for displacement along all three axes and for torsion rotation by a pendulum on the north side. The south side is fixed for movement sideways (in the y axis), has a pendulum support in the x axis and fixed for torsion rotation. For the definition of the model axis, see Figure 4-1.

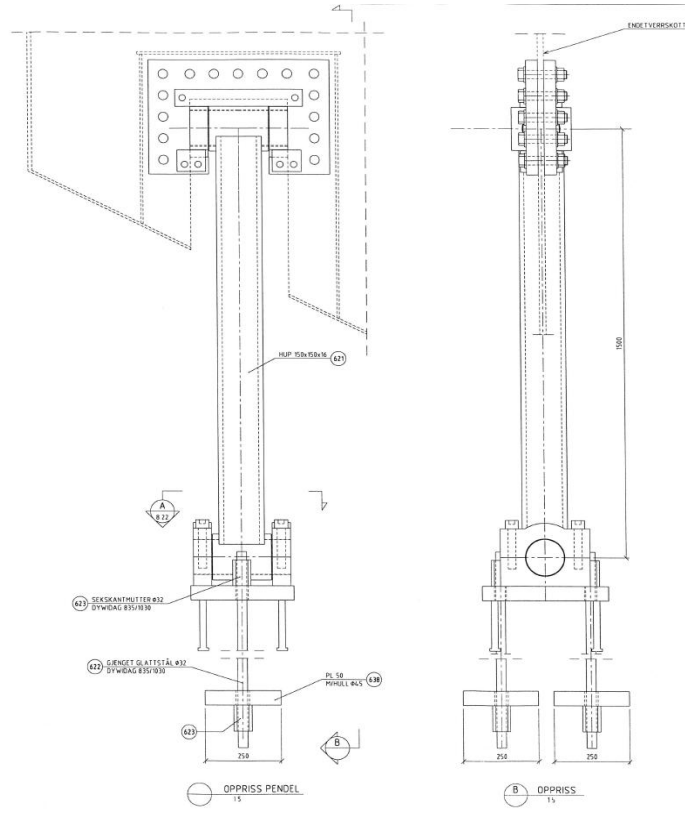


Figure 2-4: Pendulum support north side [30]

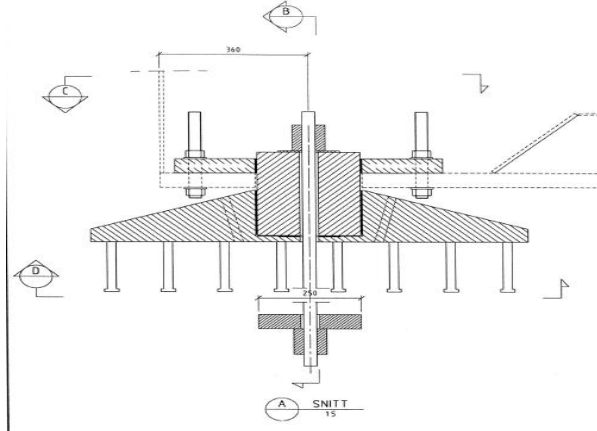


Figure 2-5: Fixed support north side [30]

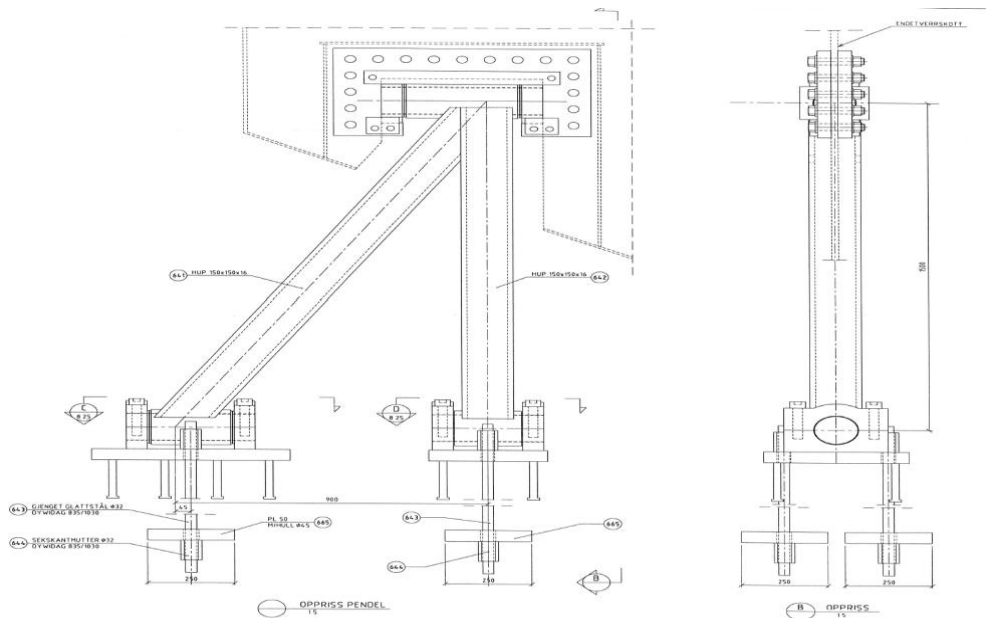


Figure 2-6: Pendulum support south side [30]

2.3. Main Cables

The main cables are the main structural elements when it comes to carrying the vertical loads of the suspension bridge. The vertical load is transmitted to the main cables by the hangers, and transported by tension up to the main towers. The main cables come in various strand configurations. The cables need to allow for vibrations and also need to handle considerable displacement coming from various loads, varying from hanger breaks to temperature loads.

The steel in the cables have higher carbon content than structural steel, 2-4 times higher. This provides 2-4 times more strength in the cable. The tradeoff is decreased ductility as the strain at breaking is only one fifth of that found in structural steel. Gimseng, chapter 2 [9] discusses the various strand and cable configurations in detail.

The cables in Lysefjord Bridge consist of a core of circular strands, and have an outer layer of z strands that are self locking to minimize the effect of a strand break.

2.4. Hanger cables

The hanger cables are the connecting elements from the bridge girder to the main cables. The spacing between the hangers depends on the characteristics of the bridge girder. The attachment detail of the hanger to the cables will vary, depending on the cable itself and the cable configuration of the bridge. The attachment detail for Lysefjord Bridge is shown in Figure 2-7

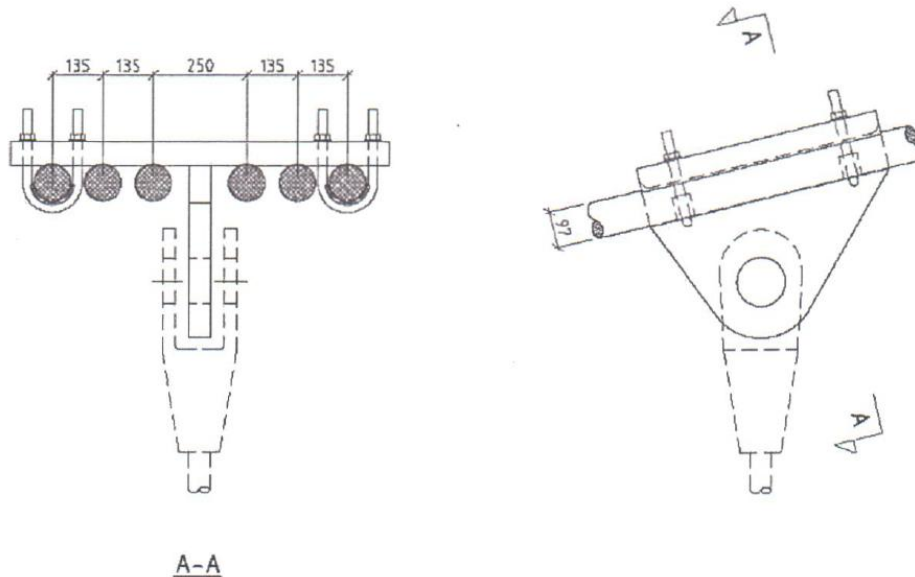


Figure 2-7: Detail of hanger attachment to main cables Lysefjord Bridge
[30]

2.5. Towers

A suspension bridge can have different tower configurations; the most common is two towers. Each tower typically consists of two columns, with two or more cross beams between the columns. The towers are subjected to compressional forces, given that ~half of the vertical load is transported to the top of the tower by the cables. The towers at Lysefjord Bridge are made out of reinforced concrete. Concrete is excellent for large compressional forces, but it also needs to withstand buckling and torsion forces.

The anchoring solution of the towers to the ground may vary. The Golden Gate Bridge towers stand on their own weight, and are not anchored at all. Lysefjord Bridge towers are bolted to the ground, making them displacement and rotationally fixed. The geometry of the Lysefjord Bridge north tower is shown in Figure 2-8.

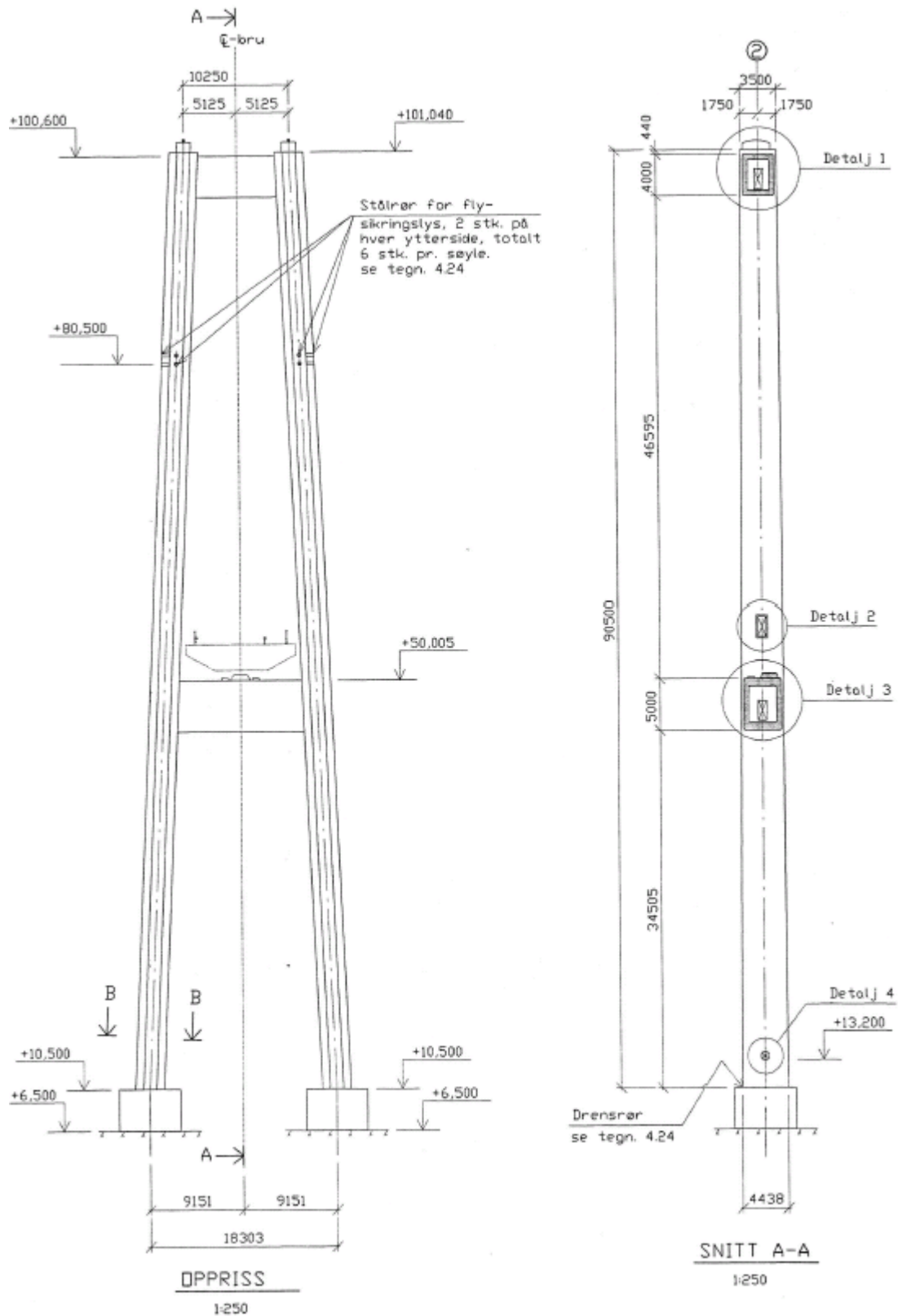


Figure 2-8: North tower Lysefjord Bridge [30]

2.6. Anchor piers

Anchor piers pull the side span cables to the ground and fix them to a given anchoring device. Typical Norwegian suspension bridges have anchoring devices that transfer the cable forces to the underlying rock. To be able to monitor the cable anchors, tunnels are built to provide access to cables and anchors.

3 Fracturing of main cables

The amount of fracturing in the main cables of Lysefjord Bridge is unique in Norway. Both the amounts of fractures are unusual, and also the trend that continue linearly throughout the years. This thesis the focus will be looking at the type of forces that apply to the bridge and their possible contribution to stress increase that may increase the risk of fracture in the cable.

For a more thorough introduction of the work already done on analyzing the cables and reasons for fractures, see [1], [3], [7] and [10]

3.1.The main cables

The main cable system of Lysefjord Bridge consist of 6 main cables at each side of the bridge girder, each cable 713 m long before dead load is applied. The main cable cross section consist of 279 wires, the outer layers consist of z wires. The z wires make them self locking in case of a wire fracture. It is assumed that the strand cross section is fully activated in a 3 meter region around the fracture.

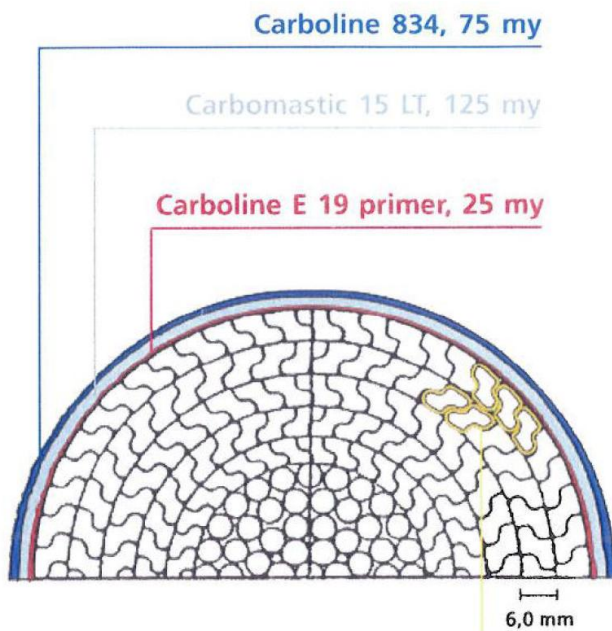


Figure 3-1: Main cable cross section Lysefjord Bridge [7]

The cables were spun on site. The cold rolling and forming of the wires provide the high yield strength of the cables. But in case of lower ductility than expected in the wire, the cold forming process may introduce cracks on the wire that may later become fractures.

Few and random wire fractures in the main cables of suspension bridges are not unusual. The unusual part is the amount of fractures in the cables in Lysefjord Bridge, together with the linear continuing trend of breakage per year. This behavior has not been seen at other suspension bridges in Norway.

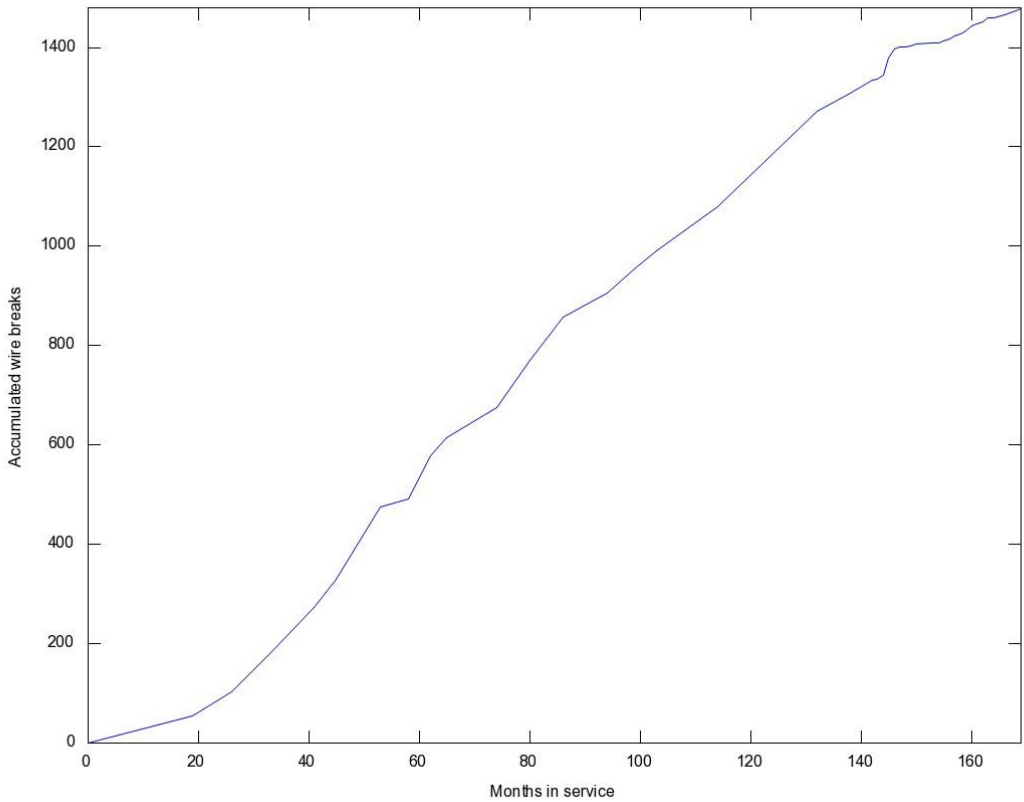


Figure 3-2: Cumulative wire breaks since bridge opening

Other bridges with wire fractures in Norway are Kjellingstraumen Bridge and Nærøysund Bridge. The Nærøysund Bridge wire fracture observations are comparable with the quality of the observations done at Lysefjord Bridge. At Nærøysund Bridge an accelerating fracture rate was found at the first two years of service, steeper than the curve at Lysefjord Bridge. Then followed a significant flattening of the curve, similar to the linear trend seen at Lysefjord Bridge.

3.2. Possible causes for wire fractures

As mentioned before, the rate of wire fractures in the main cables is worrying. The reasons for these fractures are probably a combination of several factors. Tests and reports from Blom Bakke[10], DNV[25] and Sintef[24] comment on findings of the material properties of the main cables. The reasons for the wire fractures relate to imperfections on the surface of the z wires. These initiate cracks and reduce the cross section area of the wire.

The rolling process when manufacturing the wires could cause small defects in the surface of the wires. These have been found in the main cables when cracks are observed at the edge of the z wire, see Figure 3-3.

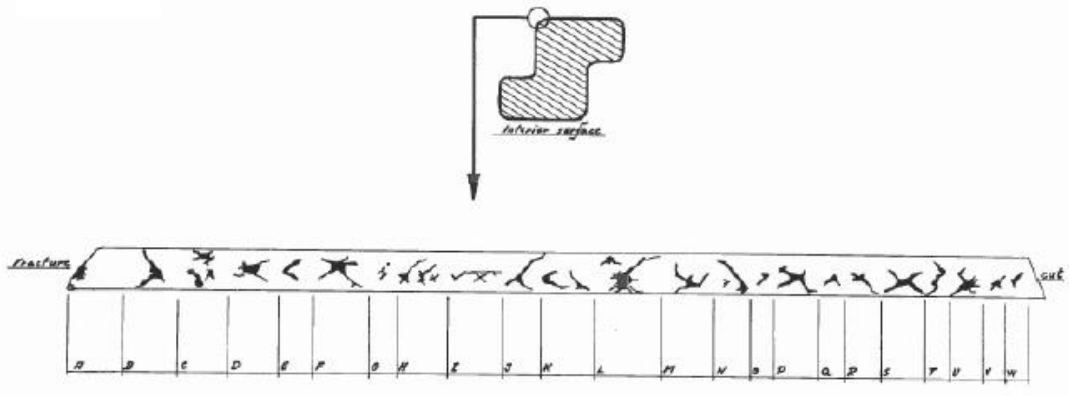


Figure 3-3: Surface defects on examined z wire from Lysefjord Bridge[27]

At the location of the defect, the cross section area is reduced by one forth and the wire has suffered a tensile overload. The initial crack is suspected to be caused by fatigue. But the true mode of cracking cannot be established when the crack surface is mechanically deformed[26].

Fractures of brittle behavior may initiate in connection with defects of a certain size when the wire is exposed to bending stresses. This may mean that either induced bending stresses or large axial stresses, or both, cause the wires to fracture.

Another possible contributor is hydrogen embrittlement. The cleaning process with an acid solution prior to galvanizing the wires may have let hydrogen diffuse into the steel, causing cracks of brittle nature [24]. It is not likely that hydrogen caused by corrosion has contributed to the fractures [25].

It is clear that the defects found in the surface of the z wires are reducing the capacity of the cable. If there are structural details that may cause stress concentration or load cases that can give localized stress concentrations, these should be looked into.

3.3. SoundPrint® acoustic monitoring system

To monitor the fracturing of the main cables, an acoustic monitoring system is mounted on Lysefjord Bridge. The system is delivered by Advitam in October 2009, and the system is monitored remotely from France. This system is a complement to the visual monitoring scheme already in place by the Norwegian Public Roads Administration. Arrays of sensors have been mounted to monitor the cables, with a slightly different sensor configuration regime on the backstays and the main span. On the backstays, each cable has sensors on each cable, see Figure 3-5. Thus fractures can be identified to both the cable number and position along the cable. In the main span, the sensor is attached to the hanger clamp, see Figure 3-4. Thus the cable number where the fracture occurred cannot be detected by the system, only the position along the cable.

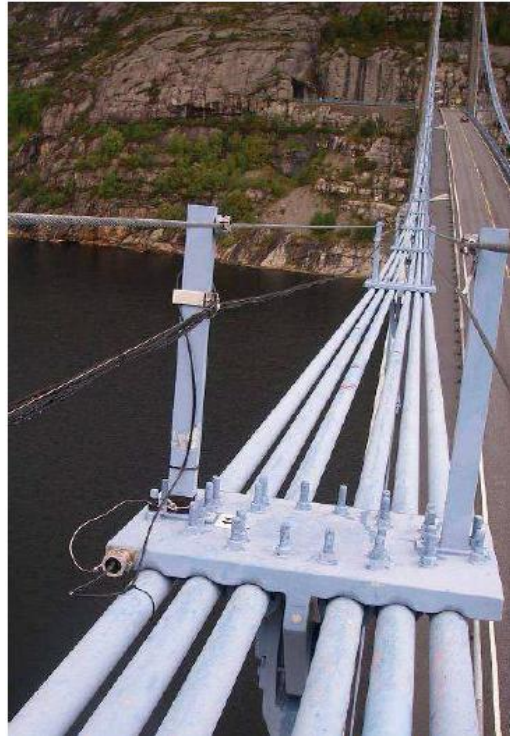


Figure 3-4: Acoustic sensor on main span



Figure 3-5: Acoustic sensor on backstay cable

The wire fractures can be roughly divided into two groups:

- Fractures more or less randomly distributed along the cable
- Stress induced fractures, localized at areas in the structure where stress concentrations can be expected.

At Lysefjord Bridge, most fractures belong to the first group, given the distribution of the fractures along the cable. As the next figures show, the wire breaks measured by Advitam has more breaks

on the south side of the bridge than on the north side. At present, no identification of wire breaks inside the cross section can be done. Only the breaks that have ruptured the outer coating can visually be detected by manual inspection [7]. The fractures are not localized at structural details that pinpoint suspectable load situations.

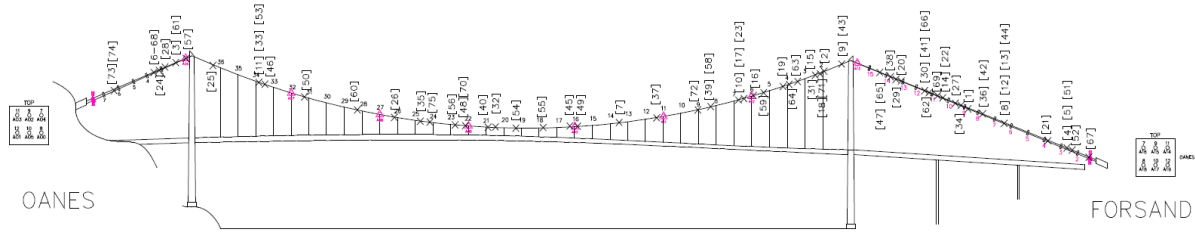


Figure 3-6: Wire breaks east cable [3]

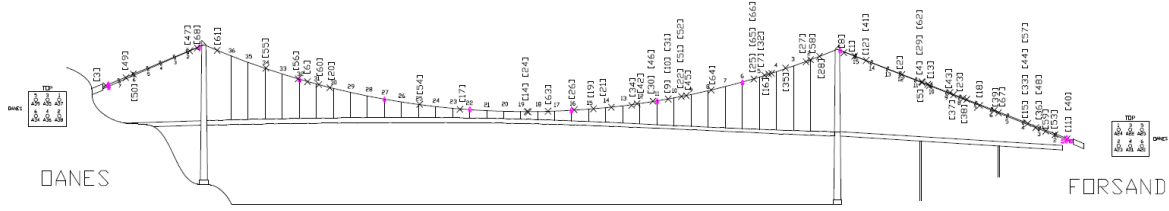


Figure 3-7: Wire breaks west cable [3]

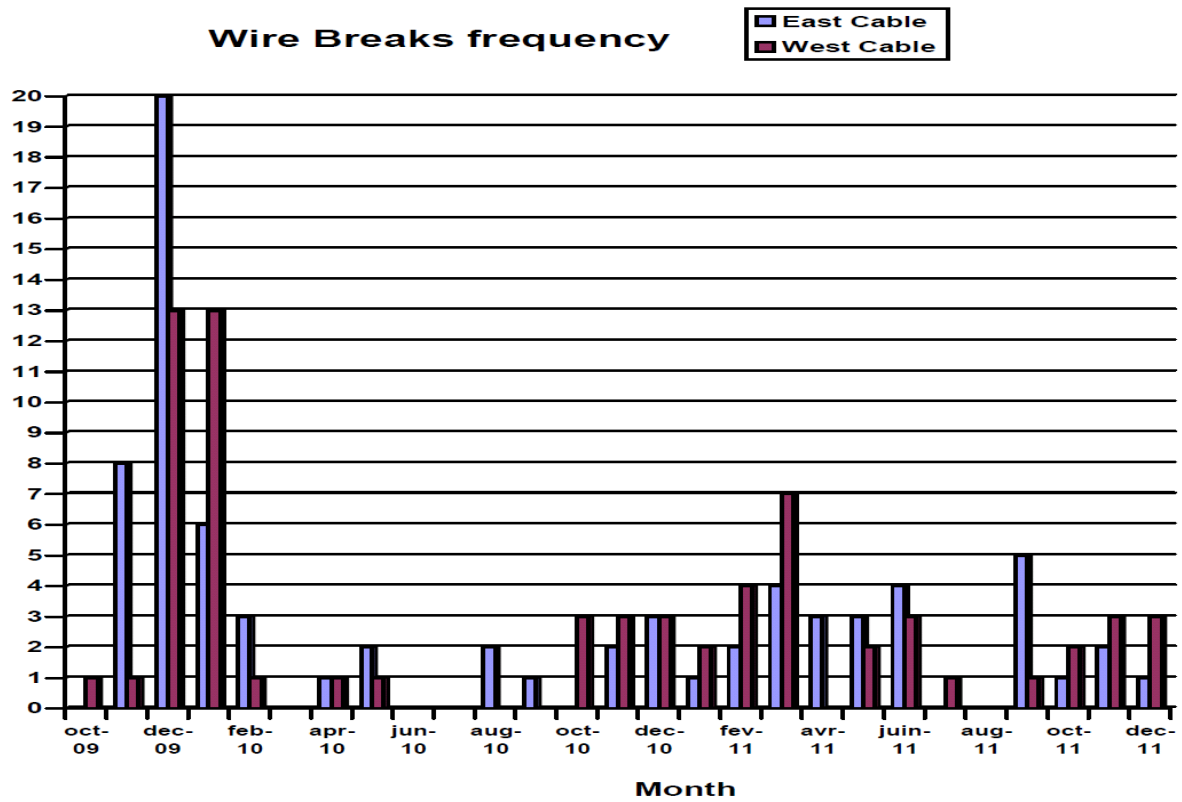


Figure 3-8: Wire breaks by month [3]

3.4. Weather around Lysefjord Bridge

To be able to correlate the wire fractures to the weather in the area of the bridge, data from a weather station at Forsand has been collected and used. The data itself has been fetched from the website www.wunderground.com, and the weather station number is <http://www.wunderground.com/weatherstation/WXDailyHistory.asp?ID=IROGALAN18>. A small Python script was written to extract the data from the website from January 2007 to December 2011. Similarly the fractures from the cables has been extracted from the Advitam reports and stored so they can be processed. The Advitam data spans from November 2009 to December 2011. Python was used for that purpose for two reasons, first it's a quite easy language to learn, and second it is the language that provides access to the ABAQUS infrastructure.

3.4.1. Wind and temperature data

The weather data is sampled every 10 minutes according to the website <http://www.lysefjordweather.com>, from which the data is provided. The wind data itself seems to be missing data at some velocities and there is also quite an amount of days without wind at this particular station. At first sight this seems unusual, and may be some topological effect at the placement of the weather station, see Figure 3-9.

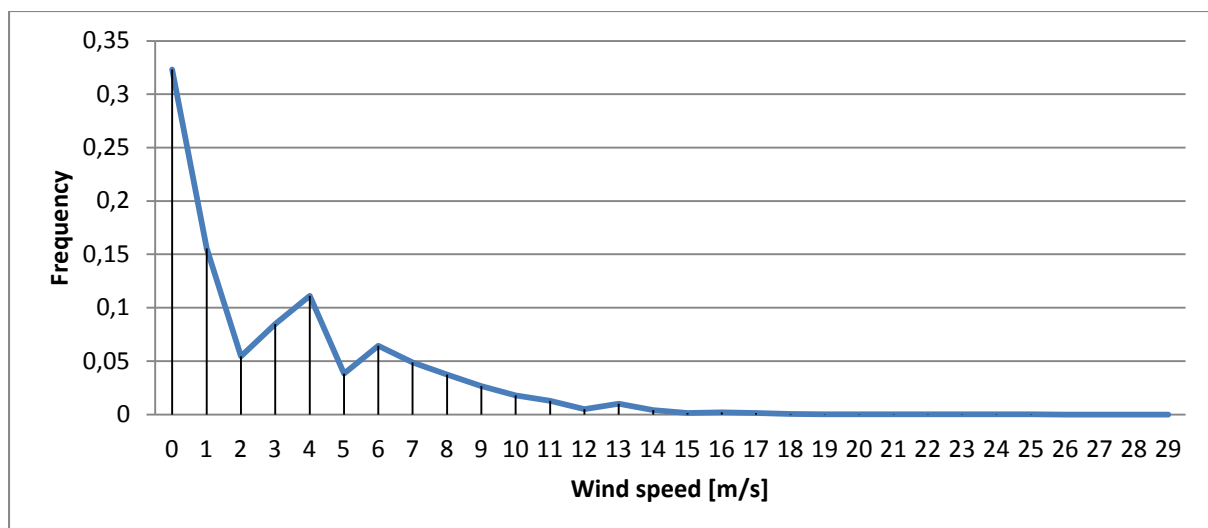


Figure 3-9: Wind velocity distribution at Forsand weather station from January 1st 2009 to December 31st 2011

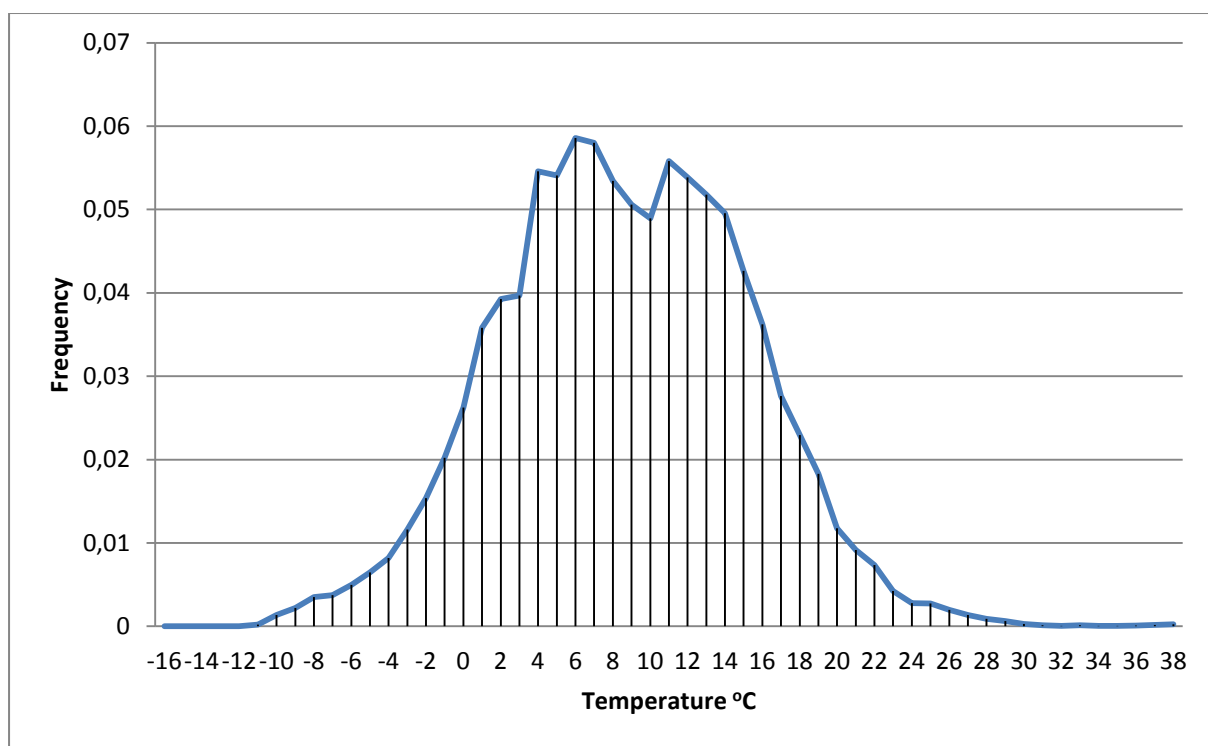


Figure 3-10: Temperature distribution at the Forsand weather station from January 1st 2009 to December 31st 2011

Table 3-1: Statistics for wind and temperature graphs

	Mean	Standard deviation
Wind Figure 3-9	3.14 [m/s]	3.40
Temperature Figure 3-10	8.63 [°C]	6.57

The wind data in Figure 3-9 resembles a Weibull distribution. Fitting the data to a Weibull distribution in Matlab, <http://www.mathworks.se/help/toolbox/stats/wblfit.html>, finds shape parameter $b = 0.3826$ and scale parameter $a = 0.0127$. The temperature data in Figure 3-10 resembles a Gauss distribution. The number of samples $N=99052$

3.4.2. Cable break data

The available Advitam data has been paired up with the weather data and shown in the next graphs with respect to temperature, wind speed and week days. Unfortunately the weather station does not have data for 19 of the fracture incidents in January 2010, so they are left out of the graph. But based on correlation with the temperature data at the Sola weather station, it is reasonably certain that the weather was below 0°C in this period. The total number of breaks in the period Advitam has measured are 143, thus the number of breaks in the graphs below are $N=124$.

Table 3-2: Statistical values for cable break data

	Mean	Standard deviation
Wind Figure 3-12	3.88 [m/s]	3.622
Temperature Figure 3-11	5.61 [°C]	6.56

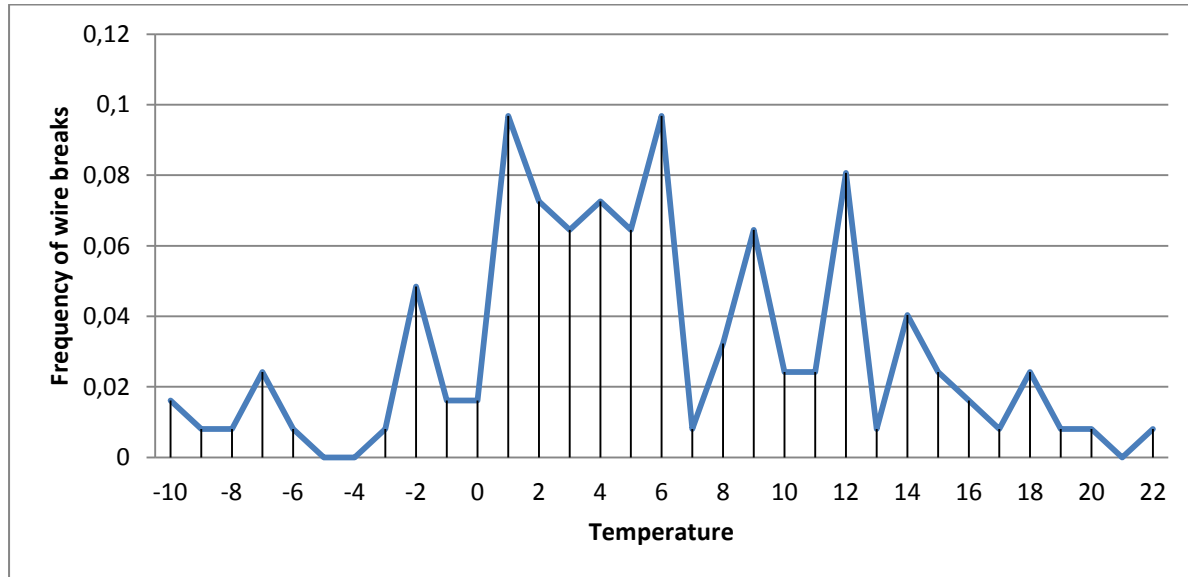


Figure 3-11: Cable breaks as function of temperature

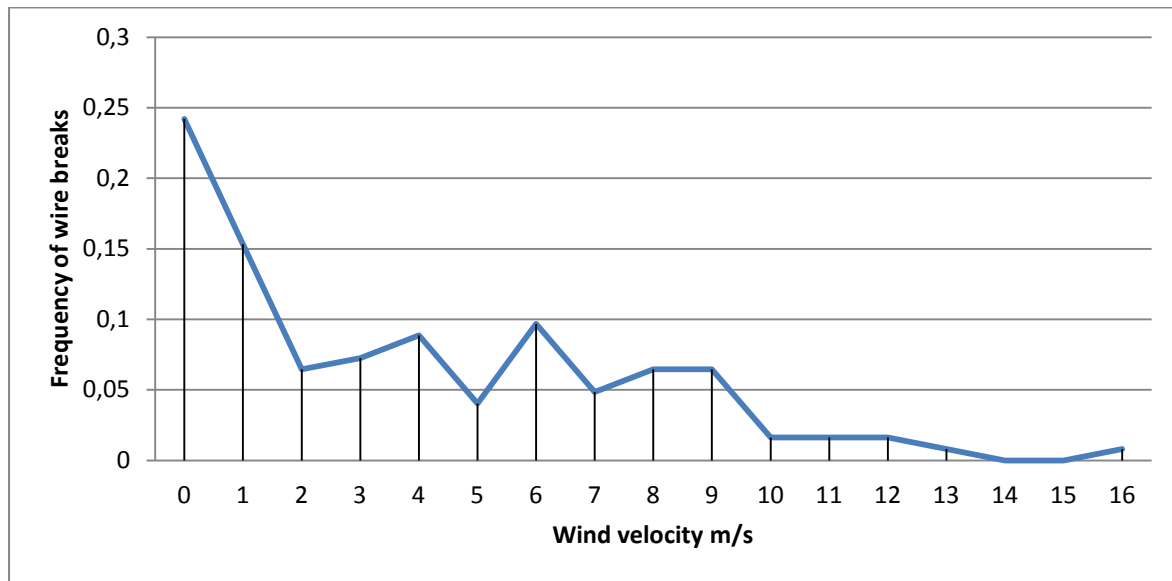


Figure 3-12: Cable breaks as function of wind velocity

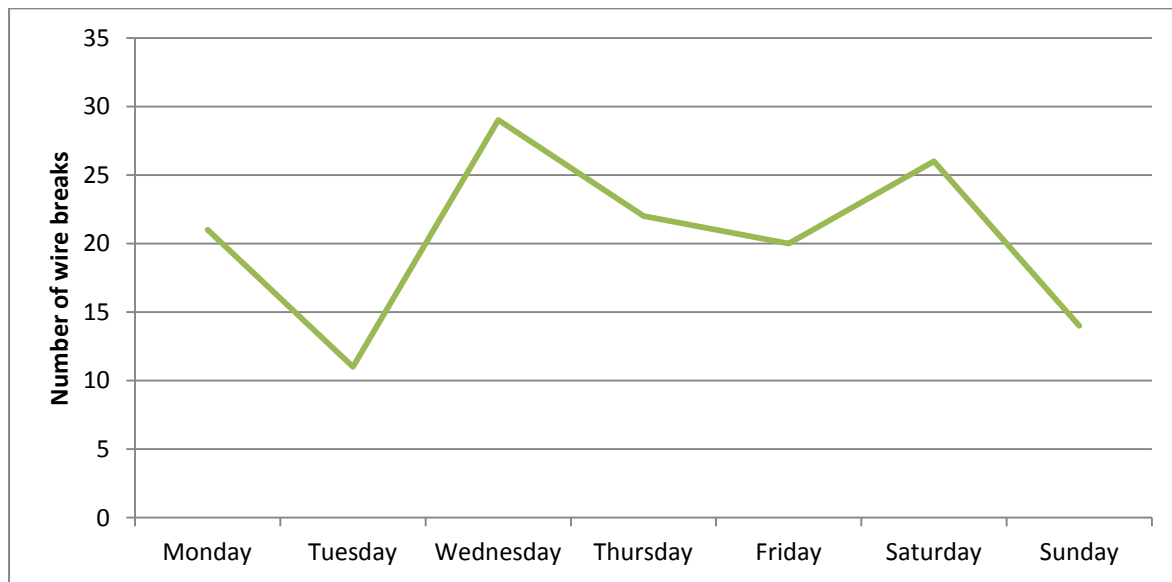


Figure 3-13: Wire breaks as function of day

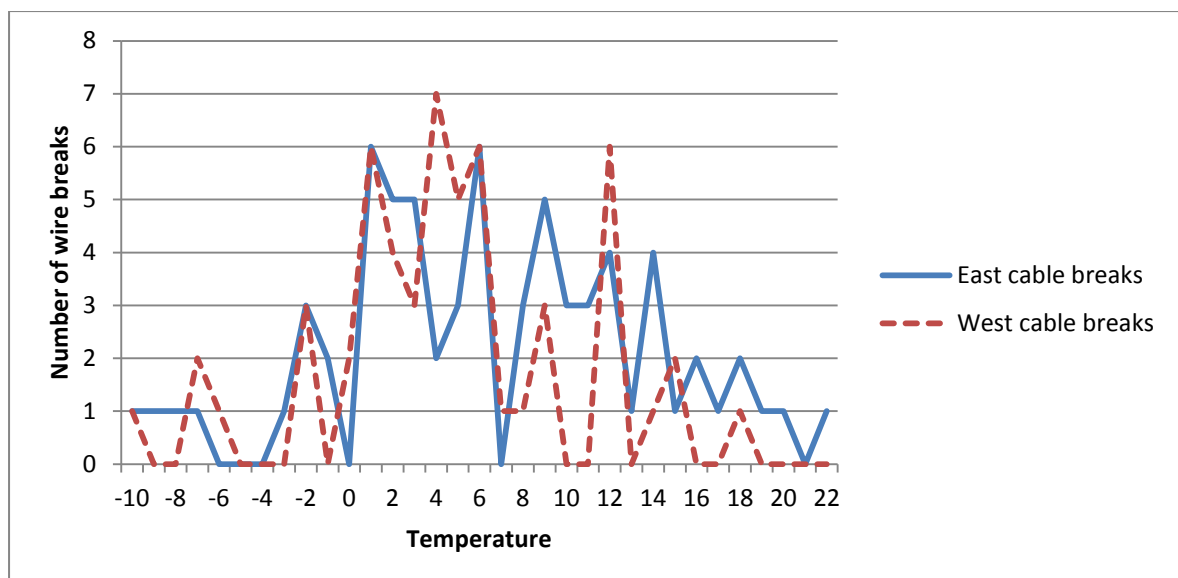


Figure 3-14: Wire breaks as function of temperature east/west side

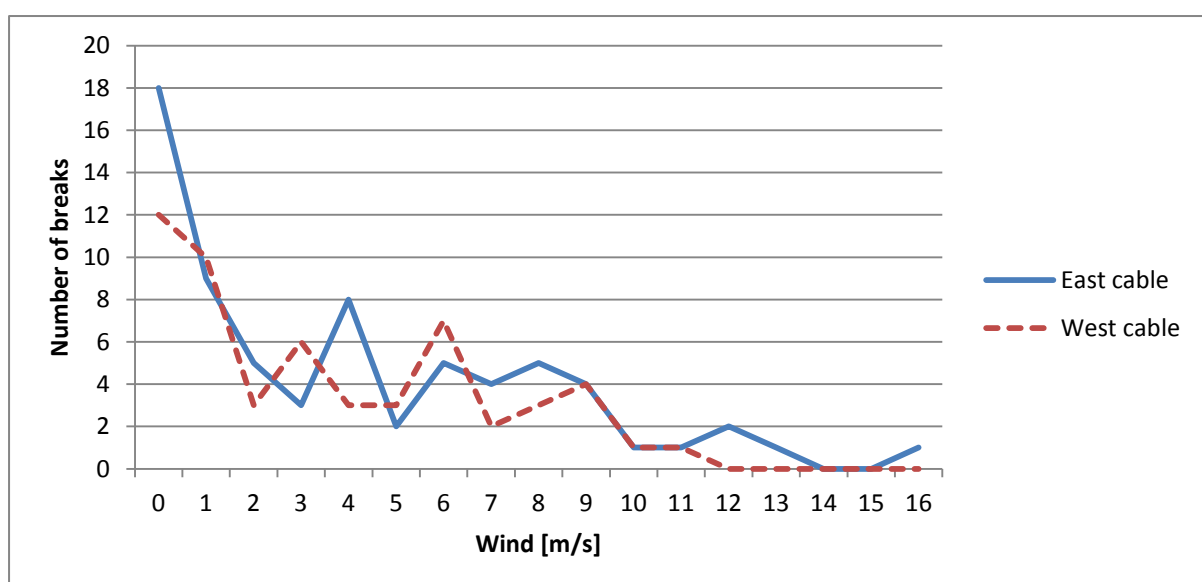


Figure 3-15: Wire breaks as function of wind east/west side

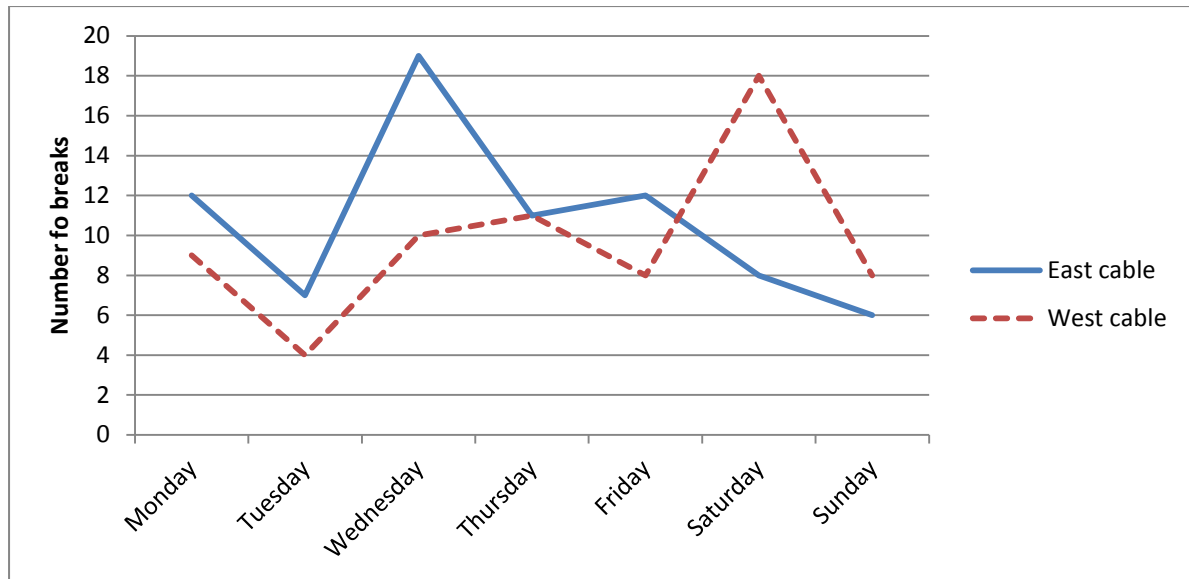


Figure 3-16: Wire breaks as function of weekday east/west side

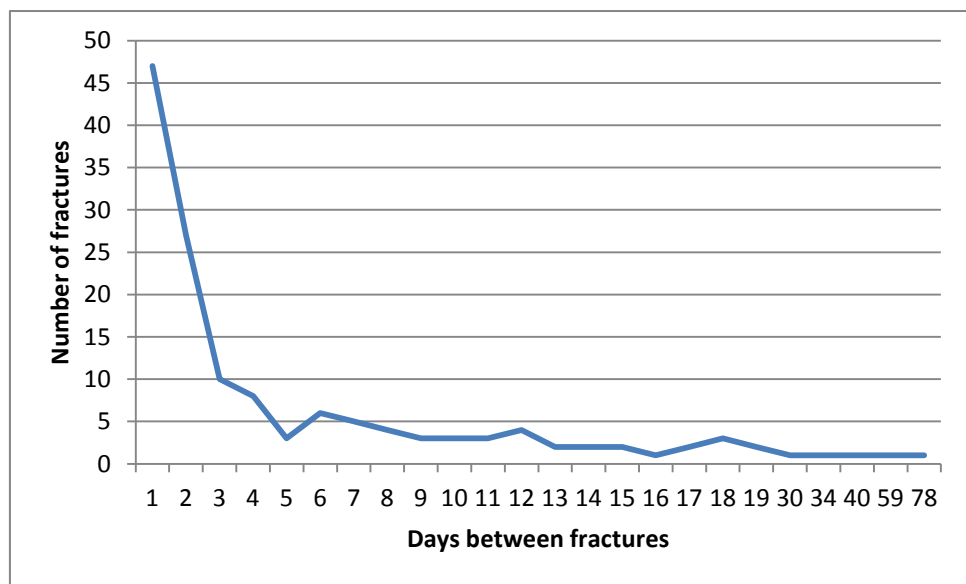


Figure 3-17: Time between wire fractures

From these graphs, a couple of observations can be made. Figure 3-11 shows that cable breaks have a correlation with temperature. The number of breaks below mean temperature is higher than above. Temperature may play a role because steel becomes more brittle when it gets colder. The mean values from the temperature curve in Table 3-1 and the temperature curve in Table 3-2 are different. The Students t test shows a correlation between the two curves.

The equations for the Students t-test can be found at http://en.wikipedia.org/wiki/Student's_t-test#Unequal_sample_sizes.2C_unequal_variance. The results based on the data found is $t=5.119$

and $df=123.31$ giving $p=2.5e-6$, which is much lower than a limit for p of 0.05. Thus the two curve means are dependent.

Figure 3-13 show that the days with the fewest breaks are on Tuesday and Sunday. It is an open question if this trend can be seen in the traffic pattern. Doing a contingency test, http://en.wikipedia.org/wiki/Contingency_table, on the data based on weekday and break/no break shows no correlation between cable break and weekday. If there was a correlation, more investigation into lorry loads might be appropriate.

The wind does not seem to have much correlation with the fractures. Almost 50% of the fractures happen at wind velocities less than 3 m/s. The reason to check wind was to see if the majority of the breaks happened at higher wind velocities, in particular around the Vortex Induced Vibration velocities. That does not seem to be the case.

If a fracture appears, often another fracture occurs within a day or two. Actually 59% of the breaks have less than three days between them. This may indicate a cable overload that happens due to the first break.

4 Finite element model

The finite element analysis program used to analyze Lysefjord Bridge is ABAQUS. ABAQUS is a very flexible system that can be used for analyzing a number of problems. The features wanted for this work is the non-linear and dynamic analysis capabilities of the program. Non linear theory is very important to use when running analysis of flexible and slender structures like a suspension bridge. As a consequence, the basic loads cannot be superimposed. Every load combination has to be run with correct load factors to get accurate results. In the following, it is assumed that all analysis will be taking non linear effects into account.

The results of these simulations will be matched with a model previously made and run in Alvsat by the NRPD. The Alvsat model seems to have some different conditions than the ABAQUS model, most noticeably that symmetry is assumed around the center of the bridge main span. Also pylon stiffness does not seem to be taken into account.

There are a number of possible analysis tools to choose from, depending on the type of analysis needed. Since this thesis will mostly look at the main span girder and cables for static and dynamic effects, ABAQUS will do the job. Some user knowledge of ABAQUS is available at the institute. If, on the other hand, analysis of traffic loads and load combinations according to Håndbok 185 [23] should be carried out, ABAQUS would not have been the natural choice. Other household software packages like NovaFrame or Brigade would be more appropriate for that task.

An ABQUS model exists for Lysefjord Bridge, made by Steigen [1]. This model will be used as the starting point for this analysis. The ABAQUS model will be used to evaluate aspects of wind, traffic and temperature loads, as well as eigenfrequencies of the bridge. The explanation of the commands used in ABAQUS can be found in various user manuals and help functions found in ABAQUS CAE. The interactive user interface is sometimes used to figure out how ABAQUS expects the command structure of the input file. This model cannot be run from the user interface of ABAQUS, because a couple of keywords used are not supported in the interactive mode.

4.1.ABAQUS software

ABAQUS is a general purpose finite element program. It has several element types, ranging from Euler-Bernoulli beams to shells. It can model contacts and other non-linear problems. Material can have linear or non linear behavior. Structure/fluid contact can also be modeled. It is also able to model incremental assembly of the structure to cover construction phases as well. Several options are available for dynamic analysis, both in the frequency domain and the time domain. Another aspect of ABAQUS is that it is not unit aware, so all dimension analysis must be done outside the software program. All program input must be in consistent units.

The models requiring FORTRAN subroutines will be run on Linux machines. FORTRAN subroutines will be needed for varying line loads and to account for wind load-deformation interactions. On a Windows platform the setup is more cumbersome, since it requires a mix of the windows runtime libraries and Intel Fortran compilers. Analysis not needing a FORTRAN subroutine will be run on Windows. An ABAQUS student version has been granted from Dassault Systems for this thesis work. This version has a limit of 1000 elements, which is sufficient for running this model.

4.2. ABAQUS model

The bridge model is built with 3-D beam elements of various types. Since this thesis is mostly looking at non linear and dynamic aspects of the bridge, reasonably simple element types have been used. To be able to run steady state dynamic analysis, FRAME3D elements cannot be used. The tower elements consist of FRAME3D elements. A linear elastic material model will be used for all elements. A non linear material model would be beneficial given the level of residual stresses in the cables were known. The model description will be assembled into a number of subfiles that will be included to make up a job to run. This reduces the redundancy in each job, and makes it easier to manage the number of files used to assemble the system with the accompanying loads.

4.2.1. Definition of directions

The enumeration regime of the model nodes and elements run in series, starting at low numbers in the north end of the bridge and increase towards south.

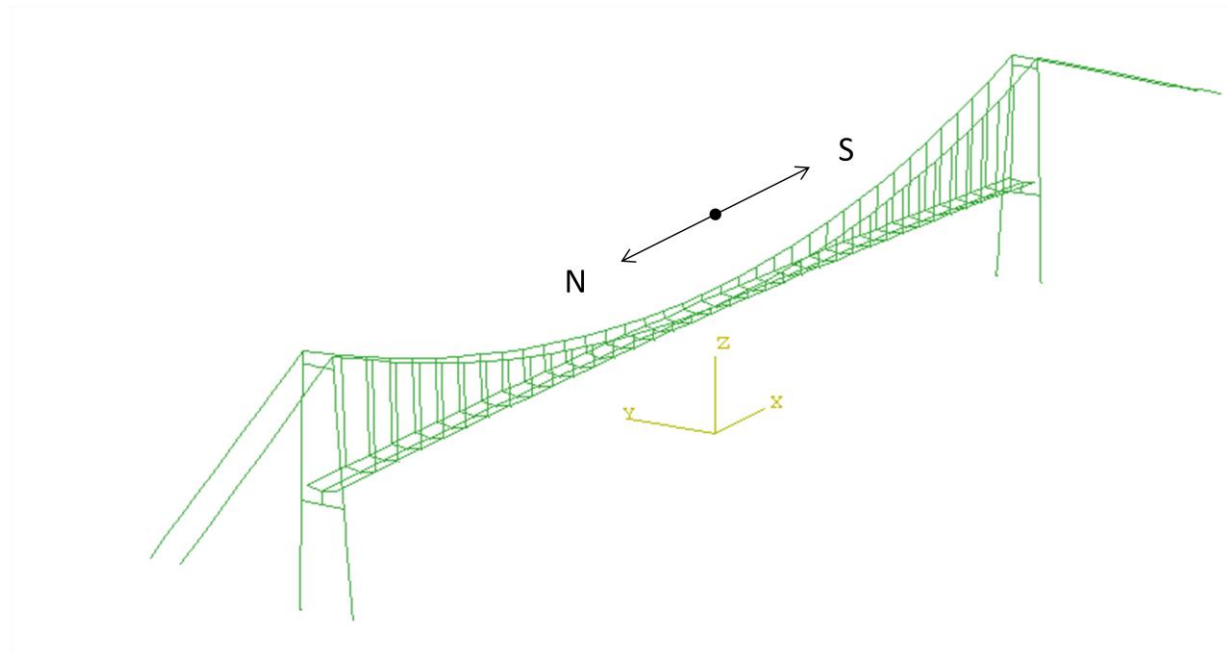


Figure 4-1: Element model of Lysefjord Bridge

The coordinate system used to model the bridge is a right-handed Cartesian coordinate system. The origin of the model is in the center of the bridge span, with positive x axis pointing due south (towards Forsand). Positive the z axis points upward, thus positive y axis points towards Lysebotn.

4.2.2. Elements

The bridge girder itself is modeled with 36 elements. An element typically spans from one hanger to the next, in general 12m. Since we are looking at the global behavior of the system, this granularity is considered good enough. For the beam element B31 with one integration point this will give a “real” value in the middle of the element. That is not enough if we were to look into the girder or cable forces in detail. A FRAME3D element would be appropriate for this task. Beam

element B31 has 2 integration points, which gives the ability to model at least parabolic line loads on the element. Parabolic line loads are sufficient for this study.

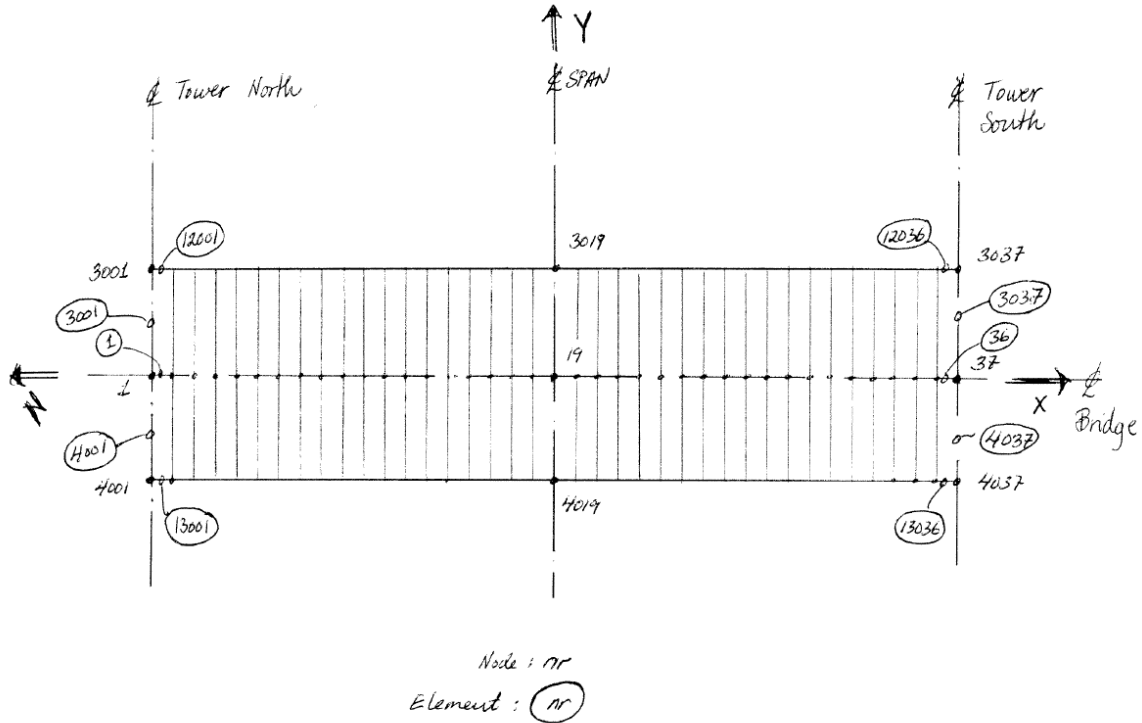


Figure 4-2: Element and node numbering scheme man span

The elements of the main span are shown, see Figure 4-2. The notation $\{a,b\}$ describes a set of nodes starting from and including a running up to and including b with increments of 1. The notation $[a,b]$ describes a set of elements starting from and including a running up to and including b with increments of 1. The east cable lines will follow node line set $\{3001, 3037\}$ in the X-Y plane and will be called element set $[1001, 1037]$. The cable element node set will be numbered $\{1001, 1037\}$. The west cable line will follow node line set $\{4001, 4037\}$ in the X-Y plane and will be called element set $[2001, 2037]$.

The bridge main cables are also modeled with 36 elements on each side, element length from hanger to hanger, and the backstay cables are modeled with the approximate same element length as the main cables. The hangers are modeled as one element from the cable down to the girder. For the cables, hangers and backstays, beam element B31 is used. Since the force of interest is the tension of the cable, this discretisation is considered appropriate. There is no simple way to describe cables, i.e. tension only elements, in ABAQUS that I've found. Given that the moment of inertia of the cables is set to 1 % of the cable cross section, these elements can be sensitive to buckling. The loading sequence is important to avoid negative values in the system matrix, a trap stepped into more than once.

Dummy elements are used to connect the bridge girder, hangers and cables together. Also dummy elements on the east and west sides of the bridge are used as aids to model the appropriate wind forces on the bridge. These elements typically follow the main element length, but the cross section

values are set to fictitiously high or low values, depending on the purpose of the dummy element. Figure 4-3 shows the lengths of the girder cross section, as well as the node points for the hanger and the mass node under the nodes for the centerline girder. The positioning of the main cable lines are also shown.

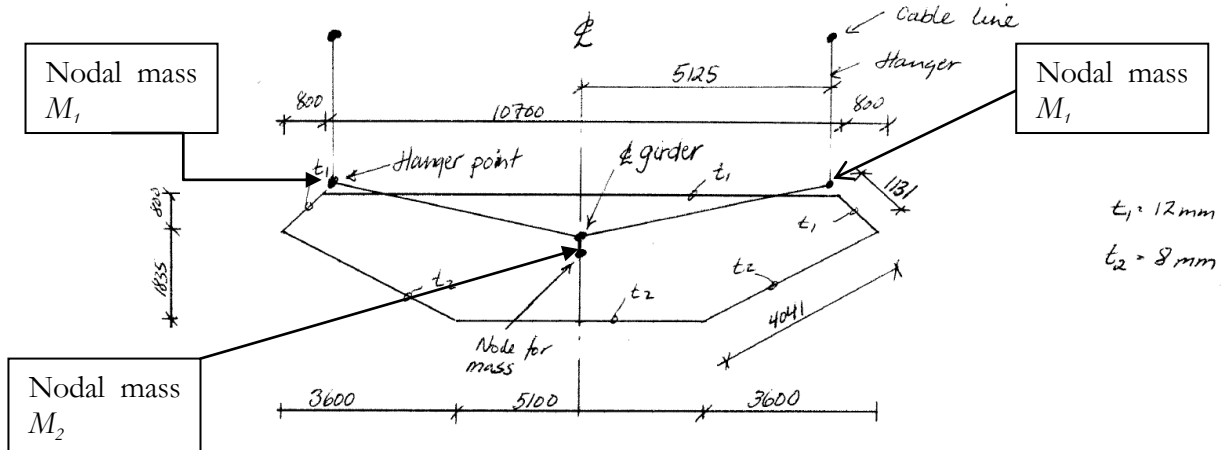


Figure 4-3: Cross section of bridge girder with cable, hanger, dummy elements and mass node points

The towers are modeled with FRAME3D elements of various lengths. ABAQUS has the option to model tapered cross sections along an element, but this option is not used. The towers contribution to the global stiffness is a point of interest; it is assumed that the choice of cross section data will have little impact on this stiffness contribution. The E modulus is not corrected for a concrete cross section in stadium 2, even though the loads and force we are looking at are normal service loads without load factors on them. This is considered correct enough, but no sensitivity analysis has been carried out to verify this assumption.

The 2 top elements of the towers that connect the cables to the towers are of type B33. Some attention to cross section axis alignment had to be made to avoid warnings from ABAQUS regarding the alignment of cross section axis from connecting elements.

The north and south viaducts of the bridge are not part of the model. The loads from the viaducts on the towers are not taken into consideration. It is assumed they have little secondary effect on the tower stiffness.

4.2.3. Boundary conditions

The following boundary conditions are used:

- Backstay cables at ground:
 - Displacement: all axis fixed
 - Rotation: all axis free
- Towers at ground:
 - Displacement: all axis fixed
 - Rotation: all axis fixed

- Girder element connected to tower cross beam:
 - North side:
 - Displacement: all axis fixed
 - Rotation:
 - X axis: fixed
 - Y,Z axis: free
 - South side:
 - Displacement:
 - X axis: modeled as a truss element connecting girder and cross beam
 - Y axis: fixed
 - Z axis: same as x axis
 - Rotation:
 - X axis: fixed
 - Y,Z axis: free

4.2.4. Model geometry

The geometry of the main bridge components are:

- Main span: 446 m
- Sag of main cables: 45 m
- Distance between main cables: 10.25 m
- Length of backstay cables north: 73.91 m
- Length of backstay cables south: 166.05 m
- Cable angle of backstay north: 33.5 degrees
- Cable angle of backstay south: 18.7 degrees
- Elevation of the top tower: 102.26 m
- Elevation of centerline road at mid span: 54.472 m
- Width of girder: 12.3 m
- Height of girder: 2.76 m

The vertical shape of the final bridge girder line is a circle, producing a curve as shown in Figure 4-4.

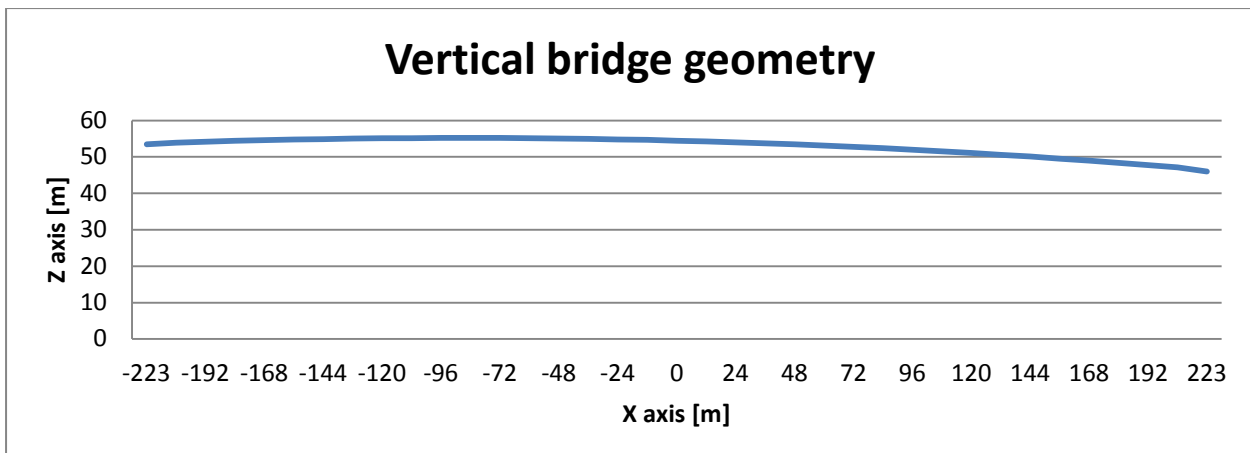


Figure 4-4: Vertical bridge geometry

The general equation for the circle is:

$$x^2 + y^2 + Dx + Ey + F = 0 \quad (4.1)$$

Solving the equation for our three points $(-223, 53.465)$, $(0, 54.472)$, $(223, 46.001)$ gives $D=175.584$, $E=10392.3$ and $F=-569056$

Similarly for the main cables, the top point of the cable and the maximum sag are given. That produces a parabola as shown in Figure 4-5

$$Y = ax^2 + b \quad (4.2)$$

$$b = 102.26 - 45 = 57.26, a = 9.049 * 10^{-4}$$

$$\text{Cable length } L = 2 \int_0^{l/2} \sqrt{1 + Y'^2} dx, l=446$$

This gives $L=470.2$ m. Doing the summation of the elements in Excel give $L=457.8$ m. The element model is according to the Excel calculations, modeled as straight lines between the nodes and not as parabolic elements. The deformed model of the cable may be more in line with the integrated parabola, but that has not been looked into.

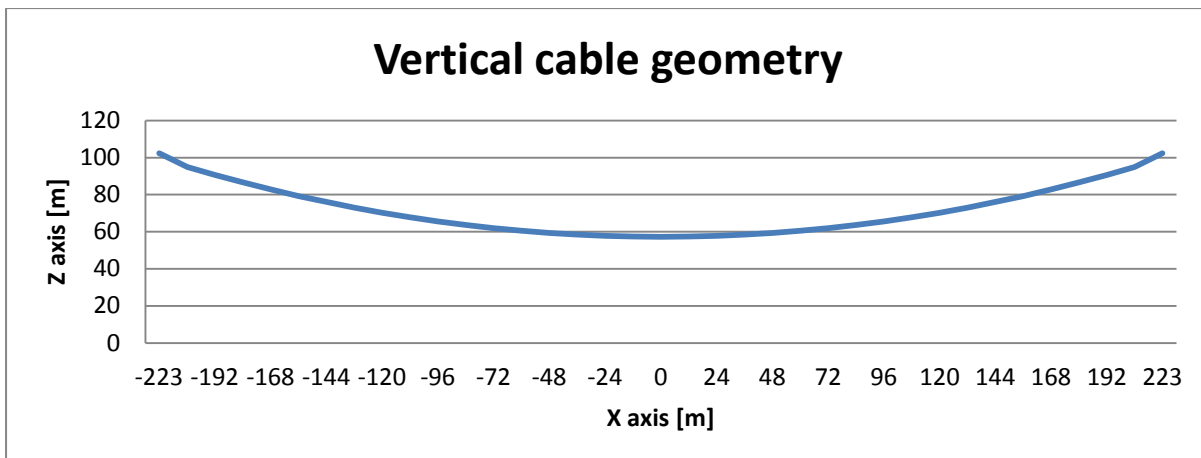


Figure 4-5: Vertical cable geometry

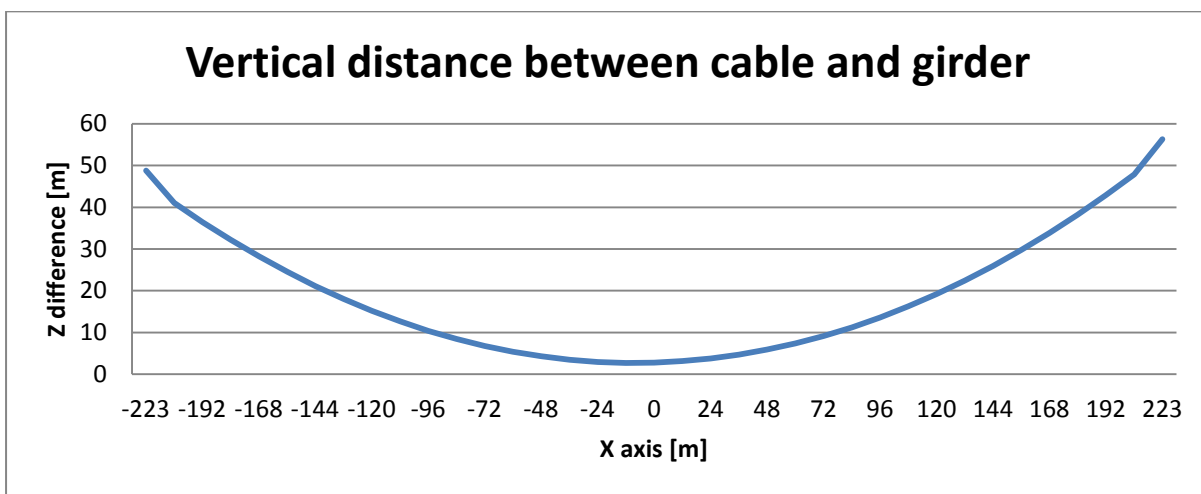


Figure 4-6: Vertical distance between cable and girder

As Figure 4-6 shows, the difference in hanger lengths will provide slightly more flexible support for the south side of the girder. That should show up in the eigenmode and deflection plots of the girder and the cables.

The towers have a tapered height of the side parallel to the X direction. The north tower has a width reducing from 4.438m at the base ($z=10.5m$) to 3.5m at the top, over a length of 90.5m. The south tower goes from a width of 4.5m at the base ($z=4.5m$) to 3.5m at the top, over a length of 96.54m. The towers will be modeled with 29 elements along the vertical axis for each leg; crossbeams will have 6 elements each.

4.2.5. Stiffness properties of the system

Cross section data has been calculated to check the numbers in the model against data used by Alvsat. In general the neutral axis, shear center and mass moment of inertia will be found. The values of the shear center, neutral axis and the mass center has been found, see APPENDIX C: Calculation of shear center for the calculations. The other options would be to make a cross section in ABAQUS and calculate the numbers from that input. An article from Sapountzakis [9] describes how to find the shear center based on the Boundary Element Method. The shear center is calculated by hand according to Boresi [8]. The mass moment of inertia is calculated about the shear center, and the mass of the cables are part of the calculation. Since Steigen[1] arrived at higher differences on the torsion eigenfrequencies between the ABAQUS and Alvsat results than for the other modes, a bit more attention has gone into understanding the mass distribution in the cross section.

4.2.5.1. Neutral axis

The neutral axis has been calculated in APPENDIX B. The following has been found

		Steigen [1]
Y [m]	1.704	1.776
I_y [m^4]	0.457	0.428
A [m^2]	0.387	0.343

4.2.5.2. Shear center

The shear center is a cumbersome to find, and since the author has never done a calculation of the shear center on a closed cross section, the exercise will be done here. Boresi [11] has an example of a closed cross section that will be followed.

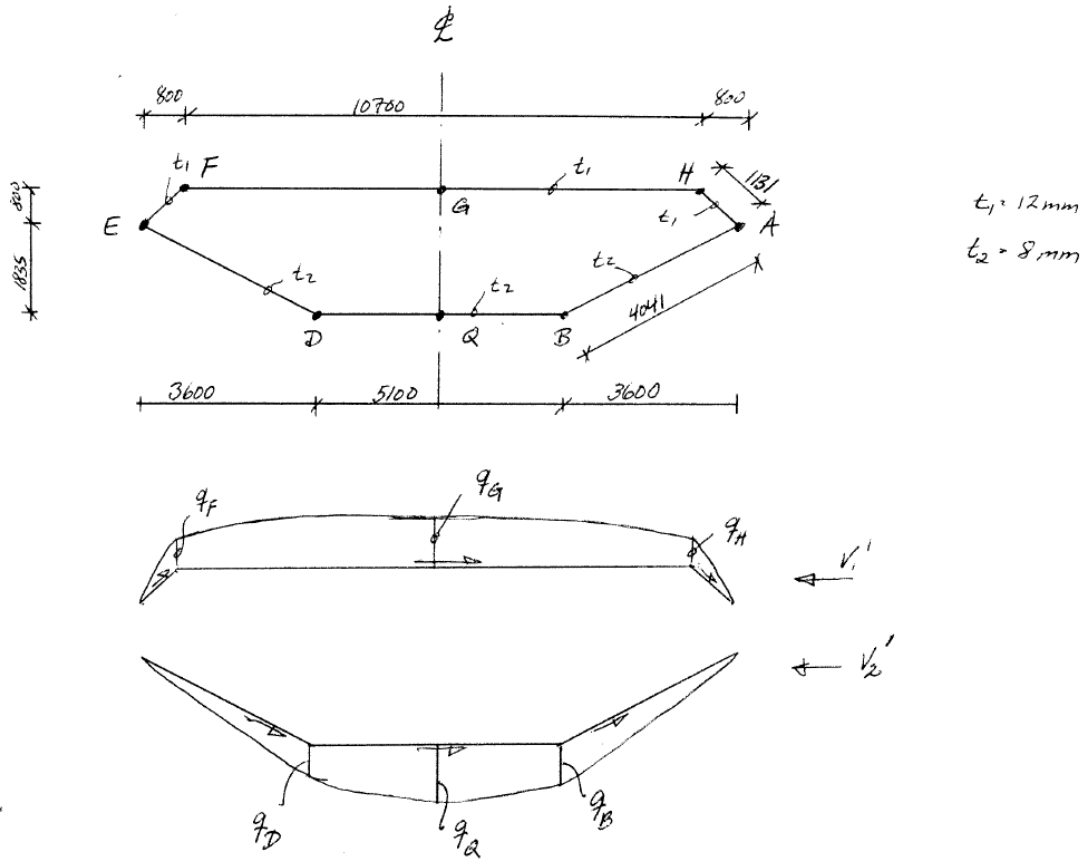


Figure 4-7: Girder cross section with initial shear stress distribution

Table 4-1: Shear calculation constants

<i>plate length l_1 [mm]</i>	1131
<i>plate length l_2 [mm]</i>	10700
<i>plate length l_3 [mm]</i>	4041
<i>plate length l_4 [mm]</i>	5100
<i>arm to plate l_2: a_1 [mm]</i>	800
<i>arm to plate l_4: a_2 [mm]</i>	1835
<i>arm to plate l_1: a_3 [mm]</i>	8697
<i>arm to plate l_3: a_4 [mm]</i>	5587
$\cos(\alpha)$ of plate l_3	$3600/4041$

As Figure 4-7 shows, the stiffening elements of the girder has not been taken into account to simplify the calculations. The calculation involves two equations where q_A needs to be found:

- the sum of shear forces = 0
- The moment around point A = 0

The value of V_1 is assumed to have the same magnitude as I_{x1} . The integral of the shear flow for the section is

$$\oint \frac{q}{t} dl = 0 \quad (4.3)$$

$$2 \int_0^{l_1} (q_A - q_1(l)) \frac{dl}{t_1} + (q_A - q_G - \frac{2}{3}(q_G - q_F)) \frac{l_2}{t_1} \\ + 2 \int_0^{l_3} (q_A + q_2(l)) \frac{dl}{t_2} + (q_A + q_G + \frac{2}{3}(q_Q \\ - q_D)) \frac{l_4}{t_2} = 0 \quad (4.4)$$

$$q_1 = \left(\frac{b}{2} - \frac{l_1 \sqrt{2}}{4} \right) l t_1 \quad (4.5)$$

$$q_2 = \left(\frac{b}{2} - \frac{l_2 \cos(\alpha)}{2} \right) l t_2 \quad (4.6)$$

For the moment calculation, the moment around point A is taken.

$$V'e - \left(q_F - q_A + \frac{2}{3}(q_G - q_F) \right) l_2 t_1 a_1 + (q_A + q_D + \frac{2}{3}(q_Q - q_D)) l_4 t_2 a_2 - \int_0^{l_1} (-q_A + q_1(l)) dl t_1 a_3 + \\ \int_0^{l_3} (q_A + q_2(l)) dl t_2 a_4 = 0 \quad (4.7)$$

Solving for e in Maple, $e = -403$ mm. \Rightarrow Shear center = 1433 mm from the bottom of the cross section. Looking at the value, it seems reasonable that the shear center has moved a bit up towards the thicker plates in the cross section, compared to half the height of the cross section.

4.2.5.3. Mass moment of inertia

$$I = m \int r^2 da \quad (4.8)$$

Since the cross section can be looked upon as discrete line segments with a given thickness, the integral turns into a summation over the girder cross section linear parts around a center point (x_c, y_c) .

$$y = y_0 + (y_1 - y_0)t \quad (4.9)$$

$$x = x_0 + (x_1 - x_0)t \quad (4.10)$$

$$s = \sqrt{(y_1 - y_0)^2 + (x_1 - x_0)^2} t \quad (4.11)$$

$$ds = \sqrt{(y_1 - y_0)^2 + (x_1 - x_0)^2} dt \quad (4.12)$$

$$L = \sqrt{(y_1 - y_0)^2 + (x_1 - x_0)^2} \quad (4.13)$$

$$I_{m_{line}} = \rho t L \int_0^1 (x - x_c)^2 + (y - y_c)^2 ds \quad (4.14)$$

$$I_{m_{line}} = \rho t L \left(\frac{1}{3} (x_1^2 + x_1 x_0 + x_0^2 + y_1^2 + y_1 y_0 + y_0^2) - x_1 x_c - x_c x_0 - y_1 y_c - y_c y_0 + x_c^2 + y_c^2 \right) \quad (4.15)$$

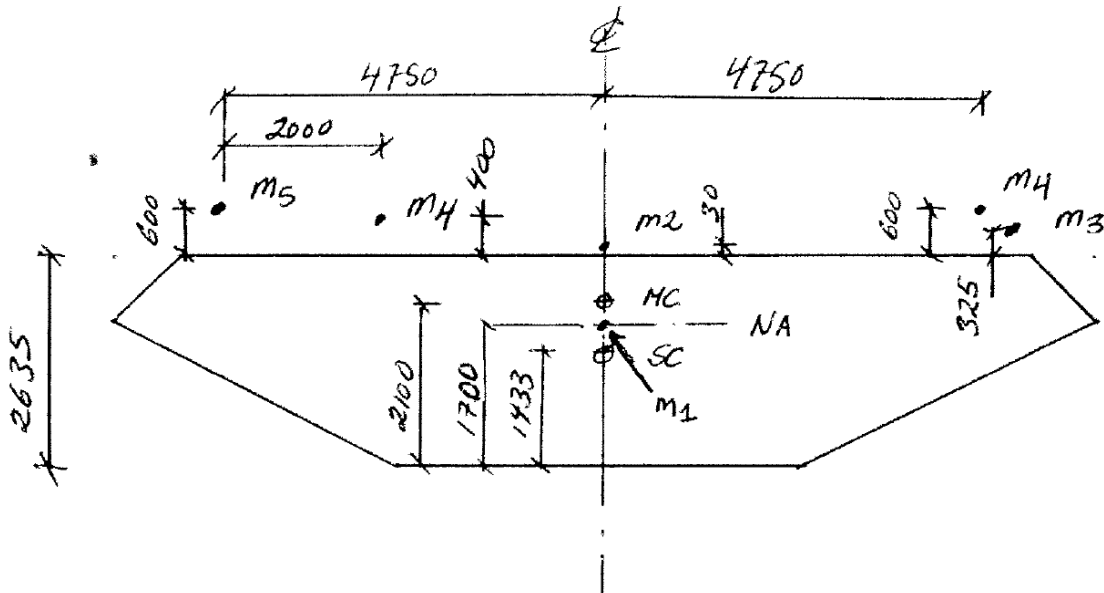


Figure 4-8: Mass positions in cross section

The 5 masses:

Table 4-2: Masses in cross section

Mass tag	Mass type	Mass [kg/m]
m1	Mass of girder	3466
m2	Mass of asphalt	1286
m3	Mass of hangers (symmetric about centerline)	95
m4	Railing type 1	150
m5	Railing type 2	100
Mass of cable	All main cables	816

A small Python script has been implemented to calculate the mass moment of inertia for the bridge girder. No plate stiffeners are taken into account. Including the cables into the calculation, $I_m =$

$74544 \frac{kg \cdot m^2}{m}$. Without the cables, $Im = 53111 \frac{kg \cdot m^2}{m}$. Alvsat uses $Im = 82430 \frac{kg \cdot m^2}{m}$. To stay consistent with the Alvsat number, $Im = 82430$ will be used.

4.2.6. Other parameters

- Temperature coefficient: $0.00001 \text{ } 1/\text{}^\circ\text{C}$
- Gravity of acceleration: 9.81 m/s^2
- Damping ratio: 0.5 \%

4.3. Basic model loads

The finite element model is used to study the following bridge characteristics:

- eigenfrequencies and eigenmodes
- deflection and stresses from:
 - self weight
 - wind
 - temperature
 - basic traffic load train
- deflection and stresses from vortex induced vibrations on
 - bridge girder
 - backstay cables

It is assumed that the level of stresses found from the above-mentioned loads will not in any way exceed the normal service stresses that the bridge is designed for.

The deflections and loads found from the dynamic VIV analysis will be compared to those established from the equivalent static load of NS-EN [22].

4.3.1. Mass distribution

The weight of the girder, cables, backstays, hangers and towers will be taken from Alvsat. The mass of the towers will be used as from the original ABAQUS model. Control calculations of the mass for the girder has been performed and compared with the values given as input to Alvsat. Based on the values found, we are in reasonable agreement with Alvsat.

The mass distribution of the girder itself will be modeled by a three point mass node approach at the nodes contained in the section where hangers meet girder. The mass for the hangers, backstays and main cables will be distributed according to the method provided by the chosen beam element type, which for the B31 beam case is a lumped mass approach. The same goes for FRAME3D beam used in the towers.

As shown in Figure 4-8, the mass in the cross section is distributed as two lumped masses M_1 , one at each hanger point, 1.267m above the shear center or on top of the bridge. The other lumped mass M_2 is situated around the shear center. Three equations are used:

- Sum of mass moment of interia =0
- Sum of masses = 0
- Center of mass preserved

With these 3 equations, m_1 , m_2 and y can be found.

$$M_2 y_1^2 + 2M_1(1.267^2 + 5.125^2) - I_m = 0 \quad (4.16)$$

$$2M_1 + M_2 = 5350 \quad (4.17)$$

$$\frac{2M_1 \cdot 2.70 + M_2(1.433 - y_1)}{5350} = 2.1 \quad (4.18)$$

Solving these three equations for $I_m = 82430$ with Maple gives $y_1 = 0.074$, $M_1 = 1478$, $M_2 = 2394$. The mass points and the masses will be modeled accordingly in the ABAQUS model.

Another option to try is to use $I_{m_2} = 58730$, which is the fraction $\frac{I_m * 53111}{74544}$ to stay consistent with the Alvsat values. Solving with this gives $y_1 = -0.28$, $M_1 = 1049$, $M_2 = 3252$. This positions the mass of the girder almost at the neutral axis, and the additional weight at the top of the girder.

4.3.1.1. Summary of masses in model

The summation of the weights can be found in Table 4-3.

Table 4-3: Weight of structure

	Length [m]	Weight [kg/m]	Total [ton]
Bridge girder	446	5350	2386
Main cable main span	458.89	408 x 2	375
Sum mass in main span			2761
Backstay cable north	87.55	365 x 2	64
Backstay cable south	174.51	365 x 2	127
Sum mass backstays			191
Towers			7919
Total			10871

The total mass found by ABAQUS is 11030 ton.

4.3.2. Wind loads

One of the most complex loads on a suspension bridge is the wind load. The wind will have a variation along the height of the bridge, as well as a lateral variation along the bridge. In addition, as the bridge girder rotates (i.e. twists) the wind load changes as a function of the angle of attack. The wind may also generate vortex induced vibrations on both the girder and cables in the main span. The literature reports of rain-wind induced vibrations occurring on the backstay cables,

which seems to be influenced by water droplets on the cables changing the aerodynamic characteristics of the cable [9]. The dimensions used for wind loads:

- Girder
 - $B = 12.3\text{m}$
 - $H = 2.76\text{m}$ (including asphalt)
- Main cable
 - $D = 0.1\text{m}$

4.3.2.1. Static wind loading

The static wind load is calculated from the mean wind speed at the height of the structure. This load consists of 3 components:

$$\text{Drag force: } D = \frac{1}{2} \rho U^2 H C_D \quad (4.19)$$

$$\text{Lift force: } L = \frac{1}{2} \rho U^2 B C_L \quad (4.20)$$

$$\text{Overturning moment: } M = \frac{1}{2} \rho U^2 B^2 C_M \quad (4.21)$$

- ρ : air density
- U : mean wind speed
- H : height of bridge girder
- B : width of bridge girder

C_D, C_L, C_M are dimensionless parameters describing the amount of wind that the actual cross section will catch. For girders on suspension bridges, these coefficients typically are found by wind tunnel experiments. The wind force will create a rotation of the girder cross section, and additional forces based on this deformation will appear. Rails on the bridge will also disturb the wind.

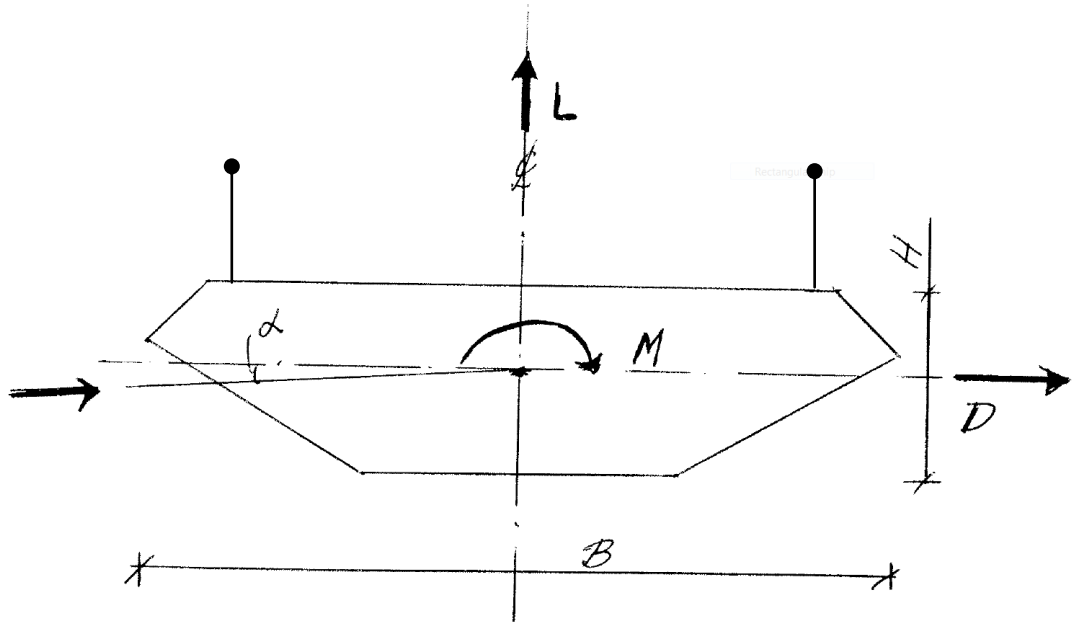


Figure 4-9 : Rotation of girder cross section

The wind coefficients refer to the shear center of the bridge girder. In this case with the shear center only $\sim 0.28\text{m}$ below the neutral axis, it is considered sufficient not to model the girder cross section with the shear center. Thus there is no need to correct the moments applied to correct the fact that the forces are applied in the neutral axis instead of the shear center.

As the wind load increases, the rotation of the girder section increases. The wind load can be split into 2 parts, one rotation independent part and one rotation dependent part. And it is assumed that linear approximation of the force coefficients as functions of the mean angle of attack, as given below will suffice for the analysis.

$$\text{Drag: } D(\alpha) = \frac{1}{2} \rho U^2 H (C_D(\alpha = 0) + \alpha C'_D(\alpha = 0)) \quad (4.22)$$

$$\text{Lift: } L(\alpha) = \frac{1}{2} \rho U^2 B (C_L(\alpha = 0) + \alpha C'_L(\alpha = 0)) \quad (4.23)$$

$$\text{Moment: } M(\alpha) = \frac{1}{2} \rho U^2 B^2 (C_M(\alpha = 0) + \alpha C'_M(\alpha = 0)) \quad (4.24)$$

The coefficients are shown in Table 4-4

Table 4-4: Wind coefficients

Coefficient	Factor
C_D	1.0
C'_D	0.0

C_L	0.1
C'_L	3.0
C_M	0.1
C'_M	1.12
C_{cable}	1.5

The cables on the bridge, both in main span and in backstay, are in most places so close to each other that they should have been corrected for the more rectangular shape of the cable configuration. But for now a simple drag factor according to a circular cable is assumed.

4.3.2.2. Mean wind speed at bridge girder

From the Alvsat input file, the mean wind speed at the girder elevation is specified to be 38 m/s. There also is a letter from Norwegian Meteorological Institute that provides this wind speed. The wind speed will be calculated according to NS_EN [22] as a check.

The basic wind velocity w_{basis} : Middle wind velocity with 10 minute duration, 10m above flat landscape for terrain category 2 and with a given return period of 50 years. The basic wind velocity for Forsand is $w_{basis} = 26$ m/s. The basic wind velocity needs adjustment for the following factors:

$$w_{corr} = C_{dir} * C_{seas} * C_{height} * C_{ret} * w_{basis} \quad (4.25)$$

- Wind direction. All directions chosen, $C_{dir}=1.0$
- Seasonal factor. Entire year chosen, $C_{seas}=1.0$
- Increasing wind speed with increasing height above level $C_{height}=1.0$
- Return period. Chosen return period is 50 years. $C_{ret}=1.0$

To account for the topology around the bridge, the place wind velocity w_{place} is needed.

$$w_{place} = C_r C_T w_{corr} \quad (4.26)$$

- Topology factor: Unclear if terrain will change the wind speed $C_T = 1.0$
- Roughness factor: $C_r = k_T \ln\left(\frac{z}{z_0}\right) = 0.17 \ln\left(\frac{50}{0.01}\right) = 1.448$

$$w_{place} = 37.6 \text{ m/s}$$

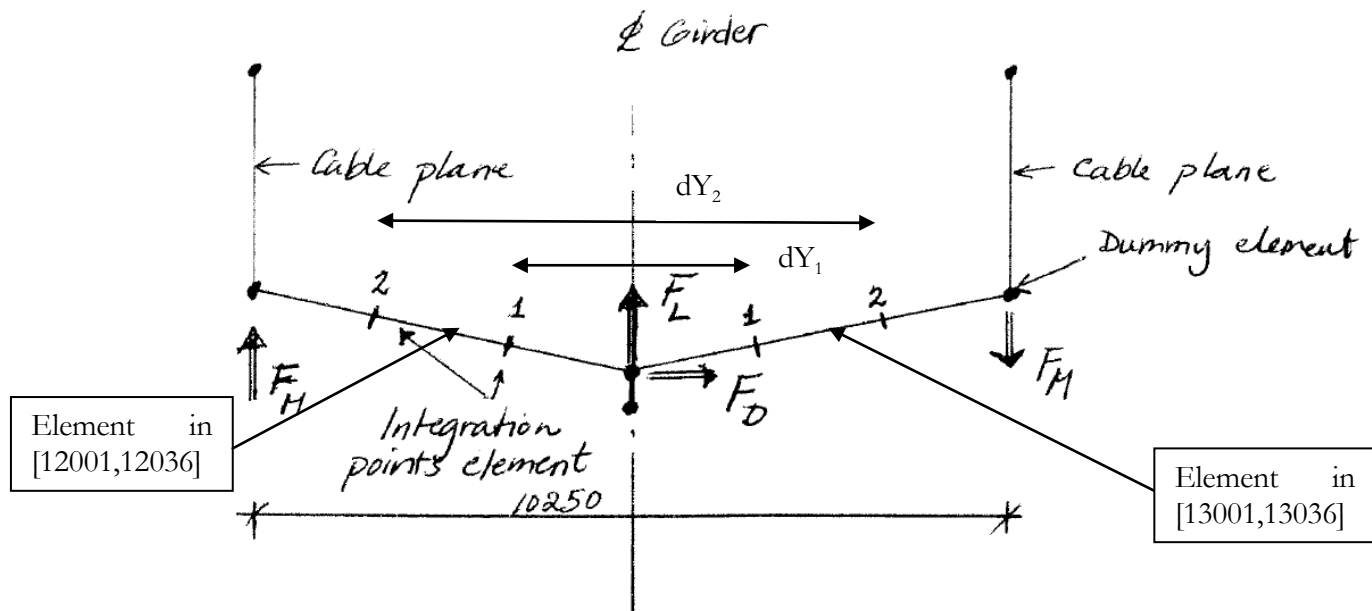
4.3.2.3. Implementation of static wind loads in ABAQUS

To simulate the loads described in the section above, we need to provide these loads to ABAQUS as a FORTRAN subroutine. Unfortunately the input parameters to the DLOAD subroutine do not have any deformation data of the cross section, only the deformed coordinates of the integration points of the element under load where the load intensity needs to be returned from the DLOAD subroutine provided.

As a workaround the user defined FORTRAN routine will be signaled to collect deformed girder data once in a while to have updated rotation angles of the girder cross section. This is achieved in the following process:

- One load case containing the angle independent loads are applied to the model, giving an initial deformation needed to start the iteration.
- One load case is used to signal to DLOAD that geometrical data can be collected from the element integration points of the elements loaded with the dummy load. No load is added to the system, DLOAD returns F=0. The element sets [3001, 3037] and [4001, 4037] as shown in Figure 4-2 and Figure 4-10 are used for this purpose, as they are in the y-z plane. The load direction is chosen as x, since no real load data is applied on the x axis in this load case
- One load case is used to signal to DLOAD that all the geometrical data has been sent, and angle calculation can be performed on the collected geometry. Here dY_i and dZ_i are calculated between integration points 1 and 2 of the neighbor elements, see Figure 4-10. Again DLOAD returns F=0. The angle $\alpha = \tan^{-1}(\frac{dZ_2}{dY_2})$ is used as the angle for the node set {1, 37}.
- Finally the load case with real angle dependent wind load are applied on element sets [1,36], [12001, 12036] and [13001, 13036]. Since the angles are recorded at the end of the elements, a linear interpolation of the deformation angles along the element is performed to find the rotation angle at the integration points of the beam in question. As seen in Figure 4-10, F_L is applied on element set [1, 36], while F_M are applied to element sets [12001, 12036] and [13001,13036].Figure 4-2

The element sets [12001, 12036] and [13001,13036] could have been used for the purpose of collecting angle information since they run parallel to the centerline girder element set [1, 36]. That would have avoided the interpolation work. But these elements are modeled as very flexible not to add to the global stiffness of the girder, thus the deformations of these elements cannot be relied upon. They only aid in transporting line loads into the cross beams element sets [3001, 3037] and [4001, 4037]. Since ABAQUS does iterations along the load history to converge, the signaling load cases as well as the real load case are called several times, thus updating the angles and the forces.



Integration points used to collect deformed geometry of cross section

Figure 4-10: Wind force diagram for bridge cross section

The wind loads run taking rotation into account will be $v = [20, 38, 60, 80, 100]$ m/s. Since the runs of the wind loads will continue until the system converges, we apply the angle dependent loads in the following manner:

- Moment load as line load pair in z direction on dummy elements F_M
- Lift load as line load in z direction on girder beam elements F_L

Rotation independent wind loads can be found in Table 4-5.

Table 4-5: Rotation independent wind forces

Force Wind [m/s]	[N] speed	F_D	F_L	F_M
20		690	307	369
38		2490	1110	1332
60		5912	2635	3162
80		10510	4684	5621
100		17250	7690	9225

The rotation dependent forces can be found in 5.4.

4.3.2.4. Dynamic wind loads

Suspension bridges with a certain length of the main span will be subjected to aerodynamic forces generated by structural motions. These motions are then in turn excited and changed by the aerodynamic forces they generate. The shape of the girder itself and the other surrounding items like hand railing will generate turbulence that again influence the air flow around the bridge. After the Tacoma Bridge incident, a lot of attention has gone into making bridge girder cross sections to minimize the impact of Vortex Induced Vibrations, flutter and galloping. In this analysis, Vortex Induced Vibration will be studied. Both static analysis based on the vertical eigenmodes and dynamic analysis in the time domain will be performed. Symmetric and asymmetric eigenmodes will be looked into, based on a possible non uniform wind velocity. It was noticed on our visit to the bridge that for certain wind directions, the southern part of the bridge is somewhat sheltered for wind forces, possibly providing asymmetric loads.

The dynamic analysis will be done in ABAQUS for a wind of 10 minute duration. These results will be compared to a static equivalent load based on the equations of NS-EN [22].

4.3.3. Temperature loads

The bridge is assumed to be in a zero tension state regarding temperature at $+10^{\circ}\text{C}$. The bridge can have an operating temperature range of $[-25, +35]$. These temperature differences will add additional forces to the structure. In addition there will be temperature gradients across the bridge girder, in particular since the top structure is dark and heats up differently than the rest of the girder. One simple temperature load will be run, with a uniform temperature decrease of $dT = -20^{\circ}\text{C}$ to see the magnitude of the temperature forces in terms of cable force increase. The temperature difference will only be run on the steel parts of the bridge.

4.3.4. Traffic loads

The bridge has quite some lorry traffic, since several factories transport goods across the bridge. Talking to one of the concrete element producers on the Forsand side, his stipulation was at least 4 lorries a day with a weight of 30 ton from their site alone crosses the bridge.

A vertical traffic load from [23] has been applied to the bridge girder. For simplicity the distribution of the loads in the neighbor spans have been according to a simply supported beam model. The same goes for the distribution of the forces between the hangers in the transversal direction. The wheel force F is set to half the axel load, $F=105[\text{kN}]$.

In the longitudinal direction of the bridge the most unfavorable load position for the cable forces is a lorry position according to Figure 4-11. Considering the beam on each side of the center hanger as simply supported, the load carried to the center hanger can be approximated to $F_T = 2.29F = 240.5 [\text{kN}]$.

In the transversal direction of the center hanger both half axel loads appear in the position shown in Figure 4-12. The support load for point A and B was found based on the assumption that the crossbeam is simply supported. These point loads are applied on the nodes where the hanger connects to the girder.

Table 4-6: Cable loads from lorry on crossbeam between hangers

F_A	$3.52F = 369.6 \text{ [kN]}$
F_B	$1.06F = 111.3 \text{ [kN]}$

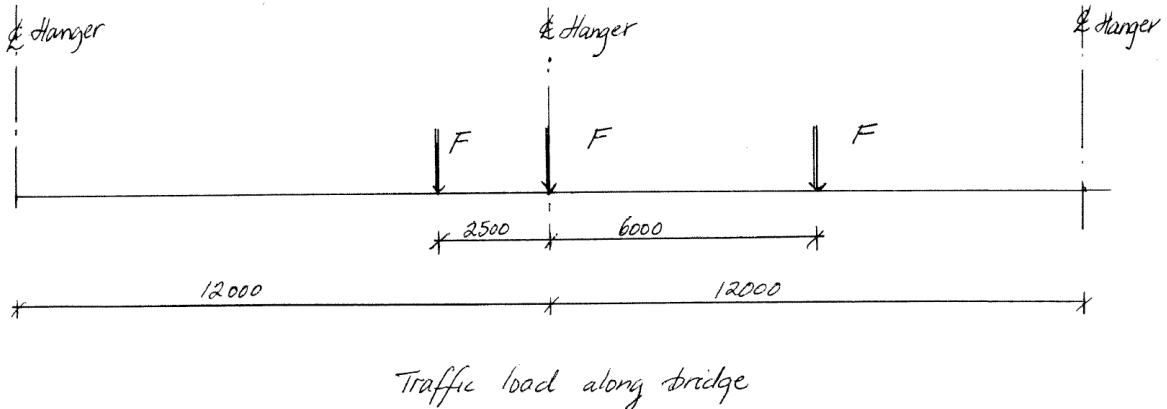
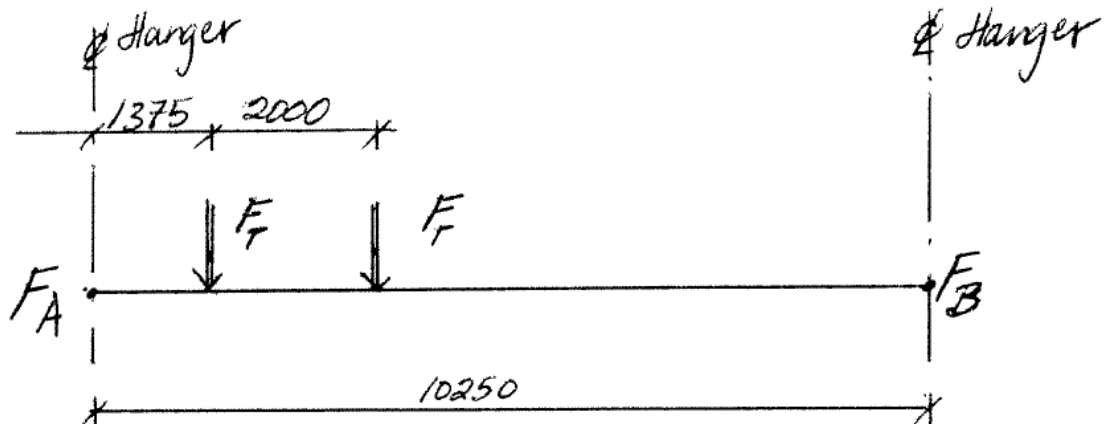


Figure 4-11: Traffic load position along bridge



These point loads have been entered into ABAQUS with the perturbation keyword. That will give a linear perturbation offset from the current state, meaning that the forces and displacements are given as if the start state was zero.

4.3.5. Earthquake loads

Even though there actually was a small earthquake in Rogaland during the time of the thesis, no analysis of earthquake loads will be performed.

5 Results of ABAQUS analysis

It must be said that ABAQUS isn't the easiest software package to run, due to its general purpose nature and the freedom of user defined subroutines. ABAQUS provides FORTRAN subroutine support for issues that cannot be solved directly out of the box. The fact that all analysis are run in nonlinear mode makes it somewhat harder, since order of loading affects the global stiffness matrix in a very different way than a linear analysis does. Also the need to write FORTRAN subroutines to apply varying line loads makes it cumbersome, contrary to other household name software packages more specialized for use in frame analysis.

On the other hand, the iterative traversal of the solver made it easier to get the angle calculations of the girder correct. The solver traverses up and down the load history to achieve convergence, providing enough passes through the FORTRAN subroutine to get updated angles without more convolved state needed in the subroutine.

The model will be run in various stages. The stages are:

- Self weight to control deformed model against theoretical model
- Eigen-frequency and mode-shape analysis
- Temperature load
- Static wind load to check stability and displacement of girder
- Dynamic analysis of VIV effects
- Static equivalent VIV analysis to compare with dynamic analysis

First we need to run only the dead load of the bridge to ensure that the deformed model is in an approximate correct state before starting analysis of the model. Then the eigenfrequencies will be calculated. These are compared to Alvsat data, but also provide the basis needed to find VIV wind speeds and mode shapes to use for the static equivalent analysis of the deformation of VIV.

5.1. Deformed model

The input model is deformed by its own deadweight to line up according to the adopted design geometry of the bridge. Writing out the deformed model coordinates with ABAQUS and performing a check, it can be seen that the difference on girder and cables are within [+0.06m, -0.04m] from the theoretical position in the z direction. That is considered sufficient.

5.1.1. Analysis of dead load

Based on the parabolic equation the horizontal force of the dead load is:

$$H = \frac{F \cdot L}{8 \cdot f} \quad (5.1)$$

The mass of the main span is $M_{mainspan} = 2761[ton]$

$$H = \frac{2761 \cdot 9.81 \cdot 446}{8 \cdot 45} = 33556[kN]$$

Abaqus result (element 1019 + 2019): $H_{Abaqus} = 32537[kN]$

Alvsat result: $H_{Alvsat} = 33731[kN]$

The difference between Alvsat and ABAQUS is 3.7%. Looking at the stresses in the cable at mid span:

$$\sigma = \frac{H}{12 \cdot A_c} = \frac{32537000}{12 \cdot 0.0074} = 366.4[MPa]$$

The cable forces will be higher approaching the towers and the north backstay cables will have the highest forces. The highest force (element 999 and 1999) $H_{max} = 2 \cdot 19118 = 38236[kN]$

$$\sigma = \frac{38236000}{12 \cdot 0.0074} = 430.6[MPa]$$

The cables used in suspension bridges in Norway today have an ultimate tensile strength of 1570[MPa]. The demand/capacity rate of the backstay cable is $\frac{430.6}{1570} = 27.4\%$. Knowing that the deadload takes most of the capacity of a suspension bridge, it is likely that the stress found from the other loads will be small compared to the stresses from the deadload.

5.2. Temperature loads

Based on a uniform temperature difference of -20 °C, the increase in the main cable forces is modest, only a 0.84% increase in the force compared to the force due to deadload. The force does have a distribution that is similar to the fracture distribution of the bridge.

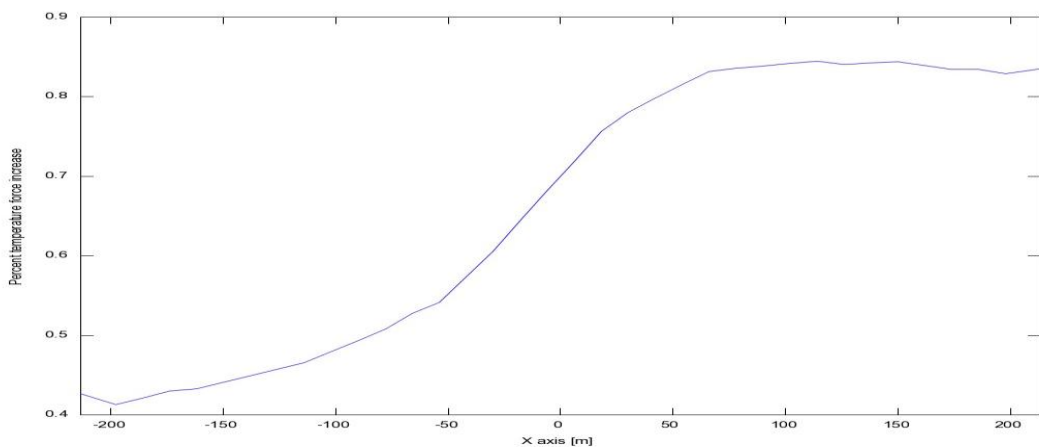
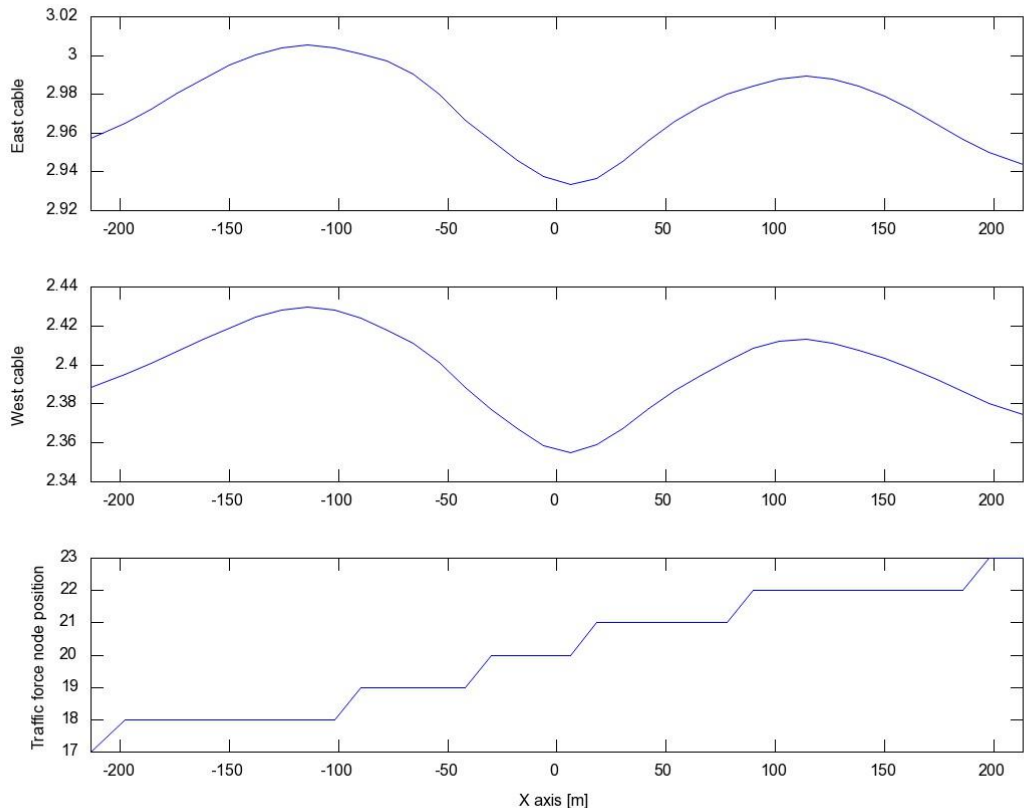


Figure 5-1: Cable force increase due to temperature

5.3. Traffic load model

The lorry load running on the east side of the bridge gives a small increase in the cable forces, but not more than 3% increase of the deadload force on the east side and 2.44% on the west side cable



5.4. Motion induced wind loads

The motion independent wind loads have been found in 4.3.2.1. The loads found from running the analysis taking rotations into account are shown in Figure 5-2 and Figure 5-3. Only forces up to 80 m/s are shown to keep a reasonable scale on the y axis. The moment

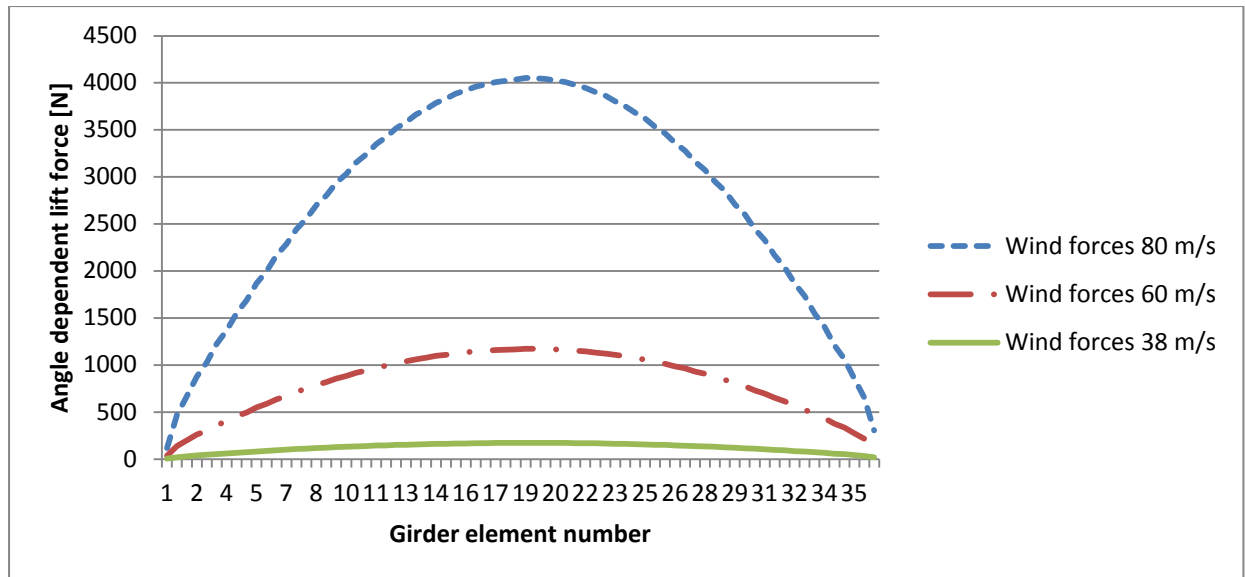


Figure 5-2: Angle dependent lift force

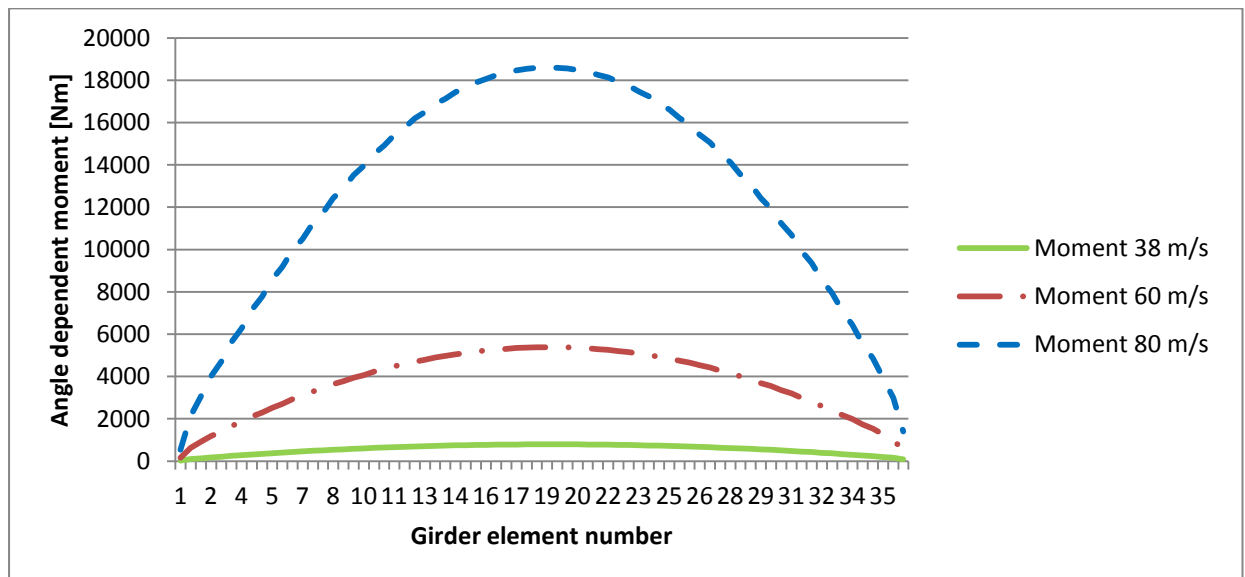


Figure 5-3: Angle dependent moment

At a wind speed of 135 m/s, the system produces negative values in the system matrix with default stability settings in ABAQUS. The ambition was to see if the system could be loaded to torsion instability, but the cause of the instability is most likely a problem with the main cable starting to be pushed upwards. In any case the girder has an excessive response. To be able to follow the loading sequence in more detail and eliminate unwanted effects, the bridge hangers were modeled as 3d trusses with no compressional capacity. At a wind velocity of 130 m/s, the upwind bridge hangers carry no load.

The equation for critical wind speed U_{div} for static torsional instability is given by Dyrbye[28]:

$$U_{div} = \sqrt{\frac{2 \cdot k_\alpha}{C'_m \cdot \rho \cdot b^2}} \quad (5.2)$$

- $k_\alpha = (2 \cdot \pi \cdot n_\alpha)^2 \cdot I_e$
- n_α : torsional natural frequency in still air
- I_e : equivalent mass moment of inertia per unit length
- b : width of girder
- ρ : air density

For equivalent mass moment of inertia, the value for the girder cross section will be used.

$$U_{div} = \sqrt{\frac{2 \cdot 6.825^2 \cdot 82430}{1.12 \cdot 1.25 \cdot 12.3^2}} = 190.4 \frac{m}{s}$$

U_{div} shows a higher value than the one found in ABAQUS.

To check the values above, the equivalent equation can be found from NS-EN [22], where k_α is torsional stiffness. A unit moment $M_x = 1000[N]$ about the X axis is applied to the girder at midpoint (node 19), found rotation $\alpha = 1.2525e-6[\text{rad}]$. To equate this to a evenly distributed torsional load, the torsional stiffness for a beam with a concentrated load at midpoint is compared to a beam with a uniform torsional line load. The stiffness equations from Byggtabeller [29]:

Concentrated load $K_p = \frac{48 * GJ}{l^3} = \frac{M_x}{\alpha}$ (5.3)

Uniform line load $K_q = \frac{384 * GJ}{5l^4}$ (5.4)

Stiffness ratio $\frac{K_q}{K_p} = \frac{8}{5l}$ (5.5)

$$K_\alpha = \frac{8}{5l} \frac{M_x}{\alpha} = 2.8642 \cdot 10^6 \quad (5.6)$$

$$U_{div_{ns}} = \sqrt{\frac{2 \cdot 2.8642 \cdot 10^6}{1.12 \cdot 1.25 \cdot 12.3^2}} = 164.5 \frac{m}{s} \quad (5.7)$$

As shown, the wind velocities for torsional instability is quite higher than the wind velocity loaded on the model taking girder deformation into account .

5.5. Eigenfrequencies and eigenmodes

The frequencies of the eigenmodes of a suspension bridge is important when dynamic response is studied. The analysis uses the center of gravity. Since this model has more elements in the backstay

cables, the eigenmodes and eigenfrequencies are harder to match up with the Alvsat values. The towers will also influence the values for both the horizontal and the torsional modes. To be able to find similar modes to compare to the Alvsat values, the number of eigenvalues needed had to be increased from 110 to 180, where the last torsional asymmetric eigenmode was found.

Looking at the energy of the different eigenmodes, both the horizontal and torsional eigenmodes have several modes with higher energy than Alvsat. Given the contributions from the cables, visual inspection to find the higher eigenmodes turned out to be difficult. Octave was used to calculate a simple energy measure $U_{mode,i}$ (squaring the displacement or rotation) and filtering the eigenmode list based on this measure.

$$U_{mode,i} = \sum u_i^2 \quad (5.8)$$

For the horizontal and vertical eigenmodes, u_y and u_z are used, thus the unit is m^2 . For the torsional eigenmodes, u_{rx} is used, thus the unit is rad^2 . The thresholds are 0.5, 1.0 and 0.03 for the horizontal, vertical and torsional eigenmodes. To find all the Alvsat eigenmodes, the threshold has to be lowered for the horizontal and torsional modes.

5.5.1. Eigenfrequency bridge girder comparison

To compare Alvsat and Abaqus, the 3 first modes where found of each type and plotted. The modes are:

- Group 1
 - HS-1: Horizontal symmetric 1st mode
 - HS-2: Horizontal symmetric 2nd mode
 - HS-3: Horizontal symmetric 3rd mode
- Group 2
 - HAS-1: Horizontal asymmetric 1st mode
 - HAS-2: Horizontal asymmetric 2nd mode
 - HAS-3: Horizontal asymmetric 3rd mode
- Group 3
 - VS-1: Vertical symmetric 1st mode
 - VS-2: Vertical symmetric 2nd mode
 - VS-3: Vertical symmetric 3rd mode
- Group 4
 - VAS-1: Vertical asymmetric 1st mode
 - VAS-2: Vertical asymmetric 2nd mode
 - VAS-3: Vertical asymmetric 3rd mode
- Group 5
 - TS-1: Torsional symmetric 1st mode
 - TS-2: Torsional symmetric 2nd mode
 - TS-3: Torsional symmetric 3rd mode
- Group 6
 - TAS-1: Torsional asymmetric 1st mode
 - TAS-2: Torsional asymmetric 2nd mode
 - TAS-3: Torsional asymmetric 3rd mode

The eigen-frequencies from Alvsat and Abaqus are presented in Table 5-1. The results from Alvsat are used as reference values. As the table shows, all the modes from Alvsat are found in ABAQUS, even though some of the 2nd and 3rd mode values do not have very much energy.

Table 5-1: Alvsat and ABAQUS values for eigenfrequencies

	Alvsat		ABAQUS			Difference [%]
	Frequency [rad/s]	Period [s]	Frequency [rad/s]	Period [s]	Number	Frequency
HS-1	0.81450	7.71417	0.80162	7.838	1	-1.58
HS-2	3.49779	1.79633	3.3513	1.8749	7	-4.19
HS-3	5.22053	1.20355	5.237	1.200	18	0.32
HAS-1	2.77863	2.26126	2.7087	2.3196	5	-2.52
HAS-2	3.75600	1.67284	3.6654	1.7142	10	-2.41
HAS-3	6.29528	0.99808	6.1162	1.027	21	-2.84
VS-1	1.79971	3.49121	1.8975	3.3113	3	5.43
VS-2	2.51538	2.49790	2.5572	2.457	4	1.66
VS-3	5.44536	1.15386	5.3778	1.1684	19	-1.24
VAS-1	1.33898	4.69252	1.3464	4.6666	2	0.55
VAS-2	3.70150	1.69747	3.6630	1.7153	9	-1.04
VAS-3	7.52991	0.83443	7.4803	0.8400	27	-0.66
TS-1	7.25328	0.86625	6.8252	0.9206	24	-5.90
TS-2	20.3611	0.30859	17.896	0.3511	77	-12.11
TS-3	34.0802	0.18436	28.384	0.2214	126	-16.71
TAS-1	13.3510	0.47062	11.673	0.5383	51	-12.57
TAS-2	27.1828	0.23115	23.149	0.2714	99	-14.84
TAS-3	41.0351	0.15312	31.938	0.1967	150	-22.17

All the modes presented in Table 5-1 involve significant response of the bridge girder. In Figure 5-4 to Figure 5-9 the associated mode shapes are presented. In ABAQUS the nodal displacement is normalized so the node with the largest displacement within the structure will have the value of 1. The modes from the Alvsat result are uncoupled, while in ABAQUS the modes can be coupled. One example can be seen in Figure 5-10, where the girder has endpoint displacements. This indicates that the towers are participating in the eigenmode as well as the girder and cables.

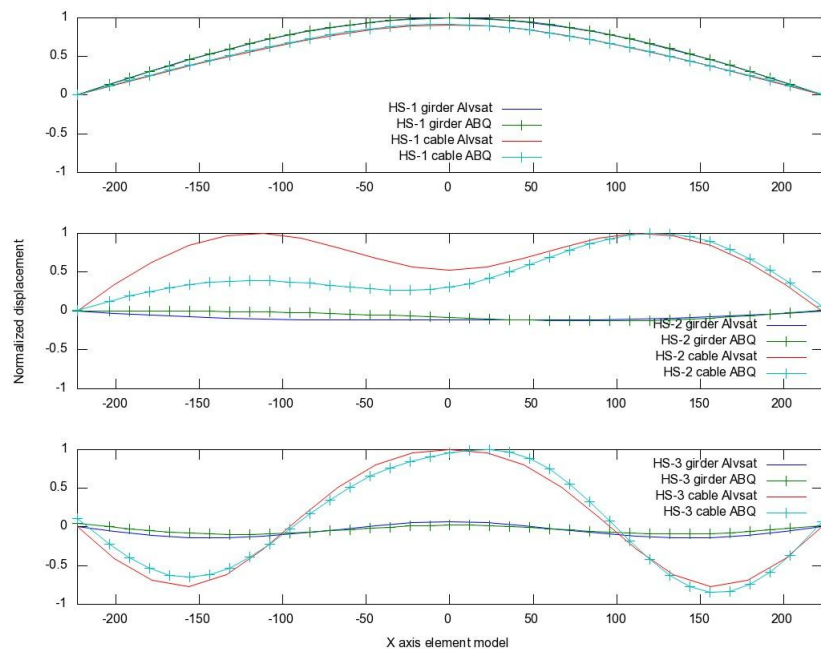


Figure 5-4: Horizontal symmetric modes

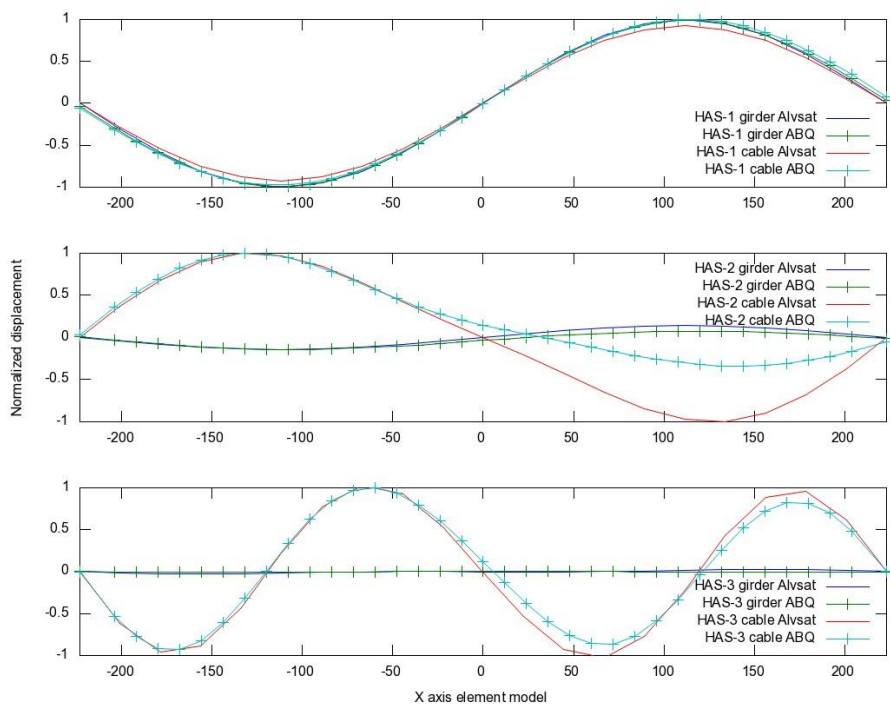


Figure 5-5: Horizontal asymmetric modes

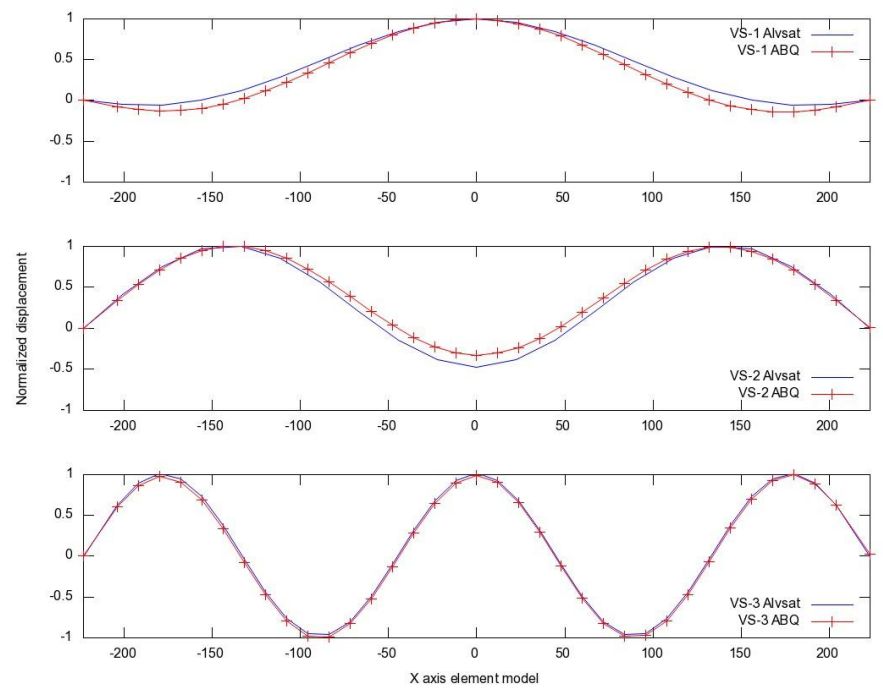


Figure 5-6: Vertical symmetric modes

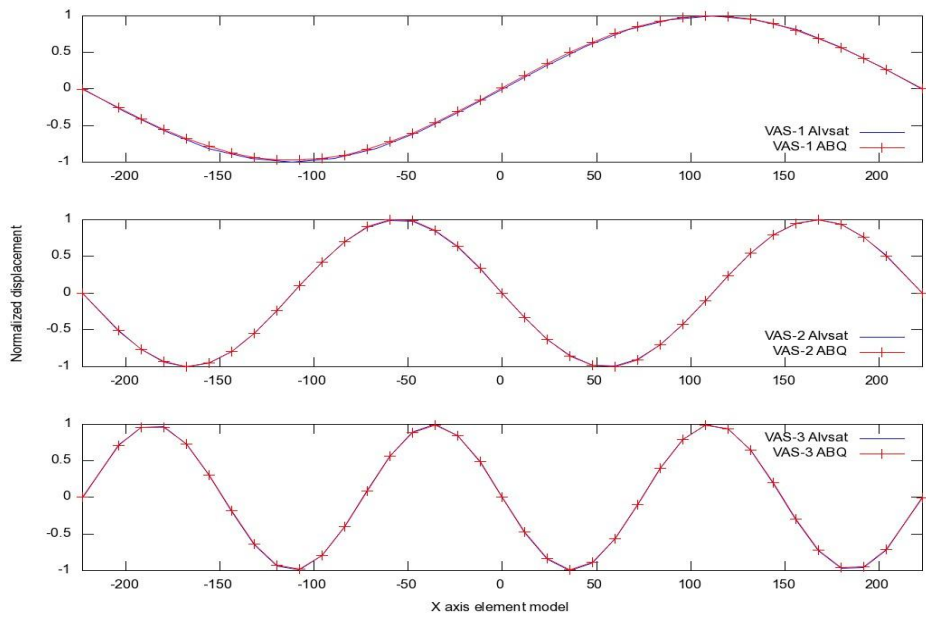


Figure 5-7: Vertical asymmetric modes

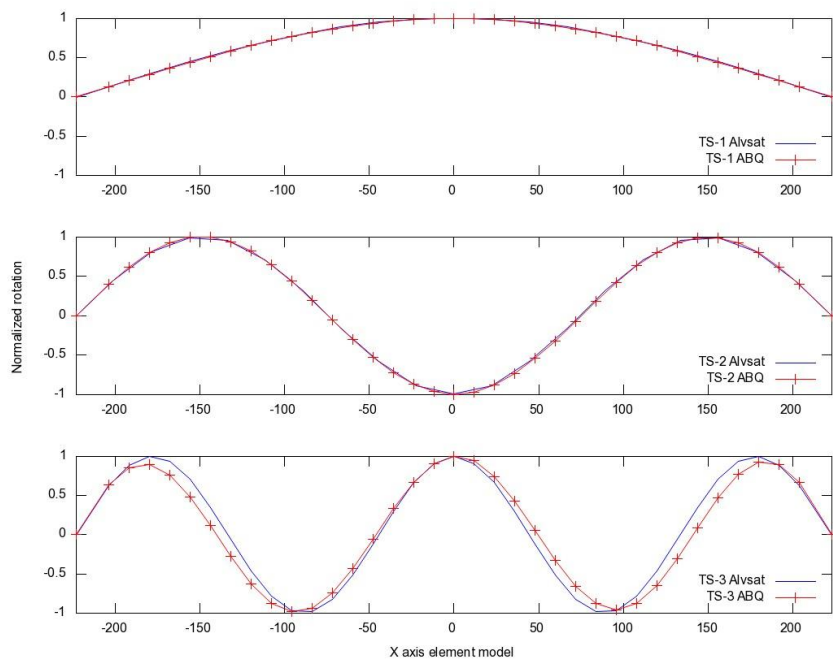


Figure 5-8:Torsional symmetric modes

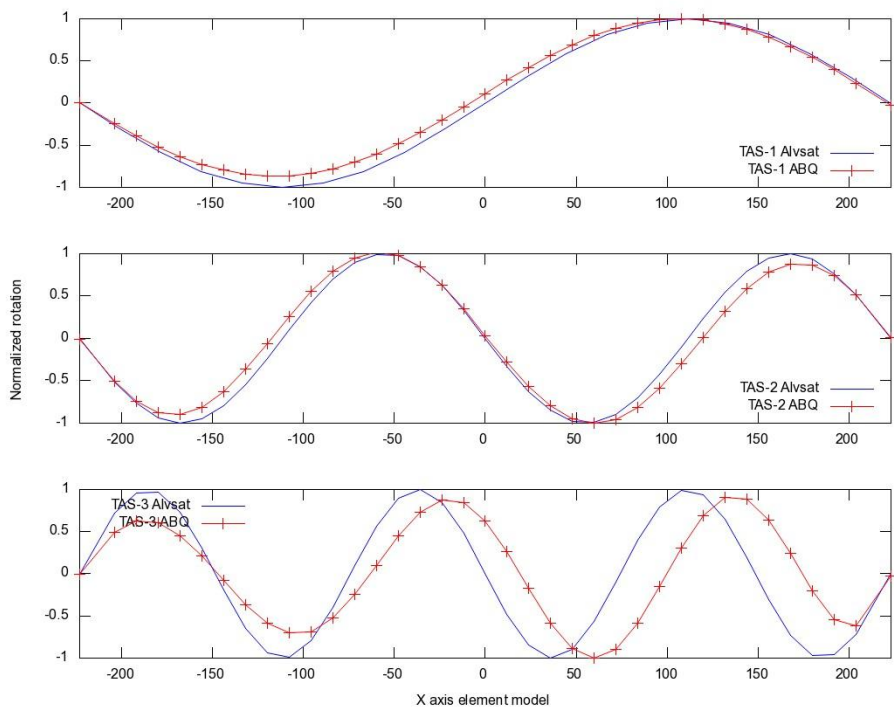


Figure 5-9: Torsional asymmetric modes

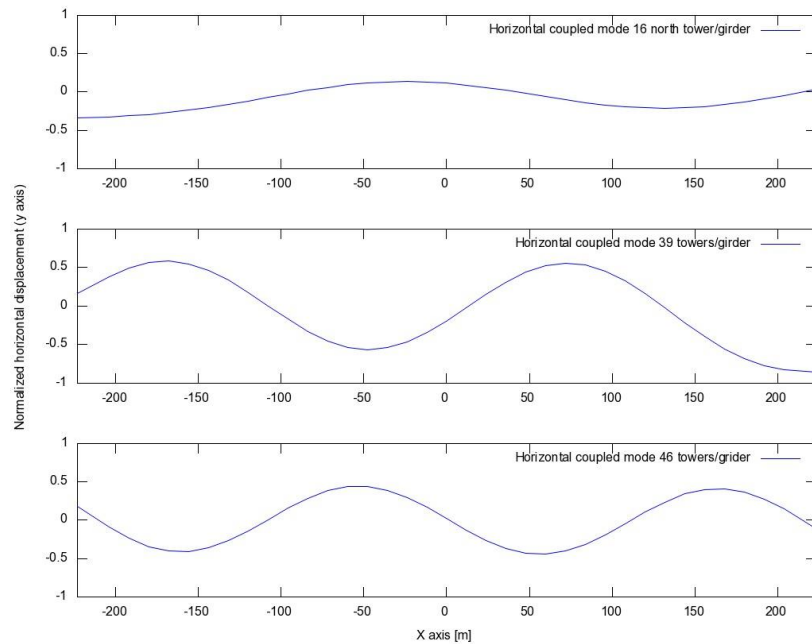


Figure 5-10: Horizontal coupled modes

As seen in Figure 5-10, there is an offset at the ends of the bridge girder, indicating tower movement in the y-direction. These modes are coupled; both the tower and the girder contribute in the modes shown. For the frequencies of the coupled modes, see Table 5-2

Table 5-2: Frequencies and periods of horizontal coupled modes

Mode	Frequency [rad/s]	Period [s]
16	4.672	1.345
39	9.405	0.668
46	11.445	0.549

The indexes that pass the energy threshold criteria for the bridge girder are shown in Table 5-3

Table 5-3: Modes above energy threshold

Horizontal modes	Vertical modes	Torsion modes
1	2	24
5	3	51
16	4	52
23	9	77
39	19	99

43	20	111
46	27	126
51	42	138
74	55	
105	56	
123	67	
	84	
	100	
	122	

Lowering the energy level threshold to 0.1 for the horizontal and vertical mode energies and 0.01 for torsion energy, the three mode index sets can be intersected to see if a mode has energy above the threshold for more than one direction. The intersection of the three index sets shows:

- No intersection of horizontal and vertical mode index sets
- No intersection of vertical and torsion mode index sets
- Intersection of horizontal and torsion mode index sets

The reason for the intersection of the horizontal and the torsion modes are the fact that the bridge girder has a circular form in the vertical plane. A simple visualization of that would be that the horizontal force needed at the highest point of the bridge will also have an arm e that provides an additional torsion force that needs to be carried to the support.

The mode numbers are shown in Table 5-4. Note that the horizontal energy unit is m^2 , while the rotational energy unit is rad^2 .

Table 5-4: Mode intersection set at threshold level

Mode number	Horizontal energy [m^2]	Rotational energy [rad^2]	Frequency [rad/s]	Period [s]
24	0.141	0.6977	6.825	0.921
51	0.884	0.5828	11.673	0.538
52	0.296	0.6262	12.042	0.522
77	0.195	0.5220	17.896	0.351
99	0.218	0.3116	23.149	0.271
105	17.200	0.0236	23.998	0.262
123	0.663	0.0294	28.252	0.222
150	0.306	0.0123	31.938	0.197

The first 6 modes from Table 5-4 are shown in Figure 5-11 and Figure 5-12.

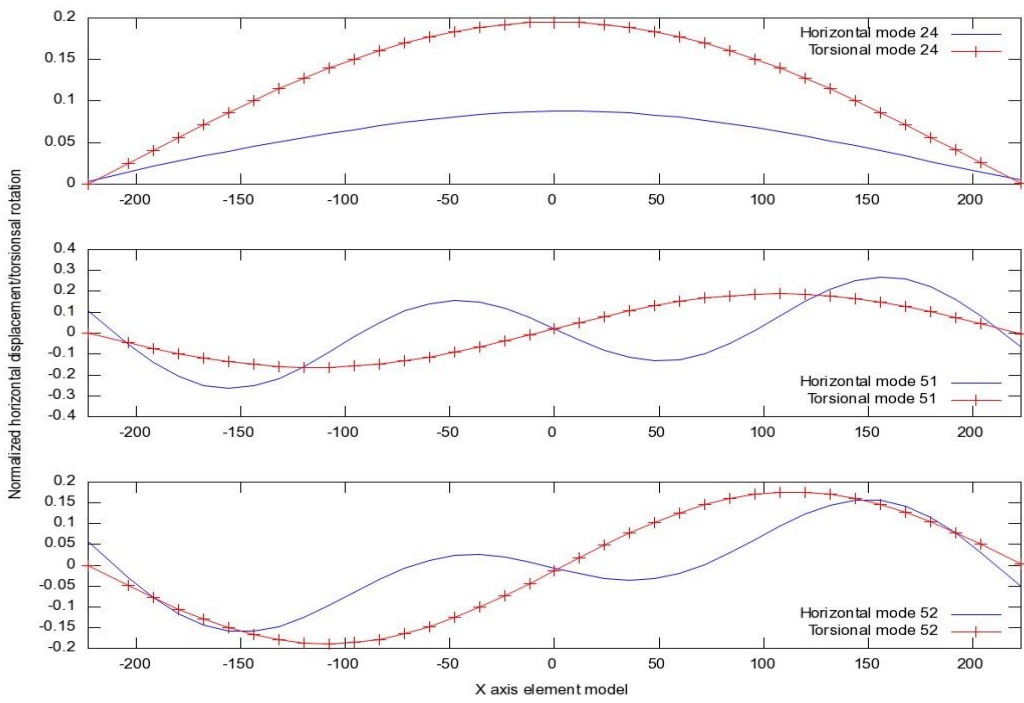


Figure 5-11: First three coupled horizontal/torsion modes

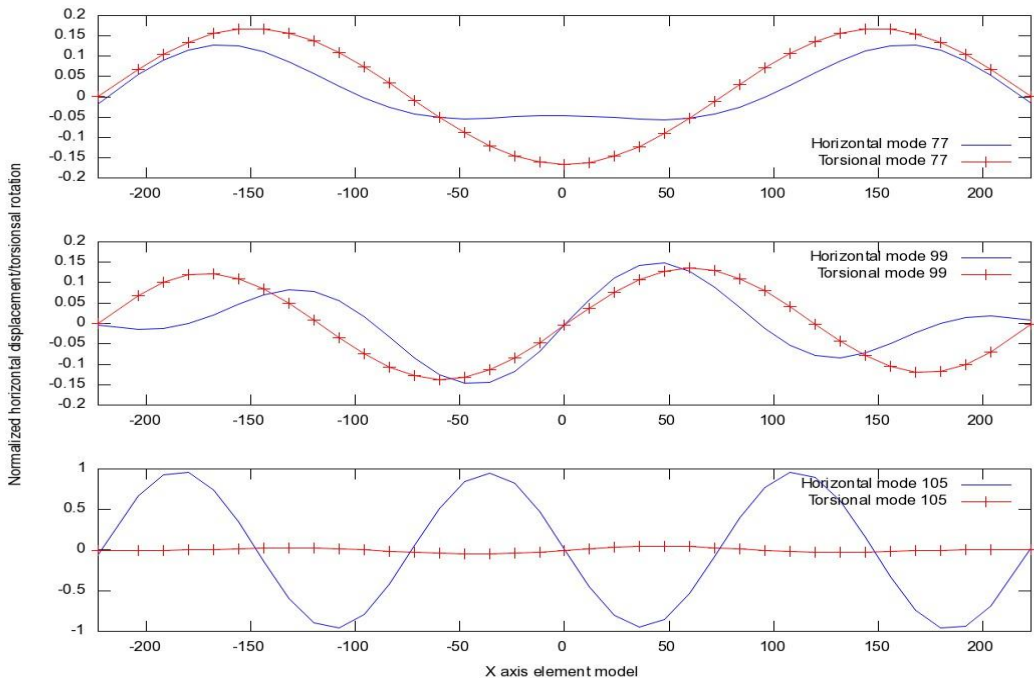


Figure 5-12: Coupled horizontal and torsional modes

Looking at the case where the cable mass is not part of the mass moment of inertia I_{m_2} of the girder, the model needs a slight change. The nodal mass M_2 is assigned to a node under the girder, see Figure 4-3. Now this mass is moved to the neutral axis point, i.e. centerline girder node, and the values of the mass weights are corrected. The mass node values can be found in chapter 4.3.1. The resulting torsional eigen-frequencies are closer to the Alvsat results, the difference now range from -11.75% to 7.19%. The horizontal and vertical eigen-frequencies are as before, the difference range from -4.2% to 5.4%, see Table 5-1. The new torsional eigen-frequencies are shown in Table 5-5

Table 5-5: Frequencies without cable mass in mass moment

	Alvsat		ABAQUS			Difference [%]
	Frequency [rad/s]	Period [s]	Frequency [rad/s]	Period [s]	Number	Frequency
TS-1	7.25328	0.86625	7.7748	0.8082	32	7.19
TS-2	20.3611	0.30859	20.165	0.3116	87	-0.96
TS-3	34.0802	0.18436	30.075	0.2089	137	-11.75
TAS-1	13.3510	0.47062	13.331	0.4713	56	-0.15
TAS-2	27.1828	0.23115	26.811	0.2344	117	-1.37
TAS-3	41.0351	0.15312	38.413	0.1636	184	-6.39

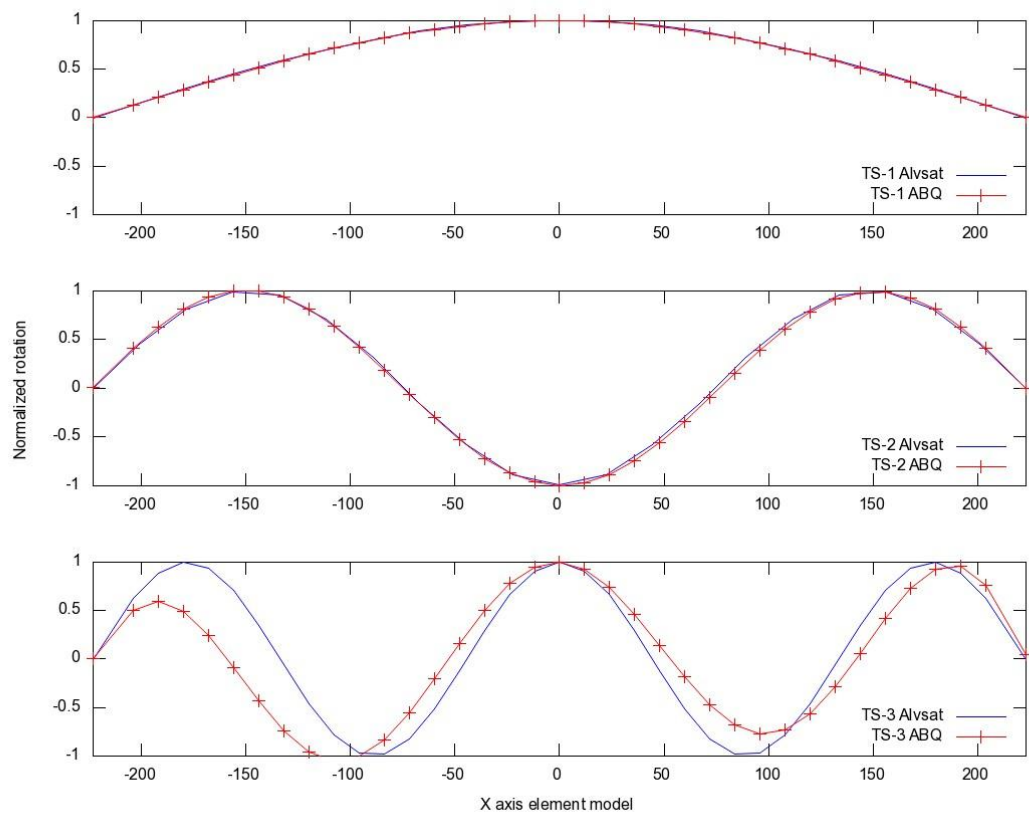


Figure 5-13: Symmetric torsional modes without cable mass in mass moment

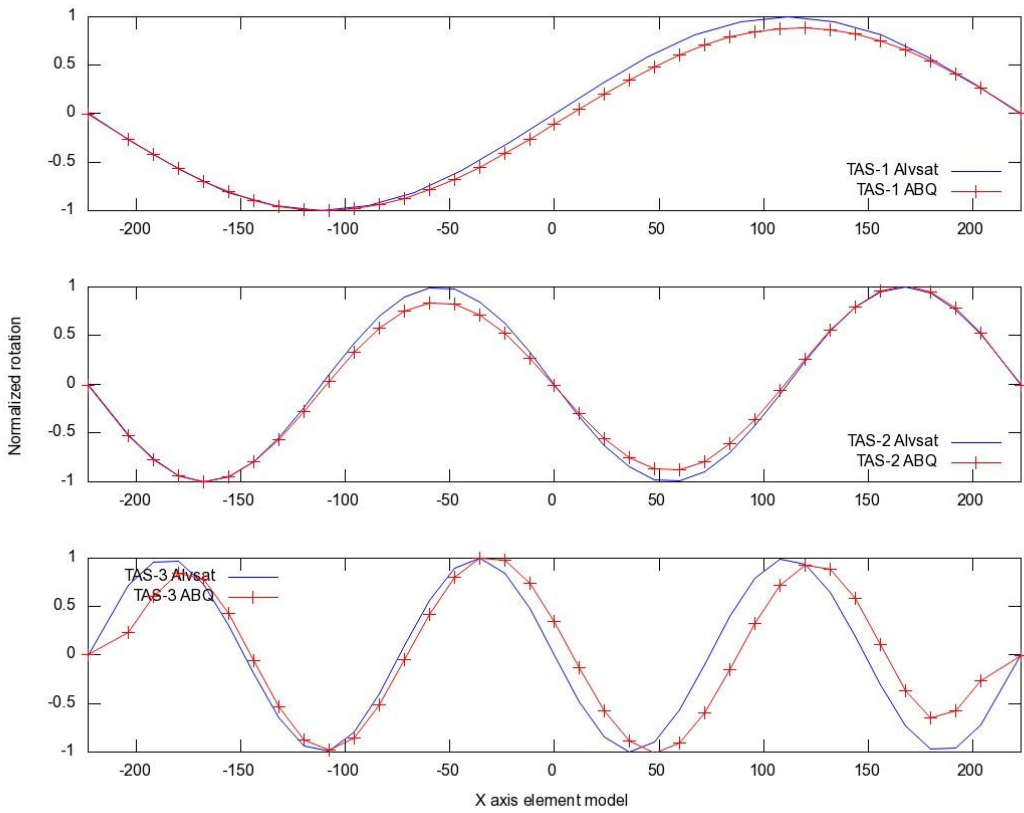


Figure 5-14: Asymmetric torsional modes without cable mass in mass moment

5.5.2. Eigenfrequencies for bridge cables

The bridge cables have more eigenmodes with energy than the bridge girder. Modeling the backstay cables with more cable elements provide more detail in that respect. This has an impact on the role the backstays play in the element model. It can be seen by looking through the modes in ABAQUS that there are a number of modes that are solely cable modes. They appear both in horizontal and vertical direction, for cables in main span and for the backstays.

Looking at the energy level for the cable modes with the same cutoff value as the girder for the main span, Table 5-6 shows the results.

Table 5-6: Number of modes with energy above threshold

	Girder	Cables main span	Mode intersections	Mode difference
Vertical direction	14	25	14	11
Horizontal direction	11	70	10	60

As expected, the cables follow the girder. But there are a number of modes where the cables deflect much more than the girder. The horizontal modes have more of these than the vertical modes, as expected. In the following 2 figures, the girder mode energy has been filtered for values > 0.1 , while the cable mode energy has been filtered for values > 1.5 . The set difference between the mode numbers have been taken to find the modes of interest.

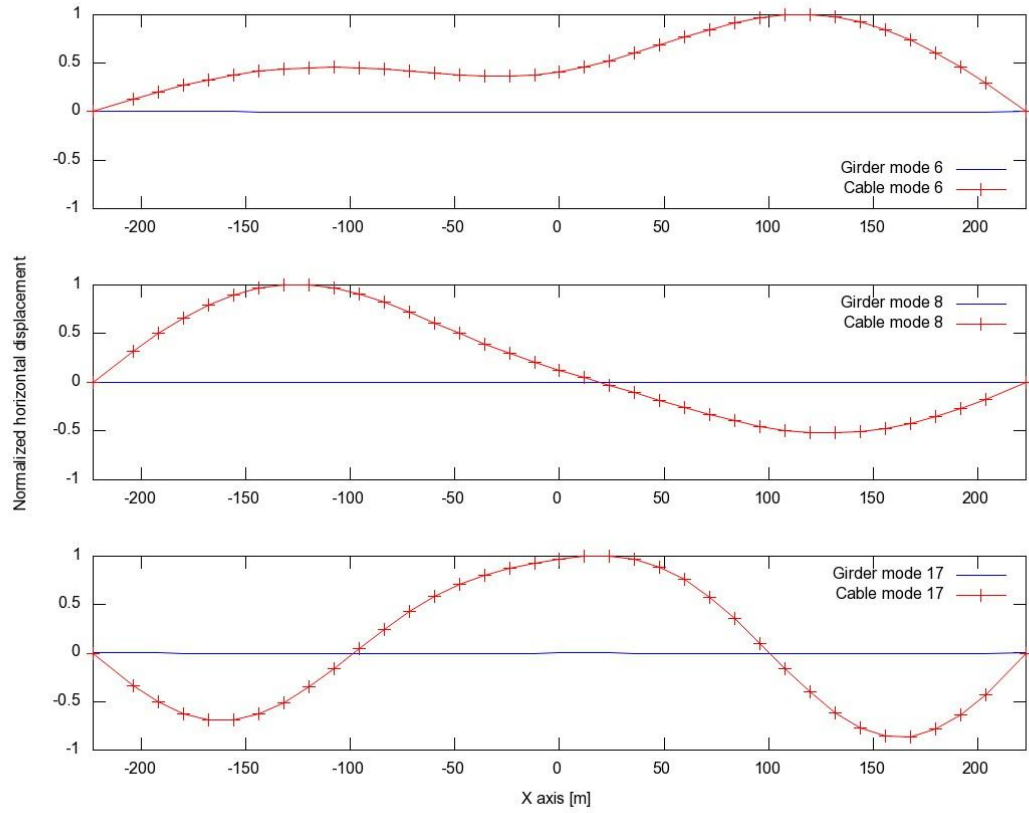


Figure 5-15: First three horizontal main cable modes with high energy and different shape

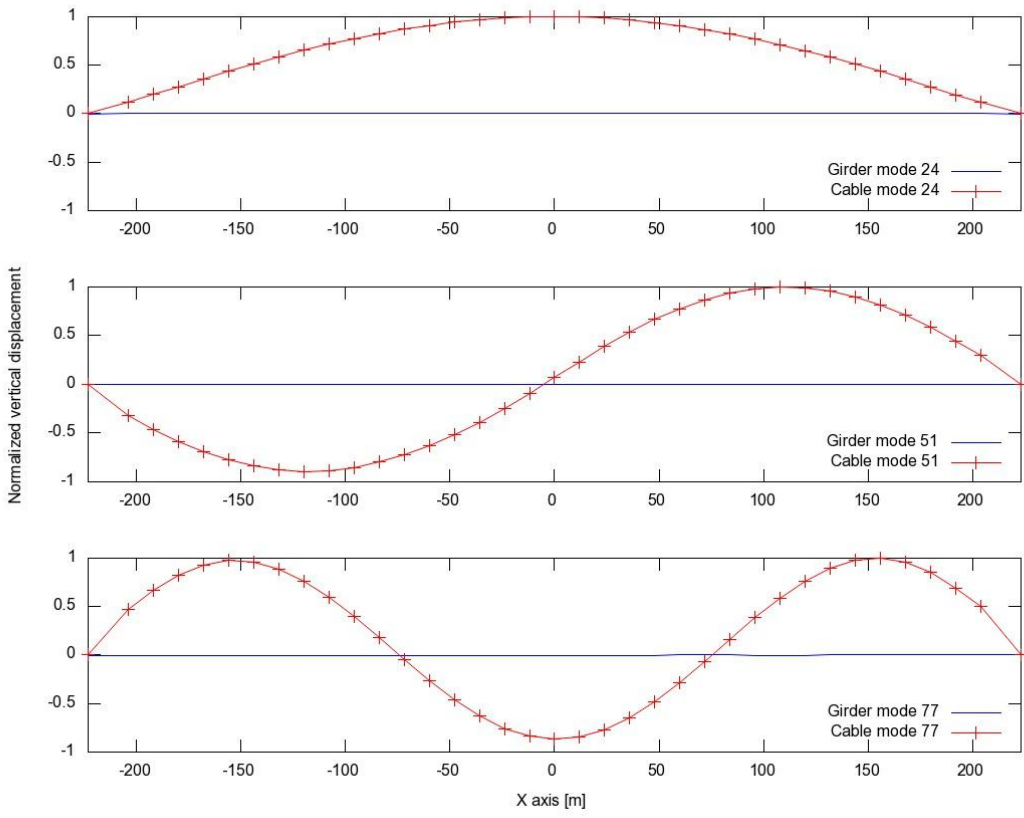


Figure 5-16: First three vertical main cable modes with high energy and different shape.

For the backstay cables, the cables on the east and the west side will “swing” in and out of phase with each other. This can best be viewed in ABAQUS CAE.

5.6. Vortex Induced Vibrations

Vortex induced vibrations of a bridge are motions of the structure excited by a force having the frequency equal to or close to that of the structure, in this case pressure variations due to vortex shedding. It has been seen that structures upstream of the wind may produce wake excitation that can set the bridge into vibrations. Varoddbroa suspension bridge in Kristiansand experienced this type of excitation after a new bridge upstream was built. The wake excitation from the new bridge put the old suspension bridge into vibrations previously unseen.

The flow around the girder cross section depends on the Reynolds number

$$R_e = \frac{U \cdot D}{\nu} \quad (5.9)$$

- U : Wind speed
- D : Height of bridge girder

- ν : Kinematic viscosity of air, 1.51×10^{-5}

Separation of the wind flow on bodies with sharp corners is less affected by the value of R_e . Wind separation is also dependent on railing and other obstacles on the bridge. When the air flow is separated, vortices are produced alternatively on the top and bottom of the girder, producing an alternating force primarily across the direction of the flow.

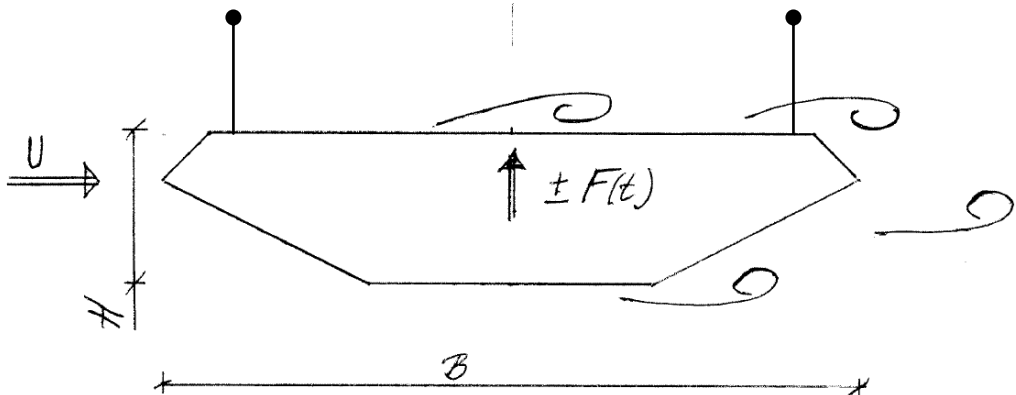


Figure 5-17: Vortexes around bridge girder

Vortex shedding frequency is:

$$f_s = \frac{S_t \cdot U}{D} \quad (5.10)$$

- S_t : Strouhal number
- U : Wind speed
- D : Height or width of the bridge girder

Strouhal number can be set to 0.11 if the width over height ratio is close to 4.5 [13]. Here the ratio is $12.3/2.76 = 4.46$, which is assumed ok $\rightarrow S_t = 0.11$

To find the critical wind velocities, the first two symmetric vertical modes and the 1st asymmetrical vertical mode with a wind velocity that varies linearly from the middle of the bridge to 1/5 of the value at the south end of the bridge are chosen. A harmonic lift force with the force coefficient of 0.5 and the frequency equal to the mode considered will be applied as a uniformly distributed load along the girder for the symmetric modes.

For the asymmetric mode, three different loads will be applied. These are:

- A harmonic lift force with a uniformly distributed load only on the northern half of the bridge with load characteristics as described above.

- A harmonic lift force consisting of a uniformly distributed load on the northern half of the bridge and a parabolic distributed load on the south side of the bridge according to the wind velocity profile mentioned above. The frequency is used uniformly along the bridge.
- A harmonic lift force as described in the bullet above, but where the vortex shedding frequency is adjusted according to the change of wind velocity. All frequencies start at the same time, no phase shifts will be applied.

The assumption is that the bridge vibration frequency will harmonize with the vortex shedding frequencies as the vibration establishes a temporary steady state of oscillation. According to NS-EN [22] the lift factors relevant for this case should be in the range of 0.6-1.0 of the lift force. As the wind velocity goes below 83% of the critical wind velocity, a quasi-static approach becomes more applicable.

The height of the girder D=2.76[m]

Table 5-7: Critical wind velocities for vortex induced vibrations

Mode number	Mode type	Eigenfrequency [Hz]	Eigenfrequency [rad/s]	Wind velocity [m/s]	Lift force [N]
2	Asym.	0.214	1.346	5.4	22
3	Sym.	0.302	1.898	7.6	44
4	Sym.	0.407	2.557	10.2	80

The lift load coefficient $C_{lift} = 0.5$ is used in all load cases. NS-EN [22] describes a distribution of lift coefficients across the wind ratios with $C_{lift} = 0.6$ for the critical wind.

5.6.1. Dynamic analysis in the time domain

Given the eigenfrequencies from the modal analysis, the velocities for vortex induced vibrations can be calculated. The analysis will be run in the time domain and simulated time will be 10 minutes. The damping ratio is set to 0.005 and applied to the appropriate cross sections. The numeric damping in ABAQUS is set to the default value. Parameters for the analysis have been discussed with O. Mikkelsen, and the analysis runs for about 30 minutes of wall clock time. There are several vertical modal shapes that can be excited into VIV, both symmetrical and perhaps also non symmetrical. The reason for trying a non symmetrical shape is based on observations on site. The wind felt when on the bridge was approximately 8-10m/s and approximately from North. After crossing half the bridge, the wind died quickly out, and at the south end the wind was barely noticeable. The map in Figure 5-18 show that Bergsholmen and Syngknuten may have a shielding effect on the bridge for certain wind directions.

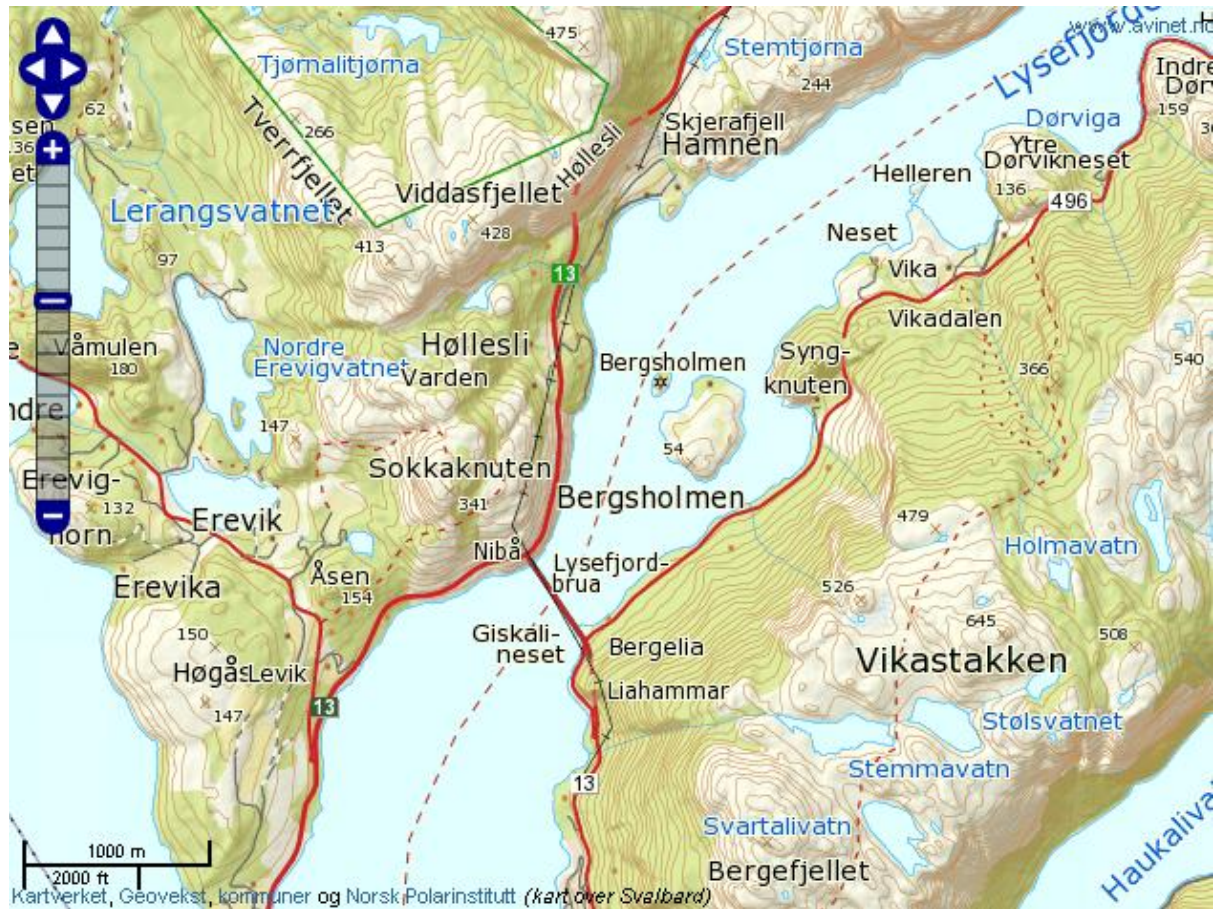


Figure 5-18: Map of Lysefjord bridge and surrounding terrain.

The load applied in ABAQUS is described in more detail above, but generally is a uniform lift load with amplitude that has a harmonic function with the same frequency as the mode in question. The node points used to plot the oscillations are the quarter points 10 and 29, together with the center point 19. The results shown below will present the displacement pattern of the bridge points, indicating that all modes mentioned with the given assumptions will contribute in bridge oscillations.

Trying out the first asymmetric mode is more an academic exercise to see if the model will oscillate with asymmetric and parabolic load. It is also a gross simplification to use a uniform load along the bridge, given that there will be variation of the wind force and hence the vortex shedding resultant force as well.

5.6.1.1. Rayleigh damping coefficients

To provide proper damping, Rayleigh damping coefficients will be calculated for mode 3 and 4

$$\xi = \frac{\alpha}{2\omega_i} + \frac{\beta\omega_i}{2} \quad (5.11)$$

Solving for $\xi = 0.005$ gives $\alpha = 0.0011$ and $\beta = 0.0024$. These values may not be good enough for the asymmetric case. The damping coefficients will be added to the “real” elements in the model, not to any of the dummy elements.

5.6.1.2. First asymmetric mode with VIV load on north half of bridge girder

This load case contains the static wind loads on girder and cables from the critical vortex shedding wind velocity. In addition a harmonic lift load is applied on the northern half of the bridge, as described earlier. Running this harmonic load case gives the following type of displacement in the quarter points along the time axis. As Figure 5-19 shows, the damping coefficients chosen are not sufficient to make the oscillations flatten out within the given time interval. The displacement unit of the figure is [m].

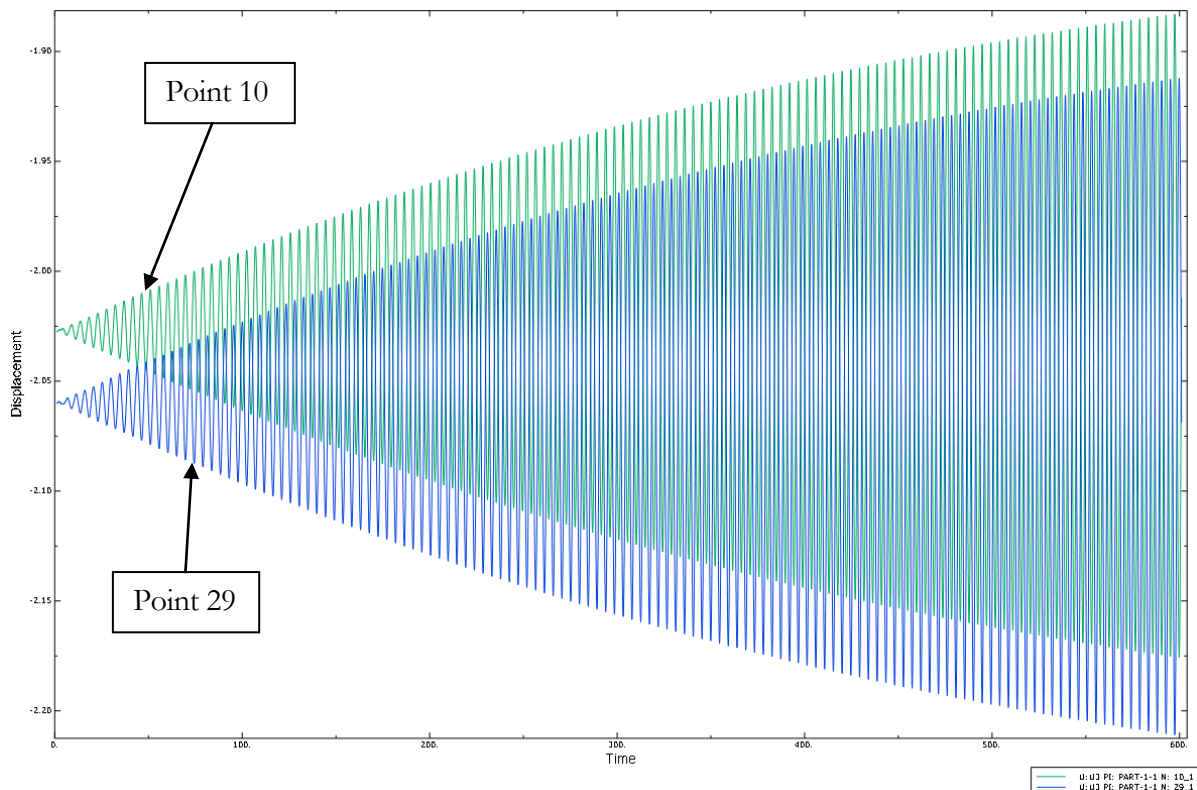


Figure 5-19: Vertical displacement in girder quarter points due to harmonic vortex shedding lift force on half the bridge

5.6.1.3. First asymmetric mode with tapered wind velocity on bridge girder

As shown in Figure 5-20, the wind velocity is assumed to decrease to 1/5 of the critical vortex shedding wind velocity at the southern end of the bridge. The drag force F_d is shown; the other wind forces will have the same distribution along the girder axis, but the magnitudes will differ due to different coefficients. The harmonic vortex shedding lift load will have the same frequency along the entire bridge girder. As Figure 5-21 shows, the displacement is roughly 0.05 m less than in Figure 5-19.

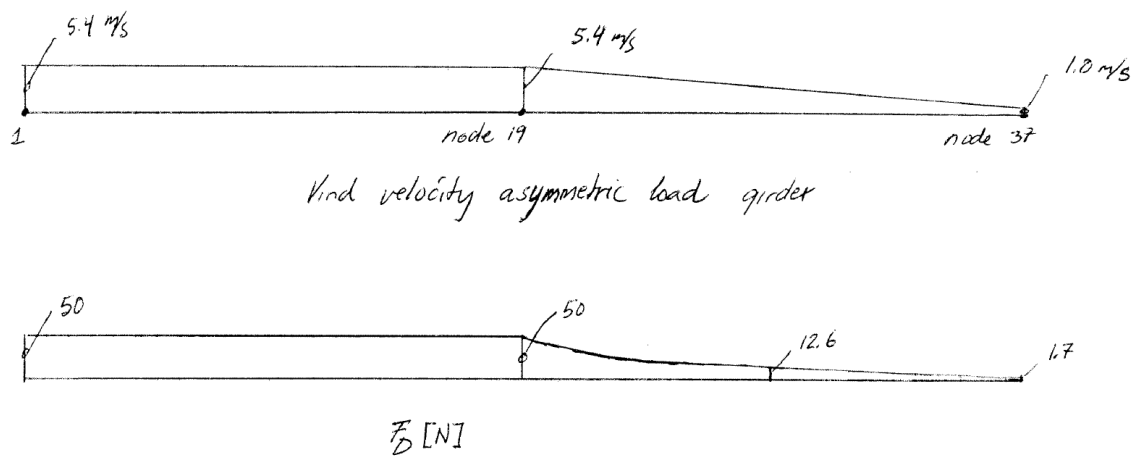


Figure 5-20: Asymmetric wind velocity and force on bridge

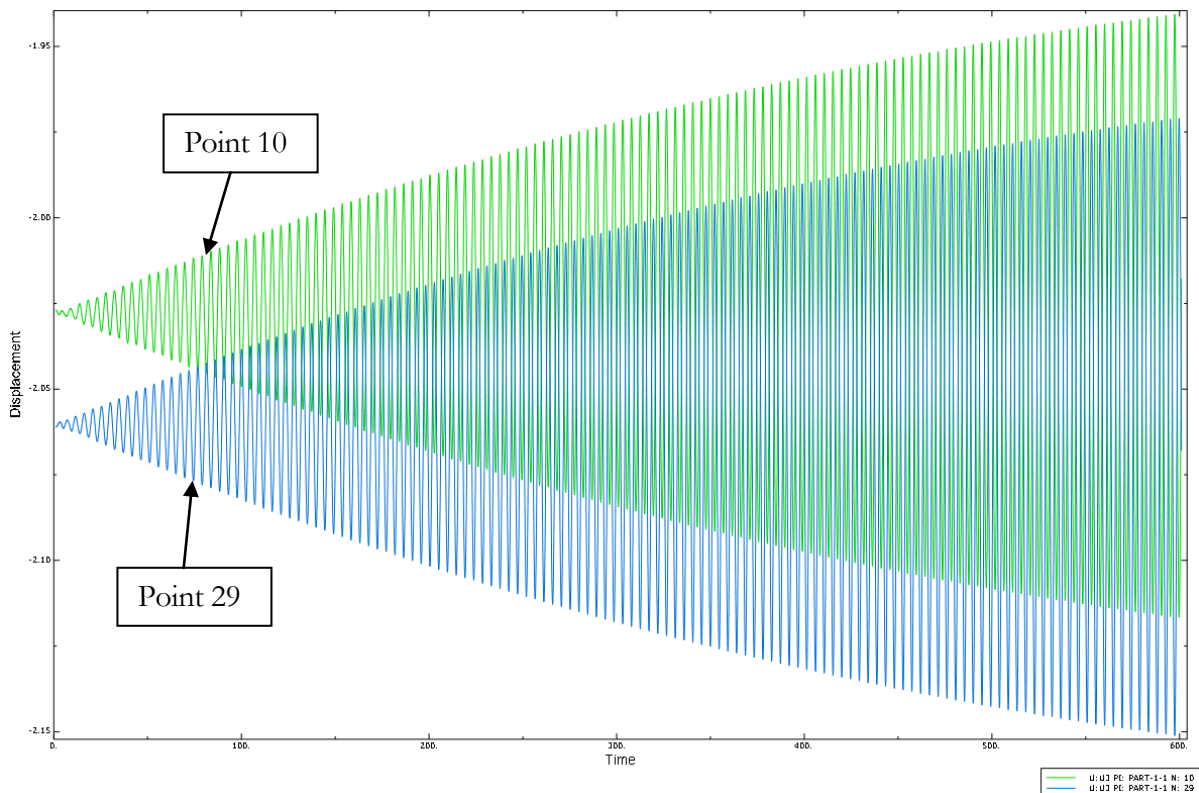


Figure 5-21: Vertical displacement [m] in girder quarter points on tapered harmonic wind lift load

5.6.1.4. First asymmetric mode with tapered wind velocity and changing vortex frequency on bridge girder

This load case is similar to the load case above, but now the vortex shedding frequencies have been corrected to reflect the velocity at each girder element. As Figure 5-22 shows, the displacements for this load case are in line with the load case in chapter 5.6.1.2 with harmonic vortex shedding lift load on only half the bridge. That indicates that the shedding frequency correction gives a more quasi-static load similar to first asymmetric case.

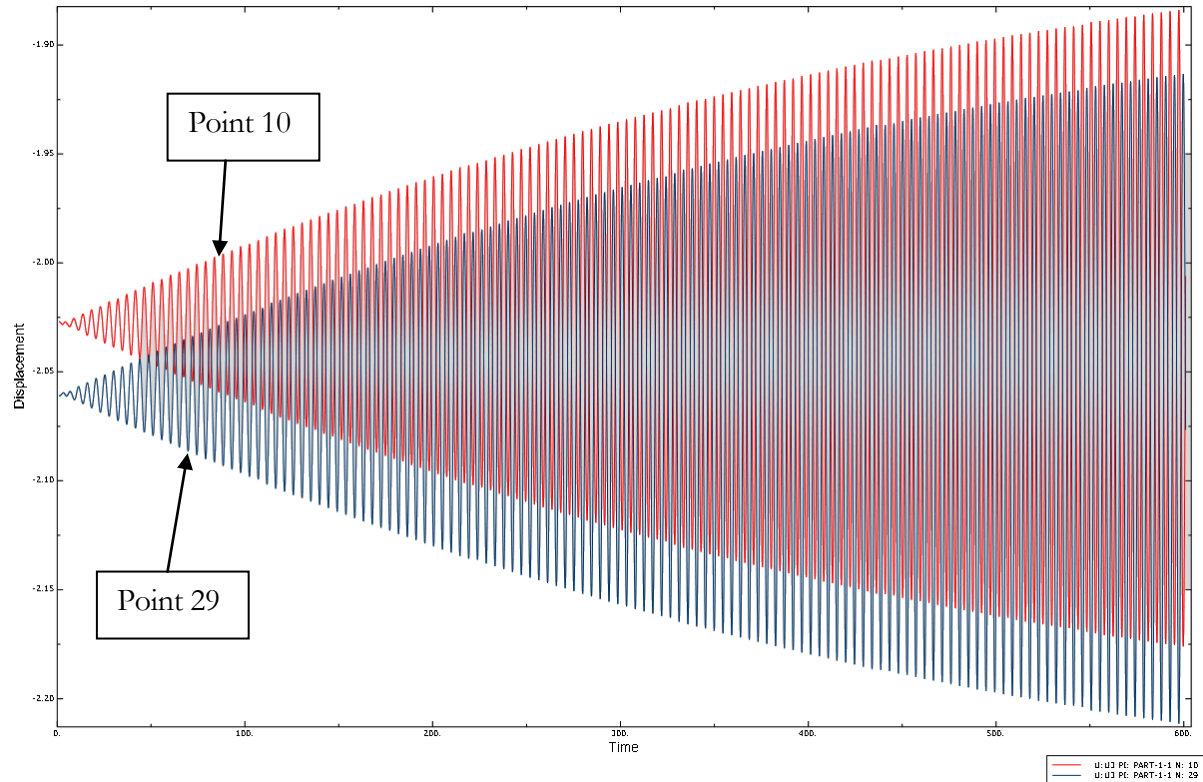


Figure 5-22: Vertical displacement [m] in girder quarter points on tapered harmonic wind lift load with varying vortex shedding frequency

5.6.1.5. First symmetric vertical mode with VIV load

This load case is a uniform harmonic vortex shedding wind lift load along the beam girder with frequency $f = f_{vs1} = 1.8975$ [rad/s] and lift coefficient $C_{lift} = 0.5$ according to the 1st symmetric vertical mode. Even though the first symmetric vertical mode is a composite of the pure modes 1 and 3, the contribution from pure mode 3 is considered small enough to be ignored in this case. See Figure 5-6 for the vertical mode shapes.

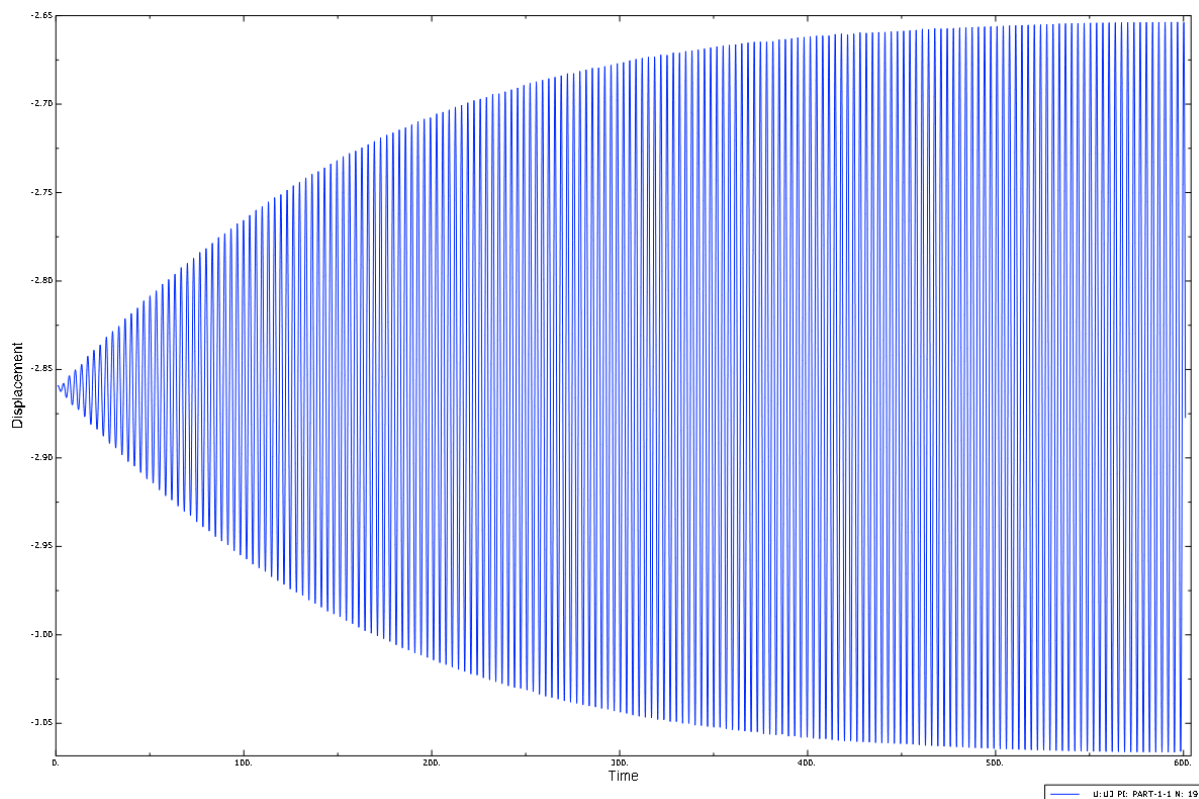


Figure 5-23: Vertical displacement [m] in center point bridge first harmonic symmetric wind lift load.

This simplified load put the bridge in motion as expected. Maximum displacement due to oscillation is 0.204[m]. Looking at the forces in the cable towards north, the loads increase is 3.5% compared to the bridge self load force. The load oscillates from 16987[kN] to 18203[kN], with the mean value of 17580[kN]. The backstay cables have a similar variation of the force, +3.7%. The oscillations contribute very little to the load picture.

5.6.1.6. Second symmetric vertical mode with VIV load

This load case is the uniform harmonic vortex shedding lift force with frequency $f = f_{vs2} = 2.557$ [rad/s] and lift coefficient $C_{lift} = 0.5$ along the girder according to the 2nd symmetric vertical mode.

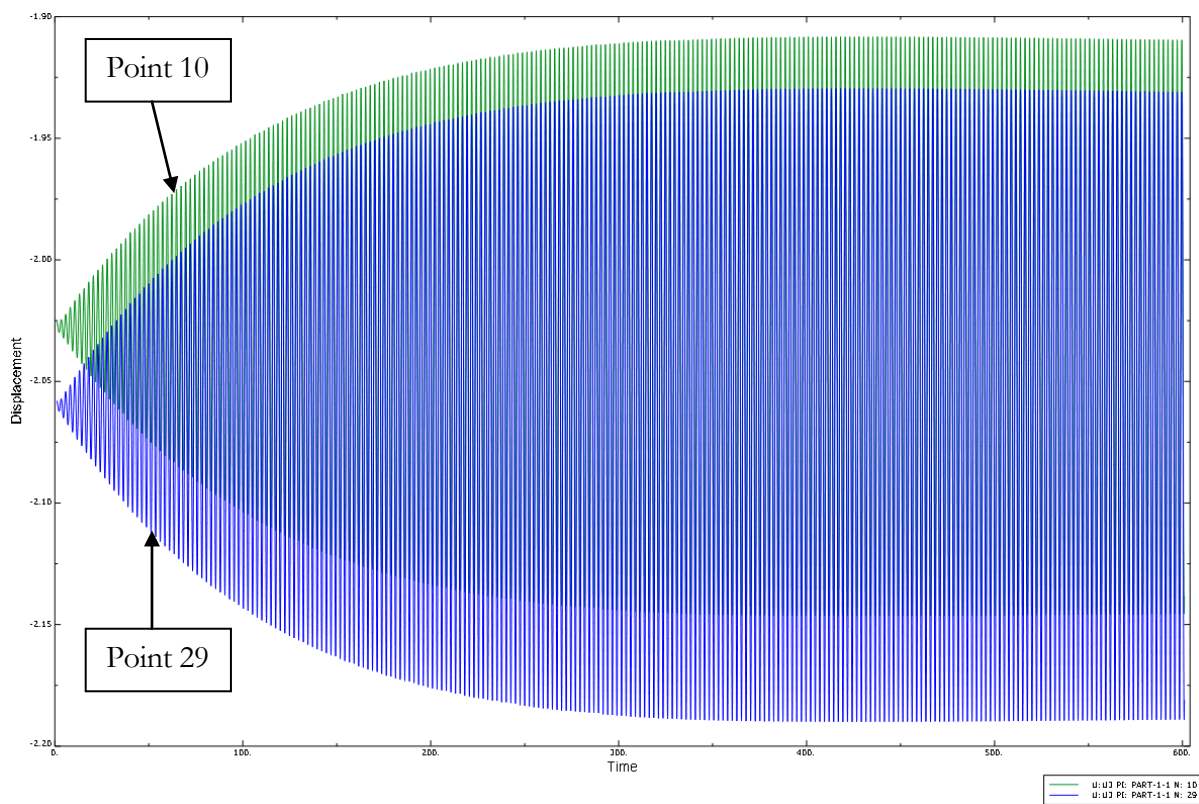


Figure 5-24: Vertical displacement [m] of quarter points on bridge VIV second symmetric lift load.

The increase in cable force is similar to the first vertical symmetrical case, around 3.7%.

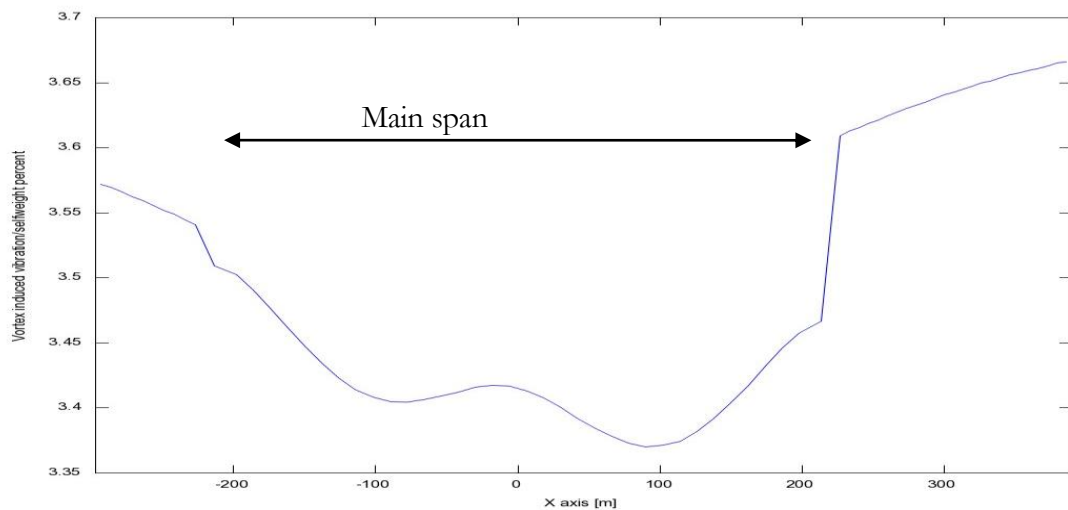


Figure 5-25: Percent increase of cable force at max oscillation due to VIV second symmetric wind lift load

5.6.2. Static equivalent load for VIV

To control that the displacements and forces found from the dynamic run of the model, an equivalent static load, representing the largest inertia forces can be calculated, as well as the associated response. NS-EN 1991[22] provides two methods for calculating the amplitude of the structure across the wind direction. This work will be based on Annex E.1.4 and E.1.5.2 of [22], which has a general formulation assumed usable for the bridge girder. Once again, ABAQUS doesn't provide the option to model a load similar to the mode function, so another FORTRAN routine needs to be devised for that. To apply this load to the girder, the X coordinates of each node is needed to interpolate the value of the mode shape at the given integration point. These are stored in the Fortran subroutine DLOAD by using a load case where a dummy load is put on cross beam elements [4001, 4037]. The next load step, the real load, can then calculate the relative coordinates to use and interpolate the lift load on the interpolation points of the elements. The mode shape used in the FORTRAN subroutine is shown in Figure 5-27

The equivalent static force due to VIV can be expressed by

$$F_w(s) = m(s) \cdot (2 \cdot \pi \cdot n_{i,y})^2 \cdot \Phi_{i,y}(s) \cdot y_{F,max} \quad (5.12)$$

- $m(s)$: mass in motion pr length unit
- $n_{i,y}$: eigenfrequency of structure
- $\Phi_{i,y}(s)$: Mode shape of structure normalized to 1 at point of largest deflection
- $y_{F,max}$: Largest displacement over time with $\Phi_{i,y}(s)$ equal 1

The largest displacement $y_{f,max}$ can be found based on the following equation:

$$\frac{y_{f,max}}{b} = \frac{1}{St^2} \cdot \frac{1}{Sc} \cdot K \cdot K_w \cdot c_{lat} \quad (5.13)$$

- St : Strouhal number
- Sc : Scruton number
- K_w : Effective correlation factor length given in E.1.5.2.4
- K : Form factor given in E.1.5.2.5
- c_{lat} : Aerodynamic excitation factor provided in table E.2

The standard shows how to find the number of lengths needed to calculate the maximum displacement. The cross flow dimension is the height $b = 2.76$ m for wind loads

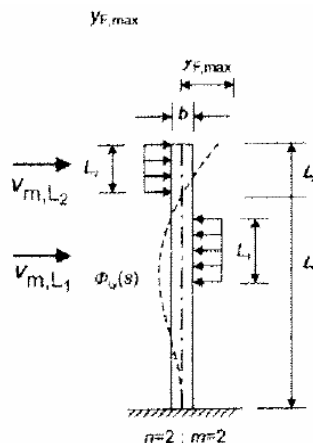


Figure 5-26: Symbol explanation [22]

The first vertical symmetric mode shape is presented in Figure 5-27

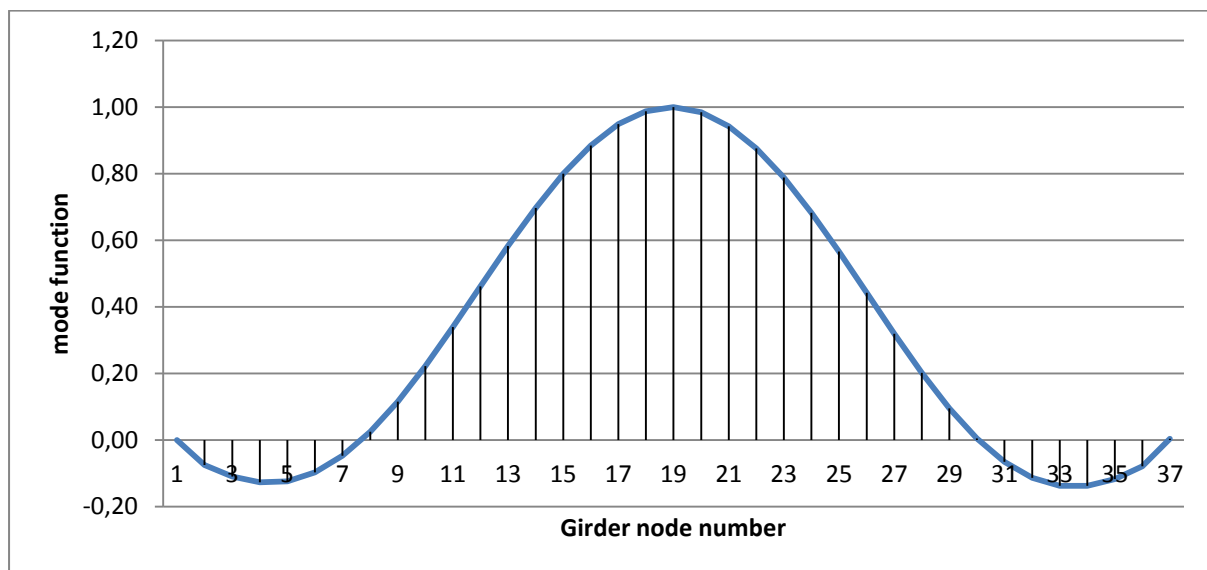


Figure 5-27: First symmetric vertical mode shape

Given the above figures, we have the current lengths in [m] provided that $\frac{y_f}{b} < 0.1$ for all spans

Table 5-8: Length coefficients

L_i	l_i
$6 \cdot b = 16.5$	87.85
$6 \cdot b = 16.5$	267.48
$6 \cdot b = 16.5$	90.67

The Scruton number:

$$S_c = \frac{2\delta_s m_{i,e}}{\rho b^2} = \frac{4\pi\xi m_{i,e}}{\rho b^2} \quad (5.14)$$

- δ_s : damping expressed by the logarithmic decrement
- ρ : air density
- $m_{i,e}$: equivalent mass pr. length for current mode shape
- b : height of cross section

$$K_w = \frac{\sum_{j=1}^n \int_0^{L_j} |\Phi_{i,y}(s)| ds}{\sum_{j=1}^m \int_0^{l_j} |\Phi_{i,y}(s)| ds} \leq 0.6 \quad (5.15)$$

- $\Phi_{i,y}$: mode shape i
- L_j : Correlation length
- l_j : Distance between zero crossing in mode shape
- n : Number of areas where VIV appear at the same time
- m : Number of local displacement maxima for the structure in the modal shape $\Phi_{i,y}$

$$K = \frac{\sum_{j=1}^m \int_0^{l_j} |\Phi_{i,y}(s)| ds}{4\pi \sum_{j=1}^m \int_0^{l_j} \Phi_{i,y}^2(s) ds} \quad (5.16)$$

Equivalent mass pr. length $m_{i,e} = 6166$.

$$\sum_{j=1}^m \int_0^{l_j} |\Phi_{i,y}(s)| ds = 171.0 \quad (5.17)$$

$$\sum_{j=1}^m \int_0^{l_j} \Phi_{i,y}^2(s) ds = 120.33 \quad (5.18)$$

The integration of K and K_w is done numerically by spline fitting the curve and re-sampling to $dX = 1.0\text{m}$ and integrating the parts. Octave was used for that.

$$K_w \approx \frac{2.15 + 16.95 + 2.34}{171} = 0.125$$

$$K \approx \frac{171}{4 \cdot \pi \cdot 120.33} = 0.113$$

$$S_c = \frac{4 \cdot \pi \cdot 0.005 \cdot 6166}{1.25 \cdot 2.76^2} = 40.687$$

The coefficient $c_{lat} = 0.5$

$$\frac{y_{f,max}}{b} = \frac{1}{0.11^2} \cdot \frac{1}{40.687} \cdot 0.113 \cdot 0.126 \cdot 0.5 = 0.0145$$

$$y_{f,max} = 0.0145 \cdot 2.76 = 0.04$$

Now the force function is found and can be applied to the girder. The load is applied in negative z direction.

$$F_w(s) = 6166 \cdot 1.898^2 \cdot \Phi_{i,y}(s) \cdot 0.04 = \Phi_{i,y}(s) \cdot 889 \frac{N}{m}$$

This load function is applied to the model to verify that the actual displacements are in the same range as $y_{f,max}$. Running the model in ABAQUS with the mentioned FORTRAN user function shows that the displacement due to the VIV static load at mid span is 0.04m. So the values are equal, but the displacement itself is far from the displacement found in the dynamic analysis.

Looking at the equations, it seems like the correlation lengths of the load play an important role. The fact that all correlations lengths are the same for this span may be one contributing factor for the difference in the resulting values.

It is unclear if the simplified harmonic load gives too large deflections, but the difference in the numbers here may suggest that. The wind variations along the bridge girder and aerodynamic damping will affect the real dynamic deflection and possibly give smaller deflections.

6 Validation of eigenfrequencies and eigenmodes

The eigenfrequencies and eigenmodes can easily be found from programs like ABAQUS and Alvsat. Given the amount of input data needed and perhaps geometrical complexity, there is a fair chance that errors may have been introduced into the model.

To check that the results from the analysis are reasonably correct, simple “hand” calculations will be done. The bases for these calculations are articles from Bleich [4] and Steinman [5]. For the vertical modes, the above mentioned references are well suited and considered classics. When it comes to torsion, the references assume that the bridge girder is a composite of trusses vertically and in some cases horizontally as well. For that reason, great measure has gone into transforming the torsion energy into internal energy of the different truss elements. Nowadays most of the girders are always a closed cross section with excellent torsion capacity. Due to that, some effort has gone into transforming Bleich’s energy approach into using the torsion internal energy directly instead transforming the girder’s cross section values into the original approach.

Maple and OpenAxiom has been used to solve the equations from Bleich with regard to ω^2 . Also all the energy equations have been solved symbolically in OpenAxiom and solved with regard to ω^2 by substitution of the bridge constants into the equations at the end.

6.1. Basic definitions

In the following, definitions will be listed to be used later in the chapter. Also values relevant to the bridge will be tabulated.

- m : mass of main span
- w : weight of main span per meter
- E : Modulus of elasticity bridge girder
- I : Moment of inertia around weak axis
- H_w : Horizontal force in cable due to dead load
- l : Length of main span
- L_E : Length of cable from hold down to hold down
- E_c : Modulus of elasticity of cable
- A_c : Cross section of cable
- m_f : Mass moment of inertia
- G : Modulus of rigidity
- f : Height of cable parabola
- b : Width between main cables
- J : Moment of torsion

For the associated values, see Table 6-1.

Table 6-1: Bridge constants

Symbol	Value
H_w	33556000 [N]
m	6166 [kg]
w	60488 [N]
E	2.1e11 [Pa]
I	0.429 [m^4]
l	446 [m]
G	0.8e11 [Pa]
J	0.929 [m^4]
L_E	720 [m]
E_c	1.8e11 [Pa]
A_c	0.05 [m^2]
f	45 [m]
b	10.25 [m]
m_I	82430 [$\frac{\text{kg}\text{m}^2}{\text{m}}$]

6.2. Basic assumptions

The theory and equation from Bleich [4] is based on the following assumptions:

- The amplitude of vibrations are small, and the additional horizontal cable force h is small compared to the initial cable force H_w due to the dead load.
- The dead load g and moment of inertia I are constant throughout each span, but may vary in different spans.
- The total mass of the bridge is assumed to be concentrated along the centerline of the bridge girder, girder fixed at one end.
- The hangers are considered inextensible, assuming that vertical deflection of cables and girder are equal.

These assumptions hold quite well for Lysefjord Bridge. In the ABAQUS model the mass has been spread to three mass points to keep the mass moment of inertia correct, and the hangers are of course elastic, since normal E modulus values have been given for them.

Bleich has used both a differential approach and an energy approach to find the symmetric and asymmetric modes of the system.

6.3. Vertical asymmetric modes

The following differential equation is found in Bleich:

$$m \frac{\partial^2 \eta}{\partial t^2} + EI \frac{\partial^4 \eta}{\partial x^4} - H_w \frac{\partial^2 \eta}{\partial x^2} + \frac{w}{H_w} h = 0 \quad (6.1)$$

- η : amplitude at distance x from the left point of attachment at time t

- h : Additional horizontal force in cable due to amplitude

The solution to the equation for the vertical asymmetric modes from equation (6.1) is

$$\omega(n) = \frac{n\pi}{l} \sqrt{\frac{g}{w}(H_w + n^2\lambda)} \quad (6.2)$$

- n : Number of sinusoidal half waves
- l : Length of main span
- $\lambda = \frac{\pi^2 EI}{l^2}$

Steinman [5] has based his equations on the fundamental equilibrium equation for a suspension bridge. The equations are identical to Bleich for vertical asymmetric modes, but presented in a different form

$$w = \frac{\partial^2}{\partial x^2} (H\eta + y \Delta H - EI \frac{\partial^2 \eta}{\partial x^2}) \quad (6.3)$$

- $H = H_w$: Horizontal cable force
- ΔH : The increment produced by displacement
- η : amplitude at distance x from the left point of attachment at time t

The Coefficient of Rigidity; $K(n)$, of the oscillating system is a significant criterion for aerodynamic stability.

$$K(n) = \frac{n^2 \pi^2}{l^2} H_w + \frac{n^4 \pi^4}{l^4} EI \quad (6.4)$$

$$\omega(n) = \sqrt{\frac{K(n)}{\frac{w}{g}}} \quad (6.5)$$

6.3.1. Asymmetric modes for the bridge

Putting the values into the Steinmann equations gives

n	$\omega(n)$	Alvsat	ABAQUS
2	1.2867 [rad/s]	1.339	1.8975
4	3.6781 [rad/s]	3.701	2.5572
6	7.5058 [rad/s]	7.530	5.3778

6.4. Vertical symmetric modes

To compute the vertical symmetric mode, the energy equation for one span suspension bridge is

$$T - V = \frac{1}{2} \left(\frac{w}{g} \omega^2 \int_0^l \eta^2 dx - EI \int_0^l \eta''^2 dx + H_w \int_0^l \eta'' \eta dx - \frac{8f}{l^2} h \int_0^l \eta dx \right) \quad (6.6)$$

$$\frac{8f}{l^2} \int_0^l \eta dx - \frac{L_E h}{E_c A_c} = 0 \quad (6.7)$$

$$\eta = a_1 \sin\left(\frac{\pi x}{l}\right) + a_3 \sin\left(\frac{3\pi x}{l}\right) \quad (6.8)$$

- T : Maximum kinetic energy as a function of η
- V : Maximum potential energy as a function of η

From the two energy equations the following equation for the 1st and 2nd vertical symmetric mode are derived. The derivation is based on the fact that the energy ($T - V$) is minimized. This is done by the Ritz method. For the full detail of the derivation, see [4]. The solution is

$$Ak + 9B(k - Ap) = 0 \quad (6.9)$$

The parameters that are part of the equation:

$$A = s\omega^2 - H_w - \lambda = s\omega^2 + C_A \quad (6.10)$$

$$B = s\omega^2 - 9H_w - 81\lambda = s\omega^2 + C_B \quad (6.11)$$

$$s = \frac{wl^2}{\pi^2 g} = \frac{ml^2}{\pi^2} \quad (6.12)$$

$$\lambda = \frac{\pi^2 EI}{l^2} \quad (6.13)$$

$$k = \frac{32f}{\pi^3} \quad (6.14)$$

$$p = \frac{\pi l}{16f} \frac{L_E}{E_c A_c} \quad (6.15)$$

Solving for ω^2 with OpenAxiom[16] gives

$$\omega^2 = \frac{\pm \sqrt{81(C_B - C_A)^2 p^2 + 144k(C_B - C_A)p + 100k^2} + 9p(-C_B - C_A) + 10k}{18ps} \quad (6.1)$$

For $n > 3$, the eigenfrequencies can be written as

$$\omega(n) = \sqrt{\frac{1}{s} (n^2 H_w + n^4 \lambda + \frac{k}{n^2 p})} \quad (6.17)$$

$$a_3 = \frac{A}{3B} a_1 \quad (6.18)$$

Table 6-2: Bleich and ABAQUS vertical symmetric frequency table

	Bleich	Alvsat	ABAQUS
ω_1 [rad/s]	1.5813	1.800	1.8975
ω_3 [rad/s]	2.4117	2.514	2.5572
ω_5 [rad/s]	5.4155	5.445	5.3778
a_{11}, a_{31}	1, -0.275	1,-.442	2.125,-0.924
a_{13}, a_{33}	1, 3.887	0.441,1	-0.95, 2.904

These frequencies found are for pure frequencies, while the symmetric vertical modes on Lysefjord are combinations of mode 1, 3 and 5. The symbols a1 and a3 in the table show the non normalized contributions of each mode.

The equations from Steinman to find the vertical symmetric eigenfrequencies:

$$\sum_{n=1,3,5..} \frac{1}{n^2} \frac{C f}{K - K(n)} = 1 \quad (6.19)$$

$K(n)$ is defined in (6.4).

$$C = \frac{512}{\pi^2} \frac{f E_c A_c}{l^2 L_E} \quad (6.20)$$

The equations from Steinman are solved in Maple, see APPENDIX D. But the resulting values are the same as those from Bleich, thus they are not repeated here.

6.5. Torsional eigenfrequencies and modes

6.5.1. Symmetric torsion modes

The symmetric torsion modes are calculated based on Bleich's equations. The equation is modified to directly include the torsion stiffness of the bridge girder, instead of the rectangular truss girder equivalent.

The potential energy of a beam in torsion [11]:

$$V_T = \int \frac{T^2}{2GJ} dx \quad (6.21)$$

$$T = GJ \frac{d\eta}{dx} = GJ\eta' \quad (6.22)$$

$$V_T = \frac{GJ}{2} \int \eta'^2 dx \quad (6.23)$$

Substitution into the energy equation

$$\begin{aligned} T - V &= \frac{1}{2} (m_I \omega^2 \int_0^l \phi^2 dx - (GJ + \frac{H_w b^2}{2}) \int_0^l \phi'^2 dx \\ &\quad - \frac{8fb}{l^2} h \int_0^l \phi dx) \end{aligned} \quad (6.24)$$

$$\frac{L_E h}{E_c A_c} - \frac{4fb}{l^2} \int_0^l \eta dx = 0 \quad (6.25)$$

$$h = \frac{E_c A_c}{L_E} \frac{4fb}{l^2} \int_0^l \eta dx \quad (6.26)$$

$$\begin{aligned} T - V &= \frac{m_I \omega^2}{2} \int_0^l \phi^2 dx - (\frac{GJ}{2} + \frac{H_w b^2}{4}) \int_0^l \phi'^2 dx \\ &\quad - \frac{E_c A_c}{L_E} \left(\frac{4fb}{l^2} \right)^2 \left(\int_0^l \phi dx \right)^2 \end{aligned} \quad (6.27)$$

Note the change from Bleich is the value of R, and the fact that Λ is removed from the equation.

$$B(A - K) - \frac{AK}{9} = 0 \quad (6.28)$$

$$A = s\omega^2 - R \quad (6.29)$$

$$B = s\omega^2 - 9R \quad (6.30)$$

$$R = \left(\frac{GJ}{2} + \frac{H_w b^2}{4} \right) \frac{\pi^2}{2l} \quad (6.31)$$

$$K = \frac{E_c A_c}{L_E} \frac{64f^2 b^2}{\pi^2 l^2} \quad (6.32)$$

$$s = \frac{m_I l}{4} \quad (6.33)$$

$$J = \frac{4A^2}{\oint \frac{dl}{t}} \quad (6.34)$$

- m_I : Mass moment of inertia
- G : Modulus of rigidity

Solving for ω^2 gives

$$\omega^2 = \frac{\pm\sqrt{5184R^2 - 1152RK + 100K^2} + 90R + 10K}{18s} \quad (6.35)$$

Table 6-3: Torsional symmetric frequencies

	Bleich	Alvsat	ABAQUS
ω_1 [rad/s]	7.4561	7.2533	6.825
ω_3 [rad/s]	20.4148	20.3611	17.896

6.5.2. Asymmetric torsion modes

For the asymmetrical case, the cable tension h becomes zero. By cancelling the term depending on h , the equation takes form of

$$T - V = \frac{1}{2}(m_I\omega^2 \int_0^l \phi^2 dx - (GJ + \frac{H_w b^2}{2}) \int_0^l \phi'^2 dx) \quad (6.36)$$

$$\phi = a_2 \sin\left(\frac{2\pi x}{l}\right) + a_4 \sin\left(\frac{4\pi x}{l}\right) + \dots \quad (6.37)$$

Differentiation of $T - V$ with respect to a_2 , a_4 , etc leads to a series of independent frequency equations defining the first, second and so on.

$$\omega_1^2 = \frac{2^2 R}{s} \quad (6.38)$$

$$\omega_3^2 = \frac{4^2 R}{s} \quad (6.39)$$

$$\omega_{n-1}^2 = \frac{n^2 R}{s} \quad (6.40)$$

	Bleich	Alvsat	ABAQUS
ω_1 [rad/s]	13.592	13.351	11.673
ω_3 [rad/s]	27.185	27.183	23.149
ω_5 [rad/s]	40.777	41.035	31.938

7 Conclusion

This thesis presents a dynamic analysis of Lysefjord Bridge, in particular looking at loads that may increase the stress levels in the main cables. Since the main cables have a steady rate of wire breaks in the main cables, some of the loads on the bridge that increase the tension levels in the cables were investigated. The finite element model from Steigen [1] was checked and used in this analysis, together with the structure and wire fracture data provided from the Norwegian Public Roads Administration. Weather data from nearby weather stations were used to compare possible loading conditions at the time of the wire fracture. The main structural components of a suspension bridge have been presented together with a brief introduction of the load carrying capabilities of the different structural components. Different load types have been analyzed to look at the increase in tensile force of the main cables, amongst these vortex induced vibrations. These appear at wind velocities that occur regularly on the bridge.

The conclusion of the work is that there is more than one reason for the fractures of the wires in the main cables. There are more cable breaks with temperatures below 10°C than above. Fractures seems to come in pairs, more than 50% of the fractures happen with time intervals less than 3 days. On the other hand over 50% of the wire fractures happen at velocities less than 3 m/s. The critical wind speeds for vortex induced vibrations of the bridge girder has been found, and the a dynamic analysis has been performed with these wind velocities in the time domain. The load setup has been very simple, no distribution of wind velocities along the bridge girder, only a uniform harmonic load.

The finite element model in ABAQUS from Steigen [1] has been checked and modified a little according to findings in the model. The outputs from the analysis have been in the same order of magnitude as findings by Steigen. The structure of the element model has been presented, and cross section data of the girder have been checked. The deformed geometry of the bridge has been checked, and are within +0.07m from the theoretical position of the bridge with the bridge deadload applied.

The load cases run on the bridge have been wind loads, lorry load train, temperature load and vortex induced vibration loads. The static wind loads have been applied up to arrival of negative values in the system matrix, but the applied wind velocity is some distance away from collapse due to the static torsional capacity. This analysis needs input from a FORTRAN load file to correct the loads according to the rotation of the girder. This exercise requires a bit knowledge of how ABAQUS solves a non linear problem and how the FORTRAN subroutine can be signaled to enter various compute states. The lorry load train input deck has been generated from Python, and the results from the run have been parsed in Python to generate the load position plot. Temperature load has just been a simple uniform temperature difference to find the distribution of the additional stresses in the cable. None of the loads run give any significant increase of the cable force, all are well within service limits.

The frequencies and modes shapes have been checked by theoretical calculations, the same has been done for the vortex induced vibration amplitudes and torsional girder collapse wind velocity. The frequency values and mode shapes are in reasonable agreement with both Alvsat and Bleich values apart from the torsion eigenmodes. Torsional eigenfrquencies differ more, thus more attention has been paid to the mass distribution in this thesis. The Bleich equation has been modified to directly incorporate the torsion stiffness of the bridge girder, thus the equations are now directly applicable for closed girder cross sections. None of the theoretical calculations have

taken tower stiffness into account, neither does Alvsat. That is probably why the ABAQUS model is slightly softer than the other calculations, since the tower is part of this model. The equivalent static check of vortex induced vibrations have been performed according to NS-EN [22], the resulting displacement found is different from the displacements found in the ABAQUS dynamic runs. The load from the hand calculation are again run in ABAQUS to check that the model gets the correct amount of deflection, and these values agree. Here yet another FORTRAN load subroutine is needed, only uniform line loads are available in ABAQUS. And the same signaling regime is used to collect appropriate data while running the loads.

Unfortunately the process of instrumenting the bridge with accelerometers and wind gauges have taken longer than hoped. It would have been interesting to check some data collected on the bridge to see if other patterns would have emerged. But hopefully there will be a chance to have a look at them at a later stage.

8 Future recommendations

As the monitoring system of wind and bridge girder movement becomes functional, the collected data will provide new insight. One suspicion is that the wind velocities will be higher than the ones found at the existing weather station at Forsand. The wind directions are assumed to be more along the direction of the fjord. On the vibrations of the bridge, can effects like vortex induced vibrations be observed on the girder measurements?

Setting up proper wind distributions based on onsite measurements is of prime interest. Running dynamic analysis with these loads and comparing these with the simplistic loads in this thesis will provide valuable insight. Hopefully the FORTRAN examples in this thesis can serve as a guideline. Other and better analysis options may be the random response analysis functionality in ABAQUS. This may require changes in the element model.

Exploring the load history of the bridge would also provide valuable insight. Finding the number of cycles both wind and traffic load applies to the structure will be very interesting. Prediction of the fatigue on the cables and thus lifetime of the bridge with the load history would be very interesting.

Running dynamics analysis in general, how can that best be done? Are there better options in ABAQUS, like steady state dynamics? Are element model changes required, what are the differences in runtime and results. What would be a more precise way to find and setup damping coefficients for the model?

On the finite element model of Lysefjord Bridge, further investigations can be done. Today the model of the bridge girder, cables and hangers are all B31 type elements. What would the runtime cost be to use higher order elements, like FRAME3D elements. There are more equations to solve, but will that be noticeable? This can be split into two parts, one for the nonlinear static analysis part and one for the nonlinear dynamic analysis part. Also the parallel option in ABAQUS could be investigated. Today all runs are done on one CPU. What difference will more CPU's have on the runtime? What does the speedup profile look like for different analysis types.

To step outside our institute a bit, making a statistical model of the wire fractures would be of interest. The report from Blom Bakke has an appendix where Norsk Regnesentral performed a statistical analysis in 2001. Today the amount of measured data is much larger, and perhaps this is an interesting topic for a thesis in the math department.

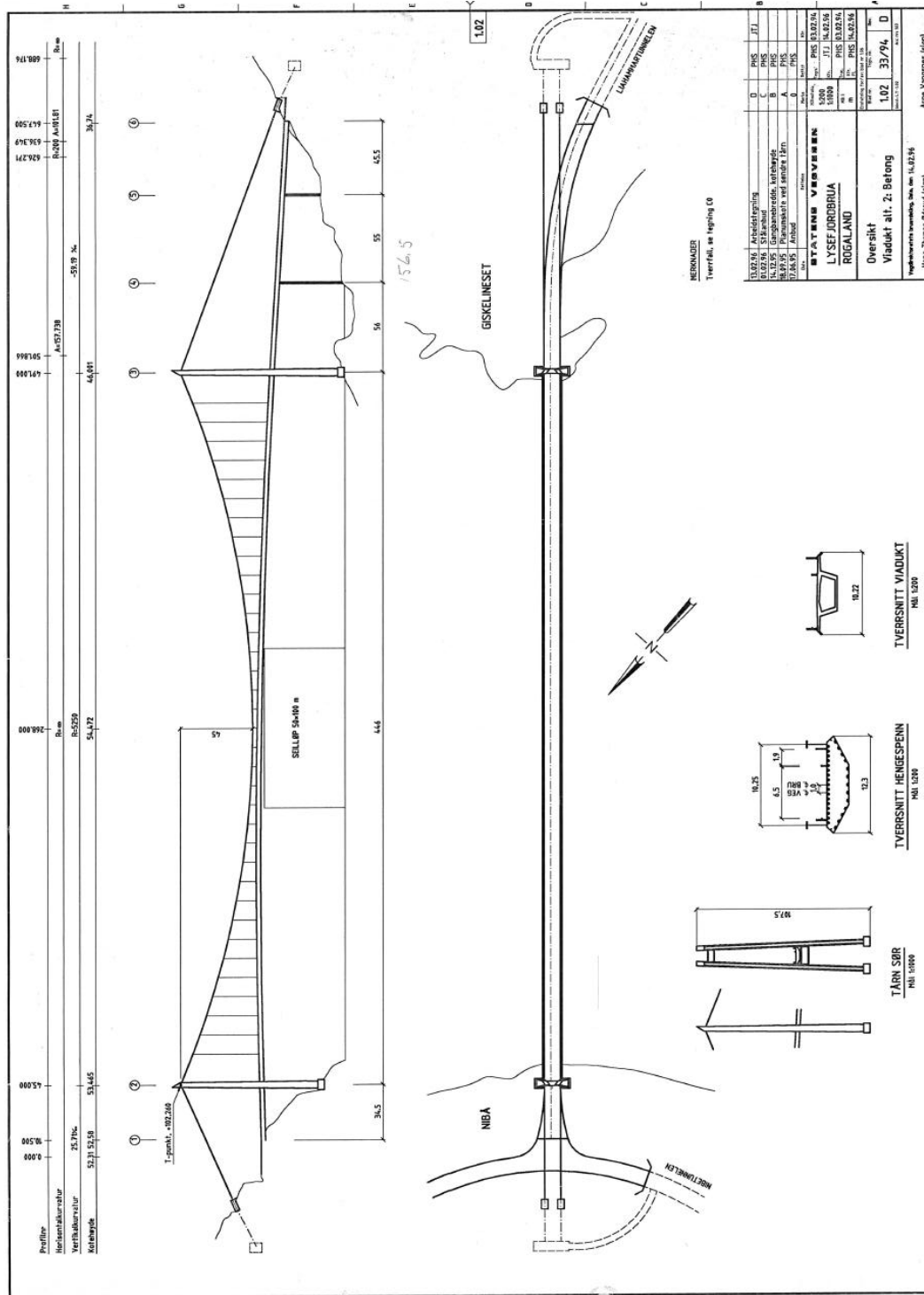
Since lifetime analysis of structures is becoming increasingly more important, an introduction course in signal analysis should be made an optional course in the curriculum.

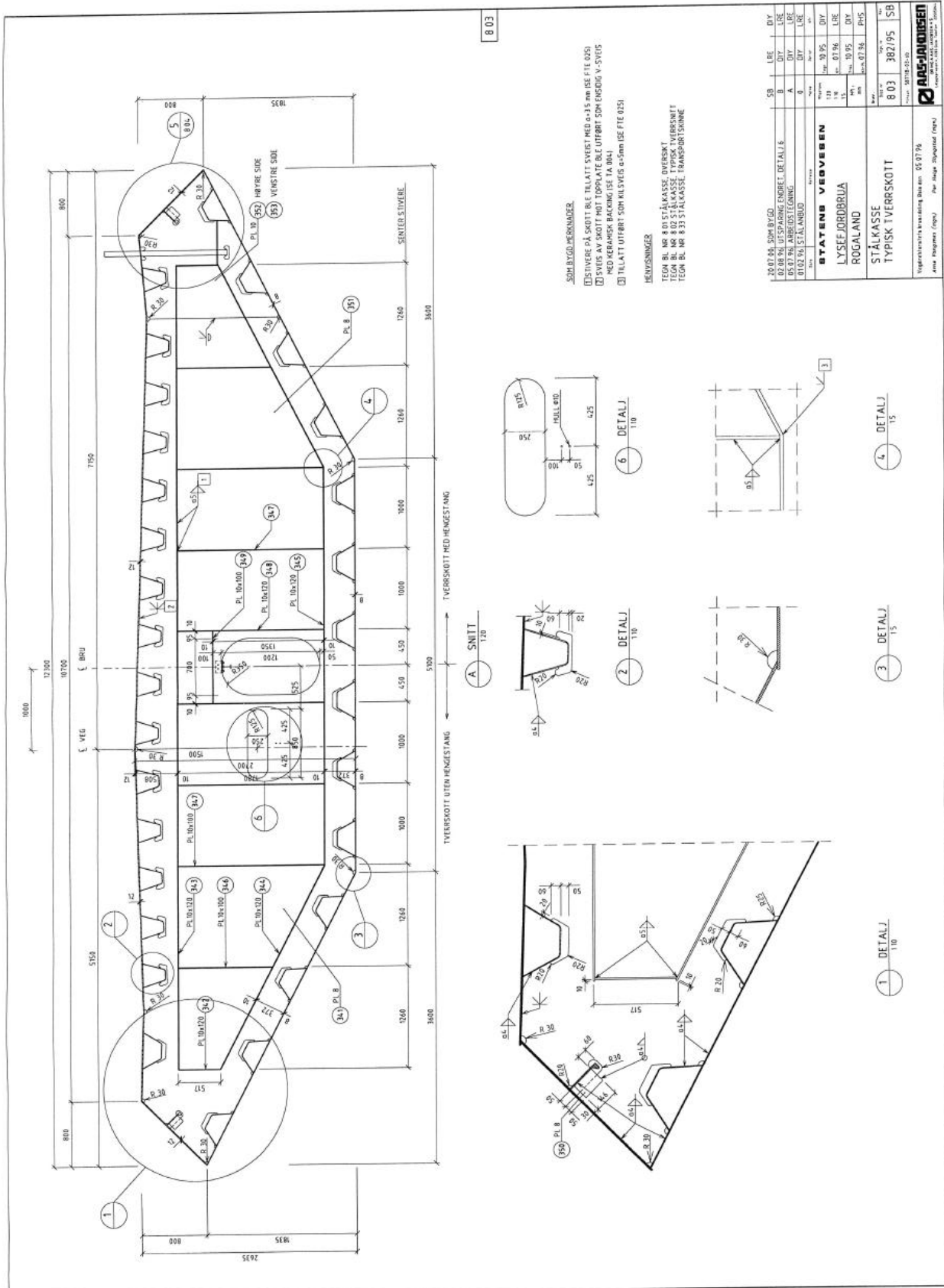
BIBLIOGRAPHY

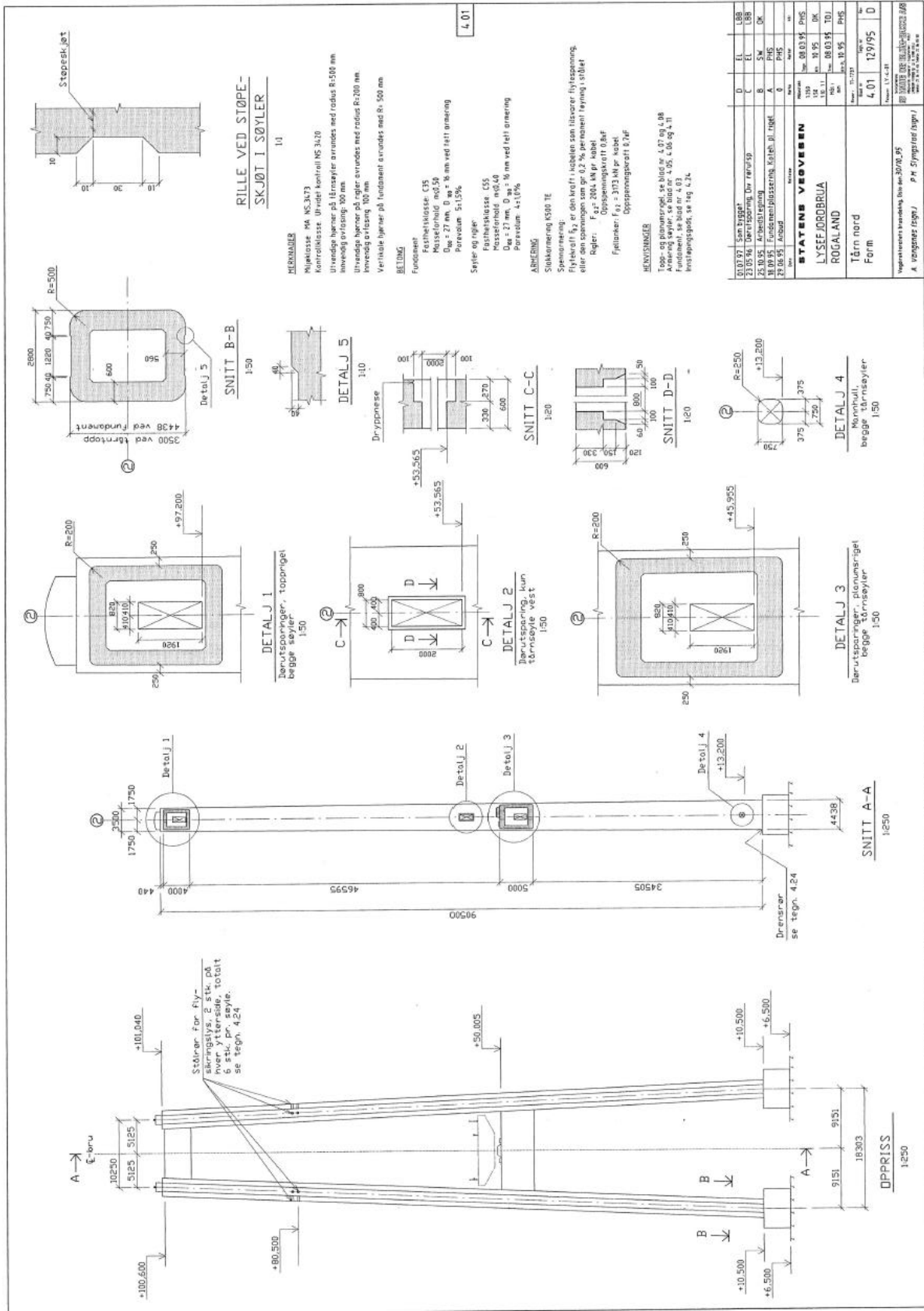
- [1] Steigen, R.O. Modeling and analysing a suspension bridge in light of deterioration of the main cable wires, Master's thesis, UiS, 2011.
- [2] AAJ. Beregninger av egenfrekvenser for lysefjordbrua. Tech. rep., Statens Vegvesen, 1999.
- [3] Auvray, M. Lysefjord suspension bridge acoustic monitoring from 01/10/2011 to 31/12/2011. Tech. Rep. NOR0159 REP 407, Advitam, 2011.
- [4] Bleich, F., McCullough, C., Rosecrans, R., and Vincent, G. S. *The mathematical theory of vibration in suspension bridges: a contribution to the work of the Advisory Board on the Investigation of Suspension Bridges*. Department of commerce, Bureau of public roads, 1950.
- [5] Steinman, D. B. Modes and natural frequencies of suspension bridge oscillations. *Journal of the Franklin Institute* 268, 3 (1959), 148 – 174.
- [6] Bjørnsen, I. P. Static and dynamic analysis of a suspension bridge excited by wind load. Master's thesis, UiS, 2007.
- [7] Ebeltoft, R. G. Lysefjord bridge, visual inspection of cable breakage. Tech. rep., Statens Vegvesen, 2008 - 2010.
- [8] Inc, A. *ABAQUS, Analysis users manual*, version 6.4 ed., 2003.
- [9] Gimsing, N. J. *Cable supported bridges, concept and design*, 3nd. ed. John Wiley and Sons, New York USA, 2012.
- [10] Gjerding-Smith, K. Rv 13 lysefjordbrua, trådbrudd i kabler, konsekvenser og tiltak. Tech. Rep. 2001-06, Sivilingeniørene Haug og Blom-Bakke AS, 2004.
- [11] Boresi, A.P,Schmidt,A.P. Advanced mechanics of materials
- [12] Sapountzakis, E.J, Mokos,V.G. A BEM solution to transverse shear loading of beams, Comput Mech(2005) 36:384-397
- .
- [13] Hjorth-Hansen, Strømmen, E., Bogunovic Jakobsen, J., Brathaug, H.-P., and Solheim, E. Wind tunnel investigations for a proposed suspension bridge across the hardanger fjord. Tech. Rep. 3, Balkema, 1993. Moan et al., (eds.).
- [14] Inc, A. *ABAQUS, Analysis users manual*, version 6.4 ed., 2003.
- [15] Maple, www.maplesoft.com.
- [16] OpenAxiom, www.open-axiom.org

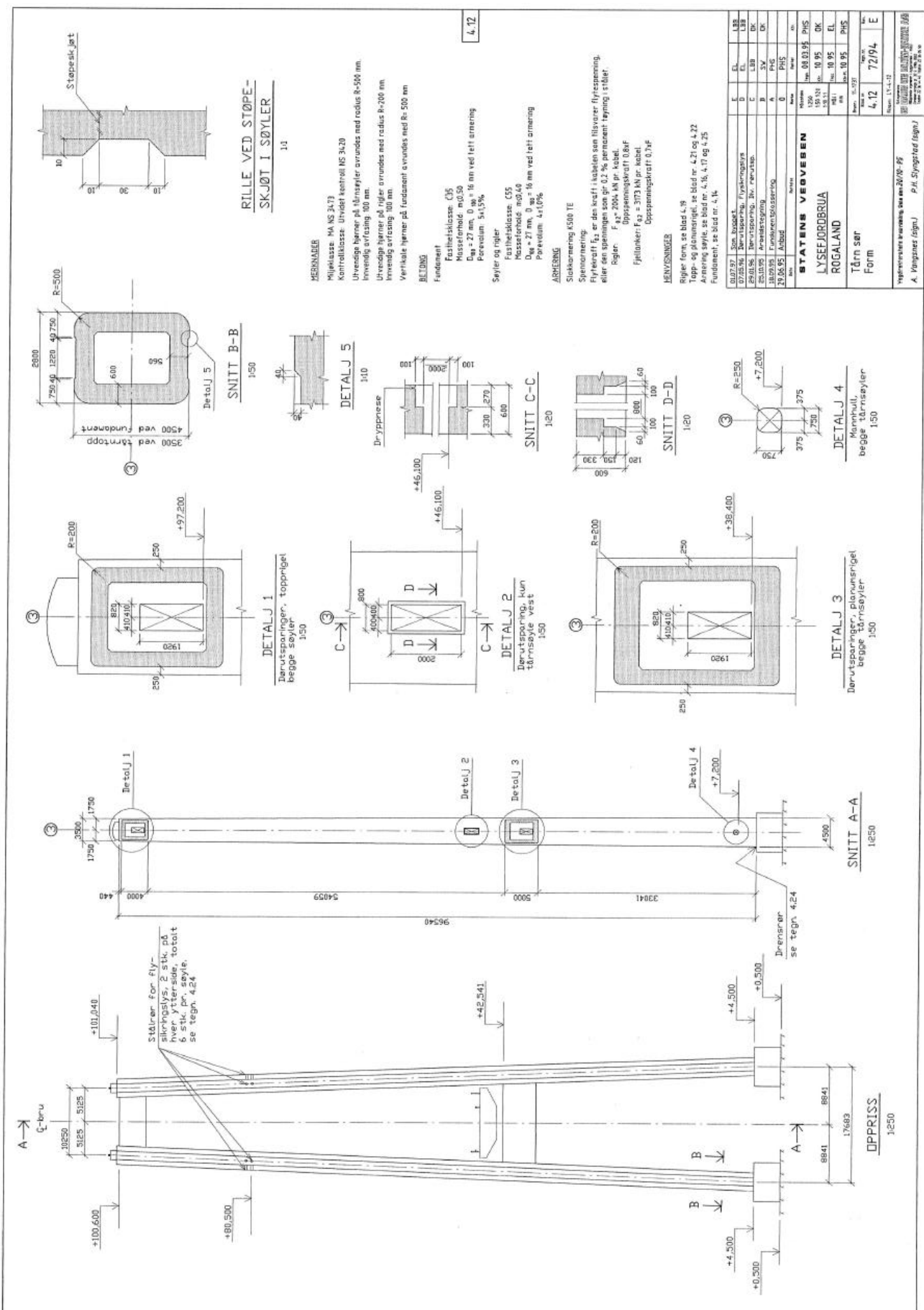
- [17] Matlab, www.mathlab.com
- [18] Octave, www.octave.org.
- [19] Python, www.python.org.
- [20] Advitam, www.advitam-group.com.
- [21] Dassault Systems, www.3ds.com
- [22] Norway, S. *Norwegian Standard NS-EN 1991-1-4:2005+NA2009, Eurocode 1:Loads on structures, wind loading, 2005/2009.*
- [23] Håndbok 185 Bruprosjektering, Statens Vegvesen
- [24] Lange, H., Lange, T., Johnsen, R., Kongstein, O. E., and Nilsen, N. I. Høyfast kabelråd med strekkfasthet 1570mpa og 1770mpa, måling av bruddseighet og effekt av hydrogensprøhet. Tech. Rep. 801059, SINTEF, 2010.
- [25] Leinum, B. H. Examination of failed z-wire rods rv13, lysefjord. Tech. Rep. 53010498, DNV, 2000.
- [26] Leinum, B. H. Examination of a 1.65 m spare main cable section rv13, lysefjord bridge. Tech. Rep. 53010389, DNV, 2001.
- [27] Strengelsrud, K. Examination of a fractured section of wire from a main cable of the lysefjord bridge. Tech. Rep. 53010389, DNV, 1999.
- [28] Dyrbye, C., Hansen, S.O. *Wind load on structures*. John Wiley and Sons Ltd, England, 1999.
- [29] Byggtabeller. Handboken Bygg, LiberFørlag Stockholm, 1983.
- [30] Drawings of Lysefjord Bridge provided by Per Slyngstad, NPRD.

APPENDIX A: DRAWINGS

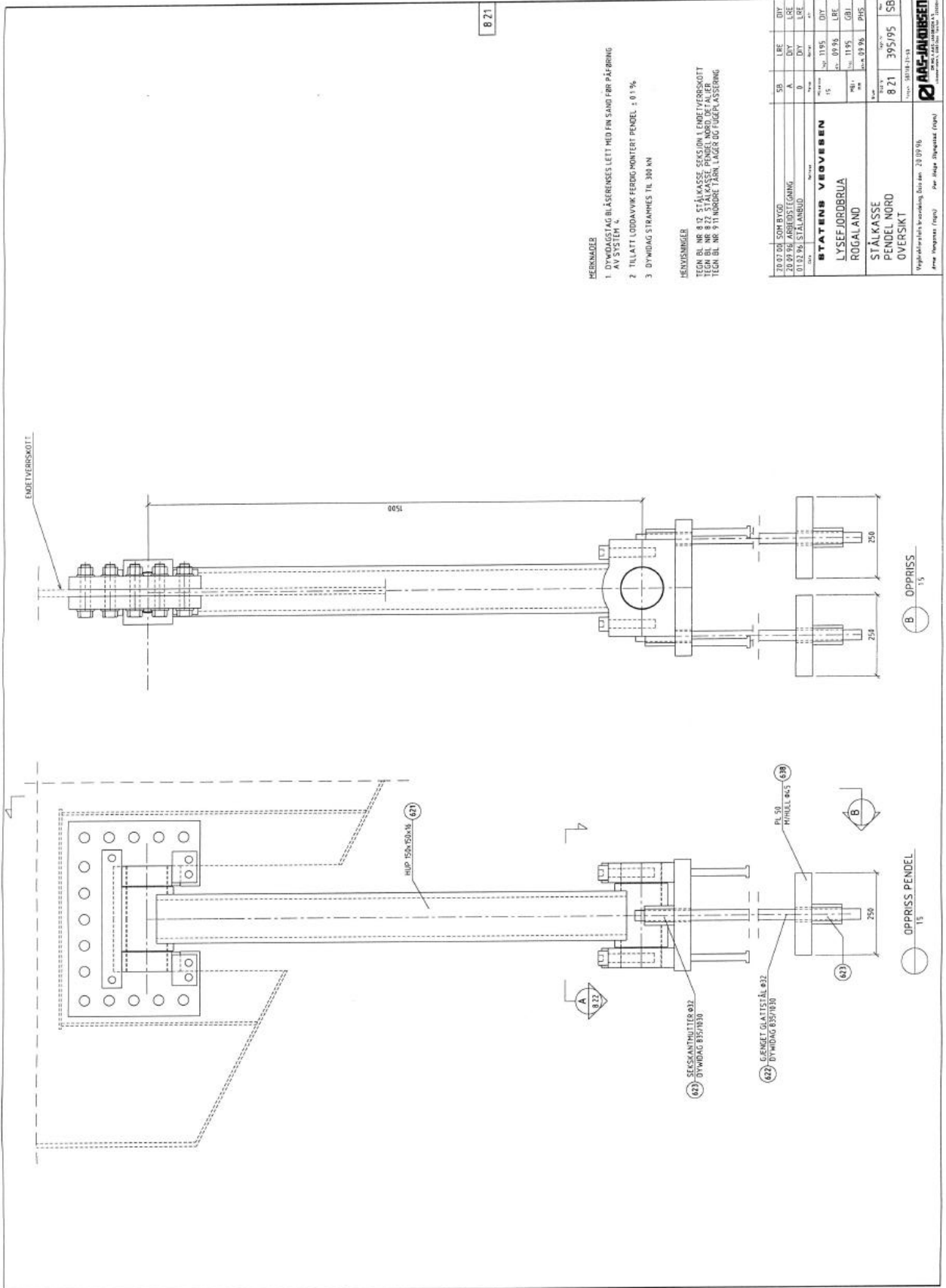


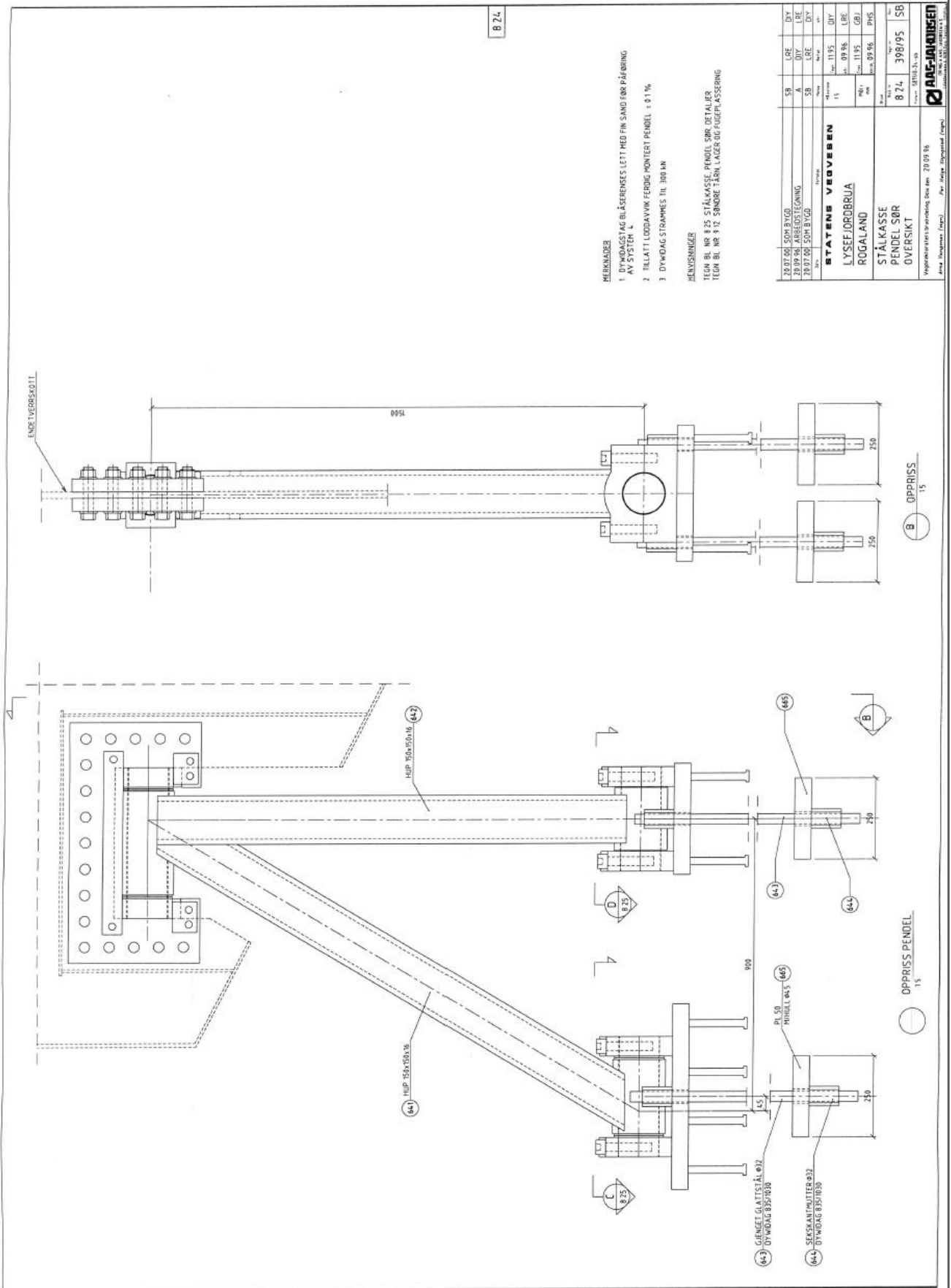


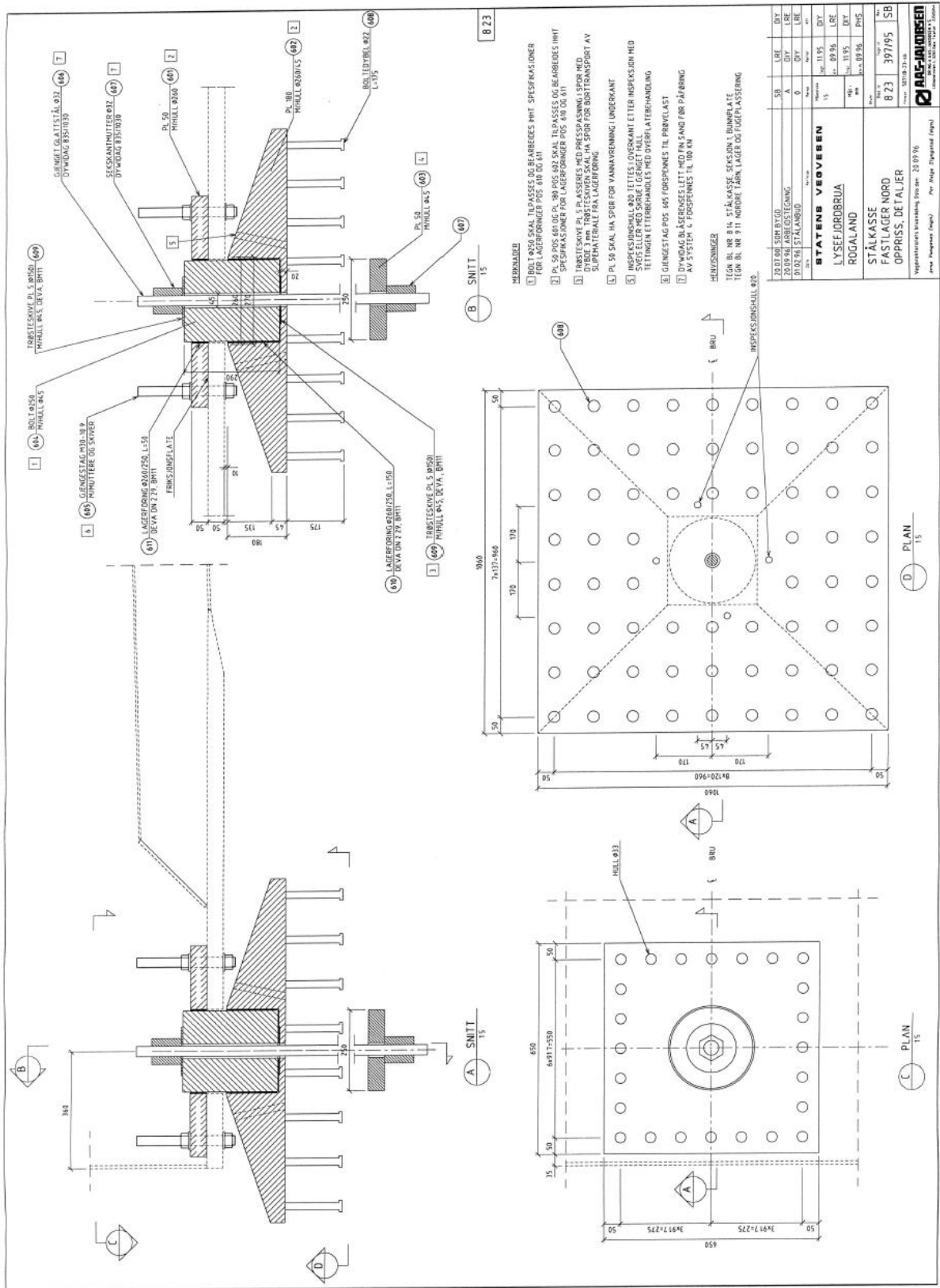


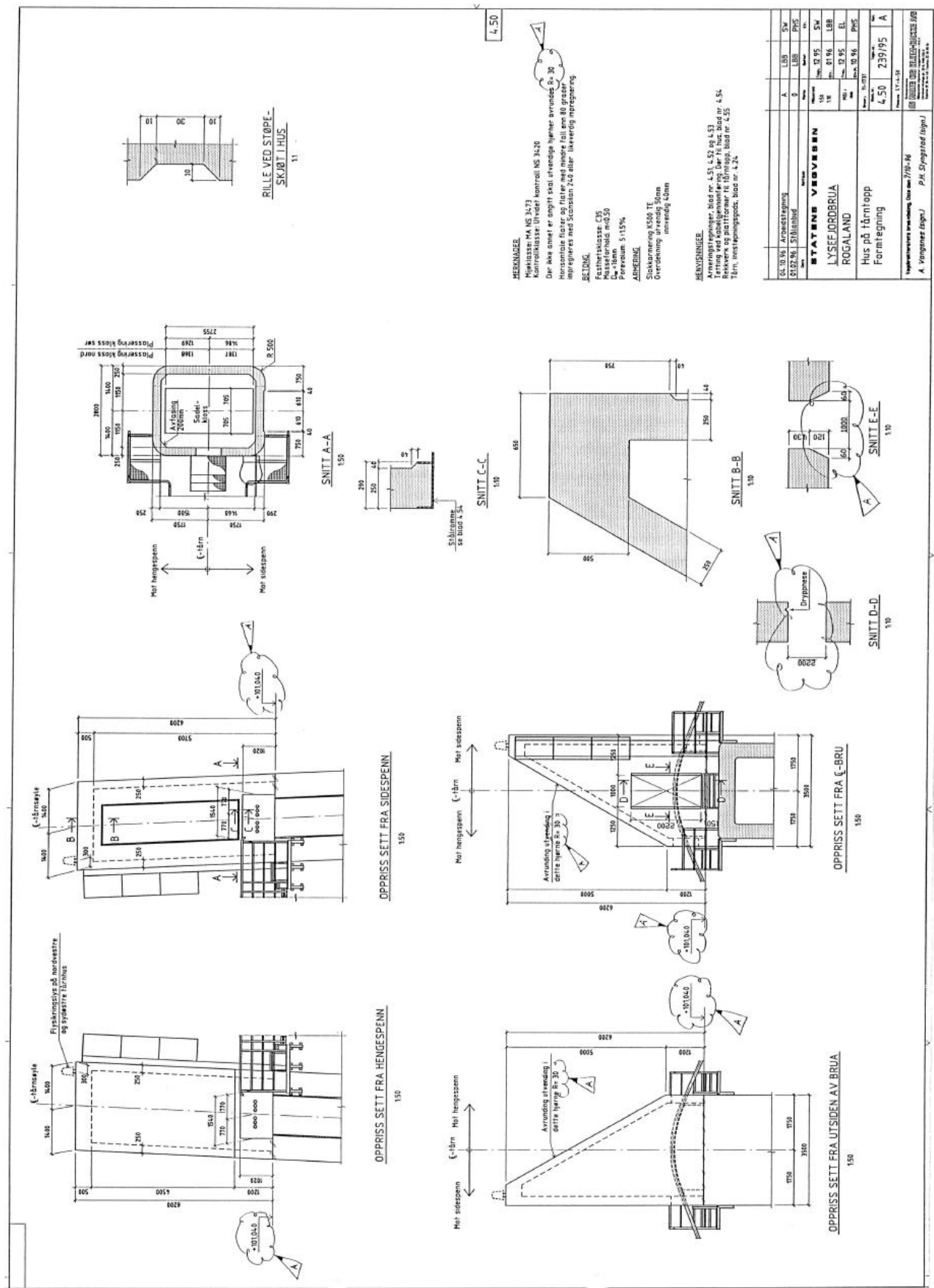


8.21

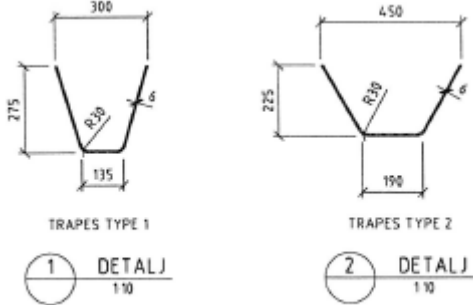








APPENDIX B: GIRDER CROSS SECTION CALCULATIONS



Stiffener type 1:

$$A1 := 6 \cdot (135 + \sqrt{269^2 + 82.5^2}) \cdot 2$$

4186.401042

$$y1 := \frac{6 \cdot \left(281.4 \cdot \left(\frac{269}{2} + 3 \right) \cdot 2 \right)}{(6 \cdot (135 + 2 \cdot 281.4))}$$

110.8985383

$$h1 := 275$$

275

$$y1m := h1 - y1$$

164.1014617

Stiffener type 2:

$$A2 := 6 \cdot (190 + 254.7 \cdot 2)$$

4196.4

$$y2 := \frac{\left(254.7 \cdot \left(\frac{219}{2} + 3 \right) \cdot 2 \right)}{(190 + 2 \cdot 254.7)}$$

81.93808979

$$h2 := 225$$

225

$$y2m := h2 - y2$$

143.0619102

Girder:

$$A := (\text{evalf}(10700 + 1131 \cdot 2) \cdot 12 + 8 \cdot (5100 + 2 \cdot 4041) + 15 \cdot A1 + 15 \cdot A2)$$

3.867420156 10^5

$$Ay := 5100 \cdot 4 \cdot 8 + 10700 \cdot 12 \cdot 2629 + 15 \cdot A1 \cdot 2458.9 + 6 \cdot A2 \cdot (8 + y2m) + 1131 \cdot 12 \cdot 2 \cdot (1835 + 400) + 4041 \cdot 8 \cdot 1835 + 2 \cdot 4 \cdot A2 \cdot (1158 + 124.8)$$

$$6.589932754 \cdot 10^8$$

$$\gamma := \frac{Ay}{A}$$

$$1703.960906$$

$$IxI := \frac{1131^3 \cdot 12}{12}$$

$$1446731091$$

Using the transposed Ix from the local system just as a reminder.

$$Ix1 := \left(IxI \cdot \cos\left(\frac{\text{Pi}}{4}\right)^2 + 1131 \cdot 12 \cdot (1835 + 400 - y)^2 \right) \cdot 2 \\ + 12 \cdot 10700 \cdot (2635 - 6 - y)^2$$

$$1.189729441 \cdot 10^{11}$$

$$IxI := \frac{8 \cdot 4041^3}{12}$$

$$43992160614$$

$$Ix2 := \left(IxI \cdot \left(\frac{3600}{4041} \right)^2 + \left(4041 \cdot 8 \cdot \left(\frac{1835}{2} - y \right)^2 \right) \right) \cdot 2 + 8 \\ \cdot 5100 \cdot (y - 4)^2$$

$$2.277261349 \cdot 10^{11}$$

$$Ixtop := A1 \cdot (2635 - 12 - y1m - y)^2 \cdot 15$$

$$3.578938520 \cdot 10^{10}$$

$$Ixbot := A2 \cdot (y - 8 - y2m)^2 \cdot 6 + 8 \cdot A2 \cdot \left(\frac{1835}{4041} \cdot 2050 \right. \\ \left. + \frac{y2m \cdot 3600}{4041} - y \right)^2$$

$$7.471072936 \cdot 10^{10}$$

$$Ix := Ix1 + Ix2 + Ixtop + Ixbot$$

$$4.571991936 \cdot 10^{11}$$

APPENDIX C: CALCULATION OF SHEAR CENTER

$$l1 := 1131$$

$$l1 := 1131$$

$$l2 := 10700$$

$$l2 := 10700$$

$$l3 := 4041$$

$$l3 := 4041$$

$$l4 := 5100$$

$$l4 := 5100$$

$$lb := 12300$$

$$lb := 12300$$

$$t1 := 12$$

$$t1 := 12$$

$$t2 := 8$$

$$t2 := 8$$

$$\text{alpha} := \arctan\left(\frac{1835}{3600}\right)$$

$$\alpha := \arctan\left(\frac{367}{720}\right)$$

$$\text{beta} := \arctan\left(\frac{1835}{(5100 + 3600)}\right)$$

$$\beta := \arctan\left(\frac{367}{1740}\right)$$

$$\text{ang} := \text{alpha} + \text{beta}$$

$$\text{ang} := \arctan\left(\frac{367}{720}\right) + \arctan\left(\frac{367}{1740}\right)$$

$$l5 := \sqrt{(5100 + 3600)^2 + 1835^2}$$

$$l5 := 5 \sqrt{3162289}$$

$$\text{arm1} := \frac{l2}{\sqrt{2}} + l1$$

$$\text{arm1} := 5350 \sqrt{2} + 1131$$

$$\text{arm2} := \text{simplify}(\text{value}(l5 \cdot \sin(\text{ang})))$$

$$\text{arm2} := \frac{110100}{434399759} \sqrt{697} \sqrt{696853872217}$$

$$\text{evalf}\left(\frac{\text{alpha} \cdot 180}{\text{Pi}}\right)$$

$$27.00894982$$

$$\begin{aligned} Ix1 := & \text{simplify}\left(\text{value}\left(\frac{t1 \cdot l2^3}{12} + 2 \cdot \text{Int}\left(t1 \cdot \left(\frac{l2}{2} + \cos\left(\frac{\text{Pi}}{4}\right)\right.\right.\right.\right. \\ & \left.\left.\left.\left.\cdot l\right)^2, l = 0 .. l1\right)\right)\right) \end{aligned}$$

$$Ix1 := 2007759064364 + 82122136200 \sqrt{2}$$

$$\begin{aligned}
Ix2 &:= \text{simplify}\left(\text{value}\left(\frac{t2 \cdot l4^3}{12} + 2 \cdot \text{Int}\left(t2 \cdot \left(\frac{l4}{2} + \cos(\text{alpha}) \cdot l\right)^2, l = 0..l3\right)\right)\right) \\
&\quad Ix2 := \frac{514774921926340800}{653089} \\
&\quad + \frac{28217688768000}{38417} \sqrt{653089} \\
q1 &:= \text{simplify}\left(\text{value}\left(\left(\frac{lb}{2} - \frac{l1 \cdot \text{sqrt}(2)}{2 \cdot 2}\right) \cdot l \cdot t1\right)\right) \\
&\quad q1 := -9 (-8200 + 377 \sqrt{2}) l \\
q2 &:= \text{simplify}\left(\text{value}\left(\left(\frac{lb}{2} - \frac{l3 \cdot \cos(\text{alpha})}{2}\right) \cdot l \cdot t2\right)\right) \\
&\quad q2 := -\frac{240}{653089} (-133883245 + 48492 \sqrt{653089}) l \\
qf &:= \text{subs}(l = l1, q1) \\
&\quad qf := 83467800 - 3837483 \sqrt{2} \\
qb &:= \text{subs}(l = l3, q2) \\
&\quad qb := 198817200 - \frac{47029481280}{653089} \sqrt{653089} \\
qg &:= qf + \frac{l2 \cdot t1 \cdot l2}{2 \cdot 4} \\
&\quad qg := 255202800 - 3837483 \sqrt{2} \\
qq &:= qb + \frac{l4 \cdot t2 \cdot l4}{2 \cdot 4} \\
&\quad qq := 224827200 - \frac{47029481280}{653089} \sqrt{653089} \\
sumqsym &:= \text{simplify}\left(\text{value}\left(\frac{2 \cdot \text{Int}(qa - q1, l = 0..l1)}{t1} + \frac{\left(qa - qf - \frac{2 \cdot (qg - qf)}{3}\right) \cdot l2}{t1} + \frac{2 \cdot \text{Int}(qa + q2, l = 0..l3)}{t2} + \frac{\left(qa + qb + \frac{2 \cdot (qq - qb)}{3}\right) \cdot l4}{t2}\right)\right) \\
&\quad sumqsym := \frac{161545624000}{3} + \frac{15133753791}{4} \sqrt{2} \\
&\quad + \frac{32735}{12} qa - \frac{53737061047560}{653089} \sqrt{653089} \\
sumq &:= \text{value}(sumqsym) \\
&\quad sumq := 2727.916667 qa - 7.29567517 \cdot 10^9 \\
qasolve &:= \text{simplify}(\text{value}(\text{solve}(sumqsym = 0, qa))) \\
&\quad qasolve := -\frac{129236499200}{6547} - \frac{45401261373}{32735} \sqrt{2} \\
&\quad + \frac{128968946514144}{4275773683} \sqrt{653089}
\end{aligned}$$

$$V := Ix1 + Ix2$$

$$\begin{aligned} V := & \frac{1826020281512761196}{653089} + 82122136200 \sqrt{2} \\ & + \frac{28217688768000}{38417} \sqrt{653089} \end{aligned}$$

$$\begin{aligned} sumMom := & V \cdot arm - \left(qf - qa + \frac{2 \cdot (qg - qf)}{3} \right) \cdot l2 \cdot t1 \cdot 800 \\ & + \left(qb + qa + \frac{2}{3} \cdot (qq - qb) \right) \cdot l4 \cdot t2 \cdot 1835 - Int(-qa \\ & + ql, l = 0..l1) \cdot t1 \cdot arm1 + Int(qa + q2, l = 0..l3) \cdot t2 \\ & \cdot arm2 \end{aligned}$$

$$\begin{aligned} sumMom := & \left(\frac{1826020281512761196}{653089} + 82122136200 \sqrt{2} \right. \\ & \left. + \frac{28217688768000}{38417} \sqrt{653089} \right) arm \\ & - 4150967966400000 + 394186253760000 \sqrt{2} \\ & + 177588000 qa - \frac{207117835557120000}{38417} \sqrt{653089} \\ & - 12 \left[\int_0^{1131} (-qa - 9(-8200 + 377\sqrt{2})l) \right. \\ & \left. dI \right] (5350\sqrt{2} + 1131) + \frac{880800}{434399759} \left[\int_0^{4041} (qa \right. \\ & \left. - \frac{240}{653089} (-133883245 + 48492\sqrt{653089})l) dI \right] \\ & \sqrt{697} \sqrt{696853872217} \end{aligned}$$

$$\begin{aligned} evalf(solve(subs(qa = qasolve, sumMom), arm)) \\ -403.3301438 \end{aligned}$$

APPENDIX D: CALCULATION OF STEINMAN EIGEN MODES

$$l := 446; \\ m := 6166; \\ s := \text{evalf}\left(\frac{m \cdot l^2}{\pi^2}\right)$$

$$1.24272058510^8$$

$$E := 2.1e11;$$

$$Iy := .429;$$

$$Ac := .05;$$

$$Ec := 1.81e11;$$

$$\text{lambda} := \text{evalf}\left(\frac{\pi^2 \cdot E \cdot Iy}{l^2}\right)$$

$$4.46999065310^6$$

$$f := 45;$$

$$k := \text{evalf}\left(\frac{32 \cdot f}{\pi^3}\right)$$

$$46.44220956$$

$$Le := 720;$$

$$p := \text{evalf}\left(\frac{\text{Pi} \cdot l \cdot Le}{16 \cdot f \cdot Ec \cdot Ac}\right)$$

$$1.54823240210^{-7}$$

$$Hw := 3.341e7$$

$$3.341 \cdot 10^7$$

$$A := s \cdot \omega^2 - Hw - \text{lambda}$$

$$1.24272058510^8 \omega^2 - 3.78799906510^7$$

$$B := s \cdot \omega^2 - 9 \cdot Hw - 81 \cdot \text{lambda}$$

$$1.24272058510^8 \omega^2 - 6.62759242910^8$$

$$eq1 := \text{simplify}(A \cdot k + 9 \cdot B \cdot (k - A \cdot p))$$

$$1.79038658110^{11} \omega^2 - 3.13761237710^{11} - 2.15191764310^{10} \omega^4$$

$$\text{solve}(eq1)$$

$$1.584063194 - 1.584063194 \cdot 2.410539866 - 2.410539866$$

$$Kn := \frac{n^2 \cdot \pi^2}{l^2} \cdot Hw + \frac{n^4 \cdot \pi^4}{l^4} \cdot E \cdot Iy$$

$$167.9603451 n^2 \pi^2 + 2.276864323 n^4 \pi^4$$

$$C := \text{evalf}\left(\frac{512 \cdot f \cdot Ec \cdot Ac}{\pi^2 \cdot l^2 \cdot Le}\right)$$

$$1.47512592110^5$$

$$eq2 := \frac{1}{n^2} \cdot \frac{C \cdot \left(\frac{f}{l}\right)}{K - Kn}$$

$$\frac{14883.55750}{n^2 (K - 167.9603451 n^2 \pi^2 - 2.276864323 n^4 \pi^4)}$$

$$eq3 := \text{add}(eq2, n \text{ in } [1, 3]) = 1$$

$$\frac{14883.55750}{K - 167.9603451\pi^2 - 2.276864323\pi^4} + \frac{1653.728611}{K - 1511.643106\pi^2 - 184.4260102\pi^4} = 1$$

eqK3List := solve(*eq3*)

$$15472.07375 \ 35828.79127$$

seq\frac{i}{m} \right), i = *eqK3List* \right)

$$1.584063194 \ 2.410539866$$

APPENDIX E: ABAQUS FILES

File lysefjord_modifisert_bru.inp

```
** The file contains the structural model
** Can't stand copying this around in every load file
** JT
**
** Changes from Ragnhilds input
** Had to change two coordinates to get the north tower straight
** Had to change the orientation of the top tower columns to better match
the direction of the cables
** Now the thing seems to work without warnings and looks right at the top
** JT
*****
**** Nodes ****
*****
*NODE
**Bridge girder(modeled from north to south)
1 , -223.1 , 0 , 52.465
2 , -204 , 0 , 53.337
3 , -192 , 0 , 53.839
4 , -180 , 0 , 54.303
5 , -168 , 0 , 54.728
6 , -156 , 0 , 55.114
7 , -144 , 0 , 55.459
8 , -132 , 0 , 55.764
9 , -120 , 0 , 56.027
10 , -108 , 0 , 56.25
11 , -96 , 0 , 56.43
12 , -84 , 0 , 56.568
13 , -72 , 0 , 56.663
14 , -60 , 0 , 56.715
15 , -48 , 0 , 56.724
16 , -36 , 0 , 56.689
17 , -24 , 0 , 56.61
18 , -12 , 0 , 56.486
19 , -0 , 0 , 56.317
20 , 12 , 0 , 56.103
21 , 24 , 0 , 55.844
22 , 36 , 0 , 55.539
23 , 48 , 0 , 55.189
24 , 60 , 0 , 54.793
25 , 72 , 0 , 54.35
26 , 84 , 0 , 53.863
27 , 96 , 0 , 53.33
28 , 108 , 0 , 52.751
29 , 120 , 0 , 52.128
30 , 132 , 0 , 51.46
31 , 144 , 0 , 50.747
32 , 156 , 0 , 49.991
33 , 168 , 0 , 49.191
34 , 180 , 0 , 48.349
35 , 192 , 0 , 47.464
36 , 204 , 0 , 46.539
```

```

37 , 223.13 , 0 , 44.987
**Anchor bolt north-west
981 , -296.906 , 5.1250 , 53.4647
**West cable main span
** Here is th error for the warning?
** The coords are mirrored, tower deflection is not
** JT
1001 , -223.2263 , 5.125 , 102.27
1002 , -204 , 5.125 , 95.302880519427
1003 , -192 , 5.125 , 91.254132341776
1004 , -180 , 5.125 , 87.457933183983
1005 , -168 , 5.125 , 83.911100046048
1006 , -156 , 5.125 , 80.61268842797
1007 , -144 , 5.125 , 77.562002529749
1008 , -132 , 5.125 , 74.758539451387
1009 , -120 , 5.125 , 72.201849992881
1010 , -108 , 5.125 , 69.891451754234
1011 , -96 , 5.125 , 67.826941335444
1012 , -84 , 5.125 , 66.007930436512
1013 , -72 , 5.125 , 64.433974857437
1014 , -60 , 5.125 , 63.10466719822
1015 , -48 , 5.125 , 62.019530758861
1016 , -36 , 5.125 , 61.178050539359
1017 , -24 , 5.125 , 60.579692339715
1018 , -12 , 5.125 , 60.224055759929
1019 , -0 , 5.125 , 60.1110118
1020 , 12 , 5.125 , 60.240615359929
1021 , 24 , 5.125 , 60.612872539715
1022 , 36 , 5.125 , 61.227641539359
1023 , 48 , 5.125 , 62.084739258861
1024 , 60 , 5.125 , 63.18404349822
1025 , 72 , 5.125 , 64.525539057437
1026 , 84 , 5.125 , 66.109290736512
1027 , 96 , 5.125 , 67.935431335444
1028 , 108 , 5.125 , 70.004206554234
1029 , 120 , 5.125 , 72.315871292881
1030 , 132 , 5.125 , 74.870737251387
1031 , 144 , 5.125 , 77.669264129749
1032 , 156 , 5.125 , 80.71190112797
1033 , 168 , 5.125 , 83.999204346048
1034 , 180 , 5.125 , 87.532014683983
1035 , 192 , 5.125 , 91.311795241776
1036 , 204 , 5.125 , 95.344277519427
1037 , 223.3363 , 5.125 , 102.27
**Anchor bolt south-west
1087 , 389.0460 , 5.1250 , 46.0009
**Anchor bolt north-east
1981 , -296.906 , -5.125 , 53.4647
**East cable main span
** Here is th error for the warning?
** The coords are mirrored, tower deflection is not
** JT
2001 , -223.2263 , -5.125 , 102.27
2002 , -204 , -5.125 , 95.302880519427
2003 , -192 , -5.125 , 91.254132341776
2004 , -180 , -5.125 , 87.457933183983
2005 , -168 , -5.125 , 83.911100046048
2006 , -156 , -5.125 , 80.61268842797
2007 , -144 , -5.125 , 77.562002529749

```

2008 , -132 , -5.125 , 74.758539451387
 2009 , -120 , -5.125 , 72.201849992881
 2010 , -108 , -5.125 , 69.891451754234
 2011 , -96 , -5.125 , 67.826941335444
 2012 , -84 , -5.125 , 66.007930436512
 2013 , -72 , -5.125 , 64.433974857437
 2014 , -60 , -5.125 , 63.10466719822
 2015 , -48 , -5.125 , 62.019530758861
 2016 , -36 , -5.125 , 61.178050539359
 2017 , -24 , -5.125 , 60.579692339715
 2018 , -12 , -5.125 , 60.224055759929
 2019 , -0 , -5.125 , 60.1110118
 2020 , 12 , -5.125 , 60.240615359929
 2021 , 24 , -5.125 , 60.612872539715
 2022 , 36 , -5.125 , 61.227641539359
 2023 , 48 , -5.125 , 62.084739258861
 2024 , 60 , -5.125 , 63.18404349822
 2025 , 72 , -5.125 , 64.525539057437
 2026 , 84 , -5.125 , 66.109290736512
 2027 , 96 , -5.125 , 67.935431335444
 2028 , 108 , -5.125 , 70.004206554234
 2029 , 120 , -5.125 , 72.315871292881
 2030 , 132 , -5.125 , 74.870737251387
 2031 , 144 , -5.125 , 77.669264129749
 2032 , 156 , -5.125 , 80.71190112797
 2033 , 168 , -5.125 , 83.999204346048
 2034 , 180 , -5.125 , 87.532014683983
 2035 , 192 , -5.125 , 91.311795241776
 2036 , 204 , -5.125 , 95.344277519427
 2037 , 223.3363 , -5.125 , 102.27
 **Anchor , bolt south-east
 2087 , 389.0460 , -5.125 , 46.0009
 **Link between bridge girder and hanger west - hanger (1.104 above NA)
 3001 , -223 , 5.125 , 53.469
 3002 , -204 , 5.125 , 54.341
 3003 , -192 , 5.125 , 54.843
 3004 , -180 , 5.125 , 55.307
 3005 , -168 , 5.125 , 55.732
 3006 , -156 , 5.125 , 56.117
 3007 , -144 , 5.125 , 56.463
 3008 , -132 , 5.125 , 56.768
 3009 , -120 , 5.125 , 57.031
 3010 , -108 , 5.125 , 57.254
 3011 , -96 , 5.125 , 57.434
 3012 , -84 , 5.125 , 57.572
 3013 , -72 , 5.125 , 57.667
 3014 , -60 , 5.125 , 57.719
 3015 , -48 , 5.125 , 57.728
 3016 , -36 , 5.125 , 57.693
 3017 , -24 , 5.125 , 57.614
 3018 , -12 , 5.125 , 57.49
 3019 , -0 , 5.125 , 57.321
 3020 , 12 , 5.125 , 57.107
 3021 , 24 , 5.125 , 56.848
 3022 , 36 , 5.125 , 56.543
 3023 , 48 , 5.125 , 56.193
 3024 , 60 , 5.125 , 55.797
 3025 , 72 , 5.125 , 55.354
 3026 , 84 , 5.125 , 54.867

3027 , 96 , 5.125 , 54.334
 3028 , 108 , 5.125 , 53.755
 3029 , 120 , 5.125 , 53.132
 3030 , 132 , 5.125 , 52.464
 3031 , 144 , 5.125 , 51.751
 3032 , 156 , 5.125 , 50.995
 3033 , 168 , 5.125 , 50.195
 3034 , 180 , 5.125 , 49.353
 3035 , 192 , 5.125 , 48.468
 3036 , 204 , 5.125 , 47.543
 3037 , 223 , 5.125 , 45.991
 **Link between bridge girder and hanger east - hanger (1.104 above NA)
 4001 , -223 , -5.125 , 53.469
 4002 , -204 , -5.125 , 54.341
 4003 , -192 , -5.125 , 54.843
 4004 , -180 , -5.125 , 55.307
 4005 , -168 , -5.125 , 55.732
 4006 , -156 , -5.125 , 56.117
 4007 , -144 , -5.125 , 56.463
 4008 , -132 , -5.125 , 56.768
 4009 , -120 , -5.125 , 57.031
 4010 , -108 , -5.125 , 57.254
 4011 , -96 , -5.125 , 57.434
 4012 , -84 , -5.125 , 57.572
 4013 , -72 , -5.125 , 57.667
 4014 , -60 , -5.125 , 57.719
 4015 , -48 , -5.125 , 57.728
 4016 , -36 , -5.125 , 57.693
 4017 , -24 , -5.125 , 57.614
 4018 , -12 , -5.125 , 57.49
 4019 , -0 , -5.125 , 57.321
 4020 , 12 , -5.125 , 57.107
 4021 , 24 , -5.125 , 56.848
 4022 , 36 , -5.125 , 56.543
 4023 , 48 , -5.125 , 56.193
 4024 , 60 , -5.125 , 55.797
 4025 , 72 , -5.125 , 55.354
 4026 , 84 , -5.125 , 54.867
 4027 , 96 , -5.125 , 54.334
 4028 , 108 , -5.125 , 53.755
 4029 , 120 , -5.125 , 53.132
 4030 , 132 , -5.125 , 52.464
 4031 , 144 , -5.125 , 51.751
 4032 , 156 , -5.125 , 50.995
 4033 , 168 , -5.125 , 50.195
 4034 , 180 , -5.125 , 49.353
 4035 , 192 , -5.125 , 48.468
 4036 , 204 , -5.125 , 47.543
 4037 , 223 , -5.125 , 45.991
 **Fictitious mass point under the bridge girder (moment of inertia)
 5002 , -204 , 0 , 53.05700
 5003 , -192 , 0 , 53.55900
 5004 , -180 , 0 , 54.02300
 5005 , -168 , 0 , 54.44800
 5006 , -156 , 0 , 54.83400
 5007 , -144 , 0 , 55.17900
 5008 , -132 , 0 , 55.48400
 5009 , -120 , 0 , 55.74700
 5010 , -108 , 0 , 55.97000

5011 , -96 , 0 , 56.15000
 5012 , -84 , 0 , 56.28800
 5013 , -72 , 0 , 56.38300
 5014 , -60 , 0 , 56.43500
 5015 , -48 , 0 , 56.44400
 5016 , -36 , 0 , 56.40900
 5017 , -24 , 0 , 56.33000
 5018 , -12 , 0 , 56.20600
 5019 , -0 , 0 , 56.03700
 5020 , 12 , 0 , 55.82300
 5021 , 24 , 0 , 55.56400
 5022 , 36 , 0 , 55.25900
 5023 , 48 , 0 , 54.90900
 5024 , 60 , 0 , 54.51300
 5025 , 72 , 0 , 54.07000
 5026 , 84 , 0 , 53.58300
 5027 , 96 , 0 , 53.05000
 5028 , 108 , 0 , 52.47100
 5029 , 120 , 0 , 51.84800
 5030 , 132 , 0 , 51.18000
 5031 , 144 , 0 , 50.46700
 5032 , 156 , 0 , 49.71100
 5033 , 168 , 0 , 48.91100
 5034 , 180 , 0 , 48.06900
 5035 , 192 , 0 , 47.18400
 5036 , 204 , 0 , 46.25900
 **Tower north, foot west
 20001 , -223 , 9.151 , 6.5
 20002 , -223.007803448276 , 9.0122 , 10.5
 20003 , -223.015606896552 , 8.8734 , 13.5833
 20004 , -223.023410344828 , 8.7346 , 16.6667
 20005 , -223.031213793103 , 8.5958 , 19.75
 20006 , -223.039017241379 , 8.457 , 22.8333
 20007 , -223.046820689655 , 8.3182 , 25.9167
 20008 , -223.054624137931 , 8.1794 , 29
 20009 , -223.062427586207 , 8.0406 , 32.0833
 20010 , -223.070231034483 , 7.9018 , 35.1667
 20011 , -223.078034482759 , 7.763 , 38.25
 20012 , -223.085837931035 , 7.6242 , 41.3333
 20013 , -223.09364137931 , 7.4854 , 44.4167
 20014 , -223.101444827586 , 7.3466 , 47.5
 20015 , -223.109248275862 , 7.2078 , 50.8463
 20016 , -223.117051724138 , 7.069 , 54.1925
 20017 , -223.124855172414 , 6.9302 , 57.5388
 20018 , -223.13265862069 , 6.7914 , 60.885
 20019 , -223.140462068966 , 6.6526 , 64.2313
 20020 , -223.148265517241 , 6.5138 , 67.5775
 20021 , -223.156068965517 , 6.375 , 70.9237
 20022 , -223.163872413793 , 6.2362 , 74.27
 20023 , -223.171675862069 , 6.0974 , 77.6163
 20024 , -223.179479310345 , 5.9586 , 80.9625
 20025 , -223.187282758621 , 5.8198 , 84.3088
 20026 , -223.195086206897 , 5.681 , 87.655
 20027 , -223.202889655172 , 5.5422 , 91.0013
 20028 , -223.210693103448 , 5.4034 , 94.3475
 20029 , -223.218496551724 , 5.2646 , 97.6938
 20030 , -223.2263 , 5.1258 , 101.04
 **Tower north, foot east
 20101 , -223 , -9.151 , 6.5

20102 , -223.007803448276 , -9.0122 , 10.5
 20103 , -223.015606896552 , -8.8734 , 13.5833
 20104 , -223.023410344828 , -8.7346 , 16.6667
 20105 , -223.031213793103 , -8.5958 , 19.75
 20106 , -223.039017241379 , -8.457 , 22.8333
 20107 , -223.046820689655 , -8.3182 , 25.9167
 20108 , -223.054624137931 , -8.1794 , 29
 20109 , -223.062427586207 , -8.0406 , 32.0833
 20110 , -223.070231034483 , -7.9018 , 35.1667
 20111 , -223.078034482759 , -7.763 , 38.25
 20112 , -223.085837931035 , -7.6242 , 41.3333
 20113 , -223.09364137931 , -7.4854 , 44.4167
 20114 , -223.101444827586 , -7.3466 , 47.5
 20115 , -223.109248275862 , -7.2078 , 50.8463
 20116 , -223.117051724138 , -7.069 , 54.1925
 20117 , -223.124855172414 , -6.9302 , 57.5388
 20118 , -223.13265862069 , -6.7914 , 60.885
 20119 , -223.140462068966 , -6.6526 , 64.2313
 20120 , -223.148265517241 , -6.5138 , 67.5775
 20121 , -223.156068965517 , -6.375 , 70.9237
 20122 , -223.163872413793 , -6.2362 , 74.27
 20123 , -223.171675862069 , -6.0974 , 77.6163
 20124 , -223.179479310345 , -5.9586 , 80.9625
 20125 , -223.187282758621 , -5.8198 , 84.3088
 20126 , -223.195086206897 , -5.681 , 87.655
 20127 , -223.202889655172 , -5.5422 , 91.0013
 20128 , -223.210693103448 , -5.4034 , 94.3475
 20129 , -223.218496551724 , -5.2646 , 97.6938
 20130 , -223.2263 , -5.1258 , 101.04
 **cross beam under the bridge girder, tower north
 20201 , -223.101444827586 , 7.3466 , 47.5
 20202 , -223.101444827586 , 4.9903 , 47.5
 20203 , -223.101444827586 , 2.4952 , 47.5
 20204 , -223.101444827586 , 0.0001 , 47.5
 20205 , -223.101444827586 , -2.495 , 47.5
 20206 , -223.101444827586 , -4.9901 , 47.5
 20207 , -223.101444827586 , -7.3466 , 47.5
 **cross beam top, tower north
 20301 , -223.218496551724 , 5.2646 , 97.6938
 20302 , -223.218496551724 , 3.5097 , 97.6938
 20303 , -223.218496551724 , 1.7548 , 97.6938
 20304 , -223.218496551724 , -0.0001 , 97.6938
 20305 , -223.218496551724 , -1.755 , 97.6938
 20306 , -223.218496551724 , -3.5099 , 97.6938
 20307 , -223.218496551724 , -5.2646 , 97.6938
 **Tower south, foot west
 30001 , 223 , 9.151 , 0.5
 30002 , 223.011596551724 , 9.0122 , 4.5
 30003 , 223.023193103448 , 8.8734 , 8.0541
 30004 , 223.034789655172 , 8.7346 , 11.6082
 30005 , 223.046386206896 , 8.5958 , 15.1623
 30006 , 223.057982758621 , 8.457 , 18.7164
 30007 , 223.069579310345 , 8.3182 , 22.2705
 30008 , 223.081175862069 , 8.1794 , 25.8246
 30009 , 223.092772413793 , 8.0406 , 29.3787
 30010 , 223.104368965517 , 7.9018 , 32.9328
 30011 , 223.115965517241 , 7.763 , 36.4869
 30012 , 223.127562068965 , 7.6242 , 40.041
 30013 , 223.139158620689 , 7.4854 , 43.4298

30014 , 223.150755172414 , 7.3466 , 46.8187
 30015 , 223.162351724138 , 7.2078 , 50.2075
 30016 , 223.173948275862 , 7.069 , 53.5963
 30017 , 223.185544827586 , 6.9302 , 56.9852
 30018 , 223.19714137931 , 6.7914 , 60.374
 30019 , 223.208737931034 , 6.6526 , 63.7628
 30020 , 223.220334482758 , 6.5138 , 67.1517
 30021 , 223.231931034482 , 6.375 , 70.5405
 30022 , 223.243527586207 , 6.2362 , 73.9293
 30023 , 223.255124137931 , 6.0974 , 77.3182
 30024 , 223.266720689655 , 5.9586 , 80.707
 30025 , 223.278317241379 , 5.8198 , 84.0958
 30026 , 223.289913793103 , 5.681 , 87.4847
 30027 , 223.301510344827 , 5.5422 , 90.8735
 30028 , 223.313106896551 , 5.4034 , 94.2623
 30029 , 223.324703448275 , 5.2646 , 97.6512
 30030 , 223.3363 , 5.1258 , 101.04
 **Tower south, foot east
 30101 , 223 , -9.151 , 0.5
 30102 , 223.011596551724 , -9.0122 , 4.5
 30103 , 223.023193103448 , -8.8734 , 8.0541
 30104 , 223.034789655172 , -8.7346 , 11.6082
 30105 , 223.046386206896 , -8.5958 , 15.1623
 30106 , 223.057982758621 , -8.457 , 18.7164
 30107 , 223.069579310345 , -8.3182 , 22.2705
 30108 , 223.081175862069 , -8.1794 , 25.8246
 30109 , 223.092772413793 , -8.0406 , 29.3787
 30110 , 223.104368965517 , -7.9018 , 32.9328
 30111 , 223.115965517241 , -7.763 , 36.4869
 30112 , 223.127562068965 , -7.6242 , 40.041
 30113 , 223.139158620689 , -7.4854 , 43.4298
 30114 , 223.150755172414 , -7.3466 , 46.8187
 30115 , 223.162351724138 , -7.2078 , 50.2075
 30116 , 223.173948275862 , -7.069 , 53.5963
 30117 , 223.185544827586 , -6.9302 , 56.9852
 30118 , 223.19714137931 , -6.7914 , 60.374
 30119 , 223.208737931034 , -6.6526 , 63.7628
 30120 , 223.220334482758 , -6.5138 , 67.1517
 30121 , 223.231931034482 , -6.375 , 70.5405
 30122 , 223.243527586207 , -6.2362 , 73.9293
 30123 , 223.255124137931 , -6.0974 , 77.3182
 30124 , 223.266720689655 , -5.9586 , 80.707
 30125 , 223.278317241379 , -5.8198 , 84.0958
 30126 , 223.289913793103 , -5.681 , 87.4847
 30127 , 223.301510344827 , -5.5422 , 90.8735
 30128 , 223.313106896551 , -5.4034 , 94.2623
 30129 , 223.324703448275 , -5.2646 , 97.6512
 30130 , 223.3363 , -5.1258 , 101.04
 **cross beam under the bridge girder, tower south
 30201 , 223.127562068965 , 7.6242 , 40.041
 30202 , 223.127562068965 , 5.1754 , 40.041
 30203 , 223.127562068965 , 2.5877 , 40.041
 30204 , 223.127562068965 , 0.0001 , 40.041
 30205 , 223.127562068965 , -2.5877 , 40.041
 30206 , 223.127562068965 , -4.1754 , 40.041
 30207 , 223.127562068965 , -7.6242 , 40.041
 **cross beam top, tower south
 30301 , 223.324703448275 , 5.2646 , 97.6512
 30302 , 223.324703448275 , 3.5097 , 97.6512

```

30303 , 223.324703448275 , 1.7548 , 97.6512
30304 , 223.324703448275 , -0.0001 , 97.6512
30305 , 223.324703448275 , -1.755 , 97.6512
30306 , 223.324703448275 , -3.5099 , 97.6512
30307 , 223.324703448275 , -5.2646 , 97.6512
**
**
** Now lets add some elements to backstays
** Approx 7 m. long each element
**
*NGEN, NSET=BACKSTAY
981, 1001, 2
1981,2001, 2
1037,1087, 2
2037,2087, 2
**
*****
**** Structural elements ****
*****
**
**Bridge girder
**
*ELEMENT , TYPE = B31 , ELSET=GIRDER
1 , 1 , 2
2 , 2 , 3
3 , 3 , 4
4 , 4 , 5
5 , 5 , 6
6 , 6 , 7
7 , 7 , 8
8 , 8 , 9
9 , 9 , 10
10 , 10 , 11
11 , 11 , 12
12 , 12 , 13
13 , 13 , 14
14 , 14 , 15
15 , 15 , 16
16 , 16 , 17
17 , 17 , 18
18 , 18 , 19
19 , 19 , 20
20 , 20 , 21
21 , 21 , 22
22 , 22 , 23
23 , 23 , 24
24 , 24 , 25
25 , 25 , 26
26 , 26 , 27
27 , 27 , 28
28 , 28 , 29
29 , 29 , 30
30 , 30 , 31
31 , 31 , 32
32 , 32 , 33
33 , 33 , 34
34 , 34 , 35
35 , 35 , 36
36 , 36 , 37

```

```

**
**
**
**
** Cable in main span
**
*ELEMENT , TYPE = B31 , ELSET=MAINCABLE
1001 , 1001 , 1002
1002 , 1002 , 1003
1003 , 1003 , 1004
1004 , 1004 , 1005
1005 , 1005 , 1006
1006 , 1006 , 1007
1007 , 1007 , 1008
1008 , 1008 , 1009
1009 , 1009 , 1010
1010 , 1010 , 1011
1011 , 1011 , 1012
1012 , 1012 , 1013
1013 , 1013 , 1014
1014 , 1014 , 1015
1015 , 1015 , 1016
1016 , 1016 , 1017
1017 , 1017 , 1018
1018 , 1018 , 1019
1019 , 1019 , 1020
1020 , 1020 , 1021
1021 , 1021 , 1022
1022 , 1022 , 1023
1023 , 1023 , 1024
1024 , 1024 , 1025
1025 , 1025 , 1026
1026 , 1026 , 1027
1027 , 1027 , 1028
1028 , 1028 , 1029
1029 , 1029 , 1030
1030 , 1030 , 1031
1031 , 1031 , 1032
1032 , 1032 , 1033
1033 , 1033 , 1034
1034 , 1034 , 1035
1035 , 1035 , 1036
1036 , 1036 , 1037
**
2001 , 2001 , 2002
2002 , 2002 , 2003
2003 , 2003 , 2004
2004 , 2004 , 2005
2005 , 2005 , 2006
2006 , 2006 , 2007
2007 , 2007 , 2008
2008 , 2008 , 2009
2009 , 2009 , 2010
2010 , 2010 , 2011
2011 , 2011 , 2012
2012 , 2012 , 2013
2013 , 2013 , 2014
2014 , 2014 , 2015
2015 , 2015 , 2016

```

```

2016 , 2016 , 2017
2017 , 2017 , 2018
2018 , 2018 , 2019
2019 , 2019 , 2020
2020 , 2020 , 2021
2021 , 2021 , 2022
2022 , 2022 , 2023
2023 , 2023 , 2024
2024 , 2024 , 2025
2025 , 2025 , 2026
2026 , 2026 , 2027
2027 , 2027 , 2028
2028 , 2028 , 2029
2029 , 2029 , 2030
2030 , 2030 , 2031
2031 , 2031 , 2032
2032 , 2032 , 2033
2033 , 2033 , 2034
2034 , 2034 , 2035
2035 , 2035 , 2036
2036 , 2036 , 2037
**
**
**
**
** Cable in backstay
**
*ELEMENT , TYPE = B31 , ELSET=BACKSTAYCABLE
981 , 981 , 983
1037 , 1037 , 1039
1981 , 1981 , 1983
2037 , 2037 , 2039
*ELGEN , ELSET=BACKSTAYCABLE
981 , 10, 2, 2
1037 , 25,2,2
1981, 10,2,2
2037 , 25,2,2
**
**
**
** Fictitious element between bridge girder and lower hanger link
**
*ELEMENT , TYPE = B31 , ELSET=DUMMY1
3001 , 1 , 3001
3002 , 2 , 3002
3003 , 3 , 3003
3004 , 4 , 3004
3005 , 5 , 3005
3006 , 6 , 3006
3007 , 7 , 3007
3008 , 8 , 3008
3009 , 9 , 3009
3010 , 10 , 3010
3011 , 11 , 3011
3012 , 12 , 3012
3013 , 13 , 3013
3014 , 14 , 3014
3015 , 15 , 3015
3016 , 16 , 3016

```

```

3017 , 17 , 3017
3018 , 18 , 3018
3019 , 19 , 3019
3020 , 20 , 3020
3021 , 21 , 3021
3022 , 22 , 3022
3023 , 23 , 3023
3024 , 24 , 3024
3025 , 25 , 3025
3026 , 26 , 3026
3027 , 27 , 3027
3028 , 28 , 3028
3029 , 29 , 3029
3030 , 30 , 3030
3031 , 31 , 3031
3032 , 32 , 3032
3033 , 33 , 3033
3034 , 34 , 3034
3035 , 35 , 3035
3036 , 36 , 3036
3037 , 37 , 3037
**
**
**
*ELEMENT , TYPE = B31 , ELSET=DUMMY2
4001 , 1 , 4001
4002 , 2 , 4002
4003 , 3 , 4003
4004 , 4 , 4004
4005 , 5 , 4005
4006 , 6 , 4006
4007 , 7 , 4007
4008 , 8 , 4008
4009 , 9 , 4009
4010 , 10 , 4010
4011 , 11 , 4011
4012 , 12 , 4012
4013 , 13 , 4013
4014 , 14 , 4014
4015 , 15 , 4015
4016 , 16 , 4016
4017 , 17 , 4017
4018 , 18 , 4018
4019 , 19 , 4019
4020 , 20 , 4020
4021 , 21 , 4021
4022 , 22 , 4022
4023 , 23 , 4023
4024 , 24 , 4024
4025 , 25 , 4025
4026 , 26 , 4026
4027 , 27 , 4027
4028 , 28 , 4028
4029 , 29 , 4029
4030 , 30 , 4030
4031 , 31 , 4031
4032 , 32 , 4032
4033 , 33 , 4033
4034 , 34 , 4034

```

```

4035 , 35 , 4035
4036 , 36 , 4036
4037 , 37 , 4037
**
**
**
**Hangers
**
*ELEMENT , TYPE = B31 , ELSET=HANGERS
5002 , 3002 , 1002
5003 , 3003 , 1003
5004 , 3004 , 1004
5005 , 3005 , 1005
5006 , 3006 , 1006
5007 , 3007 , 1007
5008 , 3008 , 1008
5009 , 3009 , 1009
5010 , 3010 , 1010
5011 , 3011 , 1011
5012 , 3012 , 1012
5013 , 3013 , 1013
5014 , 3014 , 1014
5015 , 3015 , 1015
5016 , 3016 , 1016
5017 , 3017 , 1017
5018 , 3018 , 1018
5019 , 3019 , 1019
5020 , 3020 , 1020
5021 , 3021 , 1021
5022 , 3022 , 1022
5023 , 3023 , 1023
5024 , 3024 , 1024
5025 , 3025 , 1025
5026 , 3026 , 1026
5027 , 3027 , 1027
5028 , 3028 , 1028
5029 , 3029 , 1029
5030 , 3030 , 1030
5031 , 3031 , 1031
5032 , 3032 , 1032
5033 , 3033 , 1033
5034 , 3034 , 1034
5035 , 3035 , 1035
5036 , 3036 , 1036
**
6002 , 4002 , 2002
6003 , 4003 , 2003
6004 , 4004 , 2004
6005 , 4005 , 2005
6006 , 4006 , 2006
6007 , 4007 , 2007
6008 , 4008 , 2008
6009 , 4009 , 2009
6010 , 4010 , 2010
6011 , 4011 , 2011
6012 , 4012 , 2012
6013 , 4013 , 2013
6014 , 4014 , 2014
6015 , 4015 , 2015

```

```

6016 , 4016 , 2016
6017 , 4017 , 2017
6018 , 4018 , 2018
6019 , 4019 , 2019
6020 , 4020 , 2020
6021 , 4021 , 2021
6022 , 4022 , 2022
6023 , 4023 , 2023
6024 , 4024 , 2024
6025 , 4025 , 2025
6026 , 4026 , 2026
6027 , 4027 , 2027
6028 , 4028 , 2028
6029 , 4029 , 2029
6030 , 4030 , 2030
6031 , 4031 , 2031
6032 , 4032 , 2032
6033 , 4033 , 2033
6034 , 4034 , 2034
6035 , 4035 , 2035
6036 , 4036 , 2036
**
**
**
**Fictitious mass elements under the bridge girder (moment of inertia)
**
*ELEMENT , TYPE = B31 , ELSET=DUMMY3
7002 , 2 , 5002
7003 , 3 , 5003
7004 , 4 , 5004
7005 , 5 , 5005
7006 , 6 , 5006
7007 , 7 , 5007
7008 , 8 , 5008
7009 , 9 , 5009
7010 , 10 , 5010
7011 , 11 , 5011
7012 , 12 , 5012
7013 , 13 , 5013
7014 , 14 , 5014
7015 , 15 , 5015
7016 , 16 , 5016
7017 , 17 , 5017
7018 , 18 , 5018
7019 , 19 , 5019
7020 , 20 , 5020
7021 , 21 , 5021
7022 , 22 , 5022
7023 , 23 , 5023
7024 , 24 , 5024
7025 , 25 , 5025
7026 , 26 , 5026
7027 , 27 , 5027
7028 , 28 , 5028
7029 , 29 , 5029
7030 , 30 , 5030
7031 , 31 , 5031
7032 , 32 , 5032
7033 , 33 , 5033

```

```

7034 , 34 , 5034
7035 , 35 , 5035
7036 , 36 , 5036
**
**Fictitious mass elements to create windmoment
**
*ELEMENT , TYPE = B31 , ELSET=DUMMY4
12001 , 3001 , 3002
12002 , 3002 , 3003
12003 , 3003 , 3004
12004 , 3004 , 3005
12005 , 3005 , 3006
12006 , 3006 , 3007
12007 , 3007 , 3008
12008 , 3008 , 3009
12009 , 3009 , 3010
12010 , 3010 , 3011
12011 , 3011 , 3012
12012 , 3012 , 3013
12013 , 3013 , 3014
12014 , 3014 , 3015
12015 , 3015 , 3016
12016 , 3016 , 3017
12017 , 3017 , 3018
12018 , 3018 , 3019
12019 , 3019 , 3020
12020 , 3020 , 3021
12021 , 3021 , 3022
12022 , 3022 , 3023
12023 , 3023 , 3024
12024 , 3024 , 3025
12025 , 3025 , 3026
12026 , 3026 , 3027
12027 , 3027 , 3028
12028 , 3028 , 3029
12029 , 3029 , 3030
12030 , 3030 , 3031
12031 , 3031 , 3032
12032 , 3032 , 3033
12033 , 3033 , 3034
12034 , 3034 , 3035
12035 , 3035 , 3036
12036 , 3036 , 3037
**
13001 , 4001 , 4002
13002 , 4002 , 4003
13003 , 4003 , 4004
13004 , 4004 , 4005
13005 , 4005 , 4006
13006 , 4006 , 4007
13007 , 4007 , 4008
13008 , 4008 , 4009
13009 , 4009 , 4010
13010 , 4010 , 4011
13011 , 4011 , 4012
13012 , 4012 , 4013
13013 , 4013 , 4014
13014 , 4014 , 4015
13015 , 4015 , 4016

```

```

13016 , 4016 , 4017
13017 , 4017 , 4018
13018 , 4018 , 4019
13019 , 4019 , 4020
13020 , 4020 , 4021
13021 , 4021 , 4022
13022 , 4022 , 4023
13023 , 4023 , 4024
13024 , 4024 , 4025
13025 , 4025 , 4026
13026 , 4026 , 4027
13027 , 4027 , 4028
13028 , 4028 , 4029
13029 , 4029 , 4030
13030 , 4030 , 4031
13031 , 4031 , 4032
13032 , 4032 , 4033
13033 , 4033 , 4034
13034 , 4034 , 4035
13035 , 4035 , 4036
13036 , 4036 , 4037
**
**
**
**Tower north
**
*ELEMENT, TYPE=FRAME3D,ELSET=NIVA1
20001 , 20001 , 20002
20101 , 20101 , 20102
*ELEMENT, TYPE=FRAME3D,ELSET=NIVA2
20002 , 20002 , 20003
20102 , 20102 , 20103
*ELEMENT, TYPE=FRAME3D,ELSET=NIVA3
20003 , 20003 , 20004
20103 , 20103 , 20104
*ELEMENT, TYPE=FRAME3D,ELSET=NIVA4
20004 , 20004 , 20005
20104 , 20104 , 20105
*ELEMENT, TYPE=FRAME3D,ELSET=NIVA5
20005 , 20005 , 20006
20105 , 20105 , 20106
*ELEMENT, TYPE=FRAME3D,ELSET=NIVA6
20006 , 20006 , 20007
20106 , 20106 , 20107
*ELEMENT, TYPE=FRAME3D,ELSET=NIVA7
20007 , 20007 , 20008
20107 , 20107 , 20108
*ELEMENT, TYPE=FRAME3D,ELSET=NIVA8
20008 , 20008 , 20009
20108 , 20108 , 20109
*ELEMENT, TYPE=FRAME3D,ELSET=NIVA9
20009 , 20009 , 20010
20109 , 20109 , 20110
*ELEMENT, TYPE=FRAME3D,ELSET=NIVA10
20010 , 20010 , 20011
20110 , 20110 , 20111
*ELEMENT, TYPE=FRAME3D,ELSET=NIVA11
20011 , 20011 , 20012
20111 , 20111 , 20112

```

```

*ELEMENT, TYPE=FRAME3D,ELSET=NIVA12
20012 , 20012 , 20013
20112 , 20112 , 20113
*ELEMENT, TYPE=FRAME3D,ELSET=NIVA13
20013 , 20013 , 20014
20113 , 20113 , 20114
*ELEMENT, TYPE=FRAME3D,ELSET=NIVA14
20014 , 20014 , 20015
20114 , 20114 , 20115
*ELEMENT, TYPE=FRAME3D,ELSET=NIVA15
20015 , 20015 , 20016
20115 , 20115 , 20116
*ELEMENT, TYPE=FRAME3D,ELSET=NIVA16
20016 , 20016 , 20017
20116 , 20116 , 20117
*ELEMENT, TYPE=FRAME3D,ELSET=NIVA17
20017 , 20017 , 20018
20117 , 20117 , 20118
*ELEMENT, TYPE=FRAME3D,ELSET=NIVA18
20018 , 20018 , 20019
20118 , 20118 , 20119
*ELEMENT, TYPE=FRAME3D,ELSET=NIVA19
20019 , 20019 , 20020
20119 , 20119 , 20120
*ELEMENT, TYPE=FRAME3D,ELSET=NIVA20
20020 , 20020 , 20021
20120 , 20120 , 20121
*ELEMENT, TYPE=FRAME3D,ELSET=NIVA21
20021 , 20021 , 20022
20121 , 20121 , 20122
*ELEMENT, TYPE=FRAME3D,ELSET=NIVA22
20022 , 20022 , 20023
20122 , 20122 , 20123
*ELEMENT, TYPE=FRAME3D,ELSET=NIVA23
20023 , 20023 , 20024
20123 , 20123 , 20124
*ELEMENT, TYPE=FRAME3D,ELSET=NIVA24
20024 , 20024 , 20025
20124 , 20124 , 20125
*ELEMENT, TYPE=FRAME3D,ELSET=NIVA25
20025 , 20025 , 20026
20125 , 20125 , 20126
*ELEMENT, TYPE=FRAME3D,ELSET=NIVA26
20026 , 20026 , 20027
20126 , 20126 , 20127
*ELEMENT, TYPE=FRAME3D,ELSET=NIVA27
20027 , 20027 , 20028
20127 , 20127 , 20128
*ELEMENT, TYPE=FRAME3D,ELSET=NIVA28
20028 , 20028 , 20029
20128 , 20128 , 20129
*ELEMENT, TYPE=FRAME3D,ELSET=NIVA29
20029 , 20029 , 20030
20129 , 20129 , 20130
*ELEMENT, TYPE=B31,ELSET=NIVA30
20030 , 20030 , 1001
20130 , 20130 , 2001
*ELEMENT, TYPE=FRAME3D,ELSET=CROSSBEAM1
20201 , 20201 , 20202

```

```

20202 , 20202 , 20203
20203 , 20203 , 20204
20204 , 20204 , 20205
20205 , 20205 , 20206
20206 , 20206 , 20207
*ELEMENT, TYPE=FRAME3D,ELSET=CROSSBEAM2
20301 , 20301 , 20302
20302 , 20302 , 20303
20303 , 20303 , 20304
20304 , 20304 , 20305
20305 , 20305 , 20306
20306 , 20306 , 20307
**
**
**
**
**Tower south
**
*ELEMENT, TYPE=FRAME3D,ELSET=NIVA1
30001 , 30001 , 30002
30101 , 30101 , 30102
*ELEMENT, TYPE=FRAME3D,ELSET=NIVA2
30002 , 30002 , 30003
30102 , 30102 , 30103
*ELEMENT, TYPE=FRAME3D,ELSET=NIVA3
30003 , 30003 , 30004
30103 , 30103 , 30104
*ELEMENT, TYPE=FRAME3D,ELSET=NIVA4
30004 , 30004 , 30005
30104 , 30104 , 30105
*ELEMENT, TYPE=FRAME3D,ELSET=NIVA5
30005 , 30005 , 30006
30105 , 30105 , 30106
*ELEMENT, TYPE=FRAME3D,ELSET=NIVA6
30006 , 30006 , 30007
30106 , 30106 , 30107
*ELEMENT, TYPE=FRAME3D,ELSET=NIVA7
30007 , 30007 , 30008
30107 , 30107 , 30108
*ELEMENT, TYPE=FRAME3D,ELSET=NIVA8
30008 , 30008 , 30009
30108 , 30108 , 30109
*ELEMENT, TYPE=FRAME3D,ELSET=NIVA9
30009 , 30009 , 30010
30109 , 30109 , 30110
*ELEMENT, TYPE=FRAME3D,ELSET=NIVA10
30010 , 30010 , 30011
30110 , 30110 , 30111
*ELEMENT, TYPE=FRAME3D,ELSET=NIVA11
30011 , 30011 , 30012
30111 , 30111 , 30112
*ELEMENT, TYPE=FRAME3D,ELSET=NIVA12
30012 , 30012 , 30013
30112 , 30112 , 30113
*ELEMENT, TYPE=FRAME3D,ELSET=NIVA13
30013 , 30013 , 30014
30113 , 30113 , 30114
*ELEMENT, TYPE=FRAME3D,ELSET=NIVA14
30014 , 30014 , 30015

```

```

30114 , 30114 , 30115
*ELEMENT, TYPE=FRAME3D,ELSET=NIVA15
30015 , 30015 , 30016
30115 , 30115 , 30116
*ELEMENT, TYPE=FRAME3D,ELSET=NIVA16
30016 , 30016 , 30017
30116 , 30116 , 30117
*ELEMENT, TYPE=FRAME3D,ELSET=NIVA17
30017 , 30017 , 30018
30117 , 30117 , 30118
*ELEMENT, TYPE=FRAME3D,ELSET=NIVA18
30018 , 30018 , 30019
30118 , 30118 , 30119
*ELEMENT, TYPE=FRAME3D,ELSET=NIVA19
30019 , 30019 , 30020
30119 , 30119 , 30120
*ELEMENT, TYPE=FRAME3D,ELSET=NIVA20
30020 , 30020 , 30021
30120 , 30120 , 30121
*ELEMENT, TYPE=FRAME3D,ELSET=NIVA21
30021 , 30021 , 30022
30121 , 30121 , 30122
*ELEMENT, TYPE=FRAME3D,ELSET=NIVA22
30022 , 30022 , 30023
30122 , 30122 , 30123
*ELEMENT, TYPE=FRAME3D,ELSET=NIVA23
30023 , 30023 , 30024
30123 , 30123 , 30124
*ELEMENT, TYPE=FRAME3D,ELSET=NIVA24
30024 , 30024 , 30025
30124 , 30124 , 30125
*ELEMENT, TYPE=FRAME3D,ELSET=NIVA25
30025 , 30025 , 30026
30125 , 30125 , 30126
*ELEMENT, TYPE=FRAME3D,ELSET=NIVA26
30026 , 30026 , 30027
30126 , 30126 , 30127
*ELEMENT, TYPE=FRAME3D,ELSET=NIVA27
30027 , 30027 , 30028
30127 , 30127 , 30128
*ELEMENT, TYPE=FRAME3D,ELSET=NIVA28
30028 , 30028 , 30029
30128 , 30128 , 30129
*ELEMENT, TYPE=FRAME3D,ELSET=NIVA29
30029 , 30029 , 30030
30129 , 30129 , 30130
*ELEMENT, TYPE=B31,ELSET=NIVA30
30030 , 30030 , 1037
30130 , 30130 , 2037
*ELEMENT, TYPE=FRAME3D,ELSET=CROSSBEAM1
30201 , 30201 , 30202
30202 , 30202 , 30203
30203 , 30203 , 30204
30204 , 30204 , 30205
30205 , 30205 , 30206
30206 , 30206 , 30207
*ELEMENT, TYPE=FRAME3D,ELSET=CROSSBEAM2
30301 , 30301 , 30302
30302 , 30302 , 30303

```

```

30303 , 30303 , 30304
30304 , 30304 , 30305
30305 , 30305 , 30306
30306 , 30306 , 30307
**
**
**
***** Mass elements *****
*****
**
** Mass points at the lower hanger links, at each side of the
** bridge girder (Moment of inertia)
**
*ELEMENT , TYPE = MASS , ELSET=SIDE
18002 , 3002
18003 , 3003
18004 , 3004
18005 , 3005
18006 , 3006
18007 , 3007
18008 , 3008
18009 , 3009
18010 , 3010
18011 , 3011
18012 , 3012
18013 , 3013
18014 , 3014
18015 , 3015
18016 , 3016
18017 , 3017
18018 , 3018
18019 , 3019
18020 , 3020
18021 , 3021
18022 , 3022
18023 , 3023
18024 , 3024
18025 , 3025
18026 , 3026
18027 , 3027
18028 , 3028
18029 , 3029
18030 , 3030
18031 , 3031
18032 , 3032
18033 , 3033
18034 , 3034
18035 , 3035
18036 , 3036
**
19002 , 4002
19003 , 4003
19004 , 4004
19005 , 4005
19006 , 4006
19007 , 4007
19008 , 4008
19009 , 4009

```

```

19010 , 4010
19011 , 4011
19012 , 4012
19013 , 4013
19014 , 4014
19015 , 4015
19016 , 4016
19017 , 4017
19018 , 4018
19019 , 4019
19020 , 4020
19021 , 4021
19022 , 4022
19023 , 4023
19024 , 4024
19025 , 4025
19026 , 4026
19027 , 4027
19028 , 4028
19029 , 4029
19030 , 4030
19031 , 4031
19032 , 4032
19033 , 4033
19034 , 4034
19035 , 4035
19036 , 4036
**
**
**
** Mass points under the
** bridge girder (Moment of inertia)
**
*ELEMENT , TYPE = MASS , ELSET=UNDER
10002 , 5002
10003 , 5003
10004 , 5004
10005 , 5005
10006 , 5006
10007 , 5007
10008 , 5008
10009 , 5009
10010 , 5010
10011 , 5011
10012 , 5012
10013 , 5013
10014 , 5014
10015 , 5015
10016 , 5016
10017 , 5017
10018 , 5018
10019 , 5019
10020 , 5020
10021 , 5021
10022 , 5022
10023 , 5023
10024 , 5024
10025 , 5025
10026 , 5026

```

```

10027 , 5027
10028 , 5028
10029 , 5029
10030 , 5030
10031 , 5031
10032 , 5032
10033 , 5033
10034 , 5034
10035 , 5035
10036 , 5036
**
**
**
** Mass points to attach the weight of the girder ends
**
*ELEMENT , TYPE = MASS , ELSET=END
11001 , 1
11037 , 37
**
**
**
*****
**** Dummy elements ****
*****
**
** Dummy gripping of tower leg
**
*ELEMENT, TYPE=SPRING1, ELSET=TOWERLEG
29001,20001
29101,20101
39001,30001
39101,30101
**
**
**
** Coupling between the cross beam under the bridge girder and
** the bridge girder
**
*ELEMENT, TYPE=B33, ELSET=BOUNDARY
29501,20204,1
39501,30204,37
**
**
**
*****
**** Rigidity ****
*****
**
** Bridge girder
**
**Using the beam general section option, defined by
**A,I_11,I_12,I_22,J,,Warping constant(15.3.7-2).
**
*BEAM GENERAL SECTION, ELSET=GIRDER, SECTION=GENERAL, DENSITY=0.001
0.360, 0.429, 0.0, 4.952, 0.929, ,4.762
0,1,0
210000E6, 80700E6, 0.00001
**
** USE aplha and beta from the mode 3 and 4

```

```

*DAMPING, ALPHA=0.0109, BETA=0.0024
**SHEAR CENTER
**0 , -0.283
**
**
** Coupling elements, very rigid, no mass
**
*BEAM GENERAL SECTION, ELSET=DUMMY1, SECTION=GENERAL, DENSITY=1E-12
1000,1000,0.0,1000,1000, ,
0,1,0
210000E6, 80700E6, 0.00001
*BEAM GENERAL SECTION, ELSET=DUMMY2, SECTION=GENERAL, DENSITY=1E-12
1000,1000,0.0,1000,1000, ,
0,1,0
210000E6, 80700E6, 0.00001
*BEAM GENERAL SECTION, ELSET=DUMMY3, SECTION=GENERAL, DENSITY=1E-12
1000,1000,0.0,1000,1000, ,
0,1,0
210000E6, 80700E6, 0.00001
**
**
**
** Elements for windmoment, low rigidity, no mass
**
*BEAM GENERAL SECTION, ELSET=DUMMY4, SECTION=GENERAL, DENSITY=0.00001
0.36, 0.429, 0.0, 4.952, 0.929, ,4.762
0,1,0
210000E1, 80700E1, 0.00001
**
**
** Hangers
**
*BEAM GENERAL SECTION, ELSET=HANGERS, SECTION=GENERAL, DENSITY=0.001
0.0018, 2.6E-9, 0, 2.6E-9, 5.2E-9
1,1,0
180000E6, 63077E6, 0.00001
**
**
*DAMPING, ALPHA=0.0109, BETA=0.0024
**
**
**
** Cable in main span
**
** Cable weight+hangerlink+half the hanger = 408 kg/m
**
** RHO = 408kg/m / 0.05 m2 = 8160 kg/m3
**
*BEAM GENERAL SECTION, ELSET=MAINCABLE, SECTION=GENERAL, DENSITY=8160
0.05, 0.0000026, 0, 0.0000026, 0.0000052
0,1,0
180000E6, 80700E6, 0.00001
**
**
*DAMPING, ALPHA=0.0109,BETA=0.0024
**
**
**
** Cable in backstay

```

```

**
** Cable weight = 356 kg/m
**
** RHO = 356kg/m / 0.05m2 = 7120
**
*BEAM GENERAL SECTION, ELSET=BACKSTAYCABLE, SECTION=GENERAL, DENSITY=7120
0.05, 0.0000026, 0, 0.0000026, 0.0000052
0,1,0
180000E6, 80700E6, 0.00001
**
**
*DAMPING, ALPHA=0.0109,BETA=0.0024
**
**
**
** Towers (from foundation to top)
**
*FRAME SECTION,ELSET=NIVA1,SECTION=GENERAL,DENSITY=2500
12.4264 , 8.1186 , 0.1 , 20.3957 , 30
1,0,0
4E+10,1.67E+10
*FRAME SECTION,ELSET=NIVA2,SECTION=GENERAL,DENSITY=2500
7.1176 , 6.9440 , 0.1 , 15.5673 , 16.2382
1,0,0
4E+10,1.67E+10
*FRAME SECTION,ELSET=NIVA3,SECTION=GENERAL,DENSITY=2500
7.0759 , 6.8366 , 0.1 , 15.5169 , 16.0630
1,0,0
4E+10,1.67E+10
*FRAME SECTION,ELSET=NIVA4,SECTION=GENERAL,DENSITY=2500
7.0342 , 6.7293 , 0.1 , 15.4664 , 15.8878
1,0,0
4E+10,1.67E+10
*FRAME SECTION,ELSET=NIVA5,SECTION=GENERAL,DENSITY=2500
6.9925 , 6.6219 , 0.1 , 15.4160 , 15.7127
1,0,0
4E+10,1.67E+10
*FRAME SECTION,ELSET=NIVA6,SECTION=GENERAL,DENSITY=2500
6.9508 , 6.5145 , 0.1 , 15.3655 , 15.5375
1,0,0
4E+10,1.67E+10
*FRAME SECTION,ELSET=NIVA7,SECTION=GENERAL,DENSITY=2500
6.9092 , 6.4072 , 0.1 , 15.3151 , 15.3623
1,0,0
4E+10,1.67E+10
*FRAME SECTION,ELSET=NIVA8,SECTION=GENERAL,DENSITY=2500
6.8675 , 6.2998 , 0.1 , 15.2646 , 15.1871
1,0,0
4E+10,1.67E+10
*FRAME SECTION,ELSET=NIVA9,SECTION=GENERAL,DENSITY=2500
6.8258 , 6.1925 , 0.1 , 15.2142 , 15.0119
1,0,0
4E+10,1.67E+10
*FRAME SECTION,ELSET=NIVA10,SECTION=GENERAL,DENSITY=2500
6.7841 , 6.0851 , 0.1 , 15.1637 , 14.8367
1,0,0
4E+10,1.67E+10
*FRAME SECTION,ELSET=NIVA11,SECTION=GENERAL,DENSITY=2500
6.7424 , 5.9777 , 0.1 , 15.1133 , 14.6616

```

```

1,0,0
4E+10,1.67E+10
*FRAME SECTION,ELSET=NIVA12,SECTION=GENERAL,DENSITY=2500
6.7007 , 5.8704 , 0.1 , 15.0629 , 14.4864
1,0,0
4E+10,1.67E+10
*FRAME SECTION,ELSET=NIVA13,SECTION=GENERAL,DENSITY=2500
6.6590 , 5.7630 , 0.1 , 15.0124 , 14.3112
1,0,0
4E+10,1.67E+10
*FRAME SECTION,ELSET=NIVA14,SECTION=GENERAL,DENSITY=2500
6.6173 , 5.6556 , 0.1 , 14.9620 , 14.1360
1,0,0
4E+10,1.67E+10
*FRAME SECTION,ELSET=NIVA15,SECTION=GENERAL,DENSITY=2500
6.5756 , 5.5483 , 0.1 , 14.9115 , 13.9608
1,0,0
4E+10,1.67E+10
*FRAME SECTION,ELSET=NIVA16,SECTION=GENERAL,DENSITY=2500
6.5340 , 5.4409 , 0.1 , 14.8611 , 13.7857
1,0,0
4E+10,1.67E+10
*FRAME SECTION,ELSET=NIVA17,SECTION=GENERAL,DENSITY=2500
6.4923 , 5.3336 , 0.1 , 14.8106 , 13.6105
1,0,0
4E+10,1.67E+10
*FRAME SECTION,ELSET=NIVA18,SECTION=GENERAL,DENSITY=2500
6.4506 , 5.2262 , 0.1 , 14.7602 , 13.4353
1,0,0
4E+10,1.67E+10
*FRAME SECTION,ELSET=NIVA19,SECTION=GENERAL,DENSITY=2500
6.4089 , 5.1188 , 0.1 , 14.7097 , 13.2601
1,0,0
4E+10,1.67E+10
*FRAME SECTION,ELSET=NIVA20,SECTION=GENERAL,DENSITY=2500
6.3672 , 5.0115 , 0.1 , 14.6593 , 13.0849
1,0,0
4E+10,1.67E+10
*FRAME SECTION,ELSET=NIVA21,SECTION=GENERAL,DENSITY=2500
6.3255 , 4.9041 , 0.1 , 14.6089 , 12.9098
1,0,0
4E+10,1.67E+10
*FRAME SECTION,ELSET=NIVA22,SECTION=GENERAL,DENSITY=2500
6.2838 , 4.7967 , 0.1 , 14.5584 , 12.7346
1,0,0
4E+10,1.67E+10
*FRAME SECTION,ELSET=NIVA23,SECTION=GENERAL,DENSITY=2500
6.2421 , 4.6894 , 0.1 , 14.5080 , 12.5594
1,0,0
4E+10,1.67E+10
*FRAME SECTION,ELSET=NIVA24,SECTION=GENERAL,DENSITY=2500
6.2004 , 4.5820 , 0.1 , 14.4575 , 12.3842
1,0,0
4E+10,1.67E+10
*FRAME SECTION,ELSET=NIVA25,SECTION=GENERAL,DENSITY=2500
6.1588 , 4.4747 , 0.1 , 14.4071 , 12.2090
1,0,0
4E+10,1.67E+10
*FRAME SECTION,ELSET=NIVA26,SECTION=GENERAL,DENSITY=2500

```

```

6.1171 , 4.3673 , 0.1 , 14.3566 , 12.0338
1,0,0
4E+10,1.67E+10
*FRAME SECTION,ELSET=NIVA27,SECTION=GENERAL,DENSITY=2500
6.0754 , 4.2599 , 0.1 , 14.3062 , 11.8587
1,0,0
4E+10,1.67E+10
*FRAME SECTION,ELSET=NIVA28,SECTION=GENERAL,DENSITY=2500
6.0337 , 4.1526 , 0.1 , 14.2557 , 11.6835
1,0,0
4E+10,1.67E+10
*FRAME SECTION,ELSET=NIVA29,SECTION=GENERAL,DENSITY=2500
5.9920 , 4.0452 , 0.10 , 14.2053 , 11.5083
1,0,0
4E+10,1.67E+10
**
** What happens if I change the beam direction n1 to go to global Y dir
** This removes the warning previously seen
** JT
*BEAM GENERAL SECTION,ELSET=NIVA30,DENSITY=0.00001
**5.9503 , 3.9378 , 0.10 , 14.1549 , 11.3331
**1,0,0
5.9503 , 14.1549, 0.10 , 3.9378 , 11.3331
0,1,0
4E+10,1.67E+10
**
**
*DAMPING, BETA=0.0053
**
*FRAME SECTION,ELSET=CROSSBEAM1,SECTION=GENERAL,DENSITY=2500
13.36 , 12.7516 , 0.10 , 27.8824 , 18.6318
1,0,0
4E+10,1.67E+10
*FRAME SECTION,ELSET=CROSSBEAM2,SECTION=GENERAL,DENSITY=2500
9.28 , 6.2500 , 0.10 , 12.2500 , 10.2875
1,0,0
4E+10,1.67E+10
**
**
** Dummy boundary towerleg, infinite rigid torsion spring
**
*SPRING, ELSET=TOWERLEG
6
1E+12
**
**
** Coupling between the cross beam under the bridge girder and
** the bridge girder, rigid element
**
*BEAM GENERAL SECTION,ELSET=BOUNDARY,DENSITY=0.000001
100 , 1000 , 0 , 1000 , 1000
1,0,0
4E+10,1.67E+10
**
*****
**** Assign lumped mass ****
*****
**
**
** Lumped mass along the bridge girder
** From Mathcad, fit sutch that IM = 82436:
** "SIDE" = 1478 x 12 meter between hangers = 17736

```

```

** "UNDER" = 2394 x 12 = 28728
**
*MASS, ELSET=SIDE
17736
*MASS, ELSET=UNDER
28728
**
** Weight of the last 9,5 meters have to be added as a lumped mass
** at the end of the bridge girder.
** 9,5x5350=50825
**
*MASS, ELSET=END
50825
**
***** Boundary conditions ****
*****
** Nodes for boundary conditions
**
*NSET,NSET=ROCK
981,1087,1981,2087
*NSET,NSET=TOWER
1001,1037,2001,2037
*NSET,NSET=BOUNDARY
1,37
*NSET,NSET=ALL,GENERATE
1,50000,1
*NSET,NSET=TOWERLEG
20001,20101,30001,30101
**
** Boundary conditions
**
*BOUNDARY
ROCK,1,3,0
TOWERLEG,1,5,0
**1,1,1,0
**
***** Couplings ****
*****
**
** The nodes in the top of the towers are made hinged such that
** the cables not are rigid
**
*RELEASE
20030,S2,ALLM
20130,S2,ALLM
30030,S2,ALLM
30130,S2,ALLM
**
** Coupling between cross beams and towerlegs
*MPC
**Tower north
TIE,20201,20014
TIE,20207,20114
TIE,20301,20029
TIE,20307,20129
**Tower south

```

```

TIE,30201,30012
TIE,30207,30112
TIE,30301,30029
TIE,30307,30129
**
** The cross beam under the bridge girder, and
** the bridge girder:
** Fixed in the length direction in one side of the bridge
**
*RELEASE
29501,S2,M2-T
39501,S2,M2-T
39501,S1,M2
**
*****
**** Elements ****
*****
**
*ELSET,ELSET=TOWER,GENERATE
20001,20030,1
20101,20130,1
20201,20206,1
20301,20306,1
30001,30030,1
30101,30130,1
30201,30206,1
30301,30306,1
**
*ELSET,ELSET=TOWERLEG1,GENERATE
20001,20030,1
30001,30030,1
*ELSET,ELSET=TOWERLEG2,GENERATE
20101,20130,1
30101,30130,1
**
*ELSET,ELSET=FRAME
20025,20048
20125,20148
20301,20306
**
*****
**** Nodes to put on load ****
*****
*NSET,NSET=WINDLOAD,GENERATE
2,36,1
*NSET,NSET=WINDCAB,GENERATE
1002,1036,1
2002,2036,1
**
*NSET,NSET=CENTRE
19
**
*NSET,NSET=GIRDER,GENERATE
1,37,1
*NSET,NSET=CABEL,GENERATE
1001,1037,1
2001,2037,1
*NSET,NSET=HLINK,GENERATE
3001,3037,1

```

```
4001,4037,1
**
```

File dead_load.inp

```
** STEP1: DEADLOAD
** Deadload is given as static load, with non-linear geometry
** Need to do it in a two step fashion, because of the backstay cables
**
*STEP,AMPLITUDE=RAMP,NAME=EGENVEKT,NLGEOM,INC=5000
*STATIC,STABILIZE=1E-10
1E-6,1E-6,1E-9,1E-6
**
** Cable
** Cable with half the hanger and hangerlink
** RHO-MED H.STENGER = 8524.2
** RHO-WITH HANGERS = 408kg/m / 0.0443 m2 = 9210
** RHO-WITHOUT HANGERS = 356kg/m / 0.0443m2 = 8036
** g = 9,81 x (8036/9210) = 8,5595
**
*DLOAD
MAINCABLE, GRAV, 8.5595, 0 , 0 , -1
**
** Deadload bridge girder
** Deadload bridge girder included hangerlink and half the
** hanger = 5350 kg/m
**
** 5350 x 9,81 = 52483.5
**
*DLOAD
GIRDER, PZ, -52484
**
** Deadload tower
**
*DLOAD
TOWER, GRAV, 9.81, 0 , 0 , -1
*END STEP
**
*STEP,AMPLITUDE=RAMP,NAME=EGENVEKT_BACKSTAY,NLGEOM,INC=5000
*STATIC,STABILIZE=1E-10
1E-6,1E-6,1E-9,1E-6
**
** Cable
** Need to do this in 2 steps, because the backstays need tension before
loading
**
*DLOAD
BACKSTAYCABLE, GRAV, 9.810, 0 , 0 , -1
**
*NODE PRINT, TOTALS=YES, FREQUENCY=100
RF
*NODE PRINT, TOTALS=YES, FREQUENCY=100
U
*EL PRINT, ELSET=MAINCABLE, FREQUENCY=100
SF
*EL PRINT, ELSET=GIRDER, FREQUENCY=100
SF
```

```
*EL PRINT, ELSESET=BACKSTAYCABLE, FREQUENCY=100
SF
*END STEP
```

File lysefjord_egenvekt.inp

```
*HEADING
Analysis of Lysefjord bridge
**
** Include the model
*INCLUDE, INPUT=lysefjord_modifisert_bru.inp
**
**
***** Loading and analysis *****
*****
** Dead load
*INCLUDE, INPUT=dead_load.inp
**
*STEP,NLGEOM
*FREQUENCY
150
**
*NODE PRINT, TOTALS=YES,NSET=GIRDER
U
*END STEP
**
```

File lysefjord_egenvekt.dat

1

Abaqus Student Edition 6.11-2 Date 09-May-2012 Time 10:23:43

The Abaqus Software is a product of
 Dassault Systems Simulia Corp.
 Rising Sun Mills
 166 Valley Street
 Providence, RI 02909-2499, USA

Your site id is: SE2011

```
*****  

*  

*  

*      *****  

*      * N O T I C E *  

*      *****  

*  

*  

*      Abaqus Student Edition 6.11-2  

*  

*  

*      Please make sure you are using version 6.11manuals
```

```

* plus the notes accompanying this release. *
* The Student Edition does not include technical support. *
* For more information see http://www.simulia.com. *
*
* Due to the model size limitation of the Abaqus Student *
* Edition, not all Abaqus Tutorial, Workshop, Benchmark, *
* Example and Verification problems can be run with it. *
*
* This program may not be used for commercial purposes. *
*
* Copyright 2011 Dassault Systemes *
* * * * * * * * * * * * * * * * * * * * * * * * * * * * * * * * * * *

```

PROCESSING PART, INSTANCE, AND ASSEMBLY INFORMATION

END PROCESSING PART, INSTANCE, AND ASSEMBLY INFORMATION

OPTIONS BEING PROCESSED

```

*HEADING
    Analysis of Lysefjord bridge
*INCLUDE, INPUT=lysefjord_modifisert_bru.inp

*** INPUT DATA IS READ FROM FILE lysefjord_modifisert_bru.inp

*NODE
*NGEN, NSET=BACKSTAY
*ELEMENT , TYPE = B31 , ELSET=GIRDER
*ELEMENT , TYPE = B31 , ELSET=MAINCABLE
*ELEMENT , TYPE = B31 , ELSET=BACKSTAYCABLE
*ELGEN , ELSET=BACKSTAYCABLE
*ELEMENT , TYPE = B31 , ELSET=DUMMY1
*ELEMENT , TYPE = B31 , ELSET=DUMMY2
*ELEMENT , TYPE = B31 , ELSET=HANGERS
*ELEMENT , TYPE = B31 , ELSET=DUMMY3
*ELEMENT , TYPE = B31 , ELSET=DUMMY4
*ELEMENT, TYPE=FRAME3D,ELSET=NIVA1
*ELEMENT, TYPE=FRAME3D,ELSET=NIVA2
*ELEMENT, TYPE=FRAME3D,ELSET=NIVA3
*ELEMENT, TYPE=FRAME3D,ELSET=NIVA4
*ELEMENT, TYPE=FRAME3D,ELSET=NIVA5
*ELEMENT, TYPE=FRAME3D,ELSET=NIVA6
*ELEMENT, TYPE=FRAME3D,ELSET=NIVA7
*ELEMENT, TYPE=FRAME3D,ELSET=NIVA8
*ELEMENT, TYPE=FRAME3D,ELSET=NIVA9
*ELEMENT, TYPE=FRAME3D,ELSET=NIVA10
*ELEMENT, TYPE=FRAME3D,ELSET=NIVA11
*ELEMENT, TYPE=FRAME3D,ELSET=NIVA12
*ELEMENT, TYPE=FRAME3D,ELSET=NIVA13
*ELEMENT, TYPE=FRAME3D,ELSET=NIVA14
*ELEMENT, TYPE=FRAME3D,ELSET=NIVA15
*ELEMENT, TYPE=FRAME3D,ELSET=NIVA16
*ELEMENT, TYPE=FRAME3D,ELSET=NIVA17
*ELEMENT, TYPE=FRAME3D,ELSET=NIVA18
*ELEMENT, TYPE=FRAME3D,ELSET=NIVA19
*ELEMENT, TYPE=FRAME3D,ELSET=NIVA20
*ELEMENT, TYPE=FRAME3D,ELSET=NIVA21
*ELEMENT, TYPE=FRAME3D,ELSET=NIVA22
*ELEMENT, TYPE=FRAME3D,ELSET=NIVA23
*ELEMENT, TYPE=FRAME3D,ELSET=NIVA24

```

```

*ELEMENT, TYPE=FRAME3D,ELSET=NIVA25
*ELEMENT, TYPE=FRAME3D,ELSET=NIVA26
*ELEMENT, TYPE=FRAME3D,ELSET=NIVA27
*ELEMENT, TYPE=FRAME3D,ELSET=NIVA28
*ELEMENT, TYPE=FRAME3D,ELSET=NIVA29
*ELEMENT, TYPE=B31,ELSET=NIVA30
*ELEMENT, TYPE=FRAME3D,ELSET=CROSSBEAM1
*ELEMENT, TYPE=FRAME3D,ELSET=CROSSBEAM2
*ELEMENT, TYPE=FRAME3D,ELSET=NIVA1
*ELEMENT, TYPE=FRAME3D,ELSET=NIVA2
*ELEMENT, TYPE=FRAME3D,ELSET=NIVA3
*ELEMENT, TYPE=FRAME3D,ELSET=NIVA4
*ELEMENT, TYPE=FRAME3D,ELSET=NIVA5
*ELEMENT, TYPE=FRAME3D,ELSET=NIVA6
*ELEMENT, TYPE=FRAME3D,ELSET=NIVA7
*ELEMENT, TYPE=FRAME3D,ELSET=NIVA8
*ELEMENT, TYPE=FRAME3D,ELSET=NIVA9
*ELEMENT, TYPE=FRAME3D,ELSET=NIVA10
*ELEMENT, TYPE=FRAME3D,ELSET=NIVA11
*ELEMENT, TYPE=FRAME3D,ELSET=NIVA12
*ELEMENT, TYPE=FRAME3D,ELSET=NIVA13
*ELEMENT, TYPE=FRAME3D,ELSET=NIVA14
*ELEMENT, TYPE=FRAME3D,ELSET=NIVA15
*ELEMENT, TYPE=FRAME3D,ELSET=NIVA16
*ELEMENT, TYPE=FRAME3D,ELSET=NIVA17
*ELEMENT, TYPE=FRAME3D,ELSET=NIVA18
*ELEMENT, TYPE=FRAME3D,ELSET=NIVA19
*ELEMENT, TYPE=FRAME3D,ELSET=NIVA20
*ELEMENT, TYPE=FRAME3D,ELSET=NIVA21
*ELEMENT, TYPE=FRAME3D,ELSET=NIVA22
*ELEMENT, TYPE=FRAME3D,ELSET=NIVA23
*ELEMENT, TYPE=FRAME3D,ELSET=NIVA24
*ELEMENT, TYPE=FRAME3D,ELSET=NIVA25
*ELEMENT, TYPE=FRAME3D,ELSET=NIVA26
*ELEMENT, TYPE=FRAME3D,ELSET=NIVA27
*ELEMENT, TYPE=FRAME3D,ELSET=NIVA28
*ELEMENT, TYPE=FRAME3D,ELSET=NIVA29
*ELEMENT, TYPE=B31,ELSET=NIVA30
*ELEMENT, TYPE=FRAME3D,ELSET=CROSSBEAM1
*ELEMENT, TYPE=FRAME3D,ELSET=CROSSBEAM2
*ELEMENT , TYPE = MASS , ELSET=SIDE
*ELEMENT , TYPE = MASS , ELSET=UNDER
*ELEMENT , TYPE = MASS , ELSET=END
*ELEMENT, TYPE=SPRING1, ELSET=TOWERLEG
*ELEMENT, TYPE=B33, ELSET=BOUNDARY
*NSET,NSET=ROCK
*NSET,NSET=TOWER
*NSET,NSET=BOUNDARY
*NSET,NSET=ALL,GENERATE
*NSET,NSET=TOWERLEG
*ELSET,ELSET=TOWER,GENERATE
*ELSET,ELSET=TOWERLEG1,GENERATE
*ELSET,ELSET=TOWERLEG2,GENERATE
*ELSET,ELSET=FRAME
*NSET,NSET=WINDLOAD,GENERATE
*NSET,NSET=WINDCAB,GENERATE
*NSET,NSET=CENTRE
*NSET,NSET=GIRDER,GENERATE
*NSET,NSET=CABEL,GENERATE
*NSET,NSET=HLINK,GENERATE
*INCLUDE, INPUT=dead_load.inp

```

*** INPUT DATA IS READ FROM FILE dead_load.inp

```

*BEAM GENERAL SECTION, ELSET=GIRDER, SECTION=GENERAL, DENSITY=0.001
*DAMPING, ALPHA=0.0109, BETA=0.0024
*BEAM GENERAL SECTION, ELSET=DUMMY1, SECTION=GENERAL, DENSITY=1E-12
*BEAM GENERAL SECTION, ELSET=DUMMY2, SECTION=GENERAL, DENSITY=1E-12
*BEAM GENERAL SECTION, ELSET=DUMMY3, SECTION=GENERAL, DENSITY=1E-12
*BEAM GENERAL SECTION, ELSET=DUMMY4, SECTION=GENERAL, DENSITY=0.00001
*BEAM GENERAL SECTION, ELSET=HANGERS, SECTION=GENERAL, DENSITY=0.001
*DAMPING, ALPHA=0.0109, BETA=0.0024
*BEAM GENERAL SECTION, ELSET=MAINCABLE, SECTION=GENERAL, DENSITY=8160
*DAMPING, ALPHA=0.0109,BETA=0.0024

```

```

*BEAM GENERAL SECTION, ELSET=BACKSTAYCABLE, SECTION=GENERAL,DENSITY=7120
*DAMPING, ALPHA=0.0109,BETA=0.0024
*BEAM GENERAL SECTION,ELSET=NIVA30,DENSITY=0.00001
*DAMPING, BETA=0.0053
*BEAM GENERAL SECTION,ELSET=BOUNDARY,DENSITY=0.000001
*FRAME SECTION,ELSET=NIVA1,SECTION=GENERAL,DENSITY=2500
*FRAME SECTION,ELSET=NIVA2,SECTION=GENERAL,DENSITY=2500
*FRAME SECTION,ELSET=NIVA3,SECTION=GENERAL,DENSITY=2500
*FRAME SECTION,ELSET=NIVA4,SECTION=GENERAL,DENSITY=2500
*FRAME SECTION,ELSET=NIVA5,SECTION=GENERAL,DENSITY=2500
*FRAME SECTION,ELSET=NIVA6,SECTION=GENERAL,DENSITY=2500
*FRAME SECTION,ELSET=NIVA7,SECTION=GENERAL,DENSITY=2500
*FRAME SECTION,ELSET=NIVA8,SECTION=GENERAL,DENSITY=2500
*FRAME SECTION,ELSET=NIVA9,SECTION=GENERAL,DENSITY=2500
*FRAME SECTION,ELSET=NIVA10,SECTION=GENERAL,DENSITY=2500
*FRAME SECTION,ELSET=NIVA11,SECTION=GENERAL,DENSITY=2500
*FRAME SECTION,ELSET=NIVA12,SECTION=GENERAL,DENSITY=2500
*FRAME SECTION,ELSET=NIVA13,SECTION=GENERAL,DENSITY=2500
*FRAME SECTION,ELSET=NIVA14,SECTION=GENERAL,DENSITY=2500
*FRAME SECTION,ELSET=NIVA15,SECTION=GENERAL,DENSITY=2500
*FRAME SECTION,ELSET=NIVA16,SECTION=GENERAL,DENSITY=2500
*FRAME SECTION,ELSET=NIVA17,SECTION=GENERAL,DENSITY=2500
*FRAME SECTION,ELSET=NIVA18,SECTION=GENERAL,DENSITY=2500
*FRAME SECTION,ELSET=NIVA19,SECTION=GENERAL,DENSITY=2500
*FRAME SECTION,ELSET=NIVA20,SECTION=GENERAL,DENSITY=2500
*FRAME SECTION,ELSET=NIVA21,SECTION=GENERAL,DENSITY=2500
*FRAME SECTION,ELSET=NIVA22,SECTION=GENERAL,DENSITY=2500
*FRAME SECTION,ELSET=NIVA23,SECTION=GENERAL,DENSITY=2500
*FRAME SECTION,ELSET=NIVA24,SECTION=GENERAL,DENSITY=2500
*FRAME SECTION,ELSET=NIVA25,SECTION=GENERAL,DENSITY=2500
*FRAME SECTION,ELSET=NIVA26,SECTION=GENERAL,DENSITY=2500
*FRAME SECTION,ELSET=NIVA27,SECTION=GENERAL,DENSITY=2500
*FRAME SECTION,ELSET=NIVA28,SECTION=GENERAL,DENSITY=2500
*FRAME SECTION,ELSET=NIVA29,SECTION=GENERAL,DENSITY=2500
*FRAME SECTION,ELSET=CROSSBEAM1,SECTION=GENERAL,DENSITY=2500
*FRAME SECTION,ELSET=CROSSBEAM2,SECTION=GENERAL,DENSITY=2500
*SPRING, ELSET=TOWERLEG
*MASS, ELSET=SIDE
*MASS, ELSET=UNDER
*MASS, ELSET=END
*BOUNDARY
*MPC
*RELEASE
*RELEASE
*BEAM GENERAL SECTION, ELSET=GIRDER, SECTION=GENERAL, DENSITY=0.001
*BEAM GENERAL SECTION, ELSET=DUMMY1, SECTION=GENERAL, DENSITY=1E-12
*BEAM GENERAL SECTION, ELSET=DUMMY2, SECTION=GENERAL, DENSITY=1E-12
*BEAM GENERAL SECTION, ELSET=DUMMY3, SECTION=GENERAL, DENSITY=1E-12
*BEAM GENERAL SECTION, ELSET=DUMMY4, SECTION=GENERAL, DENSITY=0.00001
*BEAM GENERAL SECTION, ELSET=HANGERS, SECTION=GENERAL, DENSITY=0.001
*BEAM GENERAL SECTION, ELSET=MAINCABLE, SECTION=GENERAL, DENSITY=8160
*BEAM GENERAL SECTION, ELSET=BACKSTAYCABLE, SECTION=GENERAL,DENSITY=7120
*BEAM GENERAL SECTION,ELSET=NIVA30,DENSITY=0.00001
*BEAM GENERAL SECTION,ELSET=BOUNDARY,DENSITY=0.000001
*FRAME SECTION,ELSET=NIVA1,SECTION=GENERAL,DENSITY=2500
*FRAME SECTION,ELSET=NIVA2,SECTION=GENERAL,DENSITY=2500
*FRAME SECTION,ELSET=NIVA3,SECTION=GENERAL,DENSITY=2500
*FRAME SECTION,ELSET=NIVA4,SECTION=GENERAL,DENSITY=2500
*FRAME SECTION,ELSET=NIVA5,SECTION=GENERAL,DENSITY=2500
*FRAME SECTION,ELSET=NIVA6,SECTION=GENERAL,DENSITY=2500
*FRAME SECTION,ELSET=NIVA7,SECTION=GENERAL,DENSITY=2500
*FRAME SECTION,ELSET=NIVA8,SECTION=GENERAL,DENSITY=2500
*FRAME SECTION,ELSET=NIVA9,SECTION=GENERAL,DENSITY=2500
*FRAME SECTION,ELSET=NIVA10,SECTION=GENERAL,DENSITY=2500
*FRAME SECTION,ELSET=NIVA11,SECTION=GENERAL,DENSITY=2500
*FRAME SECTION,ELSET=NIVA12,SECTION=GENERAL,DENSITY=2500
*FRAME SECTION,ELSET=NIVA13,SECTION=GENERAL,DENSITY=2500
*FRAME SECTION,ELSET=NIVA14,SECTION=GENERAL,DENSITY=2500
*FRAME SECTION,ELSET=NIVA15,SECTION=GENERAL,DENSITY=2500
*FRAME SECTION,ELSET=NIVA16,SECTION=GENERAL,DENSITY=2500
*FRAME SECTION,ELSET=NIVA17,SECTION=GENERAL,DENSITY=2500
*FRAME SECTION,ELSET=NIVA18,SECTION=GENERAL,DENSITY=2500
*FRAME SECTION,ELSET=NIVA19,SECTION=GENERAL,DENSITY=2500
*FRAME SECTION,ELSET=NIVA20,SECTION=GENERAL,DENSITY=2500

```

```

*FRAME SECTION,ELSET=NIVA21,SECTION=GENERAL,DENSITY=2500
*FRAME SECTION,ELSET=NIVA22,SECTION=GENERAL,DENSITY=2500
*FRAME SECTION,ELSET=NIVA23,SECTION=GENERAL,DENSITY=2500
*FRAME SECTION,ELSET=NIVA24,SECTION=GENERAL,DENSITY=2500
*FRAME SECTION,ELSET=NIVA25,SECTION=GENERAL,DENSITY=2500
*FRAME SECTION,ELSET=NIVA26,SECTION=GENERAL,DENSITY=2500
*FRAME SECTION,ELSET=NIVA27,SECTION=GENERAL,DENSITY=2500
*FRAME SECTION,ELSET=NIVA28,SECTION=GENERAL,DENSITY=2500
*FRAME SECTION,ELSET=NIVA29,SECTION=GENERAL,DENSITY=2500
*FRAME SECTION,ELSET=CROSSBEAM1,SECTION=GENERAL,DENSITY=2500
*FRAME SECTION,ELSET=CROSSBEAM2,SECTION=GENERAL,DENSITY=2500
*SPRING, ELSET=TOWERLEG
*MASS, ELSET=SIDE
*MASS, ELSET=UNDER
*MASS, ELSET=END
*RELEASE
*RELEASE
*STEP, AMPLITUDE=RAMP,NAME=EGENVEKT,NLGEOM,INC=5000
*STEP, AMPLITUDE=RAMP,NAME=EGENVEKT_BACKSTAY,NLGEOM,INC=5000
*STEP,NLGEOM
*FREQUENCY
*STEP, AMPLITUDE=RAMP,NAME=EGENVEKT,NLGEOM,INC=5000
*STEP, AMPLITUDE=RAMP,NAME=EGENVEKT_BACKSTAY,NLGEOM,INC=5000
*STEP,NLGEOM
*STEP, AMPLITUDE=RAMP,NAME=EGENVEKT,NLGEOM,INC=5000
*STATIC,STABILIZE=1E-10
*DLOAD
*DLOAD
*DLOAD
*END STEP
*STEP, AMPLITUDE=RAMP,NAME=EGENVEKT_BACKSTAY,NLGEOM,INC=5000
*STATIC,STABILIZE=1E-10
*DLOAD
*EL PRINT, ELSET=MAINCABLE, FREQUENCY=100
*EL PRINT, ELSET=GIRDER, FREQUENCY=100
*EL PRINT, ELSET=BACKSTAYCABLE, FREQUENCY=100
*END STEP
*STEP,NLGEOM
*FREQUENCY
*FREQUENCY
*END STEP
*BOUNDARY
*STEP, AMPLITUDE=RAMP,NAME=EGENVEKT,NLGEOM,INC=5000
*STATIC,STABILIZE=1E-10
*END STEP
*STEP, AMPLITUDE=RAMP,NAME=EGENVEKT_BACKSTAY,NLGEOM,INC=5000
*STATIC,STABILIZE=1E-10
*NODE PRINT, TOTALS=YES, FREQUENCY=100
*NODE PRINT, TOTALS=YES, FREQUENCY=100
*END STEP
*STEP,NLGEOM
*FREQUENCY
*FREQUENCY
*END STEP

```

P R O B L E M S I Z E

NUMBER OF ELEMENTS IS	686
NUMBER OF NODES IS	587
NUMBER OF NODES DEFINED BY THE USER	438
NUMBER OF INTERNAL NODES GENERATED BY THE PROGRAM	149
TOTAL NUMBER OF VARIABLES IN THE MODEL	3073
(DEGREES OF FREEDOM PLUS MAX NO. OF ANY LAGRANGE MULTIPLIER VARIABLES. INCLUDE *PRINT,SOLVE=YES TO GET THE ACTUAL NUMBER.)	

END OF USER INPUT PROCESSING

JOB TIME SUMMARY
 USER TIME (SEC) = 0.30000
 SYSTEM TIME (SEC) = 0.10000
 TOTAL CPU TIME (SEC) = 0.40000
 WALLCLOCK TIME (SEC) = 1

1

Abaqus Student Edition 6.11-2 DATE 09-May-2012 TIME 10:23:46

Analysis of Lysefjord bridge

STEP 1 INCREMENT 1
 TIME COMPLETED IN THIS STEP

0.00

S T E P 1 S T A T I C A N A L Y S I S

AUTOMATIC TIME CONTROL WITH -
 A SUGGESTED INITIAL TIME INCREMENT OF 1.000E-06
 AND A TOTAL TIME PERIOD OF 1.000E-06
 THE MINIMUM TIME INCREMENT ALLOWED IS 1.000E-09
 THE MAXIMUM TIME INCREMENT ALLOWED IS 1.000E-06

LINEAR EQUATION SOLVER TYPE DIRECT SPARSE

AUTOMATIC STABILIZATION WITH DISSIPATED ENERGY FRACTION = 1.000E-10

LARGE DISPLACEMENT THEORY WILL BE USED

TOTAL MASS OF MODEL

1.1029548E+07

LOCATION OF THE CENTER OF MASS OF THE MODEL

6.513799	4.5470764E-15	53.26650
----------	---------------	----------

MOMENTS OF INERTIA ABOUT THE ORIGIN		
I (XX)	I (YY)	I (ZZ)
3.8816069E+10	5.0335057E+11	4.6541096E+11

PRODUCTS OF INERTIA ABOUT THE ORIGIN		
I (XY)	I (XZ)	I (YZ)
5.7399605E-06	-1.8193880E+08	-2.0119026E-06

MOMENTS OF INERTIA ABOUT THE CENTER OF MASS		
I (XX)	I (YY)	I (ZZ)
7.5217090E+09	4.7158823E+11	4.6494298E+11

PRODUCTS OF INERTIA ABOUT THE CENTER OF MASS		
I (XY)	I (XZ)	I (YZ)
6.0666418E-06	3.6449537E+09	6.5952955E-07

M E M O R Y E S T I M A T E

PROCESS	FLOATING PT OPERATIONS PER ITERATION	MINIMUM MEMORY REQUIRED (MBYTES)	MEMORY TO MINIMIZE I/O (MBYTES)
---------	--------------------------------------	----------------------------------	---------------------------------

1	2.45E+006	18	40
---	-----------	----	----

NOTE:

- (1) SINCE ABAQUS DOES NOT PRE-ALLOCATE MEMORY AND ONLY ALLOCATES MEMORY AS NEEDED DURING THE ANALYSIS, THE MEMORY REQUIREMENT PRINTED HERE CAN ONLY BE VIEWED AS A GENERAL GUIDELINE BASED ON THE BEST KNOWLEDGE AVAILABLE AT THE BEGINNING OF A STEP BEFORE THE SOLUTION PROCESS HAS BEGUN.
- (2) THE ESTIMATE IS NORMALLY UPDATED AT THE BEGINNING OF EVERY STEP. IT IS THE MAXIMUM VALUE OF THE ESTIMATE FROM THE CURRENT STEP TO THE LAST STEP OF THE ANALYSIS, WITH UNSYMMETRIC SOLUTION TAKEN INTO ACCOUNT IF APPLICABLE.
- (3) SINCE THE ESTIMATE IS BASED ON THE ACTIVE DEGREES OF FREEDOM IN THE FIRST ITERATION OF THE CURRENT STEP, THE MEMORY ESTIMATE MIGHT BE SIGNIFICANTLY DIFFERENT THAN ACTUAL USAGE FOR PROBLEMS WITH SUBSTANTIAL CHANGES IN ACTIVE DEGREES OF FREEDOM BETWEEN STEPS (OR EVEN WITHIN THE SAME STEP). EXAMPLES ARE: PROBLEMS WITH SIGNIFICANT CONTACT CHANGES, PROBLEMS WITH MODEL CHANGE, PROBLEMS WITH BOTH STATIC STEP AND STEADY STATE DYNAMIC PROCEDURES WHERE ACOUSTIC ELEMENTS WILL ONLY BE ACTIVATED IN THE STEADY STATE DYNAMIC STEPS.
- (4) FOR MULTI-PROCESS EXECUTION, THE ESTIMATED VALUE OF FLOATING POINT OPERATIONS FOR EACH PROCESS IS BASED ON AN INITIAL SCHEDULING OF OPERATIONS AND MIGHT NOT REFLECT THE ACTUAL FLOATING POINT OPERATIONS COMPLETED ON EACH PROCESS. OPERATIONS ARE DYNAMICALLY BALANCED DURING EXECUTION, SO THE ACTUAL BALANCE OF OPERATIONS BETWEEN PROCESSES IS EXPECTED TO BE BETTER THAN THE ESTIMATE PRINTED HERE.
- (5) THE UPPER LIMIT OF MEMORY THAT CAN BE ALLOCATED BY ABAQUS WILL IN GENERAL DEPEND ON THE VALUE OF THE "MEMORY" PARAMETER AND THE AMOUNT OF PHYSICAL MEMORY AVAILABLE ON THE MACHINE. PLEASE SEE THE "ABAQUS ANALYSIS USER'S MANUAL" FOR MORE DETAILS. THE ACTUAL USAGE OF MEMORY AND OF DISK SPACE FOR SCRATCH DATA WILL DEPEND ON THIS UPPER LIMIT AS WELL AS THE MEMORY REQUIRED TO MINIMIZE I/O. IF THE MEMORY UPPER LIMIT IS GREATER THAN THE MEMORY REQUIRED TO MINIMIZE I/O, THEN THE ACTUAL MEMORY USAGE WILL BE CLOSE TO THE ESTIMATED "MEMORY TO MINIMIZE I/O" VALUE, AND THE SCRATCH DISK USAGE WILL BE CLOSE-TO-ZERO; OTHERWISE, THE ACTUAL MEMORY USED WILL BE CLOSE TO THE PREVIOUSLY MENTIONED MEMORY LIMIT, AND THE SCRATCH DISK USAGE WILL BE ROUGHLY PROPORTIONAL TO THE DIFFERENCE BETWEEN THE ESTIMATED "MEMORY TO MINIMIZE I/O" AND THE MEMORY UPPER LIMIT. HOWEVER ACCURATE ESTIMATE OF THE SCRATCH DISK SPACE IS NOT POSSIBLE.
- (6) USING "*RESTART, WRITE" CAN GENERATE A LARGE AMOUNT OF DATA WRITTEN IN THE WORK DIRECTORY.

1

Abaqus Student Edition 6.11-2

DATE 09-May-2012 TIME 10:23:47

Analysis of Lysefjord bridge

STEP 2 INCREMENT 1
TIME COMPLETED IN THIS STEP

0.00

S T E P 2 S T A T I C A N A L Y S I S

AUTOMATIC TIME CONTROL WITH -

A SUGGESTED INITIAL TIME INCREMENT OF	1.000E-06
AND A TOTAL TIME PERIOD OF	1.000E-06
THE MINIMUM TIME INCREMENT ALLOWED IS	1.000E-09
THE MAXIMUM TIME INCREMENT ALLOWED IS	1.000E-06

LINEAR EQUATION SOLVER TYPE DIRECT SPARSE

AUTOMATIC STABILIZATION WITH DISSIPATED ENERGY FRACTION = 1.000E-10

LARGE DISPLACEMENT THEORY WILL BE USED

NOTE: THE FOLLOWING CENTER OF MASS AND MOMENT OF INERTIA CALCULATIONS ARE BASED ON CURRENT POSITION

TOTAL MASS OF MODEL

1.1029548E+07

LOCATION OF THE CENTER OF MASS OF THE MODEL

6.522231 1.0584980E-08 52.79727

MOMENTS OF INERTIA ABOUT THE ORIGIN

I (XX)	I (YY)	I (ZZ)
--------	--------	--------

3.8237572E+10	5.0240593E+11	4.6504478E+11
---------------	---------------	---------------

PRODUCTS OF INERTIA ABOUT THE ORIGIN		
I (XY)	I (XZ)	I (YZ)
-17.55807	-1.6216874E+08	-6.617854

MOMENTS OF INERTIA ABOUT THE CENTER OF MASS		
I (XX)	I (YY)	I (ZZ)
7.4921385E+09	4.7119131E+11	4.6457559E+11

PRODUCTS OF INERTIA ABOUT THE CENTER OF MASS		
I (XY)	I (XZ)	I (YZ)
-16.79661	3.6359220E+09	-0.4539024

M E M O R Y E S T I M A T E

PROCESS	FLOATING PT OPERATIONS PER ITERATION	MINIMUM MEMORY REQUIRED (MBYTES)	MEMORY TO MINIMIZE I/O (MBYTES)
1	2.45E+006	18	40

NOTE:

- (1) SINCE ABAQUS DOES NOT PRE-ALLOCATE MEMORY AND ONLY ALLOCATES MEMORY AS NEEDED DURING THE ANALYSIS, THE MEMORY REQUIREMENT PRINTED HERE CAN ONLY BE VIEWED AS A GENERAL GUIDELINE BASED ON THE BEST KNOWLEDGE AVAILABLE AT THE BEGINNING OF A STEP BEFORE THE SOLUTION PROCESS HAS BEGUN.
- (2) THE ESTIMATE IS NORMALLY UPDATED AT THE BEGINNING OF EVERY STEP. IT IS THE MAXIMUM VALUE OF THE ESTIMATE FROM THE CURRENT STEP TO THE LAST STEP OF THE ANALYSIS, WITH UNSYMMETRIC SOLUTION TAKEN INTO ACCOUNT IF APPLICABLE.
- (3) SINCE THE ESTIMATE IS BASED ON THE ACTIVE DEGREES OF FREEDOM IN THE FIRST ITERATION OF THE CURRENT STEP, THE MEMORY ESTIMATE MIGHT BE SIGNIFICANTLY DIFFERENT THAN ACTUAL USAGE FOR PROBLEMS WITH SUBSTANTIAL CHANGES IN ACTIVE DEGREES OF FREEDOM BETWEEN STEPS (OR EVEN WITHIN THE SAME STEP). EXAMPLES ARE: PROBLEMS WITH SIGNIFICANT CONTACT CHANGES, PROBLEMS WITH MODEL CHANGE, PROBLEMS WITH BOTH STATIC STEP AND STEADY STATE DYNAMIC PROCEDURES WHERE ACOUSTIC ELEMENTS WILL ONLY BE ACTIVATED IN THE STEADY STATE DYNAMIC STEPS.
- (4) FOR MULTI-PROCESS EXECUTION, THE ESTIMATED VALUE OF FLOATING POINT OPERATIONS FOR EACH PROCESS IS BASED ON AN INITIAL SCHEDULING OF OPERATIONS AND MIGHT NOT REFLECT THE ACTUAL FLOATING POINT OPERATIONS COMPLETED ON EACH PROCESS. OPERATIONS ARE DYNAMICALLY BALANCED DURING EXECUTION, SO THE ACTUAL BALANCE OF OPERATIONS BETWEEN PROCESSES IS EXPECTED TO BE BETTER THAN THE ESTIMATE PRINTED HERE.
- (5) THE UPPER LIMIT OF MEMORY THAT CAN BE ALLOCATED BY ABAQUS WILL IN GENERAL DEPEND ON THE VALUE OF THE "MEMORY" PARAMETER AND THE AMOUNT OF PHYSICAL MEMORY AVAILABLE ON THE MACHINE. PLEASE SEE THE "ABAQUS ANALYSIS USER'S MANUAL" FOR MORE DETAILS. THE ACTUAL USAGE OF MEMORY AND OF DISK SPACE FOR SCRATCH DATA WILL DEPEND ON THIS UPPER LIMIT AS WELL AS THE MEMORY REQUIRED TO MINIMIZE I/O. IF THE MEMORY UPPER LIMIT IS GREATER THAN THE MEMORY REQUIRED TO MINIMIZE I/O, THEN THE ACTUAL MEMORY USAGE WILL BE CLOSE TO THE ESTIMATED "MEMORY TO MINIMIZE I/O" VALUE, AND THE SCRATCH DISK USAGE WILL BE CLOSE-TO-ZERO; OTHERWISE, THE ACTUAL MEMORY USED WILL BE CLOSE TO THE PREVIOUSLY MENTIONED MEMORY LIMIT, AND THE SCRATCH DISK USAGE WILL BE ROUGHLY PROPORTINAL TO THE DIFFERENCE BETWEEN THE ESTIMATED "MEMORY TO MINIMIZE I/O" AND THE MEMORY UPPER LIMIT. HOWEVER ACCURATE ESTIMATE OF THE SCRATCH DISK SPACE IS NOT POSSIBLE.
- (6) USING "*RESTART, WRITE" CAN GENERATE A LARGE AMOUNT OF DATA WRITTEN IN THE WORK DIRECTORY.

INCREMENT 1 SUMMARY

TIME INCREMENT COMPLETED	1.000E-06,	FRACTION OF STEP COMPLETED	1.00
STEP TIME COMPLETED	1.000E-06,	TOTAL TIME COMPLETED	2.000E-06

E L E M E N T O U T P U T

THE FOLLOWING TABLE IS PRINTED AT THE INTEGRATION POINTS FOR ELEMENT TYPE B31 AND ELEMENT SET MAINCABLE

ELEMENT	PT	FOOT- NOTE	SF1	SF2	SF3	SM1	SM2	SM3
1001	1		1.7576E+07	-111.3	-5.0246E-04	494.0	-1.1318E-03	8.1149E-03
1002	1		1.7447E+07	68.74	3.3777E-04	-208.0	1.8777E-03	7.9789E-03
1003	1		1.7328E+07	-28.41	-1.8173E-04	51.01	5.8485E-04	7.7676E-03
1004	1		1.7216E+07	10.86	3.4260E-05	-57.49	1.3154E-03	7.5646E-03
1005	1		1.7111E+07	-4.994	-5.5187E-05	-17.49	1.2050E-03	7.3294E-03
1006	1		1.7011E+07	1.265	-1.7918E-05	-36.97	1.4321E-03	7.0705E-03
1007	1		1.6918E+07	-1.351	-3.2885E-05	-32.73	1.5087E-03	6.7739E-03
1008	1		1.6832E+07	-0.4635	-2.6259E-05	-37.91	1.6322E-03	6.4305E-03
1009	1		1.6751E+07	-1.034	-2.8333E-05	-39.32	1.7179E-03	6.0236E-03
1010	1		1.6676E+07	-1.115	-2.7057E-05	-42.18	1.7969E-03	5.5308E-03
1011	1		1.6607E+07	-1.546	-2.7187E-05	-44.51	1.8528E-03	4.9199E-03
1012	1		1.6544E+07	-2.045	-2.7394E-05	-47.15	1.8889E-03	4.1449E-03
1013	1		1.6486E+07	-2.851	-2.8559E-05	-49.83	1.9039E-03	3.1427E-03
1014	1		1.6434E+07	-3.987	-3.1029E-05	-52.79	1.9030E-03	1.8336E-03
1015	1		1.6386E+07	-5.483	-3.5660E-05	-55.86	1.9030E-03	1.4059E-04
1016	1		1.6344E+07	-7.022	-4.1424E-05	-58.54	1.9365E-03	-1.9455E-03
1017	1		1.6309E+07	-7.748	-4.5205E-05	-59.66	2.0459E-03	-4.2524E-03
1018	1		1.6283E+07	-6.905	-4.0106E-05	-59.03	2.2473E-03	-6.3749E-03
1019	1		1.6267E+07	-4.883	-2.5062E-05	-58.58	2.4911E-03	-7.9021E-03
1020	1		1.6263E+07	-2.801	-7.2636E-06	-59.39	2.6948E-03	-8.7343E-03
1021	1		1.6271E+07	-1.320	6.4382E-06	-60.70	2.8119E-03	-9.0587E-03
1022	1		1.6289E+07	-0.4640	1.5664E-05	-61.66	2.8417E-03	-9.1097E-03
1023	1		1.6317E+07	-2.3361E-02	2.1127E-05	-62.01	2.8027E-03	-9.0475E-03
1024	1		1.6353E+07	0.2065	2.4521E-05	-61.72	2.7159E-03	-8.9543E-03
1025	1		1.6398E+07	0.2796	2.6648E-05	-61.02	2.5958E-03	-8.8659E-03
1026	1		1.6451E+07	0.3903	2.8289E-05	-59.67	2.4512E-03	-8.7961E-03
1027	1		1.6511E+07	0.2683	2.8322E-05	-58.44	2.2947E-03	-8.7477E-03
1028	1		1.6579E+07	0.6272	3.1257E-05	-55.60	2.1179E-03	-8.7197E-03
1029	1		1.6654E+07	-0.2379	2.6056E-05	-55.64	1.9548E-03	-8.7101E-03
1030	1		1.6736E+07	1.981	3.9465E-05	-47.07	1.7364E-03	-8.7156E-03
1031	1		1.6824E+07	-3.570	8.4598E-06	-58.94	1.6347E-03	-8.7355E-03
1032	1		1.6920E+07	10.34	8.1857E-05	-18.40	1.2453E-03	-8.7634E-03
1033	1		1.7022E+07	-24.38	-9.1246E-05	-108.2	1.5364E-03	-8.8084E-03
1034	1		1.7131E+07	62.55	3.1357E-04	131.7	2.2180E-04	-8.8424E-03
1035	1		1.7246E+07	-149.7	-6.2986E-04	-424.6	2.6846E-03	-8.9296E-03
1036	1		1.7363E+07	214.6	8.5347E-04	832.3	-2.6586E-03	-8.9177E-03
2001	1		1.7576E+07	-111.3	5.0090E-04	494.0	1.1310E-03	-8.1430E-03
2002	1		1.7447E+07	68.74	-3.3818E-04	-208.0	-1.8822E-03	-8.0063E-03
2003	1		1.7328E+07	-28.41	1.8244E-04	51.01	-5.8381E-04	-7.7944E-03
2004	1		1.7216E+07	10.86	-3.4554E-05	-57.49	-1.3186E-03	-7.5911E-03
2005	1		1.7111E+07	-4.994	5.5492E-05	-17.49	-1.2069E-03	-7.3555E-03
2006	1		1.7011E+07	1.265	1.7933E-05	-36.97	-1.4354E-03	-7.0963E-03
2007	1		1.6918E+07	-1.351	3.3044E-05	-32.73	-1.5122E-03	-6.7993E-03
2008	1		1.6832E+07	-0.4635	2.6374E-05	-37.91	-1.6364E-03	-6.4555E-03
2009	1		1.6751E+07	-1.034	2.8490E-05	-39.32	-1.7226E-03	-6.0481E-03
2010	1		1.6676E+07	-1.115	2.7235E-05	-42.18	-1.8022E-03	-5.5547E-03
2011	1		1.6607E+07	-1.546	2.7414E-05	-44.51	-1.8586E-03	-4.9431E-03
2012	1		1.6544E+07	-2.045	2.7695E-05	-47.15	-1.8952E-03	-4.1671E-03
2013	1		1.6486E+07	-2.851	2.8978E-05	-49.83	-1.9106E-03	-3.1636E-03
2014	1		1.6434E+07	-3.987	3.1626E-05	-52.79	-1.9102E-03	-1.8528E-03
2015	1		1.6386E+07	-5.483	3.6492E-05	-55.86	-1.9107E-03	-1.5740E-04
2016	1		1.6344E+07	-7.022	4.2467E-05	-58.54	-1.9446E-03	1.9319E-03
2017	1		1.6309E+07	-7.748	4.6253E-05	-59.66	-2.0544E-03	4.2428E-03
2018	1		1.6283E+07	-6.905	4.0885E-05	-59.03	-2.2565E-03	6.3696E-03
2019	1		1.6267E+07	-4.883	2.5509E-05	-58.58	-2.5013E-03	7.9005E-03
2020	1		1.6263E+07	-2.801	7.4869E-06	-59.39	-2.7059E-03	8.7357E-03
2021	1		1.6271E+07	-1.320	-6.3351E-06	-60.70	-2.8238E-03	9.0623E-03
2022	1		1.6289E+07	-0.4640	-1.5624E-05	-61.66	-2.8540E-03	9.1150E-03
2023	1		1.6317E+07	-2.3361E-02	-2.1139E-05	-62.01	-2.8153E-03	9.0543E-03
2024	1		1.6353E+07	0.2065	-2.4552E-05	-61.72	-2.7287E-03	8.9624E-03
2025	1		1.6398E+07	0.2796	-2.6733E-05	-61.02	-2.6085E-03	8.8753E-03
2026	1		1.6451E+07	0.3903	-2.8332E-05	-59.67	-2.4640E-03	8.8067E-03
2027	1		1.6511E+07	0.2683	-2.8520E-05	-58.44	-2.3070E-03	8.7595E-03
2028	1		1.6579E+07	0.6272	-3.1169E-05	-55.60	-2.1309E-03	8.7326E-03
2029	1		1.6654E+07	-0.2379	-2.6625E-05	-55.64	-1.9656E-03	8.7241E-03
2030	1		1.6736E+07	1.981	-3.8727E-05	-47.07	-1.7510E-03	8.7308E-03
2031	1		1.6824E+07	-3.570	-1.0312E-05	-58.94	-1.6403E-03	8.7515E-03
2032	1		1.6920E+07	10.34	-7.9103E-05	-18.40	-1.2674E-03	8.7809E-03
2033	1		1.7022E+07	-24.38	8.7073E-05	-108.2	-1.5277E-03	8.8259E-03
2034	1		1.7131E+07	62.55	-3.1220E-04	131.7	-2.5770E-04	8.8622E-03
2035	1		1.7246E+07	-149.7	6.4523E-04	-424.6	-2.6847E-03	8.9466E-03

2036	1	1.7363E+07	214.6	-9.0417E-04	832.3	2.7555E-03	8.9396E-03
MAXIMUM ELEMENT		1.7576E+07 2001	214.6 2036	8.5347E-04 1036	832.3 2036	2.8417E-03 1022	9.1150E-03 2022
MINIMUM ELEMENT		1.6263E+07 1020	-149.7 2035	-9.0417E-04 2036	-424.6 2035	-2.8540E-03 2022	-9.1097E-03 1022

THE FOLLOWING TABLE IS PRINTED AT THE INTEGRATION POINTS FOR ELEMENT TYPE B31 AND ELEMENT SET GIRDER

ELEMENT	PT	FOOT- NOTE	SF1	SF2	SF3	SM1	SM2	SM3
1	1		-3.4595E+05	-2.2495E+05	-2.0587E-03	-2.1505E+06	-5.1632E-02	1.157
2	1		-3.4183E+05	-4.0542E+04	2.4751E-03	-4.5325E+06	-9.2374E-02	1.545
3	1		-3.4151E+05	-4.4450E+04	2.0357E-03	-5.0302E+06	-0.1213	1.779
4	1		-3.3995E+05	-4.3892E+04	1.6541E-03	-5.5474E+06	-0.1431	1.990
5	1		-3.3711E+05	-4.2311E+04	1.2669E-03	-6.0508E+06	-0.1585	2.197
6	1		-3.3283E+05	-4.0792E+04	8.5305E-04	-6.5347E+06	-0.1669	2.403
7	1		-3.2693E+05	-3.9625E+04	4.0298E-04	-7.0013E+06	-0.1683	2.609
8	1		-3.1914E+05	-3.8929E+04	-8.8567E-05	-7.4553E+06	-0.1617	2.816
9	1		-3.0918E+05	-3.8389E+04	-6.2181E-04	-7.9003E+06	-0.1476	3.022
10	1		-2.9667E+05	-3.8220E+04	-1.2049E-03	-8.3391E+06	-0.1241	3.229
11	1		-2.8116E+05	-3.8241E+04	-1.8411E-03	-8.7746E+06	-9.1676E-02	3.435
12	1		-2.6213E+05	-3.8268E+04	-2.5327E-03	-9.2077E+06	-4.9035E-02	3.642
13	1		-2.3896E+05	-3.8260E+04	-3.2821E-03	-9.6374E+06	4.1303E-03	3.849
14	1		-2.1112E+05	-3.7945E+04	-4.0823E-03	-1.0061E+07	6.8289E-02	4.055
15	1		-1.7836E+05	-3.7123E+04	-4.9137E-03	-1.0474E+07	0.1439	4.262
16	1		-1.4132E+05	-3.5444E+04	-5.7286E-03	-1.0869E+07	0.2300	4.468
17	1		-1.0223E+05	-3.2592E+04	-6.4422E-03	-1.1235E+07	0.3253	4.674
18	1		-6.5129E+04	-2.8226E+04	-6.9369E-03	-1.1560E+07	0.4266	4.879
19	1		-3.4185E+04	-2.2378E+04	-7.1067E-03	-1.1832E+07	0.5307	5.084
20	1		-1.1438E+04	-1.5651E+04	-6.9088E-03	-1.2037E+07	0.6338	5.291
21	1	3664.	-8730.	-6.3681E-03	-1.2170E+07	0.7331	5.498	
22	1		1.2963E+04	-2030.	-5.5398E-03	-1.2227E+07	0.8247	5.706
23	1		1.8378E+04	4291.	-4.4826E-03	-1.2211E+07	0.9068	5.915
24	1		2.1413E+04	1.0204E+04	-3.2413E-03	-1.2125E+07	0.9771	6.123
25	1		2.3121E+04	1.5803E+04	-1.8460E-03	-1.1972E+07	1.031	6.333
26	1		2.4196E+04	2.1205E+04	-3.2120E-04	-1.1755E+07	1.071	6.542
27	1		2.5101E+04	2.6431E+04	1.3180E-03	-1.1475E+07	1.092	6.752
28	1		2.6132E+04	3.1733E+04	3.0636E-03	-1.1132E+07	1.093	6.962
29	1		2.7466E+04	3.7256E+04	4.9080E-03	-1.0725E+07	1.073	7.173
30	1		2.9229E+04	4.2976E+04	6.8459E-03	-1.0251E+07	1.031	7.383
31	1		3.1487E+04	4.9235E+04	8.8784E-03	-9.7047E+06	0.9646	7.594
32	1		3.4267E+04	5.6072E+04	1.1003E-02	-9.0800E+06	0.8736	7.805
33	1		3.7614E+04	6.3210E+04	1.3213E-02	-8.3712E+06	0.7553	8.020
34	1		4.1577E+04	6.9642E+04	1.5491E-02	-7.5807E+06	0.6120	8.263
35	1		4.6097E+04	7.6702E+04	1.7855E-02	-6.7089E+06	0.4500	8.682
36	1		3.6551E+04	3.2592E+05	2.3196E-02	-3.1276E+06	0.1904	10.18
MAXIMUM ELEMENT			4.6097E+04 35	3.2592E+05 36	2.3196E-02 36	-2.1505E+06 1	1.093 28	10.18 36
MINIMUM ELEMENT			-3.4595E+05 1	-2.2495E+05 1	-7.1067E-03 19	-1.2227E+07 22	-0.1683 7	1.157 1

THE FOLLOWING TABLE IS PRINTED AT THE INTEGRATION POINTS FOR ELEMENT TYPE B31 AND ELEMENT SET BACKSTAYCABLE

ELEMENT	PT	FOOT- NOTE	SF1	SF2	SF3	SM1	SM2	SM3
981	1		1.8965E+07	-11.39	-8.3418E-05	-50.45	3.6824E-04	-1.3853E-10
983	1		1.8982E+07	4.670	3.3978E-05	-80.22	5.8649E-04	-1.0059E-09
985	1		1.8998E+07	-2.176	-1.5427E-05	-69.18	5.0459E-04	1.1722E-09
987	1		1.9015E+07	1.757	1.1660E-05	-71.04	5.2123E-04	-3.8747E-09
989	1		1.9032E+07	-2.884	-1.8154E-05	-76.03	5.4987E-04	8.6121E-09
991	1		1.9049E+07	6.739	4.1960E-05	-58.96	4.4484E-04	-2.1521E-08
993	1		1.9066E+07	-16.73	-1.0406E-04	-103.2	7.1882E-04	5.7330E-08

995	1	1.9084E+07	42.19	2.6292E-04	9.569	1.7877E-05	-1.1787E-07
997	1	1.9101E+07	-106.4	-6.6445E-04	-274.9	1.7895E-03	4.2440E-07
999	1	1.9118E+07	268.8	1.6811E-03	443.9	-2.6963E-03	-4.1227E-07
1037	1	1.6611E+07	-623.1	-2.8520E-03	855.3	-4.0494E-03	-9.3297E-07
1039	1	1.6602E+07	246.1	1.1435E-03	-466.9	2.1180E-03	7.8246E-07
1041	1	1.6594E+07	-97.19	-4.5852E-04	55.15	-3.5384E-04	-6.3922E-08
1043	1	1.6586E+07	38.36	1.8369E-04	-151.1	6.3733E-04	1.0818E-07
1045	1	1.6578E+07	-15.17	-7.3681E-05	-69.79	2.4065E-04	-2.8077E-08
1047	1	1.6570E+07	5.971	2.9457E-05	-102.0	4.0006E-04	1.7535E-08
1049	1	1.6562E+07	-2.376	-1.1857E-05	-89.43	3.3669E-04	-4.7134E-09
1051	1	1.6554E+07	0.9203	4.6923E-06	-94.53	3.6255E-04	4.4725E-09
1053	1	1.6546E+07	-0.3813	-1.9352E-06	-92.64	3.5268E-04	5.6133E-10
1055	1	1.6538E+07	0.1327	7.1690E-07	-93.52	3.5711E-04	2.2298E-09
1057	1	1.6530E+07	-7.0181E-02	-3.4601E-07	-93.30	3.5582E-04	1.4899E-09
1059	1	1.6522E+07	9.8621E-03	7.7360E-08	-93.51	3.5681E-04	1.7241E-09
1061	1	1.6514E+07	-2.1380E-02	-9.1651E-08	-93.55	3.5689E-04	1.5327E-09
1063	1	1.6506E+07	-9.8015E-03	-2.7073E-08	-93.66	3.5734E-04	1.4894E-09
1065	1	1.6499E+07	-1.2282E-02	-4.2044E-08	-93.74	3.5762E-04	1.3925E-09
1067	1	1.6491E+07	-1.6428E-02	-5.5980E-08	-93.84	3.5801E-04	1.3258E-09
1069	1	1.6483E+07	-1.6374E-03	8.8046E-09	-93.90	3.5824E-04	1.3029E-09
1071	1	1.6475E+07	-4.0614E-02	-1.5266E-07	-94.05	3.5883E-04	1.2453E-09
1073	1	1.6468E+07	5.8865E-02	2.6206E-07	-93.98	3.5853E-04	1.4031E-09
1075	1	1.6460E+07	-0.1932	-7.6390E-07	-94.46	3.6045E-04	1.2298E-09
1077	1	1.6452E+07	0.4453	1.7938E-06	-93.57	3.5683E-04	1.9974E-09
1079	1	1.6445E+07	-1.172	-4.5700E-06	-96.12	3.6700E-04	9.0678E-10
1081	1	1.6437E+07	2.923	1.1244E-05	-89.98	3.4285E-04	3.9014E-09
1083	1	1.6430E+07	-7.447	-2.8087E-05	-105.8	4.0407E-04	-2.0720E-09
1085	1	1.6422E+07	18.81	6.9607E-05	-65.97	2.5304E-04	6.2342E-09
1981	1	1.8965E+07	-11.39	8.2989E-05	-50.45	-3.6865E-04	-4.5336E-11
1983	1	1.8982E+07	4.670	-3.3940E-05	-80.22	-5.8654E-04	1.8221E-10
1985	1	1.8998E+07	-2.176	1.5507E-05	-69.18	-5.0466E-04	-1.1344E-09
1987	1	1.9015E+07	1.757	-1.1815E-05	-71.04	-5.2105E-04	2.9632E-09
1989	1	1.9032E+07	-2.884	1.8440E-05	-76.03	-5.5050E-04	-7.6913E-09
1991	1	1.9049E+07	6.739	-4.2488E-05	-58.96	-4.4362E-04	2.0598E-08
1993	1	1.9066E+07	-16.73	1.0497E-04	-103.2	-7.2132E-04	-4.7702E-08
1995	1	1.9084E+07	42.19	-2.6420E-04	9.569	-1.3621E-05	1.4840E-07
1997	1	1.9101E+07	-106.4	6.6510E-04	-274.9	-1.7954E-03	-2.4701E-07
1999	1	1.9118E+07	268.8	-1.6763E-03	443.9	2.6988E-03	1.2455E-06
2037	1	1.6611E+07	-623.1	3.0026E-03	855.3	4.1500E-03	1.8950E-06
2039	1	1.6602E+07	246.1	-1.1684E-03	-466.9	-2.1059E-03	-2.5571E-07
2041	1	1.6594E+07	-97.19	4.5463E-04	55.15	3.2742E-04	3.4683E-07
2043	1	1.6586E+07	38.36	-1.7678E-04	-151.1	-6.1952E-04	-5.6215E-08
2045	1	1.6578E+07	-15.17	6.8815E-05	-69.79	-2.5177E-04	3.6228E-08
2047	1	1.6570E+07	5.971	-2.6680E-05	-102.0	-3.9522E-04	-8.1495E-09
2049	1	1.6562E+07	-2.376	1.0449E-05	-89.43	-3.3995E-04	5.2999E-09
2051	1	1.6554E+07	0.9203	-3.9797E-06	-94.53	-3.6190E-04	3.9079E-10
2053	1	1.6546E+07	-0.3813	1.6261E-06	-92.64	-3.5385E-04	2.0588E-09
2055	1	1.6538E+07	0.1327	-5.5304E-07	-93.52	-3.5746E-04	1.5216E-09
2057	1	1.6530E+07	-7.0181E-02	2.9104E-07	-93.30	-3.5653E-04	1.6541E-09
2059	1	1.6522E+07	9.8621E-03	-3.7731E-08	-93.51	-3.5737E-04	1.5443E-09
2061	1	1.6514E+07	-2.1380E-02	8.8336E-08	-93.55	-3.5752E-04	1.4697E-09
2063	1	1.6506E+07	-9.8015E-03	4.1808E-08	-93.66	-3.5793E-04	1.3923E-09
2065	1	1.6499E+07	-1.2282E-02	5.4003E-08	-93.74	-3.5823E-04	1.3159E-09
2067	1	1.6491E+07	-1.6428E-02	6.8512E-08	-93.84	-3.5861E-04	1.2413E-09
2069	1	1.6483E+07	-1.6374E-03	2.1529E-08	-93.90	-3.5887E-04	1.2213E-09
2071	1	1.6475E+07	-4.0614E-02	1.5729E-07	-94.05	-3.5941E-04	1.1630E-09
2073	1	1.6468E+07	5.8865E-02	-1.8767E-07	-93.98	-3.5922E-04	1.3194E-09
2075	1	1.6460E+07	-0.1932	7.1149E-07	-94.46	-3.6090E-04	1.1509E-09
2077	1	1.6452E+07	0.4453	-1.6078E-06	-93.57	-3.5777E-04	1.9052E-09
2079	1	1.6445E+07	-1.172	4.3778E-06	-96.12	-3.6704E-04	8.5360E-10
2081	1	1.6437E+07	2.923	-1.1082E-05	-89.98	-3.4429E-04	3.7576E-09
2083	1	1.6430E+07	-7.447	2.8781E-05	-105.8	-4.0419E-04	-1.9034E-09
2085	1	1.6422E+07	18.81	-7.4070E-05	-65.97	-2.5081E-04	5.8440E-09
MAXIMUM ELEMENT		1.9118E+07	268.8	3.0026E-03	855.3	4.1500E-03	1.8950E-06
ELEMENT		1999	1999	2037	2037	2037	2037
MINIMUM ELEMENT		1.6422E+07	-623.1	-2.8520E-03	-466.9	-4.0494E-03	-9.3297E-07
		1085	2037	1037	2039	1037	1037

N O D E O U T P U T

THE FOLLOWING TABLE IS PRINTED FOR ALL NODES

NODE	FOOT- NOTE	RF1	RF2	RF3	RM1	RM2	RM3
981		-1.5890E+07	63.87	-1.0337E+07	0.000	0.000	0.000
1087		1.5641E+07	18.02	-4.9946E+06	0.000	0.000	0.000
1981		-1.5890E+07	-63.88	-1.0337E+07	0.000	0.000	0.000
2087		1.5641E+07	-18.02	-4.9946E+06	0.000	0.000	0.000
20001		-3.5892E+05	-1.5108E+06	3.6688E+07	7.4979E+05	-4.2247E+07	0.000
20101		-3.5892E+05	1.5108E+06	3.6688E+07	-7.4979E+05	-4.2247E+07	0.000
30001		6.0843E+05	-1.1936E+06	3.2710E+07	4.8996E+05	5.9205E+07	0.000
30101		6.0843E+05	1.1936E+06	3.2710E+07	-4.8996E+05	5.9205E+07	0.000
MAXIMUM AT NODE		1.5641E+07	1.5108E+06	3.6688E+07	7.4979E+05	5.9205E+07	0.000
		2087	20101	20101	20001	30101	1
MINIMUM AT NODE		-1.5890E+07	-1.5108E+06	-1.0337E+07	-7.4979E+05	-4.2247E+07	0.000
		1981	20001	1981	20101	20101	1
TOTAL		1.278	-4.9405E-02	1.0813E+08	-0.1707	3.3916E+07	0.000

THE FOLLOWING TABLE IS PRINTED FOR ALL NODES

NODE	FOOT- NOTE	U1	U2	U3	UR1	UR2	UR3
1		6.1183E-02	-8.7749E-09	-4.9329E-03	5.0322E-09	2.0479E-02	2.1378E-10
2		7.4864E-02	-8.1215E-09	-0.3930	5.3272E-09	2.0023E-02	2.2213E-10
3		8.2377E-02	-7.5136E-09	-0.6298	5.5747E-09	1.9418E-02	2.2732E-10
4		8.8993E-02	-6.7517E-09	-0.8589	5.8598E-09	1.8748E-02	2.3230E-10
5		9.4724E-02	-5.8295E-09	-1.080	6.1785E-09	1.8008E-02	2.3677E-10
6		9.9607E-02	-4.7451E-09	-1.291	6.5303E-09	1.7202E-02	2.4060E-10
7		0.1037	-3.4816E-09	-1.492	6.9152E-09	1.6331E-02	2.4358E-10
8		0.1069	-2.0400E-09	-1.683	7.3330E-09	1.5398E-02	2.4561E-10
9		0.1095	-3.9855E-10	-1.862	7.7840E-09	1.4405E-02	2.4651E-10
10		0.1114	1.4369E-09	-2.028	8.2679E-09	1.3353E-02	2.4622E-10
11		0.1126	3.5012E-09	-2.182	8.7849E-09	1.2242E-02	2.4450E-10
12		0.1134	5.7988E-09	-2.322	9.3349E-09	1.1073E-02	2.4126E-10
13		0.1137	8.3535E-09	-2.447	9.9180E-09	9.8464E-03	2.3636E-10
14		0.1136	1.1182E-08	-2.558	1.0534E-08	8.5626E-03	2.2968E-10
15		0.1133	1.4301E-08	-2.653	1.1183E-08	7.2225E-03	2.2111E-10
16		0.1128	1.7744E-08	-2.731	1.1866E-08	5.8273E-03	2.1052E-10
17		0.1122	2.1531E-08	-2.792	1.2581E-08	4.3796E-03	1.9779E-10
18		0.1116	2.5701E-08	-2.836	1.3329E-08	2.8830E-03	1.8276E-10
19		0.1112	3.0278E-08	-2.861	1.4110E-08	1.3430E-03	1.6530E-10
20		0.1111	3.5294E-08	-2.868	1.4924E-08	-2.3324E-04	1.4524E-10
21		0.1114	4.0776E-08	-2.856	1.5772E-08	-1.8370E-03	1.2241E-10
22		0.1121	4.6774E-08	-2.824	1.6652E-08	-3.4585E-03	9.6519E-11
23		0.1135	5.3304E-08	-2.773	1.7566E-08	-5.0878E-03	6.7411E-11
24		0.1157	6.0420E-08	-2.702	1.8513E-08	-6.7152E-03	3.4750E-11
25		0.1186	6.8176E-08	-2.611	1.9494E-08	-8.3313E-03	-1.8260E-12
26		0.1226	7.6554E-08	-2.502	2.0508E-08	-9.9273E-03	-4.2393E-11
27		0.1276	8.5632E-08	-2.373	2.1556E-08	-1.1495E-02	-8.7422E-11
28		0.1338	9.5452E-08	-2.226	2.2637E-08	-1.3025E-02	-1.3725E-10
29		0.1413	1.0601E-07	-2.061	2.3753E-08	-1.4510E-02	-1.9204E-10
30		0.1501	1.1737E-07	-1.878	2.4902E-08	-1.5940E-02	-2.5223E-10
31		0.1603	1.2958E-07	-1.678	2.6084E-08	-1.7308E-02	-3.1815E-10
32		0.1719	1.4264E-07	-1.463	2.7301E-08	-1.8603E-02	-3.8996E-10
33		0.1851	1.5661E-07	-1.232	2.8551E-08	-1.9815E-02	-4.6808E-10
34		0.1997	1.7150E-07	-0.9871	2.9836E-08	-2.0933E-02	-5.5267E-10
35		0.2160	1.8738E-07	-0.7296	3.1160E-08	-2.1946E-02	-6.4440E-10
36		0.2337	2.0423E-07	-0.4605	3.2551E-08	-2.2842E-02	-7.4504E-10
37		0.2646	2.3316E-07	-1.5223E-02	3.5150E-08	-2.3508E-02	-9.3337E-10
981		0.000	0.000	0.000	6.1234E-06	8.0083E-03	-9.1672E-09
983		5.2594E-02	-2.9827E-05	-4.6106E-02	6.1195E-06	7.0536E-03	-6.2653E-09
985		9.8612E-02	-5.9628E-05	-8.2104E-02	6.1134E-06	5.5354E-03	-1.6361E-09
987		0.1380	-8.9402E-05	-0.1080	6.1082E-06	4.2262E-03	2.3375E-09

989	0.1709	-1.1915E-04	-0.1239	6.1027E-06	2.8819E-03	6.4667E-09
991	0.1972	-1.4887E-04	-0.1297	6.0970E-06	1.4431E-03	1.0760E-08
993	0.2168	-1.7857E-04	-0.1255	6.0924E-06	3.2737E-04	1.4380E-08
995	0.2299	-2.0824E-04	-0.1113	6.0849E-06	-1.6255E-03	1.9774E-08
997	0.2364	-2.3788E-04	-8.7192E-02	6.0847E-06	-1.4444E-03	2.0605E-08
999	0.2363	-2.6749E-04	-5.3096E-02	6.0660E-06	-6.6474E-03	3.3000E-08
1001	0.2297	-2.9708E-04	-9.2439E-03	6.0941E-06	1.7534E-03	1.6029E-08
1002	0.1443	-2.5321E-04	-0.3533	6.4492E-06	2.3381E-02	-9.9961E-08
1003	8.6404E-02	-2.2726E-04	-0.5943	6.6934E-06	1.7742E-02	-1.4990E-07
1004	3.5591E-02	-2.0273E-04	-0.8279	6.9203E-06	1.9116E-02	-2.0269E-07
1005	-8.0072E-03	-1.7963E-04	-1.053	7.1465E-06	1.7576E-02	-2.4045E-07
1006	-4.4560E-02	-1.5797E-04	-1.268	7.3647E-06	1.7110E-02	-2.7080E-07
1007	-7.4250E-02	-1.3776E-04	-1.473	7.5764E-06	1.6130E-02	-2.9093E-07
1008	-9.7305E-02	-1.1904E-04	-1.667	7.7793E-06	1.5267E-02	-3.0242E-07
1009	-0.1140	-1.0181E-04	-1.849	7.9723E-06	1.4271E-02	-3.0509E-07
1010	-0.1247	-8.6119E-05	-2.018	8.1533E-06	1.3242E-02	-2.9958E-07
1011	-0.1297	-7.1976E-05	-2.175	8.3196E-06	1.2143E-02	-2.8626E-07
1012	-0.1294	-5.9414E-05	-2.317	8.4678E-06	1.0986E-02	-2.6574E-07
1013	-0.1244	-4.8463E-05	-2.445	8.5929E-06	9.7647E-03	-2.3865E-07
1014	-0.1151	-3.9153E-05	-2.558	8.6884E-06	8.4767E-03	-2.0572E-07
1015	-0.1021	-3.1511E-05	-2.654	8.7454E-06	7.1152E-03	-1.6774E-07
1016	-8.5926E-02	-2.5559E-05	-2.734	8.7529E-06	5.6768E-03	-1.2546E-07
1017	-6.7277E-02	-2.1298E-05	-2.795	8.6997E-06	4.1712E-03	-7.9369E-08
1018	-4.6839E-02	-1.8694E-05	-2.838	8.5794E-06	2.6381E-03	-2.9622E-08
1019	-2.5356E-02	-1.7670E-05	-2.862	8.3974E-06	1.1215E-03	2.3559E-08
1020	-3.5913E-03	-1.8109E-05	-2.867	8.1704E-06	-3.8335E-04	7.8912E-08
1021	1.7693E-02	-1.9881E-05	-2.853	7.9181E-06	-1.9098E-03	1.3409E-07
1022	3.7719E-02	-2.2872E-05	-2.820	7.6549E-06	-3.4711E-03	1.8659E-07
1023	5.5692E-02	-2.6990E-05	-2.767	7.3888E-06	-5.0589E-03	2.3441E-07
1024	7.0809E-02	-3.2165E-05	-2.695	7.1231E-06	-6.6585E-03	2.7608E-07
1025	8.2275E-02	-3.8345E-05	-2.603	6.8588E-06	-8.2537E-03	3.1060E-07
1026	8.9311E-02	-4.5489E-05	-2.491	6.5961E-06	-9.8347E-03	3.3725E-07
1027	9.1167E-02	-5.3564E-05	-2.360	6.3347E-06	-1.1385E-02	3.5547E-07
1028	8.7132E-02	-6.2545E-05	-2.210	6.0741E-06	-1.2909E-02	3.6491E-07
1029	7.6538E-02	-7.2411E-05	-2.042	5.8141E-06	-1.4363E-02	3.6509E-07
1030	5.8772E-02	-8.3143E-05	-1.857	5.5542E-06	-1.5824E-02	3.5606E-07
1031	3.3285E-02	-9.4724E-05	-1.654	5.2944E-06	-1.7066E-02	3.3693E-07
1032	-3.9866E-04	-1.0714E-04	-1.435	5.0340E-06	-1.8628E-02	3.0911E-07
1033	-4.2676E-02	-1.2038E-04	-1.200	4.7746E-06	-1.9118E-02	2.6867E-07
1034	-9.3856E-02	-1.3442E-04	-0.9515	4.5113E-06	-2.2017E-02	2.2440E-07
1035	-0.1541	-1.4927E-04	-0.6899	4.2566E-06	-1.8469E-02	1.5550E-07
1036	-0.2221	-1.6492E-04	-0.4207	3.9787E-06	-2.9977E-02	1.1143E-07
1037	-0.3326	-1.9129E-04	-7.7595E-03	3.6075E-06	6.6221E-03	-7.8843E-08
1039	-0.3574	-1.8368E-04	-0.1184	3.5882E-06	1.9439E-02	-1.1311E-07
1041	-0.3792	-1.7607E-04	-0.2201	3.5983E-06	1.2443E-02	-9.5714E-08
1043	-0.3976	-1.6846E-04	-0.3126	3.5966E-06	1.3270E-02	-9.9237E-08
1045	-0.4128	-1.6084E-04	-0.3960	3.5996E-06	1.1005E-02	-9.4287E-08
1047	-0.4247	-1.5321E-04	-0.4701	3.6007E-06	9.9592E-03	-9.2761E-08
1049	-0.4335	-1.4559E-04	-0.5350	3.6026E-06	8.4302E-03	-8.9847E-08
1051	-0.4390	-1.3796E-04	-0.5907	3.6042E-06	7.0901E-03	-8.7490E-08
1053	-0.4413	-1.3033E-04	-0.6371	3.6059E-06	5.6735E-03	-8.4905E-08
1055	-0.4404	-1.2269E-04	-0.6743	3.6075E-06	4.2852E-03	-8.2408E-08
1057	-0.4363	-1.1505E-04	-0.7023	3.6092E-06	2.8838E-03	-7.9872E-08
1059	-0.4291	-1.0740E-04	-0.7209	3.6109E-06	1.4858E-03	-7.7349E-08
1061	-0.4187	-9.9754E-05	-0.7302	3.6125E-06	8.4537E-05	-7.4817E-08
1063	-0.4051	-9.2102E-05	-0.7303	3.6142E-06	-1.3173E-03	-7.2285E-08
1065	-0.3884	-8.4446E-05	-0.7210	3.6159E-06	-2.7208E-03	-6.9750E-08
1067	-0.3686	-7.6787E-05	-0.7024	3.6175E-06	-4.1254E-03	-6.7213E-08
1069	-0.3456	-6.9125E-05	-0.6744	3.6192E-06	-5.5315E-03	-6.4673E-08
1071	-0.3195	-6.1458E-05	-0.6371	3.6209E-06	-6.9386E-03	-6.2131E-08
1073	-0.2903	-5.3788E-05	-0.5904	3.6225E-06	-8.3479E-03	-5.9585E-08
1075	-0.2581	-4.6115E-05	-0.5343	3.6242E-06	-9.7562E-03	-5.7042E-08
1077	-0.2227	-3.8438E-05	-0.4689	3.6259E-06	-1.1172E-02	-5.4484E-08
1079	-0.1843	-3.0757E-05	-0.3940	3.6275E-06	-1.2574E-02	-5.1953E-08
1081	-0.1428	-2.3073E-05	-0.3096	3.6292E-06	-1.4014E-02	-4.9347E-08
1083	-9.8215E-02	-1.5386E-05	-0.2159	3.6308E-06	-1.5362E-02	-4.6918E-08
1085	-5.0621E-02	-7.6946E-06	-0.1127	3.6327E-06	-1.6948E-02	-4.4049E-08
1087	0.000	0.000	0.000	3.6339E-06	-1.7937E-02	-4.2244E-08
1981	0.000	0.000	0.000	-6.1238E-06	8.0083E-03	9.2119E-09
1983	5.2594E-02	2.9830E-05	-4.6106E-02	-6.1200E-06	7.0536E-03	6.3037E-09
1985	9.8612E-02	5.9633E-05	-8.2104E-02	-6.1139E-06	5.5354E-03	1.6741E-09
1987	0.1380	8.9410E-05	-0.1080	-6.1086E-06	4.2262E-03	-2.3003E-09
1989	0.1709	1.1916E-04	-0.1239	-6.1032E-06	2.8819E-03	-6.4263E-09
1991	0.1972	1.4888E-04	-0.1297	-6.0974E-06	1.4431E-03	-1.0729E-08

1993	0.2168	1.7858E-04	-0.1255	-6.0928E-06	3.2737E-04	-1.4330E-08
1995	0.2299	2.0825E-04	-0.1113	-6.0853E-06	-1.6255E-03	-1.9762E-08
1997	0.2364	2.3790E-04	-8.7192E-02	-6.0851E-06	-1.4444E-03	-2.0526E-08
1999	0.2363	2.6752E-04	-5.3096E-02	-6.0664E-06	-6.6474E-03	-3.3012E-08
2001	0.2297	2.9711E-04	-9.2439E-03	-6.0945E-06	1.7534E-03	-1.5993E-08
2002	0.1443	2.5323E-04	-0.3533	-6.4509E-06	2.3381E-02	1.0043E-07
2003	8.6404E-02	2.2728E-04	-0.5943	-6.6959E-06	1.7742E-02	1.5053E-07
2004	3.5591E-02	2.0275E-04	-0.8279	-6.9236E-06	1.9116E-02	2.0360E-07
2005	-8.0072E-03	1.7964E-04	-1.053	-7.1506E-06	1.7576E-02	2.4151E-07
2006	-4.4560E-02	1.5798E-04	-1.268	-7.3696E-06	1.7110E-02	2.7202E-07
2007	-7.4250E-02	1.3777E-04	-1.473	-7.5820E-06	1.6130E-02	2.9226E-07
2008	-9.7305E-02	1.1905E-04	-1.667	-7.7857E-06	1.5267E-02	3.0384E-07
2009	-0.1140	1.0183E-04	-1.849	-7.9794E-06	1.4271E-02	3.0656E-07
2010	-0.1247	8.6129E-05	-2.018	-8.1611E-06	1.3242E-02	3.0107E-07
2011	-0.1297	7.1987E-05	-2.175	-8.3282E-06	1.2143E-02	2.8775E-07
2012	-0.1294	5.9426E-05	-2.317	-8.4770E-06	1.0986E-02	2.6719E-07
2013	-0.1244	4.8476E-05	-2.445	-8.6028E-06	9.7647E-03	2.4004E-07
2014	-0.1151	3.9168E-05	-2.558	-8.6989E-06	8.4767E-03	2.0701E-07
2015	-0.1021	3.1529E-05	-2.654	-8.7564E-06	7.1152E-03	1.6890E-07
2016	-8.5926E-02	2.5580E-05	-2.734	-8.7644E-06	5.6768E-03	1.2646E-07
2017	-6.7277E-02	2.1323E-05	-2.795	-8.7116E-06	4.1712E-03	8.0201E-08
2018	-4.6839E-02	1.8723E-05	-2.838	-8.5917E-06	2.6381E-03	3.0253E-08
2019	-2.5356E-02	1.7704E-05	-2.862	-8.4098E-06	1.1215E-03	-2.3154E-08
2020	-3.5913E-03	1.8148E-05	-2.867	-8.1828E-06	-3.8335E-04	-7.8760E-08
2021	1.7693E-02	1.9925E-05	-2.853	-7.9304E-06	-1.9098E-03	-1.3421E-07
2022	3.7719E-02	2.2921E-05	-2.820	-7.6672E-06	-3.4711E-03	-1.8700E-07
2023	5.5692E-02	2.7043E-05	-2.767	-7.4009E-06	-5.0589E-03	-2.3512E-07
2024	7.0809E-02	3.2221E-05	-2.695	-7.1349E-06	-6.6585E-03	-2.7708E-07
2025	8.2275E-02	3.8403E-05	-2.603	-6.8704E-06	-8.2537E-03	-3.1190E-07
2026	8.9311E-02	4.5548E-05	-2.491	-6.6074E-06	-9.8347E-03	-3.3883E-07
2027	9.1167E-02	5.3624E-05	-2.360	-6.3456E-06	-1.1385E-02	-3.5732E-07
2028	8.7132E-02	6.2605E-05	-2.210	-6.0847E-06	-1.2909E-02	-3.6700E-07
2029	7.6538E-02	7.2469E-05	-2.042	-5.8242E-06	-1.4363E-02	-3.6744E-07
2030	5.8772E-02	8.3197E-05	-1.857	-5.5638E-06	-1.5824E-02	-3.5859E-07
2031	3.3286E-02	9.4773E-05	-1.654	-5.3035E-06	-1.7066E-02	-3.3973E-07
2032	-3.9858E-04	1.0718E-04	-1.435	-5.0426E-06	-1.8628E-02	-3.1192E-07
2033	-4.2675E-02	1.2041E-04	-1.200	-4.7825E-06	-1.9118E-02	-2.7190E-07
2034	-9.3856E-02	1.3445E-04	-0.9515	-4.5189E-06	-2.2017E-02	-2.2725E-07
2035	-0.1541	1.4929E-04	-0.6899	-4.2632E-06	-1.8469E-02	-1.5909E-07
2036	-0.2221	1.6492E-04	-0.4207	-3.9848E-06	-2.9977E-02	-1.1481E-07
2037	-0.3326	1.9127E-04	-7.7595E-03	-3.6141E-06	6.6221E-03	7.9708E-08
2039	-0.3574	1.8367E-04	-0.1184	-3.5943E-06	1.9439E-02	1.1536E-07
2041	-0.3792	1.7606E-04	-0.2201	-3.6043E-06	1.2443E-02	9.8148E-08
2043	-0.3976	1.6844E-04	-0.3126	-3.6028E-06	1.3270E-02	1.0129E-07
2045	-0.4128	1.6082E-04	-0.3960	-3.6057E-06	1.1005E-02	9.6601E-08
2047	-0.4247	1.5320E-04	-0.4701	-3.6069E-06	9.9592E-03	9.4921E-08
2049	-0.4335	1.4558E-04	-0.5350	-3.6087E-06	8.4302E-03	9.2080E-08
2051	-0.4390	1.3795E-04	-0.5907	-3.6103E-06	7.0901E-03	8.9681E-08
2053	-0.4413	1.3031E-04	-0.6371	-3.6120E-06	5.6735E-03	8.7109E-08
2055	-0.4404	1.2268E-04	-0.6743	-3.6136E-06	4.2852E-03	8.4600E-08
2057	-0.4363	1.1504E-04	-0.7023	-3.6153E-06	2.8838E-03	8.2064E-08
2059	-0.4291	1.0739E-04	-0.7209	-3.6170E-06	1.4858E-03	7.9534E-08
2061	-0.4187	9.9745E-05	-0.7302	-3.6187E-06	8.4537E-05	7.6999E-08
2063	-0.4051	9.2094E-05	-0.7303	-3.6203E-06	-1.3173E-03	7.4462E-08
2065	-0.3884	8.4439E-05	-0.7210	-3.6220E-06	-2.7208E-03	7.1923E-08
2067	-0.3686	7.6781E-05	-0.7024	-3.6237E-06	-4.1254E-03	6.9381E-08
2069	-0.3456	6.9119E-05	-0.6744	-3.6253E-06	-5.5315E-03	6.6837E-08
2071	-0.3195	6.1453E-05	-0.6371	-3.6270E-06	-6.9386E-03	6.4291E-08
2073	-0.2903	5.3784E-05	-0.5904	-3.6287E-06	-8.3479E-03	6.1741E-08
2075	-0.2581	4.6111E-05	-0.5343	-3.6303E-06	-9.7562E-03	5.9192E-08
2077	-0.2227	3.8435E-05	-0.4689	-3.6320E-06	-1.1172E-02	5.6632E-08
2079	-0.1843	3.0755E-05	-0.3940	-3.6337E-06	-1.2574E-02	5.4092E-08
2081	-0.1428	2.3071E-05	-0.3096	-3.6354E-06	-1.4014E-02	5.1490E-08
2083	-9.8215E-02	1.5384E-05	-0.2159	-3.6370E-06	-1.5362E-02	4.9044E-08
2085	-5.0621E-02	7.6939E-06	-0.1127	-3.6388E-06	-1.6948E-02	4.6179E-08
2087	0.000	0.000	0.000	-3.6400E-06	-1.7937E-02	4.4408E-08
3001	8.1721E-02	-1.3798E-08	-7.1911E-03	5.0320E-09	2.0479E-02	2.1515E-10
3002	9.4966E-02	-2.8127E-08	-0.3932	2.5444E-08	2.0023E-02	4.0055E-10
3003	0.1019	-2.7813E-08	-0.6299	2.5755E-08	1.9418E-02	4.3207E-10
3004	0.1078	-2.7231E-08	-0.8591	2.5894E-08	1.8748E-02	4.6532E-10
3005	0.1128	-2.6604E-08	-1.080	2.6178E-08	1.8008E-02	5.0277E-10
3006	0.1169	-2.5850E-08	-1.291	2.6527E-08	1.7202E-02	5.4449E-10
3007	0.1200	-2.5002E-08	-1.492	2.6923E-08	1.6331E-02	5.9130E-10
3008	0.1224	-2.3989E-08	-1.683	2.7354E-08	1.5398E-02	6.4428E-10

3009	0.1239	-2.2805E-08	-1.862	2.7811E-08	1.4405E-02	7.0486E-10
3010	0.1248	-2.1462E-08	-2.028	2.8304E-08	1.3353E-02	7.7546E-10
3011	0.1249	-1.9923E-08	-2.182	2.8829E-08	1.2242E-02	8.5824E-10
3012	0.1245	-1.8179E-08	-2.322	2.9381E-08	1.1073E-02	9.5579E-10
3013	0.1236	-1.6211E-08	-2.447	2.9966E-08	9.8464E-03	1.0701E-09
3014	0.1222	-1.3998E-08	-2.558	3.0577E-08	8.5626E-03	1.1996E-09
3015	0.1205	-1.1523E-08	-2.653	3.1215E-08	7.2225E-03	1.3345E-09
3016	0.1186	-8.7512E-09	-2.731	3.1878E-08	5.8273E-03	1.4467E-09
3017	0.1166	-5.6609E-09	-2.792	3.2563E-08	4.3796E-03	1.4849E-09
3018	0.1145	-2.2134E-09	-2.836	3.3269E-08	2.8830E-03	1.3930E-09
3019	0.1126	1.6110E-09	-2.861	3.4007E-08	1.3430E-03	1.1655E-09
3020	0.1109	5.8278E-09	-2.868	3.4794E-08	-2.3324E-04	8.7012E-10
3021	0.1095	1.0464E-08	-2.856	3.5635E-08	-1.8370E-03	5.8902E-10
3022	0.1087	1.5573E-08	-2.824	3.6522E-08	-3.4585E-03	3.6303E-10
3023	0.1084	2.1177E-08	-2.773	3.7448E-08	-5.0878E-03	1.9463E-10
3024	0.1089	2.7332E-08	-2.702	3.8409E-08	-6.7152E-03	7.0444E-11
3025	0.1103	3.4096E-08	-2.611	3.9401E-08	-8.3313E-03	-2.4077E-11
3026	0.1126	4.1449E-08	-2.502	4.0424E-08	-9.9273E-03	-1.0006E-10
3027	0.1161	4.9469E-08	-2.373	4.1481E-08	-1.1495E-02	-1.6559E-10
3028	0.1207	5.8203E-08	-2.226	4.2564E-08	-1.3025E-02	-2.2597E-10
3029	0.1267	6.7644E-08	-2.061	4.3677E-08	-1.4510E-02	-2.8471E-10
3030	0.1341	7.7854E-08	-1.878	4.4825E-08	-1.5940E-02	-3.4435E-10
3031	0.1429	8.8888E-08	-1.678	4.5996E-08	-1.7308E-02	-4.0659E-10
3032	0.1532	1.0073E-07	-1.463	4.7200E-08	-1.8603E-02	-4.7256E-10
3033	0.1652	1.1345E-07	-1.232	4.8447E-08	-1.9815E-02	-5.4332E-10
3034	0.1787	1.2703E-07	-0.9874	4.9762E-08	-2.0933E-02	-6.1947E-10
3035	0.1939	1.4159E-07	-0.7298	5.1072E-08	-2.1946E-02	-7.0172E-10
3036	0.2108	1.5831E-07	-0.4608	5.0724E-08	-2.2842E-02	-7.9004E-10
3037	0.2411	1.9806E-07	-1.8556E-02	3.5149E-08	-2.3508E-02	-9.3499E-10
4001	8.1721E-02	-1.3798E-08	-7.1912E-03	5.0324E-09	2.0479E-02	2.1242E-10
4002	9.4966E-02	1.1918E-09	-0.3932	-1.4789E-08	2.0023E-02	4.3702E-11
4003	0.1019	1.5972E-09	-0.6299	-1.4605E-08	1.9418E-02	2.2577E-11
4004	0.1078	1.9665E-09	-0.8591	-1.4174E-08	1.8748E-02	-7.2116E-13
4005	0.1128	2.5432E-09	-1.080	-1.3821E-08	1.8008E-02	-2.9220E-11
4006	0.1169	3.2647E-09	-1.291	-1.3467E-08	1.7202E-02	-6.3300E-11
4007	0.1200	4.1576E-09	-1.492	-1.3093E-08	1.6331E-02	-1.0414E-10
4008	0.1224	5.1885E-09	-1.683	-1.2688E-08	1.5398E-02	-1.5306E-10
4009	0.1239	6.3816E-09	-1.862	-1.2243E-08	1.4405E-02	-2.1183E-10
4010	0.1248	7.7379E-09	-2.028	-1.1769E-08	1.3353E-02	-2.8302E-10
4011	0.1249	9.2887E-09	-2.182	-1.1260E-08	1.2242E-02	-3.6924E-10
4012	0.1245	1.1035E-08	-2.322	-1.0711E-08	1.1073E-02	-4.7327E-10
4013	0.1236	1.3005E-08	-2.447	-1.0130E-08	9.8464E-03	-5.9741E-10
4014	0.1222	1.5211E-08	-2.558	-9.5085E-09	8.5626E-03	-7.4029E-10
4015	0.1205	1.7671E-08	-2.653	-8.8485E-09	7.2225E-03	-8.9229E-10
4016	0.1186	2.0414E-08	-2.731	-8.1461E-09	5.8273E-03	-1.0257E-09
4017	0.1166	2.3461E-08	-2.792	-7.4007E-09	4.3796E-03	-1.0893E-09
4018	0.1145	2.6850E-08	-2.836	-6.6109E-09	2.8830E-03	-1.0275E-09
4019	0.1126	3.0613E-08	-2.861	-5.7863E-09	1.3430E-03	-8.3490E-10
4020	0.1109	3.4791E-08	-2.868	-4.9453E-09	-2.3324E-04	-5.7964E-10
4021	0.1095	3.9419E-08	-2.856	-4.0916E-09	-1.8370E-03	-3.4420E-10
4022	0.1087	4.4537E-08	-2.824	-3.2178E-09	-3.4585E-03	-1.7000E-10
4023	0.1084	5.0159E-08	-2.773	-2.3162E-09	-5.0878E-03	-5.9804E-11
4024	0.1089	5.6333E-08	-2.702	-1.3831E-09	-6.7152E-03	-9.4376E-13
4025	0.1103	6.3113E-08	-2.611	-4.1407E-10	-8.3313E-03	2.0425E-11
4026	0.1126	7.0480E-08	-2.502	5.9125E-10	-9.9273E-03	1.5279E-11
4027	0.1161	7.8513E-08	-2.373	1.6301E-09	-1.1495E-02	-9.2566E-12
4028	0.1207	8.7248E-08	-2.226	2.7103E-09	-1.3025E-02	-4.8520E-11
4029	0.1267	9.6685E-08	-2.061	3.8281E-09	-1.4510E-02	-9.9373E-11
4030	0.1341	1.0689E-07	-1.878	4.9782E-09	-1.5940E-02	-1.6010E-10
4031	0.1429	1.1791E-07	-1.678	6.1728E-09	-1.7308E-02	-2.2970E-10
4032	0.1532	1.2973E-07	-1.463	7.4017E-09	-1.8603E-02	-3.0735E-10
4033	0.1652	1.4245E-07	-1.232	8.6554E-09	-1.9815E-02	-3.9284E-10
4034	0.1787	1.5607E-07	-0.9874	9.9108E-09	-2.0933E-02	-4.8587E-10
4035	0.1939	1.7062E-07	-0.7298	1.1248E-08	-2.1946E-02	-5.8708E-10
4036	0.2108	1.8480E-07	-0.4608	1.4378E-08	-2.2842E-02	-7.0004E-10
4037	0.2411	1.9805E-07	-1.8557E-02	3.5150E-08	-2.3508E-02	-9.3174E-10
5002	6.9258E-02	-6.6306E-09	-0.3929	5.3272E-09	2.0023E-02	2.2213E-10
5003	7.6940E-02	-5.9534E-09	-0.6297	5.5747E-09	1.9418E-02	2.2732E-10
5004	8.3744E-02	-5.1116E-09	-0.8588	5.8598E-09	1.8748E-02	2.3230E-10
5005	8.9682E-02	-4.1003E-09	-1.080	6.1785E-09	1.8008E-02	2.3677E-10
5006	9.4791E-02	-2.9173E-09	-1.291	6.5303E-09	1.7202E-02	2.4060E-10
5007	9.9080E-02	-1.5460E-09	-1.492	6.9152E-09	1.6331E-02	2.4358E-10
5008	0.1026	1.2601E-11	-1.683	7.3330E-09	1.5398E-02	2.4561E-10
5009	0.1054	1.7804E-09	-1.862	7.7840E-09	1.4405E-02	2.4651E-10

5010	0.1076	3.7513E-09	-2.028	8.2679E-09	1.3353E-02	2.4622E-10
5011	0.1092	5.9604E-09	-2.182	8.7849E-09	1.2242E-02	2.4450E-10
5012	0.1103	8.4122E-09	-2.322	9.3349E-09	1.1073E-02	2.4126E-10
5013	0.1109	1.1130E-08	-2.447	9.9180E-09	9.8464E-03	2.3636E-10
5014	0.1112	1.4131E-08	-2.558	1.0534E-08	8.5626E-03	2.2968E-10
5015	0.1112	1.7432E-08	-2.653	1.1183E-08	7.2225E-03	2.2111E-10
5016	0.1111	2.1066E-08	-2.731	1.1866E-08	5.8273E-03	2.1052E-10
5017	0.1109	2.5054E-08	-2.792	1.2581E-08	4.3796E-03	1.9779E-10
5018	0.1108	2.9433E-08	-2.836	1.3329E-08	2.8830E-03	1.8276E-10
5019	0.1109	3.4229E-08	-2.861	1.4110E-08	1.3430E-03	1.6530E-10
5020	0.1112	3.9473E-08	-2.868	1.4924E-08	-2.3324E-04	1.4524E-10
5021	0.1119	4.5192E-08	-2.856	1.5772E-08	-1.8370E-03	1.2241E-10
5022	0.1131	5.1436E-08	-2.824	1.6652E-08	-3.4585E-03	9.6519E-11
5023	0.1149	5.8223E-08	-2.773	1.7566E-08	-5.0878E-03	6.7411E-11
5024	0.1175	6.5603E-08	-2.702	1.8513E-08	-6.7152E-03	3.4750E-11
5025	0.1210	7.3634E-08	-2.611	1.9494E-08	-8.3313E-03	-1.8260E-12
5026	0.1254	8.2296E-08	-2.502	2.0508E-08	-9.9273E-03	-4.2393E-11
5027	0.1308	9.1667E-08	-2.373	2.1556E-08	-1.1495E-02	-8.7422E-11
5028	0.1375	1.0179E-07	-2.226	2.2637E-08	-1.3025E-02	-1.3725E-10
5029	0.1453	1.1266E-07	-2.061	2.3753E-08	-1.4510E-02	-1.9204E-10
5030	0.1545	1.2434E-07	-1.878	2.4902E-08	-1.5940E-02	-2.5223E-10
5031	0.1651	1.3689E-07	-1.678	2.6084E-08	-1.7308E-02	-3.1815E-10
5032	0.1771	1.5028E-07	-1.463	2.7301E-08	-1.8603E-02	-3.8996E-10
5033	0.1906	1.6460E-07	-1.232	2.8551E-08	-1.9815E-02	-4.6808E-10
5034	0.2056	1.7985E-07	-0.9871	2.9836E-08	-2.0933E-02	-5.5267E-10
5035	0.2221	1.9610E-07	-0.7295	3.1160E-08	-2.1946E-02	-6.4440E-10
5036	0.2401	2.1334E-07	-0.4605	3.2551E-08	-2.2842E-02	-7.4504E-10
20001	0.000	0.000	0.000	0.000	0.000	1.1732E-06
20002	4.1180E-04	2.0381E-05	-2.8945E-04	-3.0348E-06	2.0443E-04	5.9340E-06
20003	1.3559E-03	4.3367E-05	-6.6850E-04	-1.1853E-06	4.0610E-04	6.8772E-06
20004	2.9161E-03	6.3954E-05	-1.0428E-03	-1.4517E-06	6.0407E-04	7.5601E-06
20005	5.0809E-03	8.7458E-05	-1.4121E-03	-3.0472E-06	7.9818E-04	7.9757E-06
20006	7.8379E-03	1.1672E-04	-1.7765E-03	-5.1530E-06	9.8830E-04	8.1181E-06
20007	1.1175E-02	1.5201E-04	-2.1362E-03	-6.9125E-06	1.1743E-03	7.9811E-06
20008	1.5079E-02	1.9088E-04	-2.4912E-03	-7.4325E-06	1.3560E-03	7.5574E-06
20009	1.9536E-02	2.2808E-04	-2.8421E-03	-5.7824E-06	1.5333E-03	6.8403E-06
20010	2.4532E-02	2.5544E-04	-3.1892E-03	-9.8925E-07	1.7061E-03	5.8230E-06
20011	3.0054E-02	2.6169E-04	-3.5331E-03	7.9610E-06	1.8743E-03	4.4974E-06
20012	3.6087E-02	2.3242E-04	-3.8746E-03	2.2126E-05	2.0377E-03	2.8562E-06
20013	4.2617E-02	1.4983E-04	-4.2146E-03	4.2611E-05	2.1962E-03	8.9172E-07
20014	4.9626E-02	-7.3223E-06	-4.5541E-03	7.0570E-05	2.3497E-03	-1.4049E-06
20015	5.7765E-02	-2.2729E-04	-4.8858E-03	6.8224E-05	2.5133E-03	2.0537E-06
20016	6.6437E-02	-4.3106E-04	-5.2120E-03	6.0939E-05	2.6675E-03	5.0728E-06
20017	7.5608E-02	-6.0372E-04	-5.5323E-03	4.9685E-05	2.8120E-03	7.6489E-06
20018	8.5247E-02	-7.3370E-04	-5.8462E-03	3.5487E-05	2.9468E-03	9.7767E-06
20019	9.5322E-02	-8.1295E-04	-6.1535E-03	1.9430E-05	3.0718E-03	1.1452E-05
20020	0.1058	-8.3714E-04	-6.4538E-03	2.6602E-06	3.1868E-03	1.2670E-05
20021	0.1166	-8.0591E-04	-6.7473E-03	-1.3610E-05	3.2917E-03	1.3426E-05
20022	0.1278	-7.2306E-04	-7.0341E-03	-2.8100E-05	3.3864E-03	1.3714E-05
20023	0.1393	-5.9682E-04	-7.3145E-03	-3.9449E-05	3.4708E-03	1.3529E-05
20024	0.1510	-4.4008E-04	-7.5890E-03	-4.6223E-05	3.5448E-03	1.2866E-05
20025	0.1630	-2.7067E-04	-7.8582E-03	-4.6900E-05	3.6083E-03	1.1719E-05
20026	0.1752	-1.1169E-04	-8.1231E-03	-3.9865E-05	3.6612E-03	1.0083E-05
20027	0.1875	8.2006E-06	-8.3849E-03	-2.3403E-05	3.7035E-03	7.9538E-06
20028	0.2000	5.4427E-05	-8.6449E-03	4.3088E-06	3.7350E-03	5.3251E-06
20029	0.2125	-1.3883E-05	-8.9047E-03	4.5212E-05	3.7557E-03	2.1931E-06
20030	0.2251	-2.1070E-04	-9.1475E-03	7.0135E-05	3.7655E-03	2.0906E-06
20101	0.000	0.000	0.000	0.000	0.000	-1.1732E-06
20102	4.1180E-04	-2.0381E-05	-2.8945E-04	3.0348E-06	2.0443E-04	-5.9340E-06
20103	1.3559E-03	-4.3367E-05	-6.6850E-04	1.1853E-06	4.0610E-04	-6.8771E-06
20104	2.9161E-03	-6.3954E-05	-1.0428E-03	1.4517E-06	6.0407E-04	-7.5599E-06
20105	5.0809E-03	-8.7458E-05	-1.4121E-03	3.0472E-06	7.9818E-04	-7.9754E-06
20106	7.8379E-03	-1.1672E-04	-1.7765E-03	5.1530E-06	9.8830E-04	-8.1178E-06
20107	1.1175E-02	-1.5201E-04	-2.1362E-03	6.9124E-06	1.1743E-03	-7.9808E-06
20108	1.5079E-02	-1.9088E-04	-2.4912E-03	7.4325E-06	1.3560E-03	-7.5570E-06
20109	1.9536E-02	-2.2808E-04	-2.8421E-03	5.7824E-06	1.5333E-03	-6.8398E-06
20110	2.4532E-02	-2.5543E-04	-3.1892E-03	9.8922E-07	1.7061E-03	-5.8225E-06
20111	3.0054E-02	-2.6169E-04	-3.5331E-03	-7.9610E-06	1.8743E-03	-4.4968E-06
20112	3.6087E-02	-2.3242E-04	-3.8746E-03	-2.2126E-05	2.0377E-03	-2.8556E-06
20113	4.2617E-02	-1.4983E-04	-4.2146E-03	-4.2611E-05	2.1962E-03	-8.9101E-07
20114	4.9626E-02	7.3230E-06	-4.5541E-03	-7.0570E-05	2.3497E-03	1.4056E-06
20115	5.7765E-02	2.2729E-04	-4.8858E-03	-6.8224E-05	2.5133E-03	-2.0528E-06
20116	6.6437E-02	4.3106E-04	-5.2120E-03	-6.0939E-05	2.6675E-03	-5.0718E-06
20117	7.5608E-02	6.0372E-04	-5.5323E-03	-4.9685E-05	2.8120E-03	-7.6478E-06

20118	8.5247E-02	7.3370E-04	-5.8462E-03	-3.5487E-05	2.9468E-03	-9.7756E-06
20119	9.5322E-02	8.1295E-04	-6.1535E-03	-1.9430E-05	3.0718E-03	-1.1451E-05
20120	0.1058	8.3714E-04	-6.4538E-03	-2.6602E-06	3.1868E-03	-1.2669E-05
20121	0.1166	8.0591E-04	-6.7473E-03	1.3610E-05	3.2917E-03	-1.3424E-05
20122	0.1278	7.2307E-04	-7.0341E-03	2.8100E-05	3.3864E-03	-1.3712E-05
20123	0.1393	5.9682E-04	-7.3145E-03	3.9449E-05	3.4708E-03	-1.3528E-05
20124	0.1510	4.4008E-04	-7.5890E-03	4.6223E-05	3.5448E-03	-1.2864E-05
20125	0.1630	2.7067E-04	-7.8582E-03	4.6900E-05	3.6083E-03	-1.1717E-05
20126	0.1752	1.1169E-04	-8.1231E-03	3.9865E-05	3.6612E-03	-1.0082E-05
20127	0.1875	-8.2001E-06	-8.3849E-03	2.3403E-05	3.7035E-03	-7.9518E-06
20128	0.2000	-5.4427E-05	-8.6449E-03	-4.3088E-06	3.7350E-03	-5.3231E-06
20129	0.2125	1.3883E-05	-8.9047E-03	-4.5212E-05	3.7557E-03	-2.1910E-06
20130	0.2251	2.1070E-04	-9.1475E-03	-7.0135E-05	3.7655E-03	-2.0884E-06
20201	4.9626E-02	-7.3223E-06	-4.5541E-03	7.0570E-05	2.3497E-03	-1.4049E-06
20202	4.9622E-02	-4.9714E-06	-4.7221E-03	6.7709E-05	2.3433E-03	-1.8528E-06
20203	4.9617E-02	-2.4840E-06	-4.8619E-03	4.1090E-05	2.3366E-03	-1.4017E-06
20204	4.9615E-02	2.4902E-10	-4.9151E-03	1.8186E-09	2.3298E-03	3.1002E-10
20205	4.9617E-02	2.4845E-06	-4.8619E-03	-4.1088E-05	2.3366E-03	1.4024E-06
20206	4.9622E-02	4.9719E-06	-4.7222E-03	-6.7707E-05	2.3433E-03	1.8536E-06
20207	4.9626E-02	7.3230E-06	-4.5541E-03	-7.0570E-05	2.3497E-03	1.4056E-06
20301	0.2125	-1.3883E-05	-8.9047E-03	4.5212E-05	3.7557E-03	2.1931E-06
20302	0.2125	-9.2547E-06	-8.9798E-03	3.8341E-05	3.7557E-03	1.4627E-06
20303	0.2125	-4.6268E-06	-9.0335E-03	2.1630E-05	3.7557E-03	7.3195E-07
20304	0.2125	3.7026E-10	-9.0528E-03	-1.2466E-09	3.7557E-03	9.9990E-10
20305	0.2125	4.6276E-06	-9.0335E-03	-2.1632E-05	3.7557E-03	-7.2995E-07
20306	0.2125	9.2554E-06	-8.9798E-03	-3.8342E-05	3.7557E-03	-1.4607E-06
20307	0.2125	1.3883E-05	-8.9047E-03	-4.5212E-05	3.7557E-03	-2.1910E-06
30001	0.000	0.000	0.000	0.000	0.000	-1.5056E-06
30002	-5.7555E-04	1.8741E-05	-2.5655E-04	-4.2547E-06	-2.8542E-04	-7.0244E-06
30003	-2.1662E-03	5.3687E-05	-6.4049E-04	-7.0818E-06	-6.0667E-04	-9.1223E-06
30004	-4.8816E-03	9.9838E-05	-1.0155E-03	-1.0505E-05	-9.1824E-04	-1.0728E-05
30005	-8.6868E-03	1.5734E-04	-1.3821E-03	-1.3404E-05	-1.2199E-03	-1.1831E-05
30006	-1.3546E-02	2.2227E-04	-1.7406E-03	-1.4616E-05	-1.5112E-03	-1.2421E-05
30007	-1.9422E-02	2.8649E-04	-2.0919E-03	-1.2928E-05	-1.7921E-03	-1.2486E-05
30008	-2.6277E-02	3.3747E-04	-2.4367E-03	-7.0770E-06	-2.0622E-03	-1.2015E-05
30009	-3.4072E-02	3.5809E-04	-2.7759E-03	4.2506E-06	-2.3213E-03	-1.0995E-05
30010	-4.2768E-02	3.2646E-04	-3.1108E-03	2.2423E-05	-2.5692E-03	-9.4155E-06
30011	-5.2325E-02	2.1575E-04	-3.4425E-03	4.8864E-05	-2.8056E-03	-7.2630E-06
30012	-6.2700E-02	-6.0665E-06	-3.7725E-03	8.5057E-05	-3.0303E-03	-4.5248E-06
30013	-7.3318E-02	-2.9181E-04	-4.0466E-03	8.9201E-05	-3.2337E-03	-8.5238E-06
30014	-8.4608E-02	-5.8047E-03	-4.3153E-03	8.6804E-05	-3.4267E-03	-1.2034E-05
30015	-9.6535E-02	-8.5140E-04	-4.5780E-03	7.8776E-05	-3.6092E-03	-1.5050E-05
30016	-0.1091	-1.0871E-03	-4.8339E-03	6.6077E-05	-3.7811E-03	-1.7569E-05
30017	-0.1222	-1.2736E-03	-5.0827E-03	4.9721E-05	-3.9422E-03	-1.9587E-05
30018	-0.1358	-1.4001E-03	-5.3239E-03	3.0781E-05	-4.0924E-03	-2.1100E-05
30019	-0.1499	-1.4598E-03	-5.5573E-03	1.0387E-05	-4.2315E-03	-2.2103E-05
30020	-0.1644	-1.4499E-03	-5.7827E-03	-1.0265E-05	-4.3595E-03	-2.2592E-05
30021	-0.1794	-1.3716E-03	-6.0002E-03	-2.9913E-05	-4.4762E-03	-2.2561E-05
30022	-0.1948	-1.2305E-03	-6.2100E-03	-4.7221E-05	-4.5815E-03	-2.2006E-05
30023	-0.2105	-1.0369E-03	-6.4126E-03	-6.0778E-05	-4.6754E-03	-2.0920E-05
30024	-0.2265	-8.0611E-04	-6.6085E-03	-6.9087E-05	-4.7576E-03	-1.9300E-05
30025	-0.2427	-5.5853E-04	-6.7984E-03	-7.0562E-05	-4.8282E-03	-1.7139E-05
30026	-0.2592	-3.2016E-04	-6.9834E-03	-6.3520E-05	-4.8870E-03	-1.4432E-05
30027	-0.2758	-1.2290E-04	-7.1647E-03	-4.6170E-05	-4.9339E-03	-1.1174E-05
30028	-0.2926	-4.8744E-06	-7.3438E-03	-1.6607E-05	-4.9689E-03	-7.3599E-06
30029	-0.3095	-1.0906E-05	-7.5224E-03	-2.7205E-05	-4.9919E-03	-2.9860E-06
30030	-0.3264	-1.3599E-04	-7.6829E-03	4.4881E-05	-5.0027E-03	-2.8835E-06
30101	0.000	0.000	0.000	0.000	0.000	1.5056E-06
30102	-5.7555E-04	-1.8741E-05	-2.5655E-04	4.2547E-06	-2.8542E-04	7.0244E-06
30103	-2.1662E-03	-5.3687E-05	-6.4049E-04	7.0818E-06	-6.0667E-04	9.1222E-06
30104	-4.8816E-03	-9.9838E-05	-1.0155E-03	1.0505E-05	-9.1824E-04	1.0728E-05
30105	-8.6868E-03	-1.5734E-04	-1.3821E-03	1.3404E-05	-1.2199E-03	1.1831E-05
30106	-1.3546E-02	-2.2227E-04	-1.7406E-03	1.4616E-05	-1.5112E-03	1.2421E-05
30107	-1.9422E-02	-2.8649E-04	-2.0919E-03	1.2928E-05	-1.7921E-03	1.2486E-05
30108	-2.6277E-02	-3.3747E-04	-2.4367E-03	7.0770E-06	-2.0622E-03	1.2014E-05
30109	-3.4072E-02	-3.5809E-04	-2.7759E-03	-4.2506E-06	-2.3213E-03	1.0995E-05
30110	-4.2768E-02	-3.2646E-04	-3.1108E-03	-2.2423E-05	-2.5692E-03	9.4151E-06
30111	-5.2325E-02	-2.1575E-04	-3.4425E-03	-4.8864E-05	-2.8056E-03	7.2625E-06
30112	-6.2700E-02	6.0667E-06	-3.7725E-03	-8.5057E-05	-3.0303E-03	4.5242E-06
30113	-7.3318E-02	2.9181E-04	-4.0466E-03	-8.9201E-05	-3.2337E-03	8.5231E-06
30114	-8.4608E-02	5.8047E-04	-4.3153E-03	-8.6804E-05	-3.4267E-03	1.2033E-05
30115	-9.6535E-02	8.5140E-04	-4.5780E-03	-7.8776E-05	-3.6092E-03	1.5049E-05
30116	-0.1091	1.0871E-03	-4.8339E-03	-6.6077E-05	-3.7811E-03	1.7568E-05
30117	-0.1222	1.2736E-03	-5.0827E-03	-4.9721E-05	-3.9422E-03	1.9586E-05

30118	-0.1358	1.4001E-03	-5.3239E-03	-3.0781E-05	-4.0924E-03	2.1099E-05
30119	-0.1499	1.4598E-03	-5.5573E-03	-1.0388E-05	-4.2315E-03	2.2102E-05
30120	-0.1644	1.4499E-03	-5.7827E-03	1.0265E-05	-4.3595E-03	2.2591E-05
30121	-0.1794	1.3716E-03	-6.0002E-03	2.9912E-05	-4.4762E-03	2.2560E-05
30122	-0.1948	1.2305E-03	-6.2100E-03	4.7221E-05	-4.5815E-03	2.2004E-05
30123	-0.2105	1.0369E-03	-6.4126E-03	6.0778E-05	-4.6754E-03	2.0919E-05
30124	-0.2265	8.0611E-04	-6.6085E-03	6.9087E-05	-4.7576E-03	1.9298E-05
30125	-0.2427	5.5854E-04	-6.7984E-03	7.0562E-05	-4.8282E-03	1.7137E-05
30126	-0.2592	3.2017E-04	-6.9834E-03	6.3520E-05	-4.8870E-03	1.4430E-05
30127	-0.2758	1.2291E-04	-7.1647E-03	4.6170E-05	-4.9339E-03	1.1171E-05
30128	-0.2926	4.8845E-06	-7.3438E-03	1.6607E-05	-4.9689E-03	7.3576E-06
30129	-0.3095	1.0916E-05	-7.5224E-03	-2.7205E-05	-4.9919E-03	2.9837E-06
30130	-0.3264	1.3600E-04	-7.6829E-03	-4.4881E-05	-5.0027E-03	2.8812E-06
30201	-6.2700E-02	-6.0665E-06	-3.7725E-03	8.5057E-05	-3.0303E-03	-4.5248E-06
30202	-6.2709E-02	-4.1145E-06	-3.9810E-03	8.0241E-05	-3.0303E-03	-3.2256E-06
30203	-6.2715E-02	-2.0550E-06	-4.1522E-03	4.8400E-05	-3.0303E-03	-1.6948E-06
30204	-6.2717E-02	2.6463E-11	-4.2172E-03	2.0169E-09	-3.0303E-03	-2.8069E-10
30205	-6.2715E-02	2.0552E-06	-4.1522E-03	-4.8400E-05	-3.0303E-03	1.6943E-06
30206	-6.2712E-02	3.3182E-06	-4.0567E-03	-7.0609E-05	-3.0303E-03	2.6529E-06
30207	-6.2700E-02	6.0667E-06	-3.7725E-03	-8.5057E-05	-3.0303E-03	4.5242E-06
30301	-0.3095	-1.0906E-05	-7.5224E-03	2.7205E-05	-4.9919E-03	-2.9860E-06
30302	-0.3095	-7.2689E-06	-7.5712E-03	2.6336E-05	-4.9919E-03	-1.9914E-06
30303	-0.3095	-3.6317E-06	-7.6091E-03	1.5628E-05	-4.9919E-03	-9.9623E-07
30304	-0.3095	5.2140E-09	-7.6232E-03	-8.9391E-10	-4.9919E-03	-8.9499E-10
30305	-0.3095	3.6421E-06	-7.6091E-03	-1.5629E-05	-4.9919E-03	9.9439E-07
30306	-0.3095	7.2793E-06	-7.5712E-03	-2.6337E-05	-4.9919E-03	1.9894E-06
30307	-0.3095	1.0916E-05	-7.5224E-03	-2.7205E-05	-4.9919E-03	2.9837E-06
MAXIMUM AT NODE	0.2646	1.4598E-03	0.000	8.9201E-05	2.3381E-02	2.2591E-05
	37	30119	981	30013	2002	30120
MINIMUM AT NODE	-0.4413	-1.4598E-03	-2.868	-8.9201E-05	-2.9977E-02	-2.2592E-05
	2053	30019	4020	30113	2036	30020
TOTAL	0.3729	7.5018E-06	-439.5	1.1486E-05	-6.4561E-02	-5.2964E-07

1

Abaqus Student Edition 6.11-2

DATE 09-May-2012 TIME 10:23:48

Analysis of Lysefjord bridge

STEP 3 INCREMENT 1
TIME COMPLETED IN THIS STEP

0.00

S T E P 3 C A L C U L A T I O N O F E I G E N V A L U E S
F O R N A T U R A L F R E Q U E N C I E S

THE LANCZOS EIGENSOLVER IS USED FOR THIS ANALYSIS

Abaqus WILL COMPUTE UNCOUPLED

STRUCTURAL AND ACOUSTIC MODES

NUMBER OF EIGENVALUES 150

HIGHEST FREQUENCY OF INTEREST 1.00000E+18

MAXIMUM NUMBER OF STEPS WITHIN RUN 35

BLOCK SIZE FOR LANCZOS PROCEDURE 7

THE EIGENVECTORS ARE SCALED SO THAT

THE LARGEST DISPLACEMENT ENTRY IN EACH VECTOR

IS UNITY

INITIAL STRESS AND DISPLACEMENT EFFECTS ARE
INCLUDED IN THE STIFFNESS MATRIX

THIS IS A LINEAR PERTURBATION STEP.

ALL LOADS ARE DEFINED AS CHANGE IN LOAD TO THE REFERENCE STATE

LARGE DISPLACEMENT THEORY WILL BE USED

M E M O R Y E S T I M A T E

PROCESS	FLOATING PT OPERATIONS	MINIMUM MEMORY REQUIRED	MEMORY TO MINIMIZE I/O
---------	------------------------	-------------------------	------------------------

PER ITERATION		(MBYTES)	(MBYTES)
1	2.45E+006	16	39

NOTE:

- (1) SINCE ABAQUS DOES NOT PRE-ALLOCATE MEMORY AND ONLY ALLOCATES MEMORY AS NEEDED DURING THE ANALYSIS, THE MEMORY REQUIREMENT PRINTED HERE CAN ONLY BE VIEWED AS A GENERAL GUIDELINE BASED ON THE BEST KNOWLEDGE AVAILABLE AT THE BEGINNING OF A STEP BEFORE THE SOLUTION PROCESS HAS BEGUN.
- (2) THE ESTIMATE IS NORMALLY UPDATED AT THE BEGINNING OF EVERY STEP. IT IS THE MAXIMUM VALUE OF THE ESTIMATE FROM THE CURRENT STEP TO THE LAST STEP OF THE ANALYSIS, WITH UNSYMMETRIC SOLUTION TAKEN INTO ACCOUNT IF APPLICABLE.
- (3) SINCE THE ESTIMATE IS BASED ON THE ACTIVE DEGREES OF FREEDOM IN THE FIRST ITERATION OF THE CURRENT STEP, THE MEMORY ESTIMATE MIGHT BE SIGNIFICANTLY DIFFERENT THAN ACTUAL USAGE FOR PROBLEMS WITH SUBSTANTIAL CHANGES IN ACTIVE DEGREES OF FREEDOM BETWEEN STEPS (OR EVEN WITHIN THE SAME STEP). EXAMPLES ARE: PROBLEMS WITH SIGNIFICANT CONTACT CHANGES, PROBLEMS WITH MODEL CHANGE, PROBLEMS WITH BOTH STATIC STEP AND STEADY STATE DYNAMIC PROCEDURES WHERE ACOUSTIC ELEMENTS WILL ONLY BE ACTIVATED IN THE STEADY STATE DYNAMIC STEPS.
- (4) FOR MULTI-PROCESS EXECUTION, THE ESTIMATED VALUE OF FLOATING POINT OPERATIONS FOR EACH PROCESS IS BASED ON AN INITIAL SCHEDULING OF OPERATIONS AND MIGHT NOT REFLECT THE ACTUAL FLOATING POINT OPERATIONS COMPLETED ON EACH PROCESS. OPERATIONS ARE DYNAMICALLY BALANCED DURING EXECUTION, SO THE ACTUAL BALANCE OF OPERATIONS BETWEEN PROCESSES IS EXPECTED TO BE BETTER THAN THE ESTIMATE PRINTED HERE.
- (5) THE UPPER LIMIT OF MEMORY THAT CAN BE ALLOCATED BY ABAQUS WILL IN GENERAL DEPEND ON THE VALUE OF THE "MEMORY" PARAMETER AND THE AMOUNT OF PHYSICAL MEMORY AVAILABLE ON THE MACHINE. PLEASE SEE THE "ABAQUS ANALYSIS USER'S MANUAL" FOR MORE DETAILS. THE ACTUAL USAGE OF MEMORY AND OF DISK SPACE FOR SCRATCH DATA WILL DEPEND ON THIS UPPER LIMIT AS WELL AS THE MEMORY REQUIRED TO MINIMIZE I/O. IF THE MEMORY UPPER LIMIT IS GREATER THAN THE MEMORY REQUIRED TO MINIMIZE I/O, THEN THE ACTUAL MEMORY USAGE WILL BE CLOSE TO THE ESTIMATED "MEMORY TO MINIMIZE I/O" VALUE, AND THE SCRATCH DISK USAGE WILL BE CLOSE-TO-ZERO; OTHERWISE, THE ACTUAL MEMORY USED WILL BE CLOSE TO THE PREVIOUSLY MENTIONED MEMORY LIMIT, AND THE SCRATCH DISK USAGE WILL BE ROUGHLY PROPORTIONAL TO THE DIFFERENCE BETWEEN THE ESTIMATED "MEMORY TO MINIMIZE I/O" AND THE MEMORY UPPER LIMIT. HOWEVER ACCURATE ESTIMATE OF THE SCRATCH DISK SPACE IS NOT POSSIBLE.
- (6) USING "*RESTART, WRITE" CAN GENERATE A LARGE AMOUNT OF DATA WRITTEN IN THE WORK DIRECTORY.

E I G E N V A L U E O U T P U T

MODE NO	EIGENVALUE	FREQUENCY (RAD/TIME)	GENERALIZED MASS (CYCLES/TIME)	COMPOSITE MODAL DAMPING
1	0.64259	0.80162	0.12758	1.34522E+06 0.0000
2	1.8128	1.3464	0.21429	1.36885E+06 0.0000
3	3.6007	1.8975	0.30200	7.53148E+05 0.0000
4	6.5394	2.5572	0.40700	1.11894E+06 0.0000
5	7.3370	2.7087	0.43110	1.39764E+06 0.0000
6	10.604	3.2564	0.51827	1.27862E+05 0.0000
7	11.231	3.3513	0.53337	1.35279E+05 0.0000
8	12.862	3.5864	0.57079	1.13501E+05 0.0000
9	13.418	3.6630	0.58299	1.39603E+06 0.0000
10	13.435	3.6654	0.58337	1.28424E+05 0.0000
11	13.997	3.7412	0.59544	89109. 0.0000
12	14.902	3.8603	0.61438	62525. 0.0000
13	15.209	3.8999	0.62068	70284. 0.0000
14	15.506	3.9378	0.62672	69401. 0.0000
15	18.489	4.2999	0.68435	2.63037E+05 0.0000
16	21.823	4.6715	0.74349	1.15757E+06 0.0000
17	26.870	5.1836	0.82500	1.54412E+05 0.0000
18	27.428	5.2372	0.83353	1.76179E+05 0.0000
19	28.921	5.3778	0.85590	1.72044E+06 0.0000
20	30.074	5.4840	0.87281	3.99082E+06 0.0000
21	37.408	6.1162	0.97342	1.56534E+05 0.0000
22	37.711	6.1409	0.97736	1.97845E+05 0.0000
23	38.945	6.2406	0.99322	4.87645E+05 0.0000
24	46.583	6.8252	1.0863	8.63492E+05 0.0000
25	52.331	7.2340	1.1513	2.10342E+06 0.0000
26	55.230	7.4317	1.1828	1.55523E+05 0.0000
27	55.956	7.4803	1.1905	1.36061E+06 0.0000
28	55.966	7.4811	1.1906	1.56062E+05 0.0000
29	59.358	7.7044	1.2262	68738. 0.0000
30	59.372	7.7053	1.2263	62418. 0.0000
31	59.397	7.7069	1.2266	68669. 0.0000
32	59.549	7.7168	1.2282	63781. 0.0000
33	66.876	8.1778	1.3015	31466. 0.0000

34	67.063	8.1892	1.3034	33603.	0.0000
35	67.259	8.2011	1.3053	44510.	0.0000
36	67.306	8.2040	1.3057	45797.	0.0000
37	74.392	8.6251	1.3727	1.82748E+05	0.0000
38	74.811	8.6494	1.3766	1.73510E+05	0.0000
39	88.448	9.4047	1.4968	2.34208E+06	0.0000
40	97.364	9.8673	1.5704	2.15400E+05	0.0000
41	98.493	9.9244	1.5795	1.70157E+05	0.0000
42	99.242	9.9620	1.5855	1.36611E+06	0.0000
43	104.46	10.221	1.6267	8.08002E+05	0.0000
44	124.55	11.160	1.7762	2.14080E+05	0.0000
45	125.05	11.182	1.7797	1.87411E+05	0.0000
46	130.98	11.445	1.8215	4.31640E+05	0.0000
47	132.72	11.520	1.8335	62380.	0.0000
48	132.80	11.524	1.8341	68629.	0.0000
49	132.81	11.524	1.8341	68405.	0.0000
50	133.63	11.560	1.8398	74171.	0.0000
51	136.26	11.673	1.8579	2.67083E+06	0.0000
52	145.02	12.042	1.9166	1.22939E+06	0.0000
53	154.77	12.441	1.9800	1.77083E+05	0.0000
54	155.05	12.452	1.9818	1.78535E+05	0.0000
55	163.44	12.784	2.0347	1.48859E+06	0.0000
56	171.88	13.110	2.0865	1.70943E+06	0.0000
57	183.63	13.551	2.1567	2.02070E+06	0.0000
58	187.36	13.688	2.1785	1.79810E+05	0.0000
59	187.57	13.695	2.1797	1.80525E+05	0.0000
60	222.72	14.924	2.3752	1.79246E+05	0.0000
61	222.87	14.929	2.3760	1.79565E+05	0.0000
62	233.60	15.284	2.4325	70039.	0.0000
63	233.78	15.290	2.4335	62336.	0.0000
64	233.80	15.291	2.4336	69076.	0.0000
65	234.12	15.301	2.4352	62888.	0.0000
66	251.05	15.845	2.5218	4.57423E+05	0.0000
67	257.60	16.050	2.5544	1.26418E+06	0.0000
68	260.66	16.145	2.5696	1.84537E+05	0.0000
69	260.73	16.147	2.5699	1.92440E+05	0.0000
70	260.98	16.155	2.5711	34778.	0.0000
71	261.13	16.159	2.5719	49514.	0.0000
72	262.00	16.186	2.5761	36474.	0.0000
73	262.38	16.198	2.5780	56143.	0.0000
74	288.89	16.997	2.7051	1.23203E+06	0.0000
75	300.98	17.349	2.7611	1.79328E+05	0.0000
76	301.09	17.352	2.7617	1.79265E+05	0.0000
77	320.26	17.896	2.8482	6.93376E+05	0.0000
78	343.41	18.531	2.9494	1.80693E+05	0.0000
79	343.48	18.533	2.9496	1.80739E+05	0.0000
80	360.96	18.999	3.0238	68384.	0.0000
81	361.04	19.001	3.0241	79657.	0.0000
82	361.08	19.002	3.0243	74448.	0.0000
83	361.20	19.005	3.0248	73023.	0.0000
84	385.60	19.637	3.1253	8.91107E+05	0.0000
85	387.68	19.690	3.1337	1.79003E+05	0.0000
86	387.73	19.691	3.1339	1.78853E+05	0.0000
87	398.09	19.952	3.1755	8.12138E+05	0.0000
88	411.88	20.295	3.2300	2.18516E+06	0.0000
89	433.48	20.820	3.3136	1.78434E+05	0.0000
90	433.50	20.821	3.3137	1.78460E+05	0.0000
91	480.42	21.919	3.4884	1.78086E+05	0.0000
92	480.44	21.919	3.4885	1.78130E+05	0.0000
93	512.25	22.633	3.6022	1.09207E+05	0.0000
94	512.38	22.636	3.6026	1.15575E+05	0.0000
95	512.38	22.636	3.6026	58984.	0.0000
96	512.45	22.637	3.6029	67728.	0.0000
97	528.15	22.982	3.6576	1.74539E+05	0.0000
98	528.16	22.982	3.6576	1.74619E+05	0.0000
99	535.86	23.149	3.6842	5.30243E+05	0.0000
100	555.48	23.569	3.7511	5.69141E+05	0.0000
101	563.35	23.735	3.7775	31302.	0.0000
102	563.40	23.736	3.7777	48934.	0.0000
103	563.81	23.745	3.7791	37304.	0.0000
104	563.82	23.745	3.7791	42192.	0.0000
105	575.91	23.998	3.8194	1.27555E+06	0.0000
106	576.29	24.006	3.8207	1.75906E+05	0.0000
107	576.31	24.006	3.8207	1.84128E+05	0.0000

108	624.42	24.988	3.9770	1.72513E+05	0.0000
109	624.42	24.988	3.9770	1.72468E+05	0.0000
110	653.00	25.554	4.0670	7.14113E+05	0.0000
111	658.68	25.665	4.0847	5.32943E+05	0.0000
112	672.15	25.926	4.1262	1.77582E+05	0.0000
113	672.17	25.926	4.1263	1.77622E+05	0.0000
114	684.70	26.167	4.1646	63510.	0.0000
115	685.51	26.182	4.1670	62573.	0.0000
116	685.59	26.184	4.1673	69461.	0.0000
117	685.77	26.187	4.1678	70076.	0.0000
118	719.08	26.816	4.2678	1.73688E+05	0.0000
119	719.10	26.816	4.2679	1.73630E+05	0.0000
120	764.76	27.654	4.4013	1.70978E+05	0.0000
121	764.82	27.655	4.4015	1.70711E+05	0.0000
122	768.13	27.715	4.4110	2.79889E+05	0.0000
123	798.15	28.252	4.4964	1.23504E+06	0.0000
124	799.24	28.271	4.4994	8.0145	0.0000
125	799.25	28.271	4.4995	8.2021	0.0000
126	805.68	28.384	4.5175	1.91672E+05	0.0000
127	809.22	28.447	4.5274	1.75267E+05	0.0000
128	809.38	28.450	4.5279	1.78274E+05	0.0000
129	830.63	28.821	4.5869	5.35384E+05	0.0000
130	851.28	29.177	4.6436	1.74707E+05	0.0000
131	851.31	29.177	4.6437	1.74889E+05	0.0000
132	877.70	29.626	4.7151	69823.	0.0000
133	877.83	29.628	4.7155	62521.	0.0000
134	877.89	29.629	4.7156	69864.	0.0000
135	879.95	29.664	4.7212	63956.	0.0000
136	891.15	29.852	4.7511	1.73973E+05	0.0000
137	891.17	29.852	4.7512	1.74074E+05	0.0000
138	914.44	30.240	4.8128	1.06910E+06	0.0000
139	928.38	30.469	4.8493	1.62919E+05	0.0000
140	928.38	30.469	4.8494	1.62973E+05	0.0000
141	944.13	30.727	4.8903	34876.	0.0000
142	944.80	30.738	4.8920	34672.	0.0000
143	944.87	30.739	4.8922	49557.	0.0000
144	945.92	30.756	4.8949	51519.	0.0000
145	962.60	31.026	4.9379	1.51912E+05	0.0000
146	962.61	31.026	4.9379	1.51909E+05	0.0000
147	993.57	31.521	5.0167	1.47405E+05	0.0000
148	993.57	31.521	5.0167	1.47424E+05	0.0000
149	1014.4	31.850	5.0691	1.03960E+05	0.0000
150	1020.0	31.938	5.0831	63807.	0.0000

P A R T I C I P A T I O N F A C T O R S

MODE NO	X-COMPONENT	Y-COMPONENT	Z-COMPONENT	X-ROTATION	Y-ROTATION	Z-ROTATION
1	-1.03668E-04	1.3199	-3.17291E-06	-72.543	-6.72993E-03	0.94817
2	-3.28693E-02	3.88348E-05	2.22137E-02	-1.70869E-03	-141.74	-1.55596E-02
3	-4.36626E-03	-1.06749E-04	1.1372	7.94659E-03	8.6381	-8.23504E-02
4	-1.79237E-02	-1.73690E-04	1.0772	1.22859E-02	7.5942	-0.20695
5	3.20664E-04	3.44480E-02	5.20480E-04	-0.27344	2.01822E-02	197.90
6	-6.94317E-06	1.45955E-06	-8.57659E-05	-1.28611E-04	-2.72839E-03	4.18843E-05
7	-1.93180E-03	1.4132	4.88860E-04	-122.59	-0.14870	154.91
8	-1.25177E-04	1.17200E-06	-2.75046E-05	-8.38425E-05	-1.94270E-02	-2.54116E-04
9	-7.99533E-03	-1.44442E-05	4.83808E-03	2.82321E-04	-68.853	2.21246E-02
10	1.16917E-03	-0.42232	-6.69411E-04	23.851	8.54448E-02	-338.27
11	-5.77432E-03	3.3146	1.95595E-03	-238.66	-0.57270	669.23
12	5.77357E-05	1.57832E-06	-3.89592E-04	-1.53765E-04	0.10734	5.59928E-04
13	-0.49491	2.02344E-03	1.6638	-0.11903	-373.15	-0.43676
14	1.48434E-04	-2.56774E-02	1.32387E-04	-3.8017	-2.26671E-02	-1.6188
15	1.10309E-02	-2.9519	-7.62611E-05	206.32	0.50699	-430.56
16	1.50477E-02	-1.3175	1.02713E-03	91.882	0.85192	368.13
17	1.91256E-04	3.91904E-06	6.25178E-05	-2.83447E-04	5.78676E-03	-4.15897E-04
18	-5.08409E-02	1.4731	-9.14644E-04	-104.24	-2.9287	-136.04
19	-0.81482	-5.77413E-03	0.17819	0.46591	-47.766	1.0191
20	1.1270	5.58435E-03	0.12960	-0.48096	64.930	-0.96095
21	-1.60263E-04	5.21221E-07	-4.09574E-05	-1.05476E-04	-9.68920E-03	-1.29920E-03
22	-8.70035E-03	-1.23232E-02	2.25230E-04	14.378	-0.47576	149.29
23	-5.62907E-03	-0.32123	-6.33627E-04	-3.1199	-0.37968	-21.767
24	-4.15808E-04	2.10616E-03	1.34995E-04	8.4514	-1.88080E-02	3.0072
25	1.1381	-1.52739E-03	-9.90235E-02	-6.66470E-02	68.141	-0.58252

18	455.39	3.82291E+05	0.14739	1.91437E+09	1.51116E+06	3.26067E+09
19	1.14225E+06	57.360	54625.	3.73455E+05	3.92538E+09	1.78685E+06
20	5.06869E+06	124.45	67028.	9.23149E+05	1.68249E+10	3.68521E+06
21	4.02047E-03	4.25258E-08	2.62587E-04	1.74145E-03	14.695	0.26422
22	14.976	30.045	1.00363E-02	4.09011E+07	44781.	4.40967E+09
23	15.452	50321.	0.19578	4.74649E+06	70296.	2.31050E+08
24	0.14929	3.8304	1.57361E-02	6.16760E+07	305.45	7.80886E+06
25	2.72464E+06	4.9071	20625.	9343.0	9.76653E+09	7.13752E+05
26	1.55102E-03	2.72792E-07	1.45567E-04	2.89259E-04	46.148	7.76746E-03
27	2162.7	3.2797	39.849	8313.8	2.27896E+09	9753.2
28	13.112	6923.9	7.35172E-02	2.40229E+07	5.15554E+05	8.45049E+07
29	2.72142E-02	42.354	5.31291E-05	50894.	1210.7	3.49487E+06
30	0.96476	6.10697E-04	3.27304E-04	0.56092	994.28	50.752
31	20116.	20.436	29.130	19879.	3.50212E+07	1.74905E+06
32	83.159	48694.	0.44476	6.26943E+07	75545.	4.05969E+09
33	2.64367E-02	1.24766E-07	9.11826E-02	8.06164E-06	4765.1	1.93052E-02
34	1.00625E-02	5975.3	3.6367	25285.	1.53880E+05	3.97214E+08
35	33759.	1.88802E-02	39909.	68.333	1.35614E+09	18823.
36	1.4024	319.05	1.0165	2.09507E+06	32257.	2.30923E+07
37	3.5931	4170.8	0.18201	6.89253E+05	15940.	3.73994E+09
38	3.40742E-03	1.10733E-06	3.05190E-05	1.92238E-04	1.9062	0.26300
39	60.825	4.25368E+05	1.8404	1.10135E+08	4.12530E+05	4.42782E+10
40	19.811	1.55250E+05	4.66336E-05	3.03742E+07	1.25560E+05	3.19651E+09
41	2.68311E-04	7.33019E-06	3.19805E-02	2.53513E-03	21.129	9.21589E-02
42	80.945	0.15995	39659.	38.881	2.91389E+05	26185.
43	82.230	7.04277E+05	3.76927E-02	1.08183E+08	6.46411E+05	3.27342E+09
44	2.52698E-02	350.19	3.15167E-02	1.84072E+05	5.1978	9.73907E+08
45	1.11457E-04	1.65451E-06	4.55033E-04	3.92592E-05	36.453	3.21186E-02
46	2.4295	15144.	0.33644	4.10461E+06	10118.	7.84933E+09
47	2.92924E-02	2.33953E-04	0.19529	8.41867E-02	15528.	0.10863
48	2.04712E-02	0.22346	8.92492E-02	4.14839E+05	5971.6	3.46897E+06
49	1353.8	4.19042E-03	10678.	2.4394	8.26287E+08	27.634
50	1.12496E-02	4932.7	4.78215E-02	6.38442E+06	327.41	4.21463E+09
51	5.60060E-02	4.5451	5.09477E-02	2.36999E+05	112.57	2.43067E+08
52	7.43840E-02	172.85	9.42666E-04	1.79419E+05	974.31	7.58209E+08
53	1.80981E-04	1.74319E-06	1.94582E-03	5.40751E-04	31.272	2.2993
54	0.49759	1304.0	8.65834E-04	1.52588E+05	17262.	4.62450E+06
55	6014.0	9.5471	49.524	1357.7	2.21806E+09	34442.
56	58564.	79.230	491.87	9959.3	1.03189E+09	2.81266E+05
57	9.07591E-04	23.023	1.76249E-04	2053.8	434.00	1.03598E+08
58	3.57797E-03	9.37537E-06	1.83162E-03	4.02913E-04	5.9740	11.649
59	3.22181E-02	0.79268	3.87483E-03	10494.	8.1573	2.31109E+07
60	1.46980E-08	5.47926E-07	1.19575E-02	9.42839E-05	268.45	0.18524
61	1.11900E-02	203.87	1.65806E-04	83030.	125.35	257.90
62	3113.2	6.40470E-02	83.213	211.16	1.01668E+07	29817.
63	3.34120E-02	1.94301E-05	4.32669E-02	2.50950E-03	998.01	9.8640
64	4.73321E-05	1.4695	8.23611E-05	583.53	26.874	8.56938E+05
65	0.14366	661.22	9.17767E-03	1.98457E+06	1426.4	1.38627E+08
66	80284.	4.9411	9108.5	3649.4	5.91519E+07	7.61958E+05
67	471.07	2.78638E-02	17933.	12.801	6.22156E+05	9152.2
68	3.10786E-03	3.77911E-06	3.21429E-03	9.99350E-03	763.23	1.1513
69	2.43042E-04	80.348	6.60571E-04	2.33785E+05	4.0822	2.20365E+07
70	3.49123E-02	3.23007E-07	1.26988E-02	7.90633E-04	21.356	0.29265
71	2.70090E-03	0.40784	1.90496E-05	76.682	0.50131	6.35256E+05
72	22.165	1525.7	0.24954	6.56061E+06	3157.5	1.31464E+08
73	18871.	5.2458	266.61	18184.	4.39902E+06	64301.
74	0.31757	7629.4	2.36722E-02	2.81034E+05	174.40	1.38237E+06
75	1.14103E-04	2.68360E-06	4.42178E-02	2.63059E-04	1504.9	0.13894
76	3.51090E-03	123.49	1.42777E-04	25191.	3.3050	906.19
77	2.44969E-04	682.80	8.53442E-05	6.72142E+06	6.1518	91862.
78	2.08929E-04	1.09149E-08	0.11957	2.74874E-05	9968.6	0.42083
79	1.09265E-03	8.79675E-02	1.40266E-05	2313.6	0.52490	1.46748E+06
80	2.99930E-02	7.43974E-04	1.6021	5.2156	82209.	112.01
81	2.24831E-02	121.85	0.18279	6.78330E+05	14779.	1.39758E+07
82	338.61	4.79970E-03	3986.7	4.9428	3.25143E+08	2156.3
83	4.39681E-04	1525.0	0.12380	2.64633E+06	10086.	1.81746E+08
84	7.0487	5.49546E-04	5.0333	17.138	7.63289E+08	4578.0
85	2.41084E-03	1.36275E-05	5.1761	2.14393E-02	5485.2	6.53406E-02
86	6.04995E-03	24.949	1.40303E-05	32767.	48.855	25716.
87	7.77523E-02	9.41859E-05	4371.4	0.57369	1.40908E+08	1054.8
88	2846.0	3.0001	1590.4	3691.9	3.27605E+07	5.26988E+05
89	2.16878E-05	9.57486E-07	0.63963	3.43326E-03	19406.	4.69115E-02
90	1.44419E-03	0.52531	5.99215E-04	1756.1	7.9815	8.36327E+05
91	1.34229E-05	3.91575E-05	5.39982E-02	6.79214E-02	9131.0	8.01328E-02

92	8.95894E-03	14.377	1.63374E-05	24122.	8.97624E-02	26222.
93	5.79097E-02	118.38	7.17631E-04	2.49148E+05	889.90	3.38075E+07
94	2.80680E-02	109.92	1.03308E-03	2.88108E+05	3546.5	2.54302E+07
95	3.32912E-04	0.22643	1.6721	598.32	35728.	51713.
96	1.9555	8.43177E-02	28.605	256.21	7.50889E+06	20686.
97	3.74274E-06	5.58308E-05	0.18016	0.10497	232.54	26.803
98	1.93164E-03	1.0871	1.76384E-05	2018.2	0.68966	5.30850E+05
99	8.59476E-04	0.44392	3.84242E-04	655.41	1027.7	8.27805E+06
100	2.3493	9.49609E-05	12757.	0.13736	2.54720E+05	20.374
101	3.00141E-02	2.20467E-02	0.12907	145.87	71414.	1902.5
102	2.40071E-02	162.67	4.79632E-02	1.00994E+06	2530.8	1.28640E+07
103	57.844	1490.0	330.87	3.65566E+06	1.67934E+07	1.15176E+08
104	639.33	130.35	3857.4	3.18602E+05	1.95510E+08	1.00743E+07
105	0.36138	323.30	2.02046E-05	3.11782E+05	3.54714E-02	3.82536E+07
106	1.11516E-05	9.91858E-07	4.99629E-03	1.72691E-03	9907.9	8.3425
107	2.47496E-06	7.47116E-02	5.97415E-06	1120.6	1.5648	2.39652E+06
108	7.20332E-03	1.4841	2.15725E-04	1842.2	3.3532	6.66130E+05
109	1.09119E-05	2.39872E-04	0.77050	0.29311	20953.	122.17
110	5.23711E-02	1.31876E-02	4285.1	1.1937	2.37714E+08	1998.6
111	9.14402E-02	11.725	6.8521	1744.7	3.70879E+05	20620.
112	6.46196E-02	16.756	1.12051E-05	25794.	29.607	2.93243E+05
113	8.94144E-05	6.63959E-05	1.7004	0.12383	63360.	4.7956
114	2.5233	1602.7	8.57772E-02	2.76822E+06	13270.	1.59458E+08
115	0.20909	4.25012E-08	4.3438	9.23088E-02	3.10048E+05	0.24740
116	234.28	5.44995E-02	2187.3	90.938	1.77203E+08	5868.9
117	1.40886E-04	1.8730	4.81160E-03	42988.	2.0589	1.62051E+05
118	8.96172E-02	6.0617	8.81280E-05	4793.0	23.105	9.18730E+05
119	9.26302E-06	1.68368E-05	6.62150E-02	1.26906E-02	11994.	1.9069
120	3.1527	63.462	9.01843E-04	59985.	2811.1	1.99312E+06
121	1.52792E-02	1.91604E-05	8.96947E-02	1.93159E-02	3102.2	1.2488
122	6774.2	4.2054	3.2076	3915.8	2.88428E+08	2.42231E+05
123	2508.2	25073.	0.19316	1.89292E+07	8.15855E+06	1.23416E+09
124	1.22948E-05	7.72468E-08	1.08926E-03	1.08205E-04	11.104	6.82695E-03
125	43.152	377.23	3.18618E-03	2.76214E+05	1.40130E+05	1.80895E+07
126	201.52	681.37	9.67541E-03	3.05582E+05	6.69978E+05	6.73099E+07
127	8.47193E-03	3.24438E-05	5.43864E-03	2.20045E-02	3018.9	0.94996
128	101.37	411.65	4.08611E-03	2.02082E+05	3.42520E+05	1.85893E+07
129	2.54671E+05	312.46	0.97230	1.57322E+05	1.04007E+09	1.54367E+07
130	1.39109E-06	2.08314E-05	3.57133E-02	2.95862E-03	114.32	2.8995
131	1.7953	5.9031	3.07478E-05	816.26	9725.0	7.37803E+05
132	3.98142E-03	4.00554E-02	7.16726E-05	9411.0	173.29	2939.7
133	0.79932	2.76576E-06	0.93302	6.77457E-02	2484.9	0.47165
134	469.20	2.34727E-03	49.416	13.413	8.79638E+06	468.13
135	19.773	1769.7	9.61821E-05	1.59117E+06	1.63725E+05	1.56124E+08
136	5.17753E-04	1.16111E-04	1.12042E-03	7.63019E-02	1145.8	2.2839
137	0.13168	9.7894	8.03061E-06	6405.1	1180.4	1.91640E+05
138	0.24976	43.244	1.20239E-02	1.30591E+05	4028.8	1.48134E+06
139	4.66069E-08	2.10977E-05	1.82961E-02	3.72681E-03	30.040	12.603
140	3.48396E-03	0.34023	1.27121E-05	47.479	91.106	1.84987E+05
141	0.22529	151.58	2.15935E-02	6.08468E+05	543.88	1.59461E+07
142	8.39230E-02	7.62487E-04	3.8538	2.3190	1.18392E+05	43.188
143	8.2368	0.13049	62.132	402.83	2.91546E+05	6473.8
144	1.69236E-03	4.20119E-02	1.15853E-03	3944.2	250.17	1224.1
145	9.12870E-05	8.44076E-04	3.40477E-04	0.61221	573.70	4.15505E-04
146	2.39454E-03	1.8378	1.29699E-08	1334.8	74.421	0.19533
147	1.02374E-06	4.83919E-06	9.83238E-03	0.65767	8.6409	132.66
148	2.17614E-05	2.70229E-03	1.11901E-04	369.36	15.004	73847.
149	202.92	2.44815E-02	7364.5	200.06	5.23559E+06	4033.1
150	6.22207E-02	581.74	0.10565	1.92001E+05	8419.1	2.52308E+07
TOTAL	9.44974E+06	9.77069E+06	2.76901E+06	3.76544E+10	8.56171E+10	4.01824E+11

THE ANALYSIS HAS BEEN COMPLETED

ANALYSIS COMPLETE

JOB TIME SUMMARY
 USER TIME (SEC) = 3.9000
 SYSTEM TIME (SEC) = 0.50000

```
TOTAL CPU TIME (SEC) = 4.4000
WALLCLOCK TIME (SEC) = 6
```

File lysefjord_wind_60.inp

```
*HEADING
Analysis of Lysefjord bridge
**
*INCLUDE, INPUT=lysefjord_modifisert_bru.inp
**
**
*INCLUDE, INPUT=lysefjord_wind_sets.inp
**
**
*****
**** Loading and analysis ****
*****
**
*INCLUDE, INPUT=dead_load.inp
**
**
** Angle independent wind coming here
**
*STEP, EXTRAPOLATION=NO, AMPLITUDE=RAMP, NAME=WIND_INDEPENDENT, NLGEOM, INC=5000
*STATIC, STABILIZE=1E-10
0.1,1
**
**
*DLOAD, OP=MOD
**Moment on the sides of the bridge girder
WIND_LEFT , PZ, -3162
**
WIND_RIGHT, PZ , 3162
**
**Positive lift on the bridge girder
WIND_CENTER , PZ , 2635
**Dragload against east on the bridge girder
**Not dependent on the angle of the bridge girder
WIND_CENTER , PY , 5912
**
**Horizontal on the main cable
MAINCABLE, PY , 321
**
**
*END STEP
** Now lets signal to the subroutine that we want to record geometry
** Fortran routine will return F=0
*STEP, AMPLITUDE=RAMP, NAME=CollectGeometry, NLGEOM=NO, INC=5000
*STATIC, STABILIZE=1E-10
1E-6,5E-6,1E-9,1E-6
**
*DLOAD
WIND_SIGNAL_LEFT, PXNU, 1
WIND_SIGNAL_RIGHT, PXNU, 1
**
*END STEP
** Now lets signal to the subroutine that we want to calculate angles
```

```

** Fortran routine will return F=0
*STEP,AMPLITUDE=RAMP,NAME=CalculateAngles,NLGEOM=NO,INC=5000
*STATIC,STABILIZE=1E-10
1E-6,5E-6,1E-9,1E-6
**
*DLOAD
WIND_SIGNAL, PXNU, 2
**
*END STEP
*STEP,EXTRAPOLATION=NO,AMPLITUDE=RAMP,NAME=WIND_VAR,NLGEOM,INC=10000
*STATIC,STABILIZE=1E-10
0.05,1,,0.1
**
**
*DLOAD
**Moment on the sides of the bridge girder
** This is the wind pressure we send in, and get forces back
** from dload_wind_crossbeam.f
WIND_VAR_LEFT, PZNU , 2250
WIND_VAR_RIGHT, PZNU , 2250
WIND_VAR_CENTER, PZNU      , 2250
**
*EL PRINT, ELSET=GIRDER, FREQUENCY = 100
SF
*EL PRINT, ELSET=MAINCABLE, FREQUENCY = 100
SF
*NODE PRINT, TOTALS=YES, FREQUENCY=100
RF
*NODE PRINT, TOTALS=YES
U
*END STEP
**

```

File lysefjord_wind_8_amp.inp

```

*HEADING
Analysis of Lysefjord bridge
**
** Include the model
*INCLUDE, INPUT=lysefjord_modifisert_bru.inp
**
**
** Lets setup some sets for wind load
**
*ELSET, ELSET=WIND_LEFT, GENERATE
12001,12036,1
*ELSET, ELSET=WIND_RIGHT, GENERATE
13001, 13036,1
*ELSET, ELSET=WIND_CENTER, GENERATE
1,36,1
*ELSET, ELSET=WIND_SIGNAL
19
**
**
*NSET, NSET=MAINCABLE, generate
1001,1037,1
2001,2037,1

```

```

** Lets add the amplitude
*AMPLITUDE, NAME=my_curve, DEFINITION=PERIODIC
**N, w, t0, A0,
**A1,B1,A2,B2
**1, 1.9105 , 1.0, 0.0
1, 1.8975, 1.0, 0.0
0.0,1.0
*****
**** Loading and analysis ****
*****
**
** STEP1: DEADLOAD
**
*INCLUDE, INPUT=dead_load.inp
**
** Angle independent wind coming here
**
*STEP, AMPLITUDE=RAMP,NAME=WIND_INDEPENDENT,NLGEOM,INC=5000
*STATIC,STABILIZE=1E-10
0.1,1
**
**
*DLOAD,OP=MOD
**Moment on the sides of the bridge girder
WIND_LEFT , PZ, -59
**
WIND_RIGHT, PZ , 59
**
**Positive lift on the bridge girder
WIND_CENTER, PZ , 49.2
**Dragload against east on the bridge girder
**Not dependent on the angle of the bridge girder
WIND_CENTER, PY , 110.4
**
**Horizontal on the main cable
MAINCABLE, PY , 5.8
**
**
*EL PRINT, ELSET=GIRDER, FREQUENCY = 100
SF
*EL PRINT, ELSET=MAINCABLE, FREQUENCY = 100
SF
*EL PRINT, ELSET=BACKSTAYCABLE, FREQUENCY = 100
SF
*NODE PRINT, TOTALS=YES, FREQUENCY=100
RF
*NODE PRINT, TOTALS=YES
U
*END STEP
**
**
*STEP,NAME=WIND_VAR,NLGEOM,INC=50000
*DYNAMIC, HALFINC scale factor=1000,INITIAL=NO, ALPHA=-0.05

```

```

**DYNAMIC, HALFINC scale factor=1000, INITIAL=NO, ALPHA=0
.1,600,,,1
**
**
*DLOAD, AMPLITUDE=my_curve
**Moment on the sides of the bridge girder
WIND_CENTER, PZ , 24.6
**
*OUTPUT, FIELD, FREQ=1
*Element OUTPUT, ELSESET=GIRDER
SF
*NODE OUTPUT, NSET=GIRDER
U
*Element OUTPUT, ELSESET=MAINCABLE
SF
*NODE OUTPUT, NSET=MAINCABLE
U
*Element OUTPUT, ELSESET=BACKSTAYCABLE
SF
*EL PRINT, ELSESET=GIRDER, FREQUENCY = 100
SF
*EL PRINT, ELSESET=MAINCABLE, FREQUENCY = 100
SF
*NODE PRINT, NSET=GIRDER, FREQUENCY = 100
U
*NODE PRINT, NSET=CABEL, FREQUENCY = 100
U
*END STEP
**
**

```

File lysefjord_wind_8_viv_static.inp

```

*HEADING
Analysis of Lysefjord bridge
**
** Include the model
*INCLUDE, INPUT=lysefjord_modifisert_bru.inp
**
**
*INCLUDE, INPUT=lysefjord_wind_sets.inp
**
**
***** Loading and analysis ****
*****
** STEP1: DEADLOAD
*INCLUDE, INPUT=dead_load.inp
**
** Now store the x coords on the model, so we can calc wind
*STEP,NAME=REGISTER_GEOM,NLGEOM,INC=50000
*STATIC,STABILIZE=1E-10

```

```

0.1,1
**
**
*DLOAD
**Moment on the sides of the bridge girder
DUMMY1 , PXNU , 1
**
*END STEP
**
*STEP,NAME=WIND_VAR,NLGEOM,INC=50000
*STATIC,STABILIZE=1E-10
0.1,1,,0.1
**
**
** The static VIV
** m*(2*pi*freq)^2*phi_y(s)*y_max
** 6166*(1.8975)Â²*phi_y(s)*0.635
**
*DLOAD
**Now we send in the line load intensity to fortran
WIND_VAR_CENTER , PZNU , -5398
**
*EL PRINT, ELSET=GIRDER, FREQUENCY = 100
SF
*EL PRINT, ELSET=MAINCABLE, FREQUENCY = 100
SF
*NODE PRINT, NSET=GIRDER, FREQUENCY = 100
U
*NODE PRINT, NSET=CABEL, FREQUENCY = 100
U
*NODE PRINT, TOTALS=YES, FREQUENCY=100
RF
*END STEP
**
**

```

APPENDIX F: FORTRAN FILES

File dload_wind_crossbeam.f

```

SUBROUTINE DLOAD(F,KSTEP,KINC,TIME,NOEL,NPT,LAYER,KSPT,COORDS,
1      JLTYP,SNAME)
C
C      INCLUDE 'ABA_PARAM.INC'
C
C      DIMENSION TIME(2),COORDS(3)
C      CHARACTER*80 SNAME

C
C      Lets make some saving stuff:
C      Left side is positive y axis. Stand in origin and face towards
increasing x values
C      Define the elements that are used for angle calculation
C
      integer left_element_begin, left_element_end, num_left_elems
      integer cent_element_begin, cent_element_end, num_cent_elems
      integer right_element_begin, right_element_end, num_right_elems
      integer right_moment_begin, right_moment_end, num_right_mom_elems
      integer left_moment_begin, left_moment_end, num_left_mom_elems
      integer num_integration_points, num_coords
      integer x_index, y_index, z_index
      integer signal_type, lift_type
      real width, height, moment_arm
      real Cl, Cm
      logical initiated

C
C      Here is where we setup the element layout system.
C      Left side is assumed positive Y, rigth side negative y
C
      parameter(left_element_begin=3001, left_element_end=3037,
+      num_left_elems = left_element_end - left_element_begin +1)
      parameter(cent_element_begin=1, cent_element_end=36,
+      num_cent_elems= cent_element_end - cent_element_begin +1)
      parameter(right_element_begin=4001, right_element_end=4037,
+      num_right_elems= right_element_end - right_element_begin +1)
      parameter(left_moment_begin=12001, left_moment_end=12036,
+      num_left_mom_elems = left_moment_end - left_moment_begin +1)
      parameter(right_moment_begin=13001, right_moment_end=13036,
+      num_right_mom_elems= right_moment_end - right_moment_begin +1)

      parameter(num_integration_points=2, num_coords=3)
      parameter(x_index=1, y_index=2, z_index=3)
      parameter(signal_type=41, lift_type=42)
C      Bridge cross section data
      parameter(width=12.3, height=2.76, moment_arm=10.25)
C      Coefficients for variable wind load
      parameter(Cl=3, Cm=1.12)

      real left_side(num_left_elems,num_integration_points,

```

```

+      num_coords)
real right_side(num_left_elems,num_integration_points,
+      num_coords)
double precision angle(num_left_elems,
+      num_integration_points)

C
C      Static variables to keep state
save left_side, right_side, angle
save initiated

real delta_l, delta_z, loc_angle, loc_moment, loc_force
real start_angle, end_angle, element_length
real element_dist
logical is_left, is_center, is_q_positive
integer element_index
integer i,j,k

data initiated/.FALSE./

C
C      Functions
C
Logical in_closed_set
real drag_coefficient
real lift_coefficient
real moment_coefficient

C
if( .NOT. initiated) then
do 10 i = 1, num_left_elems
   do 20 j=1,num_integration_points
      do 30 k=1,3
         left_side(i,j,k)=0
         right_side(i,j,k)=0
30      continue
         angle(i,j) = 0
20      continue
10      continue
      initiated = .TRUE.
      print *, "initiated"
endif

C
C      Find element index
C
is_left = .FALSE.
is_center = .FALSE.
if(in_closed_set(NOEL,left_element_begin,left_element_end)) then
   is_left = .TRUE.
   element_index = NOEL - left_element_begin + 1
elseif(in_closed_set(NOEL,left_moment_begin,left_moment_end)) then
   is_left = .TRUE.
   element_index = NOEL - left_moment_begin + 1
elseif(in_closed_set(NOEL,right_moment_begin,right_moment_end))
$      then
   element_index = NOEL - right_moment_begin + 1
elseif (in_closed_set(NOEL,cent_element_begin,cent_element_end))
$      then
   element_index = NOEL - cent_element_begin + 1
   is_center = .TRUE.
else
   element_index = NOEL - right_element_begin + 1

```

```

        endif
C
C      Is it a signal?
C
C      if (JLTYP .EQ. signal_type) then
C        Collect or calculate angles
          if (F .EQ. 1.0) then
            print *, "Register ", NOEL, NPT
            if (is_left) then
C        then we are on the left side of the stuff
              left_side(element_index, NPT, 1)=Coords(1)
              left_side(element_index, NPT, 2)=Coords(2)
              left_side(element_index, NPT, 3)=Coords(3)
            elseif (is_center) then
            else
              right_side(element_index, NPT, 1)=Coords(1)
              right_side(element_index, NPT, 2)=Coords(2)
              right_side(element_index, NPT, 3)=Coords(3)
            endif
          else
            print *, "Calc angles"
            call calc_angles(left_side, right_side, angle,
$              num_left_elems, num_integration_points)
          endif
C        return zero force, just for signalling
          F = 0
        else
C        Now we do the calculations
C        First we have to look at the angle
C
C        Now it is more elaborate, needs to find the angles in the integration
point
C        Use integration point 2 since that gives us the longest distance
C
C        print *, "Element" ,NOEL, NPT, element_index
start_angle = angle(element_index, 2)
end_angle = angle(element_index+1, 2)
element_dist = Coords(1) - left_side(element_index, 2,1) -
element_length = left_side(element_index + 1, 2,1) -
$      left_side(element_index, 2,1)
loc_angle = start_angle+ element_dist*(end_angle-start_angle)/
$      element_length
C        print *, "angles", start_angle, end_angle
C        print *, "Element dist", element_dist,element_length, loc_angle
loc_angle = loc_angle/180*3.14159265
is_q_positive = .FALSE.
if ( F .GE. 0 ) then
  is_q_positive = .TRUE.
endif

        if (is_center) then
C        Do some lift stuff
C
C        This is temporary stuff for missing an element
          F=F*width*C1*loc_angle
          if (is_q_positive) then
C            F = -F
          endif
        else

```

```

C
C      Moment type
C
        loc_moment = F*width*width*Cm*loc_angle
        F = loc_moment/moment_arm
        if(in_closed_set(NOEL, left_moment_begin, left_moment_end) )
$          then
            if (is_q_positive) then
                F = -F
            endif
        else
C      Right side of things
            if( .NOT. is_q_positive) then
                F=-F
            endif
            endif
        endif
C
C      Need to scale according to time, we assume ramp
C      Hopefully this will improve convergence
C      Time has to be setup to be something like 0.1,1
C      So we can use the factor directly as scale
C
100     FORMAT(A, I7, I7,I7, F10.1, I7, I7, F10.6)
        F = F*TIME(1)
        write (*,100) "Hit wind", NOEL, NPT, JLTYP, F, KSTEP, KINC,
$           TIME(1)
        endif
c$$$  print *, "Coords: ", COORDS(2), Coords(3)
c$$$  print *, KStep, KINC
c      print *, Time(1), Time(2)
c$$$  print *, NOEL, NPT, JLTYP
      RETURN
      END

C
C      check that we are in intervals
C
LOGICAL FUNCTION in_closed_set(val, min_val, max_val)
implicit none
integer val, min_val, max_val
in_closed_set = val .GE. min_val .AND. val .LE. max_val
return
end

SUBROUTINE set_array(val, loc_matrix, num_elems,
+      num_integration_points)
implicit none
double precision loc_matrix(num_elems,num_integration_points)
integer num_elems, num_integration_points
double precision val
integer i,j

do 10 i = 1, num_elems
    do 20 j=1,num_integration_points
        loc_matrix(i,j)= val
20    continue
10   continue
      return

```

```

end

SUBROUTINE calc_angles(left_side, right_side, angle, num_elems,
+      num_integration_points)
implicit none
real left_side(num_elems,num_integration_points,3)
real right_side(num_elems,num_integration_points, 3)
double precision angle(num_elems,num_integration_points)
integer num_elems, num_integration_points
real delta_l, delta_z
double precision loc_angle
integer i, j

do 10 i = 1, num_elems
    do 20 j=1,num_integration_points
        delta_l = left_side(i,j,2)-right_side(i,j,2)
        delta_z = -left_side(i,j,3)+right_side(i,j,3)
        loc_angle = atan2(delta_z, delta_l)
        angle(i,j)=loc_angle/3.14159265*180
        print *, "Angle", i, j, angle(i,j)
20    continue
10    continue
return
end

```

File dload_viv_ns_load.f

```

SUBROUTINE DLOAD(F,KSTEP,KINC,TIME,NOEL,NPT,LAYER,KSPT,COORDS,
1      JLTYP,SNAME)
C
INCLUDE 'ABA_PARAM.INC'
C
DIMENSION TIME(2),COORDS(3)
CHARACTER*80 SNAME

C
C      Lets make some saving stuff:
C      Left side is positive y axis. Stand in origin and face towards
increasing x values
C      Define the elements that are used for angle calculation
C
integer cent_element_begin, cent_element_end, num_cent_elems
integer signal_element_begin,signal_element_end, num_signal_elems
integer num_integration_points, num_coords
integer x_index, y_index, z_index
integer signal_type, lift_type
real width, height, moment_arm
real Cl, Cm
logical initiated
C
C      Here is where we keep the loads for the
static load eq to the dynamic load
C
real loads(37)
real phi_3(37)
real x_coords(37)
real force

```

```

real length
real amp

C Here is where we setup the element layout system.
C Left side is assumed positive Y, rigth side negative y
C
parameter(cent_element_begin=1, cent_element_end=36,
+      num_cent_elems= cent_element_end - cent_element_begin +1)
parameter(signal_element_begin=3001, signal_element_end=3037,
+      num_signal_elems= signal_element_end-signal_element_begin +1)
parameter(num_integration_points=2, num_coords=3)
parameter(x_index=1, y_index=2, z_index=3)
parameter(signal_type=41, lift_type=43)
C Bridge cross section data
parameter(width=12.3, height=2.76, moment_arm=10.25)
C Coefficients for variable wind load
parameter(Cl=3, Cm=1.12)

integer element_index
integer i,j,k

C Load data
C
data phi_3/ 3.3583E-04,-7.5217E-02,-0.1098,-0.1271,-0.1235,
$   -9.6850E-02,-4.7014E-02,2.4741E-02,0.1157,0.2221,0.3390,
$   0.4611,0.5824,0.6971,0.7996,0.8848,0.9485,0.9874,0.9996,
$   0.9844,0.9424,0.8758,0.7878,0.6828,0.5658,0.4427,0.3195,
$   0.2019,9.5575E-02,5.3114E-03,-6.5036E-02,-0.1128,-0.1368,
$   -0.1374,-0.1166,-7.8277E-02,3.5761E-03/

data loads/-1.2,-438.2,-642.9,-751.6,-742.7,-604.6,-335.3,
$   58.4,561.9,1153.6,1806.6,2490.1,3171.3,3816.8,4394.9,
$   4876.6,5237.9,5460.4,5532.6,5450.6,5218.3,4847.2,4355.8,
$   3768.6,3114.9,2426.9,1738.4,1082.5,490.3,-11.2,-400.4,
$   -662.7,-791.6,-789.4,-668.3,-450.4,8.3/

C Just use the rough x dirs as a start
data x_coords/37*0/
save x_coords

C Functions
C
C
C Find element index
C
if (in_closed_set(NOEL,signal_element_begin,signal_element_end))
$  then
    if (JLTYP .EQ. signal_type) then
C Register the coords for cross beams as starters
        x_coords(NOEL-signal_element_begin+1)=COORDS(1)
        F=0
        print *, 'Element: ', NOEL
    endif
endif
if (in_closed_set(NOEL,cent_element_begin,cent_element_end)) then
    if (JLTYP .EQ. lift_type) then
C Do some lift stuff

```

```

length = x_coords(NOEL+1) - x_coords(NOEL)
amp    = phi_3(NOEL+1) - phi_3(NOEL)
force = phi_3(NOEL) + amp*(COORDS(1)-x_coords(NOEL))/length
F=F*force*TIME(1)
endif
C
C Need to scale according to time, we assume ramp
C Hopefully this will improve convergence
C Time has to be setup to be something like 0.1,1
C So we can use the factor directly as scale
C
100 FORMAT(A, I7, I7,I7, F10.1, I7, I7, F10.3, F10.3, F10.5)
      write (*,100) "Hit wind", NOEL, NPT, JLTYPE, F, KSTEP, KINC,
$      COORDS(1),COORDS(3), TIME(1)
      endif
      RETURN
      END

C
C check that we are in intervals
C
LOGICAL FUNCTION in_closed_set(val, min_val, max_val)
implicit none
integer val, min_val, max_val
in_closed_set = val .GE. min_val .AND. val .LE. max_val
return
end

```